Sílvia Marisa Janeiro Fontenete

Towards the development of detection methods for *Helicobacter pylori* within the human body

Tese de Candidatura ao grau de Doutor em Patologia e Genética Molecular submetida ao Instituto de Ciências Biomédicas Abel Salazar da Universidade do Porto.

Orientador:
Doutor Nuno Filipe Azevedo
Categoria - Investigador auxiliar.
Afiliação - Faculdade de Engenharia da Universidade do Porto.

Coorientadores:
Prof. Maria do Céu Fontes Herdeiro Figueiredo
Categoria – Professor auxiliar.
Afiliação – Faculdade de Medicina da Universidade do Porto.

Prof. Jesper Wengel
Categoria – Professor catedrático.
Afiliação – University of Southern Denmark.

This work was financially supported by: Project UID/EQU/00511/2013-LEPABE, by the FCT/MEC with national funds and when applicable co-funded by FEDER in the scope of the P2020 Partnership Agreement; Project NORTE-07-0124-FEDER-000025 - RL2_ Environment&Health, by FEDER funds through Programa Operacional Factores de Competitividade – COMPETE, by the Programa Operacional do Norte (ON2) program and by national funds through FCT - Fundação para a Ciência e a Tecnologia: DNA mimics Research Project PIC/IC/82815/2007 and PhD grant, SFRH/BD/72999/2010.

"Do your work with your whole heart and you will succeed."

Elbert Hubbard.

Aos meus Pais.

ACKNOWLEDGMENTS

My first words of acknowledgement I express them to my supervisor Professor Nuno Azevedo for his constant advice, guidance, insight and inestimable support. I would like to express my gratitude for the opportunity he gave me to become part of his team.

Special thanks go to my co-supervisor Professor Jesper Wengel, who kindly welcomed me in his lab at Nucleic Acid Center, where I could familiarize with nucleic acid chemistry and developed part of my work.

I would like to thank to my co-supervisor Professor Céu Figueiredo for the excellent scientific guidance and support, as well as critical revision of all my work.

Special thanks to BEL's laboratory for the good mood in the laboratory, the exchange of ideas and all help. In particular, I am grateful to Ana Luísa, Luciana, Anabela, Carla, Joana Malheiro, Inês e Catarina for all the fun we have had in the last years. Special thanks go to Andreia Azevedo and Joana Barros for their friendship, good moments in the lab and support in this thesis (you will always be in my heart!). I also thank to my collegue Joana Lima for supporting me and for helping me with proofreading of my thesis.

I would like to thank to all people from University of Southern Denmark who contributed with their time, expertness, instrumentation and advice to my project. Special thanks to Per Trolle Jorgensen, Joan Hansen and Tina Hansen for their valuable technical assistance, information and help. I would like to thank to my colleagues Torben Højland, Christina Udesen, Nicola Derbyshire, Harvey Lou, Kathrine Wich and Kira Astakhova for their friendship and for being available for scientific discussions.

To IPATIMUP team under the supervision of Professor Céu Figueiredo, I would like to express my gratitude. Special thanks go to Marina Leite for the scientific ideas and for always being available.

The *in vivo* studies were performed at Laboratory of Microbiology, Parasitology and Hygiene (LMPH), University of Antwerp, under the supervision of Professor Paul Cos to whom I would like to express my gratitude for the opportunity to work in his research group and receiving me so well. I would like to express my gratitude to Davie Cappoen

and to the PhD student Maíra, Bieke and Freya for the precious help, for receiving me so well and for providing me a pleasant stay in Antwerp.

My deepest thanks are extended to my friends from TPC team; Ankita, Dario, Maxime, Marc and Rebecca for the good moments we shared in Belgium.

I am deeply thankful to my parents for supporting me in every way possible. When I was geographically distant, you have always been available, encouraging me and giving me support.

I also would like to thank to Nuno, without your support the distance would be much harder to overcome, thank you for being part of my life.

Finally, I want to thank to Fundação para a Ciência e Tecnologia for the financial support (SFRH/BD/72999/2010).

ABSTRACT

Gastric cancer is the 5th most common cancer in the world, with an estimated 950,000 new cases diagnosed in 2012. It is also the 3rd leading cause of cancer death in both worldwide. *Helicobacter pylori* (*H. pylori*) is a gastric pathogen that causes chronic inflammation and significantly increases the risk of developing gastric diseases, including gastric cancer. The global prevalence of *H. pylori* infection in humans is of more than 50%, and therefore it represents a public health issue. *H. pylori* can be detected after endoscopy by histology, culture and urease tests, but all biopsy-based methods are liable to sampling errors. For that reason, the development of novel, fast and efficient diagnostic methods is extremely important. Confocal Laser Endoscopy is a recent technology that has been tested to identify specific cellular and subcellular changes on the surface of the gastric mucosa. However, there is no specific staining to detect *H. pylori in vivo*. Fluorescence *in situ* hybridization (FISH) using rRNA-targeted probes is a molecular technique that allows the specific identification of bacteria in different types of samples without prior cultivation. The *in vivo* use of FISH, also called fluorescence *in vivo* hybridization (FIVH), has proved to be a challenge, in part due to the need of highly resistant oligonucleotides able to hybridize in human body conditions. The development of nucleic acid chemistry allowed the synthesis of new nucleic acid mimics that possess advantages comparatively with the typical DNA or RNA probes. These new mimics may be used to design FISH probes and increase the efficiency of the detection. Locked nucleic acid (LNA) has been developed as a novel RNA derivative nucleotide analog being able to hybridize with DNA or RNA according to Watson-Crick base-pairing rules with higher selectivity.

The general aim of this thesis was to explore the applicability of nucleic acid mimics for the *in vivo* diagnostic of *H. pylori*.

In the first stage of this work, different designs of locked nucleic acid (LNA) based probes were compared relatively to their ability to hybridize and detect *H. pylori*. Different FISH protocols and denaturant agents were also evaluated. Results showed that small LNA probes with 10 to 15 base pairs (bp) have higher efficiencies of hybridization comparatively to 18 bp LNA probes. Additionally, 2'-*O*-methyl RNA (2'OMe9 monomers showed to improve the hybridization in this type of probes. However, the performance of each probe showed to be very dependent on the combinations between length, nucleic acid composition and backbones modifications, being the 10_HyP_LNA/2'OMe PO and

10_HyP_LNA/2'OMe PS probes considered the best designs in the set of probes studied. Consequently, the designs that displayed high efficiency were selected for further studies.

The quantitative comparison of results between the different probes by microscopy is only possible if a suitable bioimaging tool is used. However, due to the lack of user-friendly and validated tools to quantify fluorescence intensity in slides, a new set of semi-automated and automated image analysis tools (FISHji) were developed to be used with the software ImageJ. Results demonstrated that FISHji3, FISHji4 and FISHji5 showed the highest correlation with flow cytometry data. These methods not only allow the fluorescence quantification in FISH samples but are also able to analyse non-specific stains such as propidium iodide.

Other characteristic that is necessary to take into account when new probes for FISH are designed is the ability of each probe to detect and discriminate mismatches. As such, the capacity of mismatch discrimination of some nucleic acid mimics (DNA, PNA, LNA/DNA, LNA/2'OMe and LNA/UNA) was assessed by thermodynamic analysis and *in vitro* studies using *H. pylori* and *H. acinonychis*. PNA and LNA/2'OMe probes yielded high specificity both against naked DNA and RNA sequences and *in vitro* in the identification of the corresponding target microorganism (*H. pylori*).

The performance of FIVH directly in the human body implies that the full process has to be carried out at 37 ºC during the whole reaction. Therefore, LNA-based probes that were previously developed (10_HyP_LNA/2'OMe PO and 10_HyP_LNA/2'OMe PS probe) were employed to identify *H. pylori* at human body temperature *in vitro*. The results showed that the 10_HyP_LNA/2'OMe PS probe was able to detect *H. pylori* at 37 ºC with high sensitivity and specificity *in vitro* in bacterial samples and in biopsies of infected patients.

Regarding the human stomach environment, the integrity, sensitivity and specificity of the previously probe was then studied using acid pH. Additionally, a simple, fast and non-toxic FISH protocol was developed. The cytotoxicity of the probe was also tested on a gastric cell line through the analysis of cell viability and apoptosis induction. The 10_HyP_LNA/2'OMe PS probe showed high signal-to-noise ratio in the detection of *H. pylori* in all pH conditions tested. The sensitivity and specificity of the probe was maintained using the new FISH methodology.

The validation of the study was achieved using fluorescence *in vivo* hybridization (FIVH) for the detection of *H. pylori* SS1 in infected C57BL/6 mice. After 15 days of post-infection FIVH was performed using 0.5 µM and 2 µM of 10_HyP_LNA/2'OMe PS probe. Fluorescence were analysed *ex vivo* by microscopy in mucus samples, cryosections and paraffin-embedded tissue slides. Results showed that the 10_HyP_LNA/2'OMe PS probe displayed high specificity *in vivo* allowing direct observation of the location and distribution of the *H. pylori SS1* within the mice stomach mucosa.

In summary, the 10_HyP_LNA/2'OMe PS probe could efficiently detect *H. pylori* not only in varying *in vitro* conditions but also directly *in vivo* in the gastric mucosa. This work offers a set of new LNA-based FISH protocols and studies that can be used for other researches in the microbiology field. Furthermore, a new approach is also presented for the diagnostic of *H. pylori*. These studies should be extended to other emergent microbes for the development of methods to identify important bacteria directly *in vivo*, not only in a diagnostic perspective but also to understand the interaction mechanisms involving the microbiome within the human body.

RESUMO

O cancro gástrico é o quinto cancro mais comum em todo o mundo, com um número estimado de novos casos diagnosticados de 950.000 em 2012. Este cancro é também a terceira causa de morte por cancro em todo o mundo, em ambos os sexos. *Helicobacter pylori* (*H. pylori*) é uma bactéria presente no estômago que causa inflamação crónica e aumenta significativamente o risco de desenvolvimento de doenças gástricas. A prevalência global da infeção por *H. pylori* em humanos é superior a 50 %, representando desta forma um problema de saúde público. *H. pylori* pode ser detectada após endoscopia por histologia, cultura e testes de urease, no entanto, todos os métodos baseados em biópsia são passíveis a erros. Por esta razão, o desenvolvimento de métodos de diagnóstico rápidos e eficientes são de extrema importância. A endoscopia a laser confocal é uma tecnologia recente, que tem sido utilizada na identificação de alterações celulares e subcelulares na superficie da mucosa gástrica. No entanto, não existem métodos de coloração específicos para *H. pylori in vivo.*

A hibridação *in situ* fluorescente (FISH) em conjunto com sondas específicas para ARN ribossomal é uma técnica molecular que permite a identificação de uma bactéria, em diferentes tipos de amostras, sem necessidade de cultivo prévio. O uso de FISH *in vivo*, também chamado de hibridação *in vivo fluorescente* (FIVH), tem-se revelado ser um desafio, em parte devido à necessidade de oligonucleotídeos altamente resistentes com capacidade para hibridarem nas condições existentes no corpo humano. O desenvolvimento da química dos ácidos nucleicos permitiu a síntese de novos mímicos de ácidos nucleicos com vantagens comparativamente ao ADN e ARN. Estes novos mímicos podem ser utilizados no desenho de sondas FISH permitindo o aumento da eficiência destas sondas. O *Locked nucleic acid* (LNA) foi desenvolvido como um novo nucleotídeo derivado e análogo ao RNA, hibridando especificamente com sequências de DNA e RNA de acordo com as regras de emparelhamento de Watson-Crick.

O objetivo geral desta tese foi explorar a aplicabilidade dos mímicos de ácidos nucleicos para o diagnóstico *in vivo* de *H. pylori*.

Durante a primeira parte deste trabalho, diferentes desenhos de sondas de LNA foram comparados relativamente à sua capacidade de hibridar e detetar *H. pylori*. Diferentes protocolos FISH e distintos agentes desnaturantes foram também analisados. Os resultados mostraram que pequenas sondas de LNA com 10 a 15 pares de bases (pb) têm maior eficiência na hibridação comparativamente com sondas de LNA de 18 pb. Adicionalmente, monómeros 2'OMe mostraram uma melhoria na hibridação neste tipo de sondas. No entanto, a performance de cada sonda demonstrou ser muito dependente das

combinações entre o tamanho, composição de ácidos nucleicos e modificações nos *backbones*, sendo as sondas 10_HyP_LNA/2'Ome PO e 10_HyP_LNA/2'Ome PS consideradas as melhores, no conjunto de sondas estudadas. Consequentemente, os desenhos das sondas que dispõem elevada eficiência foram selecionados para estudos futuros.

A comparação quantitativa dos resultados obtidos para diferentes sondas só é possível se uma ferramenta de bioimagem for utilizada. No entanto, devido à falta de ferramentas validadas de uso fácil e de forma a quantificar a fluorescência em lâminas, um novo conjunto de ferramentas semi-automáticas e automáticas (FISHji) foram desenvolvidas, para o uso com o programa ImageJ. Os resultados demostraram que os métodos FISHji3, FISHji4 e FISHji5 revelaram maior correlação com os dados obtidos por citometria de fluxo. Estes métodos não só permitiram a quantificação de fluorescência em amostras de FISH mas também permitiram a análise de amostras marcadas com corantes não específicos tais como o iodeto de propídio.

Outra caraterística importante que é necessária ter em conta quando novas sondas de FISH são desenhadas é a capacidade de detetar e discriminar *mismatches*. Desta forma, a capacidade de discriminar *mismatches* para alguns mímicos de ácidos nucleicos (DNA, PNA, LNA/DNA, LNA/2'OMe e LNA/UNA) foi acedida através de análises termodinâmicas e estudos *in vitro* utilizando *H. pylori* e *H. acinonychis*. As sondas de PNA e LNA/2'OMe mostraram elevada especificidade quer para ADN e ARN isolados em suspensão quer no interior de células para a identificação do microrganismo alvo, *H. pylori*.

Para a realização de FIVH diretamente no corpo humano, é necessário que todo o processo seja efetuado a 37 ºC durante toda a reação. Desta forma, as sondas de LNA que foram previamente desenhadas **(**10_HyP_LNA/2'Ome PO e 10_HyP_LNA/2'Ome PS) foram utilizadas *in vitro* para identificar *H. pylori* à temperatura do corpo humano. Os resultados mostraram que a sonda 10_HyP_LNA/2'Ome PS foi eficaz na deteção de *H. pylori* a 37 ºC apresentando elevada sensibilidade e especificidade *in vitro,* em amostras bacterianas e em biópsias de pacientes infetados.

Tendo em conta o ambiente do estômago humano, a integridade, a sensibilidade e a especificidade da sonda referida anteriormente foi estudada, utilizando pH ácido. Adicionalmente, um protocolo FISH simplificado, rápido e não tóxico foi desenvolvido. A citotoxicidade da sonda foi também testada em uma linha celular gástrica, através da análise de viabilidade celular e indução da apoptose. A sonda 10_HyP_LNA/2'Ome PS mostrou elevada deteção de racio sinal/ruído de H. *pylori* em todas as condições de pH testadas. A sensibilidade e a especificidade da sonda foram mantidas utilizando o novo protocolo de FISH desenvolvido.

A validação do estudo foi efetuada utilizando FIVH para a deteção de *H. pylori SS1* em ratinhos C57BL/6 infetados. Após 15 dias de período pós-infeção, FIVH foi efetuado utilizando 0.5 µM e 2 µM de sonda 10_HyP_LNA/2'Ome PS. A fluorescência foi analisada *ex vivo* através de microscopia em amostras de muco, crioseções e lâminas de tecidos parafinados. Os resultados revelaram que a sonda 10_HyP_LNA/2'OMe PS tem elevada sensibilidade e especificidade *in vivo*, permitindo a observação direta da localização e distribuição de *H. pylori SS1* na mucosa gástrica dos ratinhos.

Resumindo, a sonda 10_HyP_LNA/2'OMe PS pode detetar eficazmente *H. pylori* não só em diversas condições *in vitro* mas também diretamente na mucosa gástrica *in vivo*. Este trabalho oferece um conjunto de novos protocolos de LNA-FISH e estudos que poderão ser utilizados por outros investigadores na área de microbiologia. Para além disso, uma nova abordagem é também apresentada para o diagnóstico de *H. pylori*. Estes estudos devem ser alargados a outros microrganismos emergentes para o desenvolvimento de métodos de identificação de importantes bactérias, diretamente *in vivo*, não só em uma perspetiva de diagnóstico mas também para compreender mecanismos de interação existentes entre o microbioma e o corpo humano.

TABLE OF CONTENTS

Chapter II - Application of locked nucleic acid-based probes in fluorescence in situ hybridization

LIST OF FIGURES

Chapter I- Background and aims

Chapter II - Application of locked nucleic acid-based probes in fluorescence *in situ* hybridization

Chapter III - FISHji: new ImageJ macros for the quantification of fluorescence in epifluorescence images

Chapter IV - Mismatch discrimination in Fluorescent in situ hybridization using different types of nucleic acids

Chapter V – Hybridization-based detection of *Helicobacter pylori* at human body temperature using advanced Locked Nucleic Acid (LNA) probes

Chapter VI – Towards fluorescence in vivo hybridization (FIVH) detection of H. pylori in gastric mucosa using advanced LNA probes

Chapter VII - Fluorescence *in vivo* hybridization (FIVH) for detection of *Helicobacter pylori* infection in a C57BL/6 mouse model

Supplemental material

LIST OF TABLES

Chapter I- Background and aims

Chapter II - Application of locked nucleic acid-based probes in fluorescence *in situ* hybridization

Chapter III - FISHji: new ImageJ macros for the quantification of fluorescence in epifluorescence images

Chapter IV - Mismatch discrimination in Fluorescent in situ hybridization using different types of nucleic acids

Chapter V – Hybridization-based detection of *Helicobacter pylori* at human body temperature using advanced Locked Nucleic Acid (LNA) probes

Chapter VI – Towards fluorescence in vivo hybridization (FIVH) detection of H. pylori in gastric mucosa using advanced LNA probes

Chapter VII - Fluorescence *in vivo* hybridization (FIVH) for detection of *Helicobacter pylori* infection in a C57BL/6 mouse model

Supplemental material

ABBREVIATIONS AND ACRONYMS

ºC	Celsius degrees
%	Percent
Ω	Overlap index
g	Times gravity
kcal	Kilocalories
M	Molar
min	Minutes
mM	Millimolar
mol	Mole
mW	Milliwatts
MW	Molar weight
nm	Nanometer
rpm	Revolutions per minute
µM	Micromolar
µg	Microgram
µL	Microliter
µm	Micrometer

AEEA	8-amino-3,6-diaxaoctanoic acid
AFU	Arbitrary fluorescence units
AGS	Gastric adenocarcinoma cell line
ANOVA	One-way analysis of variance
ATCC	American Type Culture Collection
BaP	Benzo(α)pyrene
B/C	Brightness and contrast
BLAST	*Basic local alignment search tool*
α-CA	α-carbonic anhydrase
CagA	Cytotoxin-associated gene A
CagA PAI	*Cag* pathogenicity island
CFU	*Colony-forming unit*
CLE	Confocal laser endomicroscopy
CO_2	Carbon dioxide
CPP	Cell penetrating peptides
CT	Cholera toxin
Cy	Cyanine
DAIME	Digital image analysis program

DAPI	4',6-diamidino-2-phenylindole
DMT	Dimethoxytrityl
DNA	Deoxyribonucleic acid
Ea	Activation energy
EDTA	Ethylenediamine tetraacetic acid
ELISA	Enzyme-linked immunosorbent assay
EUCAST	European committee on antimicrobial susceptibility testing
HCO_3^-	Bicarbonate
HE	Hematoxylin and eosin
HPLC	High Performance Liquide Chromatography
IE-HPLC	IonExchange HPLC
FA	Formamide
FAM	*Fluorescein* amidite
FCS	Fetal calf serum
FBS	Fetal bovine serum
FDA	*Food and drug administration*
FISH	Fluorescence *in situ* hybridization
FIVH	Fluorescence *in vivo* hybridization
FITC	Fluorescein isothiocyanate
G	Gibbs free energy
Ig	Immunoglobulin
IL	Interleukin
LNA	Locked nucleic acid
LoG	Laplacian of Gaussian
LT	Heat-labile enterotoxin
MALDI	*Matrix-assisted laser desorption ionization*
MALDI-TOF	MALDI time-of-flight mass spectrometry
MALT	Mucosa-associated lymphoid tissue
Mb	Megabase pairs
MFI	Mean fluorescence intensity
MIC	Minimum inhibitory concentration
miRNA	MicroRNA
MOI	Multiplicity of infection
N_2	Nitrogen
NA	Numeral aperture
NaCl	S*odium chloride*
NaH_2PO_4	Sodium Dihydrogen Phosphate
NH_3	Ammonia
NN	Nearest-neighbour
O_2	Oxygen

OCT	Optimal cutting temperature compound
O.D.	Optical density
PBS	*Phosphate-buffered* saline
pCLE	Probe-based confocal laser endoscopy
PCR	Polymerase chain reaction
PF	Paraformaldehyde
PI	Propidium iodide
PLGA	*Poly(lactic-co-glycolic acid*
PMNs	*Polymorphonuclear neutrophils*
PNA	Peptide nucleic acid
PO	Phosphate
PPI	Proton-pump inhibitors
PS	Phosphorothioate
RDP-II	Ribosomal Database Project II
RPMI	Roswell Park Memorial Institute medium
RNA	Ribonucleic acid
ROI	Region of interest
RP-HPLC	Reversed phase HPLC
rRNA	Ribossomal RNA
RSM	Response surface methodology
RUT	Rapid urease test
SDS	Dodecil sodium sulfate
SPF	Specific-pathogen-free
SPSS	Statistical Package for the Social Sciences
T_H	Hybridization temperature
T_m	Melting temperature
TRITIC	Tetramethylrhodamine isothiocyanate
Tris-HCl	Tris(hydroxymethyl)aminomethane hydrochloride
TSA	Trypticase soy agar
TSB	Tryptic soy broth
UBT	Urea breath test
UNA	Unlocked nucleic acid
VacA	Vacuolating cytotoxin A
2'OMe	2'-*O*-methly RNA
4-NQO	4-nitroquinoline-oxide

SCIENTIFIC OUTPUT

Papers in peer reviewed journals

Fontenete S., Guimarães N., Wengel J., Azevedo N.F. *Prediction of melting temperatures in fluorescence in situ hybridization (FISH) procedures using thermodynamic models.* Crit Rev Biotechnol. (2015) Jan 14:1-12. (**Chapter I**)

Fontenete S., Carvalho D., Guimarães N., Madureira P., Figueiredo C., Wengel J., Azevedo N.F. *Application of locked nucleic acid-based probes in fluorescence* in situ *hybridization*. (Submitted) **(Chapter II)**

Fontenete S., Carvalho D., Lourenço A., Guimarães N., Madureira P., Figueiredo C., Wengel J., Azevedo N.F. *FISHji: new ImageJ macros for the quantification of fluorescence in epifluorescence* images. (Submitted) (**Chapter III)**

Fontenete S., Barros J., Guimarães N., Madureira P., Figueiredo C., Wengel J., Azevedo N.F *Mismatch discrimination in fluorescent in situ hybridization using different types of nucleic acids.* Appl Microbiol Biotechnol. 2015 May;99(9):3961-9. doi: 10.1007/s00253-015-6389-4. Epub 2015 Jan 21. (**Chapter IV**).

Fontenete S., Guimarães N., Leite M., Figueiredo C., Wengel J., Azevedo N.F. *Hybridization-based detection of Helicobacter pylori at human body temperature using advanced Locked Nucleic Acid (LNA) probes.* PLos One (2013) Nov 22;8(11):e81230. doi: 10.1371/journal.pone.0081230. **(Chapter V).**

Fontenete S., Leite M., Guimarães N., Madureira P., Ferreira RM., Figueiredo C., Wengel J., Azevedo N.F. *Towards Fluorescence In Vivo Hybridization (FIVH) Detection of H.pylori in Gastric Mucosa Using Advanced LNA Probes.* PLos One (2015) 0(4): e0125494. doi:10.1371/journal.pone.0125494 **(Chapter VI)**

Fontenete S., Leite M.,Cappoen D., Santos R., Figueiredo C., Wengel J., Cos P., Azevedo N.F. *Fluorescence in vivo hybridization (FIVH) for detection of Helicobacter pylori infection in a C57BL/6 mouse model.* (Submitted) **(Chapter VII)**

Books Chapters

Fontenete S., Guimarães N., Azevedo N. *Biofilm transcriptomics handbook. Quantifying gene expression from pathogenic bacterial biofilms.* Nuno Cerca (2011) ISBN: 978-972-97810-8-7

Abstracts in international refereed journals

Fontenete S., Guimarães N., Leite M., Figueiredo C., Wengel J., Azevedo N.F. *FISH-based method for in vivo detection of H. pylori in gastric mucosa using advanced LNA probes.* Helicobacter, Special Issue: The Year in Helicobacter 2013. Guest Editors: Francis Mégraud and Peter Malfertheiner, September 2013, Volume 18, Issue Supplement s1, Pages 1–162.

Oral communications

Fontenete S., Leite M., Cappoen D., Guimarães N., Madureira P., Cos P., Figueiredo C., Wengel J., Azevedo N.F. Fluorescence *in vivo* Hybridization (FIVH) detection of *Helicobacter pylori*. Doctoral Congress in Engineering, 11-12 June 2015, Porto, Portugal.

Poster communications

Fontenete S., Carvalho D., Guimarães N., Madureira P., Figueiredo C., Wengel J., Azevedo N.F. *Evaluation of fluorescent Locked Nucleic Acid advanced probes by fluorescent in situ hybridization (FISH): a new analytical approach using FISHji.* 3rd Symposium in Applied Bioimaging, 16-17 October 2014, Porto, Portugal.

Fontenete S., Guimarães N., Leite M., Madureira P., Figueiredo C., Wengel J. and Azevedo N.F. *In Vivo Detection of Helicobacter Pylori in Gastric Mucosa Using Advanced LNA Probes By FISH*. XXI International Roundtable of Nucleosides, Nucleotides and Nucleic Acids, IS3NA, 24-28 August, 2014, Poznan, Poland.

Fontenete S., Guimarães N., Leite M., Madureira P., Figueiredo C., Wengel J., Azevedo N.F. *FISH-based method for in vivo detection of H. pylori in gastric mucosa using advanced LNA probes* XXVIth International Workshop of European Helicobacter study group (EHSG), 12th-14th September 2013, Madrid, Spain.

Fontenete S., Guimarães N., Azevedo N. *Nucleic acid mimics hybridization at human body temperature in Heliobacter pylori*". COST Action TD1004, October 28-30, 2012, London, England.

Chapter I

Background and Aims

Bacterial infectious diseases are one of the most frequent causes of human mortality worldwide and it is considered that the lack of accessibility and application of high quality diagnostic tests for these diseases contributes greatly to this problem [1]. A decrease in the amount of time required to perform a diagnosis would offer potential benefits for the management of infectious diseases. In fact, rapid and accurate diagnosis is fundamental to apply more rational therapies (e.g. antimicrobial therapies) leading to more effective treatments and improving the chances of a positive outcome for the patients. Furthermore, the fast identification of a pathological bacterium lowers the risk of its nosocomial transmission. However, the diagnosis can be a complex process. This section will focus on the detection of *Helicobacter pylori* (*H. pylori*) a well-known risk factor for gastric inflammation, peptic ulcer disease and cancer in humans [2,3].

1.1. Helicobacter pylori

H. pylori is one of the most common infectious agent worldwide, colonizing the human stomach of over 50% of the global population [4]. Marshall and Warren isolated and demonstrated for the first time that this infection was associated with human disease, and for that reason they were awarded the Nobel prize in Physiology and Medicine in 2005 [5,6].

1.1.1. Phylogeny

The human body is infected by diverse microbial communities that can be present in both healthy [7,8] and unhealthy individuals [9,10]. For more than a century, different investigators have reported the presence of spiral microorganisms within the human stomach [11]. However, only about 30 years ago, Robin Warren described the isolation and culture of a spiral-shaped bacterium on the human gastric mucosa. This bacterium was first named *Campylobacter pyloridis* [6] being renamed as *Helicobacter pylori* in 1989 [12].

The genus *Helicobacter* belongs to the subdivision of the *Proteobacteria*, order *Camplylobacter*, family *Helicobacter*. Depending on their localization, *Helicobacter species* can be classified into gastric and enterohepatic (non-gastric) subgroups. *Gastric Helicobacter* species have the gastric mucus secreting cells as target cells, live mainly in the surface of the mucus layer and can adhere to cells close to the intercellular junctions [13]. Enterohepatic *Helicobacter* species colonize the intestine and hepatobiliary system and have been also associated with chronic hepatic and intestinal diseases [14-16].

1.1.2. Microbiology of H. pylori

H. pylori is a gram-negative bacterium generally spiral or slightly curved, measuring 2 to 4 µm in length and 0.5 to 1.0 µm in width. In the spiral form, the bacterium has 2 to 6 unipolar flagella with approximately 2.5 µm in length [17,18]. *H. pylori* can also appear as a rod, while coccoid shapes could appear as a response to physical and chemical stresses such as prolonged *in vitro* culture, antibiotic treatment and increased oxygen tension [19-23]. Some authors observed that this morphological change is a manifestation of the cell death [20,24]. *H. pylori* exhibits strong adaptation to its natural habitat, lacking several of the biosynthetic pathways commonly present in less specialized bacteria [25]. In culture, *H. pylori* is microaerophilic with optimal growth at O_2 levels of 2 to 5%, CO_2 levels of 5 to 10% and high humidity. This bacterium has an optimal growth at 37℃ and at neutral pH [26,27]. It is a fastidious microorganism and requires complex growth media, which are frequently supplemented with blood or serum.

1.1.3. Genome

The first *H. pylori* genome sequenced (strain 26695) consists of a circular chromosome with 1.67 Mb in size, 1590 predicted coding sequences and an average G+C content of 39% [28]. Other *H. pylori* genome sequences available have 1.5 to 1.7 Mb in size [29]. About 6% to 7% of the genes are specific to each strain, with almost half of these genes being clustered into a single hypervariable region [25]. *H. pylori* isolates from unrelated humans exhibit a high level of genetic diversity [30,31]. *H. pylori* has developed to adapt to the harsh environment of the human stomach, and there are several genetic variants in subpopulations of this bacterium [32]. Strain-specific genetic diversity appears to be involved in the capacity of these bacteria to cause different outcomes in different human hosts [33,34]. In this process of adaptation, bacteria accumulated a high degree of genetic heterogeneity caused by genomic rearrangements, gene insertions and deletions [35]. Point mutations and inversions are also very common. Typically, 92% to 99% of the alleles are identical in nucleotide sequences for different *H. pylori* strains [30,36].

1.1.4. Epidemiology of H. pylori infection

H. pylori is estimated to be the most prevalent chronic infection worldwide and affects more than 50% of the population [37,38]. The prevalence of *H. pylori* infection has however been changing over the years [38]. The overall prevalence is lower in developed countries than in underdeveloped regions as a result of better sanitary conditions and treatments procedures [39,40]. In Europe, the prevalence of *H. pylori* is lower in Northern

countries than in Southern and Eastern countries [41]. In Portugal, *H. pylori* infection remains among the highest in Europe [40]. High prevalence of this infection is also observed in Turkey, Mexico and Asian countries [42-47].

Several risk factors for *H. pylori* infection have been investigated. Significant differences in prevalence have been reported relatively to lifestyle habits (e.g. smoking and alcoholism consumption) and socioeconomic status [47,48]. Socioeconomic status includes specific conditions such as levels of hygiene, density of living, sanitation and education [49]. Factors such as gender do not seem associated with an increased risk of infection [44,45,50,51].

Despite of the scientific effort to determine the principal transmission routes of *H. pylori* infection, the way how the infection is transmitted still remains unclear. Person-to-person contact is considered to be the most common route of infection (e.g. within the family), of which the most relevant pathways correspond to the gastro-oral, oral-oral and fecal-oral routes [52-54]. However, zoonotic transmission and food/water could be critical in terms of successful colonization of the human host [49]. The iatrogenic mode of transmission, in which endoscopes that have been in contact with the gastric mucosa of one individual are used for another patient, has been discussed years ago [55]. However, it was shown that adequate disinfection procedures eliminate the transmission risk of this microorganism [56,57].

1.1.5. Pathogenesis of H. pylori infection

1.1.5.1. Clinical outcomes of H. pylori infection

Some authors consider *H. pylori* as part of the normal gastric biota although its role in disease is well recognized [30]. *H. pylori* colonization induces gastric inflammation in infected individuals, but only a small percentage develop more severe clinical outcomes, such as peptic ulcer disease, gastric mucosa-associated lymphoid tissue (MALT) lymphoma and gastric carcinoma [58,59]. Although this infection increases the risk of developing disease, the majority of the infections are asymptomatic [60,61].

H. pylori initially causes a brief acute infection, in the great majority of the cases *H. pylori* subsists for decades establishing a chronic infection [62]. It has been postulated that the difference in outcomes of *H. pylori* infection depends on the topography and patterns of gastritis (Figure 1.1). As such, individuals with chronic antral-predominant gastritis have an increased risk of developing duodenal ulcer, while individuals with corpus-predominant or pangastritis have increased risk of developing gastric ulcer and gastric carcinoma [63].

Epidemiological, clinical and experimental data showed a very close relationship between *H. pylori* and gastric carcinoma development and this bacterium was classified as a group 1 carcinogen by the World Health Organization [64-66]. The ability of *H. pylori* to induce disease depends not only on the bacterium but also on environmental and host factors, such as gene polymorphisms [33,67,68] .

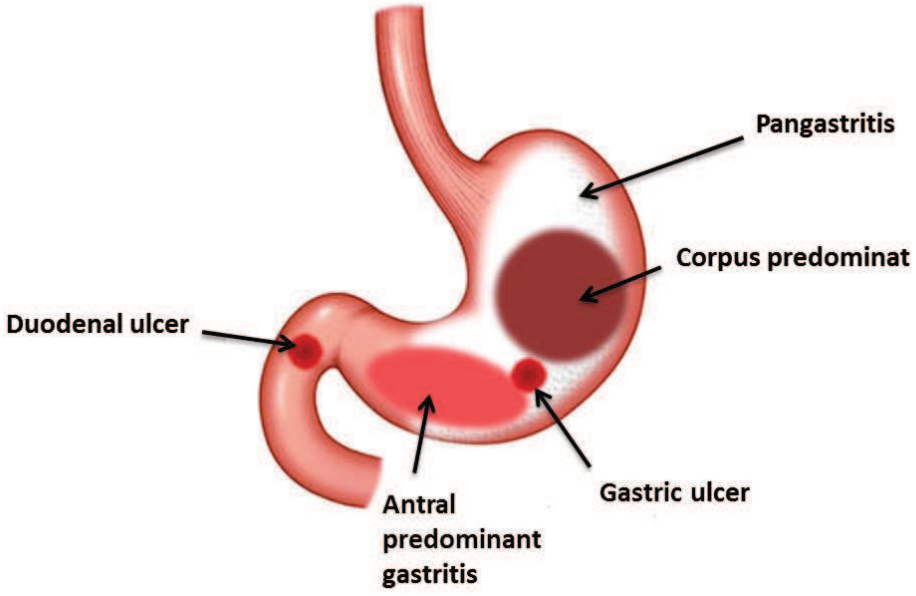

Figure 1.1 - Typical *Helicobacter pylori*-associated pathologies. Adapted from Testerman and Morris [63].

1.1.5.2. H. pylori localization, distribution and orientation in the stomach

Several studies have been performed to determine the localization of *H. pylori* in the human stomach. While some show that the antrum and the cardia have higher intensities of *H. pylori* colonization, other studies demonstrated an equal distribution of the infection in all sites of the stomach [69-72].

The colonization of *H. pylori* has been found not only on the surface mucus cells but also in the mucus layer of the stomach [73]. Intracellular *H. pylori* has also been reported [74-76]. In gerbils, *H. pylori* colonizes a mucus layer located 0-25 μm above the tissue surface [69]. Although the mucus layer is a physical barrier which acts to prevent pathogens from colonizing and interacting with the underlying cells, *H. pylori* can overcome this barrier and interact with the epithelium [77]. *H. pylori* can penetrate the 300 μm thickness of the human mucus through a pH gradient that ranges from 1 (lumen) to 7 (epithelium) [78]. This is only possible because *H. pylori* raises the pH through urea and modifies the mucus, thus enabling the bacterium to move through it [79-81].

H. pylori adheres to gastric epithelial cells with specific tissue tropism [82]. The interaction of *H. pylori* with gastric epithelial cells is mediated by adhesins present in the outer membrane of this bacterium. Adhesion increases bacterial resistance to cleansing mechanisms and provides them nutrients required to initiate colonization [69]. After *H. pylori* binding to the cells, different host cells signaling pathways are activated, which influences inflammation and promotes disease development [83-86].

1.1.5.3. Virulence factors of H. pylori

Studies have been performed to understand the mechanisms involved in the pathogenesis of *H. pylori* related with colonization, inflammation and carcinogenesis (Figure 1.2) [87-91].

To survive in the harsh acid environment of the gastric mucosa and grow in the gastric niche, *H. pylori* has developed different acid acclimation mechanisms [92]. One of these is the adjustment of periplasmic pH acid environment, as the preservation of an intracellular neutral pH is critical to the survival of bacteria in the stomach [93]. *H. pylori* can survive in the stomach at a pH lower than 2.5 due to the production and regulation activity of the urease enzyme and α-carbonic anhydrase (α-CA) [94]. Urease hydrolyses urea to NH_3 and CO_2, raising the pH in the vicinity of *H. pylori* and in the periplasm of the bacterium, maintaining the proton motive force. Urease is present in the bacterial cytoplasm and its activity is controlled by a proton-gated urea channel, UreI [95]. However, some authors hypothesized that UreI and urease expression are necessary but not sufficient for colonization of the human stomach [96,97]. Therefore, the role of α-CA may be crucial in the conversion of CO_2 to HCO_3^- , which acts as a periplasmic buffer maintaining the pH close to 6.1 (gating pH of UreI) [96].

In addition to urease, other virulence factors that also play a fundamental function in *H. pylori* gastric colonization are the adhesins and other outer-membrane proteins (BabA, SabA, and OipA) that allow bacteria to bind to the epithelial cells and may also modulate host cellular pathways involved in the inflammation [98-100]. Additional virulence factors produced by *H. pylori* such as fragments of peptidoglycan can also deregulate host intercellular signalling pathways [99,101].

Undoubtedly, the major pathogenic factors of *H. pylori* are CagA (cytotoxin-associated gene A) and VacA (Vacuolating cytotoxin A). CagA is encoded by the terminal gene of the *cag* pathogenicity island (PAI). The remaining genes of the *cag* PAI encode the type IV secretion system. [102,103]. This system is a protein complex that allows the bacterium to inject CagA into eukaryotic cells [104]. Infection with *H. pylori* strains containing the *cag*

PAI and CagA increases the risk of severe inflammation, peptic ulcer disease and gastric carcinoma comparatively to infection with strains that do not contain the *cag* PAI [35].

H. pylori VacA is a toxin with multiple functions in the host cells. It induces the formation of large intracellular vacuoles in infected mammalian cells [105-107]. This protein is secreted into the extracellular space but also remains localized in the *H. pylori* surface. Although VacA is conserved among all *H. pylori* strains, it has a high level of genetic diversity. A specific allelic combination, the s1m1 type is correlated with the most active vacuolating activity and the bacteria with this feature play a key role in peptic ulcer and cancer pathogenesis [34,108,109]. VacA also reduces the mitochondrial transmembrane potential, releases cytochrome c from the mitochondria, activates caspase 8 and 9 and induces apoptosis [98]. Several studies also suggest that VacA has immunomodulatory proprieties contributing for *H. pylori* persistence [110,111].

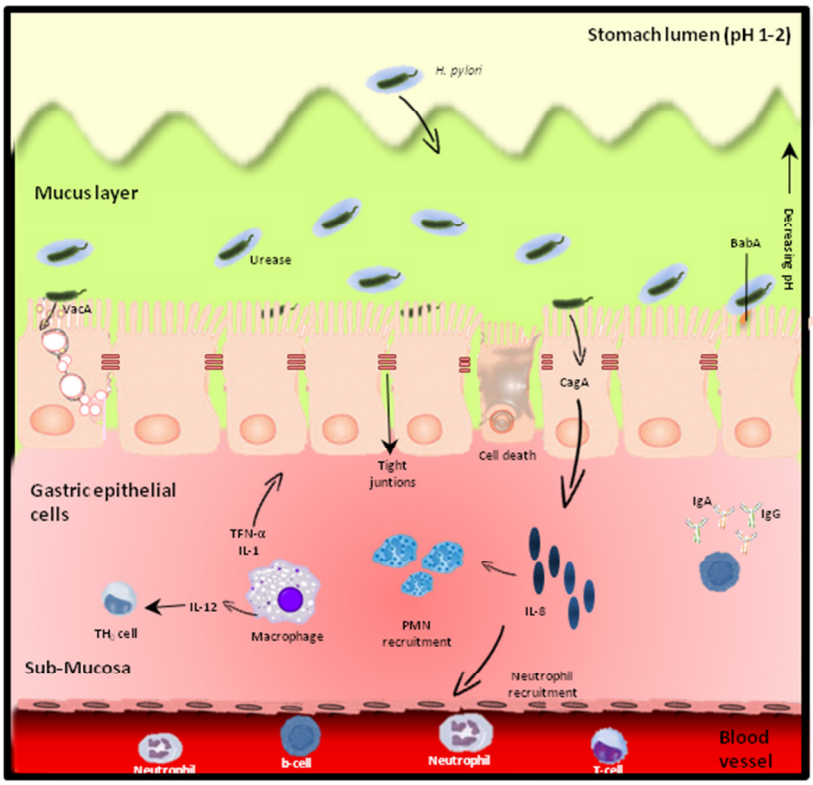

Figure 1.2 - Persistent *H. pylori* infection. The interaction between *H. pylori* and the host response leads to persistent colonization and chronic gastritis. *H. pylori* binds to gastric epithelial cells through adhesins, such as BabA. When CagA is translocated into the cells, production of interleukin (IL)-8 and other chemokines is induced. These chemokines lead to the recruitment polymorphonuclear cells (PMNs), resulting in inflammation. CagA can cause disruption of the epithelial barrier and VacA is secreted into cells and the submucosa inducing vacuolization and apoptosis. The chronic phase of *H. pylori* gastritis is associated to adaptive lymphocyte response with the initial innate response. Cytokines produced by macrophages (IL-12) activate recruited cells as helper T cells (T_H0), recruiting T_H1 and B cells.

1.2. Diagnosis of *Helicobacter pylori* infection

During the last years, several methods have been developed for *H. pylori* detection. These methods can be considered non-invasive or invasive and each of them has certain advantages and disadvantages that will be described in the next sections.

1.2.1. Non-invasive tests

Direct detection of *H. pylori* by endoscopy has proved to be a valuable test, and is hence considered to be the reference method. Nonetheless, several drawbacks promoted the development of non-invasive methods. The major concern is the invasiveness of the procedure that causes discomfort for many patients. Although anesthesia can be used, the risk of this procedure is increased [112]. The most widely used non-invasive methods will be discussed next.

1.2.1.1. Serology

The first non-invasive method to be developed for *H. pylori* detection was serology. Because *H. pylori* induces a specific systemic immune response, antibodies are produced and can be detected in serum samples [113]. The most common serology-based test is the enzyme-linked immunosorbent assay (ELISA) test, which detects the total amount of immunoglobulin (IgG response predominant) in the serum. Latex agglutination and Western blotting are also available and used when it is necessary to know a response from an antibody to a specific antigen. The sensitivity and specificity of these tests depend on the antigen used. However, in general the sensitivity ranges between 90% and 97% and the specificity between 40% and 96% [114-116].

Based on reverse-flow immunochromatography, Schrier *et al.,* developed a highly specific test to detect human IgG antibodies against *H. pylori* in the serum, named FlexSure® HP kit (SmithKline Diagnostics) [117]. This test shows a high negative predictive value and is an easy and fast method suitable to small laboratories with low volume of *H. pylori* testing [118-121]. Other immunoassays have been developed, such as lateral flow systems [122,123].

Serology is a recommended non-invasive test for initial screening (requiring confirmation by histology or/and culture) and for large epidemiological studies [124,125]. The major drawback of serology is that the detection of antibodies does not allow to distinguish between active infection and a previous exposure to *H. pylori* [126].

1.2.1.2. Urea Breath Test (UBT)

The first demonstration of UBT to detect gastric urease activity was performed in 1954 by Kornberg *et al.* on a cat [127]. However, it was only in 1987 and 1988 that it was demonstrated that it was possible to detect *H. pylori* in humans using urea labelled with ^{13}C or ^{14}C [128,129].

In this test, the patient ingests a solution containing [^{13}C]-labeled or [^{14}C]-labeled urea, which in case of infection will be hydrolyzed by *H. pylori* producing labeled CO_2. This compound will be absorbed by the blood and exhaled in expired air [130]. The inclusion of a citric acid solution proved to increase the sensitivity of the method [131]. The acidity of the medium activates the uptake of urea via UreI, making urea accessible to the urease [132,133]. Consequently, the increase of urease activity leads to the increase in labeled CO_2 excretion [132]. The urea dose was standardized at 50 to 75 mg, because the concentration of the gastric urea should exceed the urease rate of urea hydrolysis (K_{max}) (10 mg) [130]. Thus, [^{13}C] urea is diluted in a citric acid solution and administered to the patient. In general, protocols use two breath samples, one collected before and another collected 10-15 minutes after urea ingestion. The cut-off level has to be adapted to different factors, such as the test meal, the dose and type of urea or the pre- and post-treatment setting [134].

Although unavailable on a global scale due to its high cost, UBT is highly accurate and reproducible, having the highest values of sensitivity (88%-95%) and specificity (95%-100%) among the non-invasive tests in adults [135-137]. In pediatric populations the UBT showed heterogeneous accuracy, with values of sensitivity and specificity ranging from 75% to 100% [138].

It is considered safe to perform the UBT many times on a single patient, including pregnant women and children [139,140]. This test is considered the gold standard for determining the success of *H. pylori* eradication treatment [141]. Other studies showed that this method can be unreliable under specific conditions [142,143].

1.2.1.3. Stool tests

H. pylori is excreted through feces as a non-culturable bacterium due to the action of biliary salts [144]. The identification of *H. pylori* in stool specimens can be achieved by molecular methods such as polymerase chain reaction (PCR) or ELISA for detection of *H. pylori* antigens [145,146]. This assay can be used for the initial diagnosis of *H. pylori* infection or for confirmation of eradication after treatment. Stool antigen testing has a sensitivity of 94% and a specificity of 92% [147]. This method is relevant for children, as it

provides a safe diagnosis for a low cost [126,148]. *H. pylori* isolation from stool is not used as a routine diagnostic test [124,149,150]. On the other hand, using breath test and stool antigen test, patients must stop taking proton-pump inhibitors (PPIs) and antibiotics for at least 2 weeks or 4 weeks, respectively, before testing [151,152]

1.2.2. Invasive tests

Invasive tests were the first to be used in *H. pylori* diagnosis. In clinical settings, the stomach is accessed by an endoscope and biopsy specimens are obtained, allowing to assess the degree of pathology in the stomach.

1.2.2.1. Endoscopy

Endoscopic images can contribute to improve the early detection of typical lesions recurrent in gastric cancer. Endoscopy also provides biopsy samples that can be used in different diagnostic tests such as histology, culture, rapid urease test or molecular tests that are mostly based on PCR.

Several imaging techniques for gastric cancer have evolved increasing the precision and allowing the improvement of the diagnosis of pre-neoplasic lesions on a macroscopic level [153]. In recent years, the development of new endoscopic equipments to include narrow band imaging, chromoendoscopy or confocal laser endomicroscopy (CLE) has revolutionized the field [154-156].

CLE allows the observation of living tissue and also the vascular networks in the bronchial and gastrointestinal tract during endoscopy [157,158]. Through this it technique is possible to acquire high-quality images with a magnification of up to 1000-times, which enables the visualization of capillary structures in the mucosal layer. Histological images can be obtained through a miniprobe-based confocal fluorescence microscopy [159]. After the injection of an unspecific dye such as fluorescein or acriflavine it is possible for example to assess microcirculatory alterations in the gastrointestinal mucosal tissue [160-162]. The grey-scale images acquired *in vivo* can be comparable to conventional hematoxylin and eosin (HE) slides. In the case of using fluorescently labeled antibodies as molecular probes, it is possible to obtain similar results to immunohistochemical techniques [163-165]. The main goal of this methodology is not only diagnosing gastric carcinoma *in vivo* through a detailed examination of the mucosal surface and subsurface but also screening for potential therapeutic targets [166]. The innovative introduction of probe-based confocal laser endoscopy (pCLE) allows a spatial resolution in the micro-scale (1 micron) through light in the visible spectral region. pCLE enables the analysis at

histological level but using a flexible miniaturized fiberoptic probe of 1.5 to 2.6 mm outer diameter inserted through the working channel of a standard endoscope. This system has greater versatility relatively to endoscope-based CLE (eCLE) and it has been approved for clinical use in the respiratory [167,168] and gastrointestinal tract [169,170]. Therefore, the presence of particular pathological features and the presence of *H. pylori* could be detected in the future. However, the diagnosis of *H. pylori* in the gastric mucosa by this type of endoscopy has not yet been established with specific staining.

1.2.2.2. Histology

Histology was the first method used for the detection of *H. pylori*. Histological examination also allows the characterization of the inflammation and lesions present in the gastric mucosa. Following the Sydney classification system, gastric biopsy samples should be collected from 5 sites: the lesser curvature of the corpus, the greater curvature of the antrum, the middle portion of the greater curvature of the corpus and the incisura angularis [171]. The analysis of fewer biopsy samples can lead to sampling errors or false negatives. Biopsies are immediately introduced into a fixative of 10 (vol/vol) formaldehyde, which maintains the morphology of the bacteria and with which most stains can be used [130].

There is no specific staining for *H. pylori*. Conventional HE stain is not well suited for *H. pylori* detection. Special histochemical stains such as modified Giemsa and Genta, as well as the silver Warthin-Starry stain can be used. It has been shown that immunohistochemical stains with polyclonal/monoclonal *H. pylori* antibodies has a better sensitivity and specificity than histochemical stains [172]. Guidelines suggest that at least two different stains should be used on biopsy samples [173].

Through the histological analysis it is possible to distinguish morphological differences of *H. pylori* when compared other *Helicobacter* present in the human stomach. *H. heilmanii* sensu lato can be acquired from cats and dogs (zoonotic infection) and cause chronic gastritis [174-176]. These groups of bacteria are longer than *H. pylori,* non-adherent to epithelial cells and normally colonize in aggregates the crypts' lumen [177].

The sensitivity and specificity of histological tests for *H. pylori* detection is dependent on the pathologist's experience and varies from 53% to 90% [178-180]. These values are highly influenced by the site, number and size of the biopsies collected [181]. Prior treatment for infection will affect the sensitivity and specificity of the method [172,182].

1.2.2.3. Culture

H. pylori can be cultured from gastric biopsies. The plates are incubated in a micro-aerobic environment during 5 to 7 days at 37 ºC. The colonies can be identified by Gram stain and biochemical tests such as urease, oxidase and catalase. This diagnostic method has high specificity (about 100%) and sensitivity (90%) when performed under optimal conditions [183]. However, low sensitivity of culture has been reported, generally due to careless conservation of the biopsies or due to the effects of previous *H. pylori* treatment [130]. Biopsy specimens should be transported with refrigeration and processed for culture ideally within 6 h [184,185]. Additionally, culture is a tedious and time consuming procedure [186,187].

Culture has the advantage of allowing antimicrobial susceptibility determinations, such as clarithromycin. There are several commercial assays available [188]. The disc diffusion (Oxoid^{TM}) is one of the most widely used tests; in here, an antibiotic coated disc is placed directly onto the agar plate inoculated with *H. pylori* and the zone of bacterial growth inhibition is determined [189]. However, the E-test for *H. pylori* culture-based antimicrobial susceptibility is the recommended test by the European Committee on Antimicrobial Susceptibility Testing (EUCAST) [190]. Through E-test it is possible to determine the minimum inhibitory concentration (MIC) [191].

When culture is not possible, molecular tests that allow clarithromycin susceptibility determination such as PCR or fluorescence *in situ* hybridization should be performed in gastric biopsies [137].

1.2.2.4. Rapid urease test (RUT)

The rapid urease test is based on the capacity of *H. pylori* urease enzyme to produce ammonia, which will increase the pH. The increased pH can then be detected by the indicator phenol red, allowing the identification of active microorganisms [192]. Therefore, biopsies obtained by endoscopy are placed on a reactive strip or agar gel medium with urea, and if *H. pylori* is present urease breaks the urea down into ammonia and CO_2, with results being visible after 1 hour (up to 24h, depending on the number of bacteria in the biopsy and the type of kit) [173]. The other urease positive bacteria present in the stomach e.g. *Streptococci* and *Staphylococci*, produce lower amounts of urease and thus do not interfere in a short time detection [193]. Several commercial RUT are available with varying formats (e.g. gel-based tests, paper-based tests and liquid-based tests) [194,195]. The first commercial kits introduced into the market were based on agar (the CLO test); recent kits are strip-based tests such as PyloriTek, where biopsy specimens are

sandwiched between a reagent strip with a pH indicator and a pad containing urea [196,197]. The test is fast, accurate, and inexpensive, having 95%-100% of specificity and 85%-95% of sensitivity [195]. The sensitivity is mainly affected by the number of bacteria present in the biopsy (10^4 minimum required for a positive result). False negative results can appear after a pre-treatment with proton pump inhibitors, antibiotics or in case of achlorhydria where the luminal pH is higher [198].

1.2.2.5. Molecular tests

Molecular tests available include PCR which can be used for *H. pylori* detection and characterization of the bacterial genome [199-204]. PCR can be used in samples obtained by invasive or non-invasive methods, as gastric biopsy specimens, gastric juice, saliva or feces [205-209]. This technique can be applied when it is not possible to employ culture methods, because few bacterial cells are present or when the isolation of *H. pylori* failed due to contamination [173]. PCR can be used for testing clarithromycin resistance directly in fresh or in formalin fixed, paraffin-embedded gastric biopsies, through the identification of mutations in the 23S rRNA gene [210,211]. This test is particularly useful to detect primary resistance to clarithromycin in the case of failure of a therapy with an antibiotic [212]. Numerous other assays have been developed to detect mutations leading to resistance, especially to macrolides and fluoroquinolones [213-215]. The study of the potential virulence of this bacterium has also been performed in key genes such as *cagA* and *vacA* [215-217]. The characterization of these genes may have an important role in the identification of patients with high risk of disease development [215,217-219].

Real-time quantitative PCR assays allow quantification of the *H. pylori* present in biopsy specimens and can to be more sensitive than conventional PCR methods [220].

An advantage of PCR based methods is that deoxyribonucleic acid (DNA) does not require very demanding transport or storage conditions [221,222]. One of the disadvantages of PCR as a routine test is that it is expensive compared with culture, histology and the rapid urease test. In addition, it may lead to false-positive results that can be caused, for instance, by DNA fragments of dead bacteria present in the gastric mucosa of patients after treatment [209,223]. Other drawback of PCR is the existence of *Taq* polymerase inhibitors that reduce the sensitivity of the reaction [224]. Moreover, the contamination of samples with exogenous DNA can affect the specificity of this method [225].

FISH has been used to detect clarithromycin resistance with reported values for sensitivity and specificity of 95% and 100%, respectively [226,227]. This diagnostic method will be described in detail in the next topic.

1.3. Treatment of *Helicobacter pylori* infection

The first therapeutics against *H. pylori* were performed in 1984 leading to the suppression or elimination of bacteria, but the reported suppression was transient [228-230]. Optimal treatment for *H. pylori* has not been defined for all patients, because there is not a single antibiotic treatment that can eradicate the infection and the rates of antibiotic resistance vary by region. Consequently, there are many schemes for treating *H. pylori* infection, which generally consist of a combination of various antibiotics (e.g. clarithromycin, amoxicillin, metronidazole, tetracycline, fluoroquinolones, tinidazole) with anti-secretory agents such as PPIs or with bismuth salts [231-233].

The failure of bismuth-based dual therapies led to the development of triple therapies involving the combination of bismuth salt, metronidazole and tetracycline [234]. The addition of anti-secretory agents to bismuth-based antibiotic therapies allowed an increase in the efficiency with 95% eradication success [235,236]. PPIs were introduced in therapeutic strategies in 1989 [237] allowing the clearance of *H. pylori* in the antrum but not in the body mucosa and therefore requiring at least one additional antibiotic [238]. PPIs elevate the gastric pH after activation in the secretory canalicular space of the parietal cell increasing the bioavailability and efficacy of antibiotics [239].

The triple therapy with PPI, clarithromycin and amoxicillin or metronidazole has become universal since 1994 [240,241]. This therapy has become a standard during almost a decade due to its consistently high eradication rates [242,243]. However, in the last years a lower rate of success of the clarithromycin-containing triple therapy has been observed (10-30%). There are several explanations for the failure of the triple therapy; nonetheless, the most important one is the increase of *H. pylori* resistance to clarithromycin [137]. Because of that, it is currently recommended the attribution of specific treatments according to clarithromycin resistance rates of the population to be treated (Table 1.1) [137]. Different combinations of known antibiotics or new tailored treatments have also been suggested [193,244-246]. One of these strategies is the sequential treatment that includes a 5 day period with PPI and amoxicillin, followed by a 5 day period with PPI, clarithromycin and metronidazole [247-249]. It has been also proposed the non-bismuth quadruple therapy, where three antibiotics are taken simultaneously together with a PPI [190,250].

In general, to determine the success of eradication treatment, non-invasive tests should be performed, such as the UBT or a stool test. Testing should be performed at least 4 weeks after the end of the treatment [137].

Table 1.1 - Summary of treatment lines depending on the clarithromycin resistance. Adapted from Megraud *et al.,* [251]

Regions of low clarithromycin resistance	
First-line treatment	Clarithromycin-containing treatments are recommended; Bismuth-containing quadruple therapy is an alternative;
Second-line treatment	Bismuth-containing quadruple therapy or levafloxacin-containing triple therapy;
Third-line treatment	Treatment should be guided by antimicrobial testing.
Regions of high clarithromycin resistance	
First-line treatment	Bismuth-containing quadruple therapy is recommended; Sequential treatment or nonbismuth-containing quadruple therapy are an alternative;
Second-line treatment	Levofloxacin containing triple therapy is recommended;
Third-line treatment	Treatment should be guided by antimicrobial testing.

Several groups have tried to develop a vaccine against *H. pylori* [252,253]. In the past few years, different immunization strategies such as antigens and adjuvants have been tested in animal models [254]. Earlier studies started in 1992 in a mouse model infected with *H. felis*. In this first study, oral vaccination was developed with bacterial antigens and mucosal adjuvants, demonstrating a protective immune response again *H. felis* [255]. In recent years a new vaccine approach comprised new antigens, new antigen combinations or new adjuvants [256]. Promising antigens were urease, katalase, CagA, VacA, HpaA, AlpaA, BabA and NapA. These antigens can be used with adjuvants (e.g. cholera toxin (CT), CpG-oligonculeotide, heat-labile enterotoxin (LT)) [257-259]. Different routes were used such as oral, intranasal, rectal, intraperitoneal, intramuscular and subcutaneous. Phase I clinical trials performed in humans revealed antigen-specific humoral and cellular responses, however it did not show satisfactory protection against a challenge infection [260,261]. Although the *H. pylori*-specific vaccination research have discovered useful antigens, adjuvants and delivery routes, all the studies undertaken to develop a successful vaccine for humans have failed until now.

1.4. Fluorescence *in situ* hybridization

Since it was first developed, fluorescence *in situ* hybridization (FISH) has become one of the most frequently used molecular techniques in the microbiology field [262]. FISH is a powerful molecular method with widespread use in environmental and in medical applications for the identification, visualization, and quantification of organisms of interest in microbial communities [262-267]. Different FISH assays have been recently developed for the direct identification of a wide range of gram-positive and gram-negative bacteria in clinical samples [268,269]. This methodology has also been used to detect the resistance status of *H. pylori* to antibiotic therapies (e.g. creaFAST® *H. pylori* Combi-Kit, Probe4pylori®, Oxoid Ltd) [270,271].

FISH is based on the annealing of fluorescently-labeled oligonucleotides (commonly called probes) to a specific complementary target sequence, enabling its detection and quantification. When FISH is used as an identification method in bacteria, the target sequences are mainly selected within the 16S rRNA or 23S rRNA since these regions can be used as phylogenetic markers. When the sample is exposed to light of specific wavelengths, fluorescence can be detected by epifluorescence microscopy or fluorescence-activated flow cytometry [272]. Therefore, this method can be used to detect, quantify and characterize (in combination with other techniques) a specific group of bacteria present in clinical samples [273]. One of the most important advantages of FISH is the fact of being a cultivation-independent method, allowing the analysis of microbial communities composition and their dynamics, directly on the sample [265].

The design of adequate probes is a crucial step, and a previous and accurate analysis through available databases is required to achieve good levels of specificity and sensitivity [274-276]. The probes are synthesized and usually coupled to the 5'of the oligonucleotide with a fluorescent label dye (e.g. cyanine (Cy): Cy3, Cy5, Fluorescein amidite (FAM), Alexa fluor® dyes) [277,278]. FISH protocols in bacteria are usually composed by three steps: fixation/permeabilization, hybridization and washing (Figure 1.3). Fixation and permeabilization are typically joined in one operation with the objective to render the cell wall permeable to the nucleic acid probe while, at the same time, guaranteeing that cell lysis and extensive nucleic acid degradation will not occur. During hybridization, the probe is placed in contact with the target cells, and if complementary (or near-complementary) sequences are present, hybridization will take place. The specificity of this binding event, i.e. the ability of the method to discriminate the target organisms from the remaining cells, is further ensured by a washing step where all loosely-bound probes are washed away.

Specificity can be theoretically predicted using 16S rRNA comparative sequence analysis, as probes are designed to confer a required level of taxonomic specificity (e.g. species, genus, class), and then implemented in the laboratory by optimizing the hybridization and washing conditions [279]. Finally, visualization by either fluorescence microscopy or flow cytometry allows the researcher to observe if successful hybridization has occurred.

The reaction stringency can be adjusted by parameters such as temperature, salt buffers or denaturants components. However, it is necessary to consider some important details in the optimization of this technique. Therefore, a successful hybridization is dependent on several factors such as the conditions at which the hybridization step is carried out and the ribosomal content of cells [280]. The effect of ribosomal proteins, the affinity of the probe, technical factors like the type of fluorophore used, and the microscope's optical quality are also very important [266,280-282]. Due to the large number of factors involved, the development of new FISH procedures remains highly empirical and time-consuming. One of the ways to decrease the effort associated with method development is to be able to predict under which conditions a new probe will work. For instance, if a suitable mathematical model is available that allows the researcher to predict the temperature at which the hybridization step should be carried out, the need for trial-and-error experiments where several temperatures are tested can be minimized.

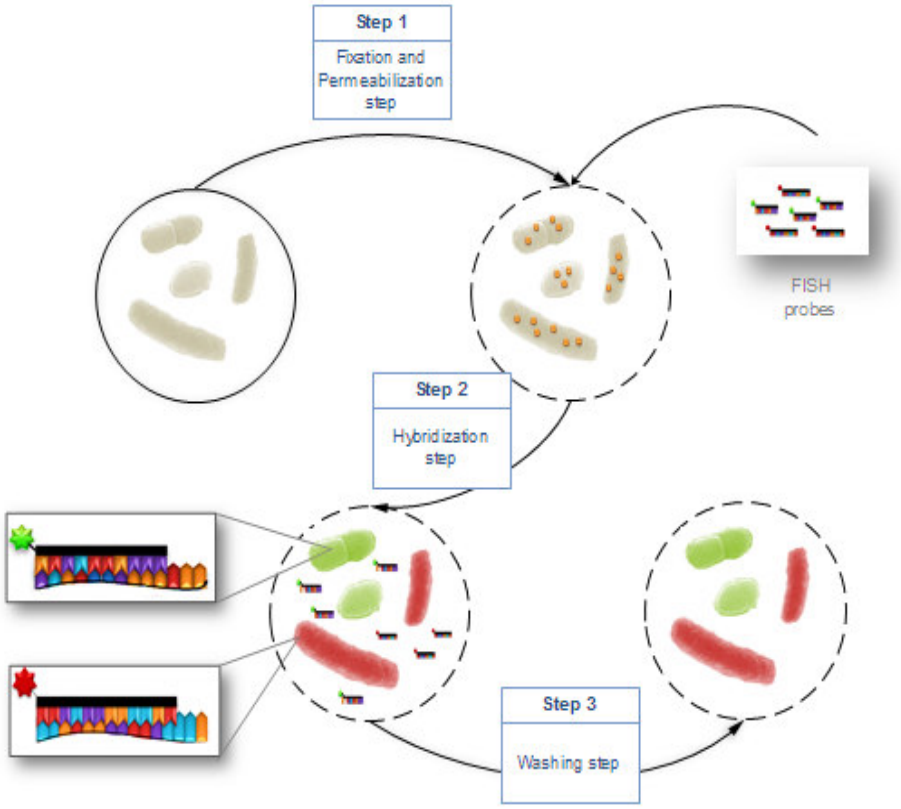

Figure 1.3 - Basic steps of fluorescence *in situ* hybridization in bacteria.

1.4.1. Factors that influence fluorescence in situ hybridization

Low fluorescence ratio in hybridized cells may be related with different factors, such as low ribosomal content of cells, difficulty in permeating cells walls and crowding interactions [266]. These drawbacks can be circumvented by optimizations in the experimental protocol adjusting the most important factors involved in FISH performance. Some of these factors are mentioned below.

1.4.1.1. Effect of fixative

Chemical cell fixation is part of the FISH protocol that serves to increase the permeability of the cell membranes allowing the entry of the probe into the cells and to stabilize cell integrity (preventing nucleic acid from degradation) [265]. Fixatives can be divided in two classes: cross-linked agents such as aldehydes (e.g. paraformaldehyde, glutaraldehyde) and precipitant agents such as ethanol. Cross-linking agents act by adding covalent reactive groups which may induce cross-links between proteins, nucleic acids and between nucleic acids and proteins [283,284]. This method preserves the natural structure of proteins such as their secondary/tertiary structures [285]. Precipitant agents remove free water and hence precipitate proteins and inactivate enzymes. The denaturation of the proteins occurs by the breaking down of the hydrophobic bonds (responsible by the tertiary structures) [286].

Paraformaldehyde is the most common fixative agent in FISH in microorganisms. Though, rRNA FISH using unfixed samples has been reported [287-289]. Alcohol enables molecular dehydration acting on the hydroxymethyl adducts [290]. Additionally, ethanol proved to be more effective for fixation of members of the *Firmicutes and Actinobacteria* [291].

Consequently, it is necessary to take into account the different efficiencies of fixative agents in the permeabilization of the bacterial cell wall to improve significantly the detection rates with bacterium-specific probes [292].

1.4.1.2. Effect of denaturant and sodium concentration

The denaturing agent (e.g. formamide (FA), urea or dodecil sodium sulfate (SDS)) and sodium ions are two of the most important ingredients used in FISH reactions with DNA probes, and are also two of the most likely to impact hybridization temperature (TH). These two chemicals are used to adjust the stringency conditions of the hybridization [293].

FA acts by allowing a more exposed surface in the molecule, leading in turn to a thermodynamically more favourable reaction [294]. Earlier studies suggested that this effect of FA was due to its ion-solvating power [295,296] and the ability to increase the solubility of free bases [295]. In fact, by increasing the hydrophobic character of the solvent, the activity coefficients and free energies of the bases were decreased, favoring the denatured state [297,298]. Initially, it was demonstrated that the T_m of DNA duplexes decrease linearly by approximately 0.65 °C per volume fraction of FA [299-302]. Though, these earlier studies considered the effects of FA independently of DNA base content. In theory, the concentration of a denaturant that is used in a FISH process should depend of the oligonucleotide sequence and the hybridization sequence, therefore the optimization of denaturant concentration is crucial for an efficient hybridization. Urea has also been used as a denaturant in FISH protocols in order to reduce the toxicity from FA [303].

Sodium ions interact with nucleic acid duplexes stabilizing the electrostatic repulsions between the duplex strands [304]. Consequently, low salt concentrations affect the formation of the hybrid (in negatively-charged oligonucleotides) and causes reannealing of the duplex. Subsequently, depending of the probe charge, adjustments on the sodium concentration in each FISH experiment may be necessary.

1.4.1.3. Type of fluorochrome

The use of different fluorochromes can influence the yield of the hybridization [305]. Fluorescein and rodhamine-derivates (e.g. fluorescein isothiocyanate (FITC), Rhodamine, and tetramethylrhodamine isothiocyanate (TRITIC)) are commonly-used dyes in microbiology. Nevertheless, due to limitations such as bleaching limits, they have been replaced by Cy series (e.g. Cy2, Cy3, Cy5) or Alexa fluor dyes. Fluorochromes with high quantum yields and extension coefficient, such as Cy have been preferred to overcome some problems related with low fluorescence intensity and sensitivity to pH. These types of fluorochromes have significant higher staining and are more resistant to photobleaching [306]. However, this type of fluorochromes has the tendency to increase the background signal. This drawback can be easily overcome by improving the hybridization efficiency and adjusting the stringency of the reaction [305]. The choice of the correct fluorochromes is especially important in multiplex studies, where several types of probes and consequently spectrally distinct fluorochromes have to be selected.

1.5. Nucleic acid analogues

Limitations on the use of DNA and RNA oligonucleotides have been reported including their toxicity, sensitivity to nucleases and low specificity for target nucleic acids [307,308]. Therefore, the last decade has observed an increased interest in the chemistry and biology of nucleic acid analogues by the scientific community.

Nucleic acids analogues have the remarkable ability of sequence-specific hybridization through Watson-Crick base pairing. The geometry of Watson-Crick base pairs is mediated by hydrogen bonds, which are responsible for the association of complementary bases, a process that is crucial for the storage of genetic information [309]. Additionally, it is possible to conjugate these analogues with other molecules such as fluorescent dyes, amino acids or nanoparticles [310-312].

Due to these characteristics, many unnatural nucleosides have been developed for diverse purposes, such as enhancement of the affinity and selectivity towards RNA sequences [313], control of gene expression [314] and as therapeutic agents [315]. Consequently, in general a new nucleic acid analogue is designed, synthesized and evaluated with a view to improve the efficiency of the native DNA or RNA through the changing of their bio-physical properties [316,317]. Several unnatural nucleotides have been established through the modification or the replacement of the nucleic acid base (e.g. *C*5-modified uridine nucleosides), phosphate backbones (phosphorothioates) or the sugar-phosphate backbone. Examples of nucleic acid analogues with modifications in the sugar-phosphate backbone include the 2'-*O*-methyl RNA (2'OMe), the locked nucleic acid (LNA), the peptide nucleic acid (PNA) and more recently the unlocked nucleic acid (UNA) (Figure 1.4) [318-323].

Although traditionally FISH employs DNA probes [324-326], this type of probes can present some shortcomings. For instance, it has been shown that for DNA sequences the capacity of mismatch discrimination is often difficult to achieve [307]. Low resistance to exo- and endonucleases resulting in low stability in *in vivo* and *in vitro* applications, are examples of DNA-FISH protocols limitations. More recently, the research based on nucleic acid mimics promoted important improvements in this methodology [321,327,328]. In general, nucleic acid mimics showed better mismatch discrimination, higher resistance to nucleases and higher chemical stability than standard DNA probes [329-331].

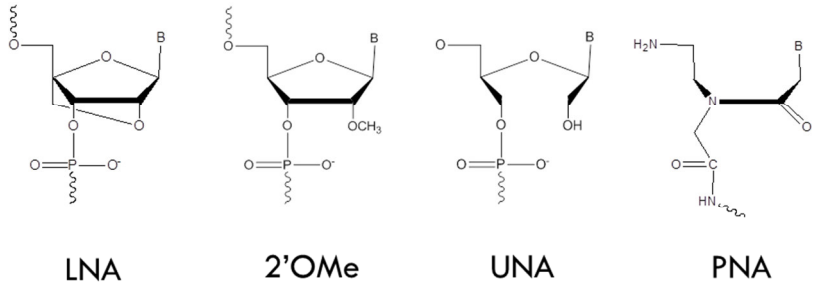

Figure 1.4 - Structures of the monomers of selected nucleic acid analogues.

1.5.1. LNA

LNAs are modified unnatural RNA nucleotides that have recently began to be used in FISH [307,332,333]. The pentose ring of LNA nucleotides is conformationally locked in a C3'-endo/N-type sugar conformation by an O2' to C4' methylene linkage [328,334]. The use of LNA residues mixed with DNA, RNA and 2'OMe allows the stabilization of the duplex during the hybridization and allows a more sensitive detection [307,335,336]. Additionally, this stability is evident in biological media where the presence of only three LNAs at the 5' and 3' ends is enough to increase the half-life of the oligonucleotide [337]. LNA oligonucleotides show low toxicity in biological systems and efficient transfection into mammalian cells [338]. Due to these atypical properties of LNAs, they have been used as an antisense molecule both *in vitro* and *in vivo*, exhibiting very high affinity and specificity towards complementary DNA and RNA [333,339,340]. LNA has successfully been applied as specific probes in miRNA northern blot analysis [341,342], as capture probes in microarrays [343] and as probes for *in situ* detection [344,345]. Moreover, these molecules are potential drug candidates to be used in oligonucleotides based therapeutics for example to inhibit gene expression [346-350].

LNA has important advantages, namely the possibility of being synthesized using conventional phosphoramidite chemistry which allows automated synthesis of chimeric oligonucleotides such as LNA/DNA or LNA/RNA and good aqueous solubility [351]. Furthermore, LNA probes offer high design flexibility comparatively to the PNA probes. The introduction of LNA into an oligonucleotide raises the melting temperature (T_m) of the hybrid, depending on the length and the position in the oligonucleotide. It has been shown that the number of LNA substitutions needs to be optimized to allow a higher hybridization efficiency and specificity [307,352]. It has also been observed that single LNA modifications in the inner positions of a DNA or RNA oligonucleotide has equal effect on the stability, in spite of the chemical nature of the LNA nucleotides used [339,353].

The helical preorganization of single stranded oligonucleotides was suggested to be the reason for this LNA nucleotide stabilization [335]. Similarly, LNA/DNA probes in which LNA and DNA nucleotides alternate have shown strong increase of affinity [307]. However, the thermodynamic origin of LNA's enhanced base pairing stability has not been clearly delineated, although it has been suggested that the decreased entropy of duplex formation and the improved stacking in the duplex both play a part. Additionally, enthalpy has been reported to be improved [354].

LNA is now in itself a molecule that serves as the basis for many other nucleic acid modifications, such as 2'- amino- LNA nucleotides and "doubled-headed" LNA [355].

1.5.2. 2'OMe

2'OMe RNA is a natural sugar modification that can be found in most of the organisms. The 2'OMe chemistry offers several advantages for biotechnological applications as this molecule is nuclease resistant and has a great affinity for RNA targets [356]. More specifically, the oligoribonucleotides containing the 2'OMe have been studied as diagnostic probes. Some studies showed that the 2'OMe oligoribonucleotides probes have higher target affinity than 2'-deoxy-oligoribonucleotides probes [356]. In addition, 2'OMe RNA probes can be designed to target living cells because they do not affect cell viability [357]. One of the most interesting features of these oligoribonucleotides probes is the fact that there is a high discrimination between matched and mismatched RNA targets, when short probes are used. Therefore, these probes have revealed fast hybridization kinetics, increased T_m and ability to bind to targets [358]. More recently, it was demonstrated that LNA/2'OMe probes have better results in the detection of miRNA than LNA/DNA probes [359]. This was also proven by thermodynamic studies, using naked probes, indicating that these probes have a greater binding affinity than the LNA/DNA probes [335].

Many studies have shown the huge potential *in vivo* therapeutic application of this nucleic acid analogue [360,361]. The uptake of these oligonucleotides has been improved by the coupling of nanoparticles as cell penetrating peptides (CPP) [360], copolymers [362], nanoplexes [363] chitosan coated *Poly(lactic-co-glycolic acid* (PLGA) nanoparticles [364] or dendrimers [365]. Still, the use of these probes *in vivo* as a diagnostic tool has not been investigated.

1.5.3. UNA

An UNA, 2'-3'-seco-RNA is an acyclic RNA mimic monomer with a highly flexible structure due to the open ribose ring, which is cleaved between the 2'- and 3'- carbons [366].

Pasternak and Wengel performed a detailed thermodynamic study providing useful features for an approximate prediction of the thermodynamic stability of UNA [367]. Because the UNA is an acyclic nucleoside, it leads to a decrease in duplex stability. A destabilization due to the incorporation of a UNA monomer depends on either where this mimic is positioned and the length of the duplex [368]. In fact, UNA nucleotide residues cause destabilization of RNA duplexes by 4.0-6.6 kcal/mol (internal positions) or 0.5-1.5 kcal/mol (terminal positions). The destabilizing properties of UNA nucleotides are slightly dependent on the nature of the flanking bases. Many other features must also be taken into account to predict the thermodynamic stability of UNA-modified RNA duplexes. A single UNA monomer in the centre of a DNA/DNA duplex and a RNA/RNA duplex leads to a decrease of T_m of 7-10 °C [368] and 5-10 °C [367,369], respectively. The UNA monomers can also increase or decrease the specificity of oligonucleotide binding. For example, the incorporation of a UNA on the opposite site of a mismatch causes a decrease in the ability of the oligonucleotide to distinguish between matched and mismatched duplexes [369,370]. However, depending on the incorporation conditions (exact positioning) of UNA monomers, there might be a significant specificity increase [366,369]. These characteristics, along with the fact that UNA has demonstrated compatibility with RNase H activity, allows the use of this mimic in the gene silencing context [367,371,372]. Other derivatives of UNA monomers are currently being developed. One example is the pyrene-derivatized UNA monomer, in which the distal amine piperazino moiety is conjugated through amine bond formation. These monomers have the advantage (compared to unmodified UNA) of improved mismatch discrimination. Thus, this feature can be very important in the use of these mimics as antisense molecules and in the detection and analysis of genes [373].

1.5.4. PNA

PNA is an uncharged synthetic DNA analogue, where the sugar phosphate backbone is replaced by *N*-(2-aminoethyl) glycine units [321,374-376]. PNA monomers were described for the first time by Nielsen *et al*. [374]. These monomers bind with complementary DNA and RNA sequences to form a Watson-Crick double helices. Moreover, these molecules can generate triple helix structures and perform strand invasion. PNA forms various hybrid complexes such as PNA:PNA, PNA:DNA and PNA:RNA duplexes, and PNA:PNA:PNA and PNA:DNA:PNA triplexes [377]. Due to its thermodynamic characteristics, PNA presents several advantages for FISH experiments. For instance, PNA:target duplexes are more stable under physiological salt conditions (being resistant to nuclease and

protease degradation) and have more favourable hybridization properties than the corresponding unmodified DNA or RNA duplexes [321,378,379]. PNA probes can be shorter than other nucleic acid probes because their enhanced binding properties [380]. Due to its neutral charge, PNA has very high affinity for DNA/RNA owing to the lack of charge repulsion of the peptide-like backbone [321,381,382]. Another important hallmark of the properties of a PNA is its stability and versatility [383]. Their extreme stability in acid environment (where DNA would undergo depurination) represents yet another advantage [384].

The higher specificity and sensitivity of PNA have been exploited in order to develop several diagnostic applications [271,385,386]. PNAs duplex formation is greatly destabilized by a single-base mismatch, enabling the use of these nucleic acid mimics in diagnostic protocols for point mutation identification [387]. Due to this highly sensitive hybridization, PNA nucleic acid probes have been employed in the identification of nucleic acid of disease-associated bacteria, fungi, virus or other pathogens [388-391]. More specifically, PNA probes have been demonstrated to be useful for rRNA detection in ISH and FISH assays [388,392,393]. Moreover, PNA probes hybridize independently of the salt concentration, therefore, conditions where the stability of the secondary structures of the target rRNA are decreased can be selected. This allows PNA probes to hybridize to less accessible target sites [394] PNA has also been used in PCR molecular diagnosis protocols. The capacity of some PNAs to bind dsDNA has also promoted their use in antisense technology [395]. However, these nucleic acid mimics have low efficiency in cell entry, probability due to the non-ionic structure of PNA [396,397]. New chemical modifications have been developed to enhance these biophysical properties, while maintaining the highly desirable hybridization properties [396]. Examples include the change of the backbone to add negative or positive charges [398] or the attachment of a cationic amino acid to improve the aqueous solubility [399].

Until now, PNA is the only mimic with Food and Drug Administration (FDA) certified methods based on PNA-FISH for clinical bacteriology, commercializing by AdvanDx. Several PNA FISH® tests for rapid identification of different bacteria (*S. aureus*, *E. faecalis*, *E. coli*, *P. aeruginosa* and *K. pneumoniae*) have been developed [393,400,401]. More recently, the same company launched new products, such as QuickFISH®, that takes only 20 min to be performed [402,403]. These probes have been shown to possess higher sensitivity and specificity (e.g. sensitivity, 99.1%; specificity, 99.6% in methicillin-resistant *S. aureus* organisms) [403-405] and all have gained FDA clearance.

1.5.5. Phosphorothioate oligonucleotides

Phosphorothioate oligonucleotides contain non-bridging sulfur backbones, which means that oxygen is replaced by sulfur in the backbone (PS) of analogues or derivatives [406]. Interestingly, these substitutions do not disrupt hydrogen bonding between the nucleobases. PS was initially introduced by Fritz Eckstein in the 1970's mainly with the synthesis of adenosine 5'-phosphorothioate which had an unexpected resistance to phosphatases [406]. The development of phosphoramidite technology allowed the expansion of PS-oligos syntheses for therapeutic applications in a large scale [407]. PS modification blocks or reduces the ability of several nucleases to degradation. This modification can be placed uniformly in a sequence or can be strategically inserted in a critical position leaving some unmodified linkages. PS modification lowers T_m by approximately 0.25 °C (in 2'OMe oligonucleotide duplexes with an RNA target) per modified linkage and consequently reduces binding affinity [408].
PS backbones are present in a large number of oligonucleotides in clinical trials. Additionally, the two oligonucleotides (Vitravene and Mipomersen) approved by the FDA as drugs are fully phosphorothioated [409-412].

1.5.6. Synthesis and properties of nucleic acid analogues

1.5.6.1. The phosphoramidite method

The use of the phosphoramidite method by the application of solid-phase technology and automation was developed by Marvin Caruthers in the 1980s and it is now established as a standard method [413]. Since then, the method of chemical synthesis of oligonucleotides has been the phosphoramidite four-steps of coupling, capping, oxidation/thiolation and detritylation repeated until all the bases have been incorporated in the 3' to 5' direction (Figure 1.5). The first step is detritylation of the support-bound 3'-nucleoside where the 5'DMT protecting group (4,4'-dimethoxytrityl) is removed from the first pre-attached nucleoside to the resin (detritylation). Although standard solid-phase supports have the first base pre-attached to the resin, for some nucleic acid analogues these columns are not readily available and it is necessary to use universal supports. These supports do not have a base attached and therefore, the first base is added in the first coupling step. This involves activation and coupling of the nucleoside phosphoramidite. For that, nucleosides are mixed with tetrazole (or a derivative) and dissolved in acetronitrile, allowing the formation of a new phosphorus-oxygen bond and creating a support-bond phosphite triester. The second step is the capping that allows blocking the unreacted 5'-hydroxyl groups. A mixture composed by acetic anhydride and

N-methylimidazole acetylates alcohols the 5'-hydroxyls groups inert to subsequent and make reactions. This step is crucial to avoid deletion mutation of the desired oligonucleotide. The phosphite-triester (P(III)) formed during the coupling step must be converted to a stable (P(v)) species. The newly-formed phosphite triester internucleotide bond is then converted to the corresponding phosphorothioate or phosphodiester with a thiolating or oxidation reagent, respectively (step 3). The fourth step of the phosphoramidite oligo synthesis is the detritylation, which involves the removal of the DMT protecting group at the 5'-end of the resin-bound DNA chain, allowing that the primary hydroxyl group can react with the next nucleotide phosphoramidite. In the end of the oligonucleotide synthesis, cleavage from the support can be carried out automatically or manually by an ammoniacal solution. The oligonucleotide deprotection is based on the exposure of the oligonucleotide in concentrated aqueous ammonia and then this solution is heated to remove the protecting groups from the heterocyclic bases and phosphates. After evaporation the oligonucleotide can be purified [414]. Contrarily, the cleavage of an oligonucleotide from universal supports involves two steps, ester hydrolysis followed by dephosphorylation (breaking of a P-O bound).

One of the principal advantages of solid-phase is the easy methodologies (filtration and washing steps) that can be used to separate the immobilized product from other reagents and by-products. This method also allows the synthesis of small quantities of material (0.2 to 1 µmol scale), which is crucial because of the high cost of the reagents. This technique also has some drawbacks. An example is the high coupling yield needed in every chain extension step. Although using this methodology, the coupling efficiencies are typically very high (98-99%), incomplete capping of coupling failures may occur, resulting in deletion sequences (being the major impurities in solid-phase oligonucleotide synthesis). Other impurities can result from incomplete detritylation or incomplete oxidation/thiolation, which makes the purification process crucial for some applications (e.g. cells or bacteria) [415,416].

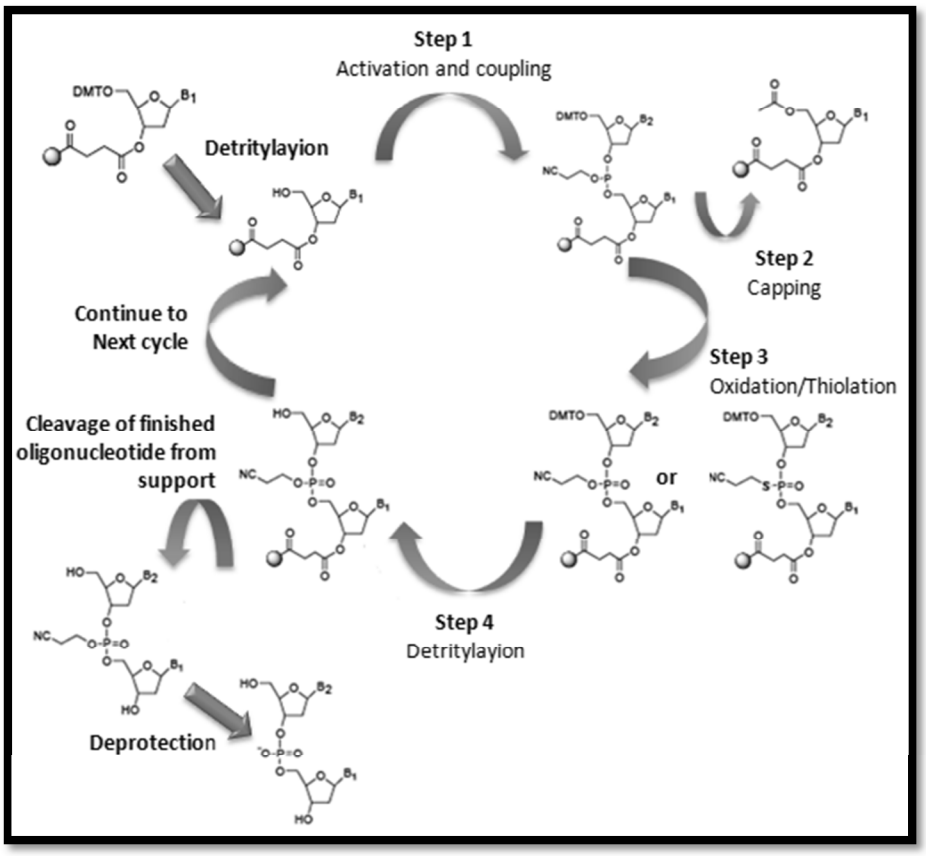

Figure 1.5 - The phosphoramidite oligonucleotide synthesis cycle. The 5' hydroxyl group from the first nucleoside attached to the solid is removed (detritylation). The next nucleoside is coupled in the presence of an activator (step 1). Any unreacted 5' hydroxyl is capped (step 2), and the phosphite triester is oxidized or thiolated to provide a phosphotriester or phosphorothioate linkage, respectively (step 3). To allow the incorporation of the next nucleotide, detritylation occurs through the removal of the DMT protecting group at the 5'-end of the resin-bound DNA chain (step 4). This cycle continues until the oligonucleotide sequence is completed. In the end of the oligo synthesis, the oligonucleotide is cleaved from the support and deprotected. Adapted from Brown T *et al*., [414].

1.5.6.2. Solid-phase PNA synthesis

The process of PNA synthesis is very similar to the solid-phase peptide synthesis. In chemical terms, the carboxylic acid must be activated, being converted to *O*-acylisourea (by reaction with a carbodiimide), which is spontaneously converted to a reactive 1-hydroxybenzotriazole ester. The following step in PNA synthesis is an amide bond coupling reaction between two amino acids where the carboxylic acid is firstly activated (benzotriazole uranium salt) and the following reactions end with the formation of a hydroxybenzotrazole ester. In the final step, the protecting groups are removed and the cycle of each PNA synthesis ends [417].

1.6. Melting temperature prediction of oligonucleotide probes

When FISH first appeared, most studies were performed at the same temperature (46 °C) during the hybridization step [418-420]. This temperature was maintained constant by testing different probe designs and altering the concentration of denaturing agents, in the hybridization solution. The arrival of multiplex methods (the use of more than one probe in the same experiment to detect multiple microorganisms), together with a better understanding of the hybridization mechanisms, changed this approach. Because in a multiplex experiment probes have to operate at the same temperature and concentrations of denaturing agents, the current approach is to predict the temperature at which the probes will work based on the sequence of the probe and taking into account the compounds of the hybridization solution used in the experiment [307]. Still to date, there are no mathematical models that can accurately predict the optimal T_m, for a given oligonucleotide probe. As such, the more easily calculated T_m of an oligonucleotide is calculated instead [421]. T_m can be defined as the temperature at which half of the nucleic-acid strands are forming a duplex and the other half are single stranded, i.e. the temperature at which the dissociation factor is 0.5 [422]. Typically, T_m is used as an indication for the T_H, but the relationship between these temperatures has not been clearly defined in the literature. It appears sensible to state, however, for hybridization to occur as efficiently as possible, it would be desirable that all sites have bound probes. It hence follows that T_m overestimates T_H by a value that is related to the slope of the melting curve and to the dissociation fraction that is considered acceptable for the FISH procedure (Figure 1.6). For strands that are not completely complementary, i.e. that contain one or more mismatches to the target sequence, it is usually desirable that the dissociation factor is close to 1 at the T_H.

Examining Figure 1.6, it would be reasonable to consider that the hybridization would be successful if it was performed at a temperature equal or lower than the T_H. However, in the initial state of the dissociation fraction curves, the nucleic acids are already in the duplex configuration, and as such do not require energy so called activation energy (Ea) to form a duplex. FISH, on the other hand, starts with two single stranded strands that will require Ea to hybridize [294]. This implies that low temperatures will make the hybridization process very slow, and consequently there is a narrow range of TH at which FISH will provide satisfactory results. The narrow range allows researchers to increase the temperature to minimize non-target hybridization, if specificity is an issue, whereas the opposite may be true if sensitivity is the biggest issue.

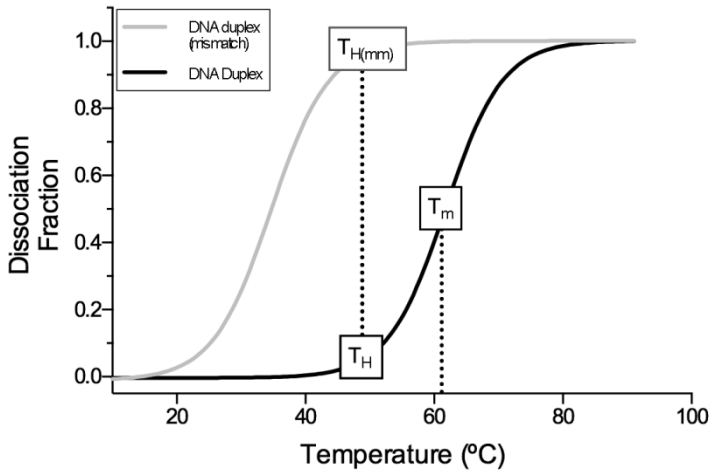

Figure 1.6 - Melting temperature (T_m) and dissociation fraction curves are showed for completely complementary strands (DNA duplex) and for strands with one mismatch (DNA duplex mismatch). The T_H is presented as the hybridization temperature for DNA duplex and T_H (mm) represents the hybridization temperature for the DNA duplex containing one mismatch (DNA duplex (mismatch)). The values used to design the curves are hypothetical.

T_m is intrinsically related with other thermodynamic properties such as the Gibbs Free Energy (G). This energy is a thermodynamic quantity which can be used as an indicator of whether a reaction is thermodynamically favourable or not. When ΔG is negative ($\Delta G<0$) the reaction will be favourable or spontaneous, and the more negative the value the more favourable is the reaction. An estimation of these parameters (and also their correlation) can now be obtained by the nearest-neighbour model (NN), which relies on the assumption that the stability of a base pair depends on the identity and orientation of the adjacent base pair (neighbour base pair) [423,424]. While very useful, the NN model was developed to deal with the thermodynamics of nucleic acid hybridization in general, and does not take into account all parameters and chemical compounds involved in the hybridization step of a FISH procedure. After, other models for prediction of the T_m value were developed. These first thermodynamic models were based on thermodynamic parameters calculated for DNA or RNA oligonucleotides, but with the appearance of the new DNA or RNA mimics it has become necessary to adjust these models or to develop novel models. The most used models to calculate thermodynamic parameters for DNA/RNA mimics oligonucleotides have been derived from the ones used for DNA oligonucleotides and provide important information about the conditions at which the FISH procedure should be performed, helping to decrease the time involved in method optimization [335,382,425]. However, the results often lack accuracy because these all

models are not specific for FISH since they were designed for other molecular biology techniques, such as PCR. Additionally, they do not take into account all parameters and chemical compounds (e.g. for salt and denaturant constituents) involved in the hybridization step of a FISH procedure. Furthermore, these methods only allow us to predict the T_m which is used as a reference for the hybridization temperature as illustrated above when the T_m values predicted by the models were compared with the T_H's used in the experiments. In short, the thermodynamic models already developed for DNA, RNA and DNA/RNA mimics only allow researchers to obtain an indication of the range of the hybridization temperature. If possible, one should always confirm the predicted T_m values through two independent models due to the occurrence of potential deviations.

1.7. Aims

The general aim of the work presented in this thesis was to develop a new methodology based on FISH using nucleic acid mimics for the *in vivo* diagnosis of *Helicobacter pylori*. Particularly, the present thesis is focusing on the potential use of LNA as a strategy to detect *H. pylori* directly in the gastric mucosa.

Nucleic acid analogues such as LNA have several advantages comparatively to their nucleic acid counterparts (DNA or RNA), for example higher chemistry stability, higher efficiency in target detection and better capacity to discriminate mismatches [426,427]. As such, LNA have revealed a multitude of properties that make them suitable to clinical applications [428]. Considering their enhanced detection properties, it is essential to study their diagnostic capacity against clinically-relevant microorganisms. Consequently, the initial approach consisted on the evaluation of the capacity of LNA probes to detect *H. pylori*. Different designs were developed, synthetized and their hybridization efficiency assessed by measuring fluorescence intensities using flow cytometry and bioinformatics tools. Chemical stability studies were also performed to analyse all probes in order to understand their biophysical characteristics. These studies will be described in Chapters II, III and IV to provide important keys about the most efficient designs to be used in *H. pylori* detection, as well as to elucidate the specific characteristics of the different nucleic acid analogues.

Another aim of this study is the use of LNA probes to detect *H. pylori* at normotemperature (37 °C), based on the results from Chapter II. Using FISH, probes were compared by means of microscopy and flow cytometry analysis. Sensitivity and specificity of the probe which showed the best performance in *H. pylori* detection was also studied, using different *Helicobacter* species, non-*Helicobacter* species, *H. pylori* strains and clinical isolates. Several studies were performed in order to achieve a preliminary protocol to detect *H. pylori in vivo*. These results will be presented in Chapter V.

H. pylori can be found in the human gastric mucosa which is an acid environment. To reach an *in vivo* diagnostic protocol it is therefore important that the methodology is non-toxic and acid resistant. For this, a wide optimization of the standard FISH protocol was performed. Each optimization was investigated carefully to maintain high efficient detection of *H. pylori*. Extensive analyses of the previously described probe were also performed in order to determine the sensitivity and specificity at low stringency conditions (low pH and low hybridization temperature, 37 °C) using different *Helicobacter* species, non-*Helicobacter* species, *H. pylori* strains and clinical isolates. To mimic human gastric conditions, a simulated gastric juice was also used. In order to ascertain the potential

application *in vivo* of this method, cytotoxicity and genotoxicity assays using a gastric cell line were also performed. Data generated in this part of the thesis will be presented in Chapters VI and VII.

To ascertain the potential use of the probe and of the developed methodology, *in vivo* studies using *H. pylori*-infected C57BL/6 mice were also an aim of the thesis. In order to assess the suitability and protocol efficiency of the FIVH for *H. pylori* detection, fluorescence signal was evaluated *ex vivo* in mucus samples, cryosections and paraffin-embedded slides from the corpus and antrum of the stomach mucosa using microscopy. *In vivo* studies will be presented in Chapter VII.

In this thesis, a paper reviewing the findings of the literature regarding the thermodynamic of nucleic acid mimics (Appendix I) is also included, and has been partially used in the Introduction.

The present thesis reports the work performed at the BEL Group Lab at LEPABE, Laboratory for Process Engineering, Environment, Biotechnology and Energy, Faculty of Engineering (University of Porto), Cancer Genetics Group Lab at IPATIMUP, Institute of Molecular Pathology and Immunology of the University of Porto, Nucleic Acid Center at the Department of Physics, Chemistry and Pharmacy (University of Southern Denmark) and at LMPH Group Lab at Faculty of Pharmaceutical, Biomedical and Veterinary Sciences (University of Antwerp).

1.8. References

1. Sharma K., Mishra A.K., Mehraj V., Duraisamy G.S. Advances and applications of molecular cloning in clinical microbiology. Biotechnol Genet Eng Rev (2014); 30: 65-78.
2. Marshall B.J. The Campylobacter pylori story. Scand J Gastroenterol Suppl (1988); 146: 58-66.
3. Lee A. The microbiology and epidemiology of Helicobacter pylori infection. Scand J Gastroenterol Suppl (1994); 201: 2-6.
4. Parsonnet J. Helicobacter pylori. Infect Dis Clin North Am (1998); 12: 185-197.
5. Marshall B.J., Warren J.R. Unidentified curved bacilli in the stomach of patients with gastritis and peptic ulceration. Lancet (1984); 1: 1311-1315.
6. Robin Warren J., Marshall B. Unidentified curved bacilli on gastric epithelium in active chronic gastritis. The Lancet (1983); 321: 1273-1275.
7. Beck J.D., Eke P., Heiss G., Madianos P., Couper D., Lin D., et al. Periodontal Disease and Coronary Heart Disease: A Reappraisal of the Exposure. Circulation (2005); 112: 19-24.
8. Sokol H., Pigneur B., Watterlot L., Lakhdari O., Bermúdez-Humarán L.G., Gratadoux J.-J., et al. Faecalibacterium prausnitzii is an anti-inflammatory commensal bacterium identified by gut microbiota analysis of Crohn disease patients. Proceedings of the National Academy of Sciences (2008); 105: 16731-16736.
9. Bercik P., Denou E., Collins J., Jackson W., Lu J., Jury J., et al. The Intestinal Microbiota Affect Central Levels of Brain-Derived Neurotropic Factor and Behavior in Mice. Gastroenterology (2011); 141: 599-609.e593.
10. Bercik P., Verdu E.F., Foster J.A., Macri J., Potter M., Huang X., et al. Chronic Gastrointestinal Inflammation Induces Anxiety-Like Behavior and Alters Central Nervous System Biochemistry in Mice. Gastroenterology (2010); 139: 2102-2112.e2101.
11. Bizzozero G. Ueber die schlauchförmigen Drüsen des Magendarmkanals und die Beziehungen ihres Epithels zu dem Oberflächenepithel der Schleimhaut. Archiv für mikroskopische Anatomie (1889); 33: 216-246.
12. Goodwin C.S., Armstrong J.A. Microbiological aspects of Helicobacter pylori (Campylobacter pylori). Eur J Clin Microbiol Infect Dis (1990); 9: 1-13.
13. Hazell S.L., Lee A., Brady L., Hennessy W. Campylobacter pyloridis and gastritis: association with intercellular spaces and adaptation to an environment of mucus as important factors in colonization of the gastric epithelium. J Infect Dis (1986); 153: 658-663.
14. Fox J.G. The non-H pylori helicobacters: their expanding role in gastrointestinal and systemic diseases. Gut (2002); 50: 273-283.
15. Zhang L., Day A., McKenzie G., Mitchell H. Nongastric Helicobacter species detected in the intestinal tract of children. J Clin Microbiol (2006); 44: 2276-2279.
16. O'Rourke J.L., Grehan M., Lee A. Non-pylori Helicobacter species in humans. Gut (2001); 49: 601-606.
17. Goodwin C.S., Worsley B.W. Microbiology of Helicobacter pylori. Gastroenterol Clin North Am (1993); 22: 5-19.

18. O'Toole P.W., Lane M.C., Porwollik S. Helicobacter pylori motility. Microbes Infect (2000); 2: 1207-1214.
19. Sisto F., Brenciaglia M.I., Scaltrito M.M., Dubini F. Helicobacter pylori: ureA, cagA and vacA expression during conversion to the coccoid form. Int J Antimicrob Agents (2000); 15: 277-282.
20. Kusters J.G., Gerrits M.M., Van Strijp J.A., Vandenbroucke-Grauls C.M. Coccoid forms of Helicobacter pylori are the morphologic manifestation of cell death. Infect Immun (1997); 65: 3672-3679.
21. Catrenich C.E., Makin K.M. Characterization of the morphologic conversion of Helicobacter pylori from bacillary to coccoid forms. Scand J Gastroenterol Suppl (1991); 181: 58-64.
22. Nilsson H.O., Blom J., Abu-Al-Soud W., Ljungh A.A., Andersen L.P., Wadstrom T. Effect of cold starvation, acid stress, and nutrients on metabolic activity of Helicobacter pylori. Appl Environ Microbiol (2002); 68: 11-19.
23. Azevedo N.F., Almeida C., Cerqueira L., Dias S., Keevil C.W., Vieira M.J. Coccoid Form of Helicobacter pylori as a Morphological Manifestation of Cell Adaptation to the Environment. Appl Environ Microbiol (2007); 73: 3423-3427.
24. Bumann D., Habibi H., Kan B., Schmid M., Goosmann C., Brinkmann V., et al. Lack of Stage-Specific Proteins in Coccoid Helicobacter pylori Cells. Infect Immun (2004); 72: 6738-6742.
25. Alm R.A., Ling L.-S.L., Moir D.T., King B.L., Brown E.D., Doig P.C., et al. Genomic-sequence comparison of two unrelated isolates of the human gastric pathogen Helicobacter pylori. Nature (1999); 397: 176-180.
26. Scott D.R., Marcus E.A., Weeks D.L., Sachs G. Mechanisms of acid resistance due to the urease system of Helicobacter pylori. Gastroenterology (2002); 123: 187-195.
27. Stingl K., Altendorf K., Bakker E.P. Acid survival of Helicobacter pylori: how does urease activity trigger cytoplasmic pH homeostasis? Trends in Microbiology (2002); 10: 70-74.
28. Tomb J.F., White O., Kerlavage A.R., Clayton R.A., Sutton G.G., Fleischmann R.D., et al. The complete genome sequence of the gastric pathogen Helicobacter pylori. Nature (1997); 388: 539-547.
29. Lara-Ramirez E.E., Segura-Cabrera A., Guo X., Yu G., Garcia-Perez C.A., Rodriguez-Perez M.A. New implications on genomic adaptation derived from the Helicobacter pylori genome comparison. PLoS ONE (2011); 6: e17300.
30. Blaser M.J., Berg D.E. Helicobacter pylori genetic diversity and risk of human disease. J Clin Invest (2001); 107: 767-773.
31. Linz B., Schuster S.C. Genomic diversity in Helicobacter and related organisms. Res Microbiol (2007); 158: 737-744.
32. McClain M., Shaffer C., Israel D., Peek R., Cover T. Genome sequence analysis of Helicobacter pylori strains associated with gastric ulceration and gastric cancer. BMC Genomics (2009); 10: 3.

33. Figueiredo C., Machado J.C., Pharoah P., Seruca R., Sousa S., Carvalho R., et al. Helicobacter pylori and interleukin 1 genotyping: an opportunity to identify high-risk individuals for gastric carcinoma. J Natl Cancer Inst (2002); 94: 1680-1687.
34. van Doorn L.J., Figueiredo C., Sanna R., Plaisier A., Schneeberger P., de Boer W., et al. Clinical relevance of the cagA, vacA, and iceA status of Helicobacter pylori. Gastroenterology (1998); 115: 58-66.
35. Yamaoka Y. Pathogenesis of Helicobacter pylori-Related Gastroduodenal Diseases from Molecular Epidemiological Studies. Gastroenterol Res Pract (2012); 2012: 371503.
36. Suerbaum S., Smith J.M., Bapumia K., Morelli G., Smith N.H., Kunstmann E., et al. Free recombination within Helicobacter pylori. Proceedings of the National Academy of Sciences (1998); 95: 12619-12624.
37. Go M.F. Review article: natural history and epidemiology of Helicobacter pylori infection. Aliment Pharmacol Ther (2002); 16 Suppl 1: 3-15.
38. Brown L.M. Helicobacter pylori: epidemiology and routes of transmission. Epidemiol Rev (2000); 22: 283-297.
39. Rehnberg-Laiho L., Rautelin H., Koskela P., Sarna S., Pukkala E., Aromaa A., et al. Decreasing prevalence of helicobacter antibodies in Finland, with reference to the decreasing incidence of gastric cancer. Epidemiol Infect (2001); 126: 37-42.
40. Bastos J., Peleteiro B., Barros R., Alves L., Severo M., de Fatima Pina M., et al. Sociodemographic determinants of prevalence and incidence of Helicobacter pylori infection in Portuguese adults. Helicobacter (2013); 18: 413-422.
41. van Blankenstein M., van Vuuren A.J., Looman C.W., Ouwendijk M., Kuipers E.J. The prevalence of Helicobacter pylori infection in the Netherlands. Scand J Gastroenterol (2013); 48: 794-800.
42. Ozaydin N., Turkyilmaz S.A., Cali S. Prevalence and risk factors of helicobacter pylori in Turkey: a nationally-representative, cross-sectional, screening with the (1)(3)C-Urea breath test. BMC Public Health (2013); 13: 1215.
43. Alvarado-Esquivel C. Seroepidemiology of helicobacter pylori infection in pregnant women in rural durango, Mexico. Int J Biomed Sci (2013); 9: 224-229.
44. Adlekha S., Chadha T., Krishnan P., Sumangala B. Prevalence of helicobacter pylori infection among patients undergoing upper gastrointestinal endoscopy in a medical college hospital in kerala, India. Ann Med Health Sci Res (2013); 3: 559-563.
45. Benberin V., Bektayeva R., Karabayeva R., Lebedev A., Akemeyeva K., Paloheimo L., et al. Prevalence of H. pylori infection and atrophic gastritis among symptomatic and dyspeptic adults in Kazakhstan. A hospital-based screening study using a panel of serum biomarkers. Anticancer Res (2013); 33: 4595-4602.
46. Vilaichone R.K., Mahachai V., Shiota S., Uchida T., Ratanachu-ek T., Tshering L., et al. Extremely high prevalence of Helicobacter pylori infection in Bhutan. World J Gastroenterol (2013); 19: 2806-2810.

47. Dorji D., Dendup T., Malaty H.M., Wangchuk K., Yangzom D., Richter J.M. Epidemiology of Helicobacter pylori in Bhutan: the role of environment and Geographic location. Helicobacter (2014); 19: 69-73.
48. Hanafi M.I., Mohamed A.M. Helicobacter pylori infection: seroprevalence and predictors among healthy individuals in Al Madinah, Saudi Arabia. J Egypt Public Health Assoc (2013); 88: 40-45.
49. Azevedo N.F., Guimaraes N., Figueiredo C., Keevil C.W., Vieira M.J. A new model for the transmission of Helicobacter pylori: role of environmental reservoirs as gene pools to increase strain diversity. Crit Rev Microbiol (2007); 33: 157-169.
50. Mana F., Vandebosch S., Miendje Deyi V., Haentjens P., Urbain D. Prevalence of and risk factors for H. pylori infection in healthy children and young adults in Belgium anno 2010/2011. Acta Gastroenterol Belg (2013); 76: 381-385.
51. den Hollander W.J., Holster I.L., den Hoed C.M., van Deurzen F., van Vuuren A.J., Jaddoe V.W., et al. Ethnicity is a strong predictor for Helicobacter pylori infection in young women in a multi-ethnic European city. J Gastroenterol Hepatol (2013); 28: 1705-1711.
52. Didelot X., Nell S., Yang I., Woltemate S., van der Merwe S., Suerbaum S. Genomic evolution and transmission of Helicobacter pylori in two South African families. Proc Natl Acad Sci U S A (2013); 110: 13880-13885.
53. Osaki T., Okuda M., Ueda J., Konno M., Yonezawa H., Hojo F., et al. Multilocus sequence typing of DNA from faecal specimens for the analysis of intra-familial transmission of Helicobacter pylori. J Med Microbiol (2013); 62: 761-765.
54. Urita Y., Watanabe T., Kawagoe N., Takemoto I., Tanaka H., Kijima S., et al. Role of infected grandmothers in transmission of Helicobacter pylori to children in a Japanese rural town. J Paediatr Child Health (2013); 49: 394-398.
55. Tytgat G.N. Endoscopic transmission of Helicobacter pylori. Aliment Pharmacol Ther (1995); 9 Suppl 2: 105-110.
56. Cronmiller J.R., Nelson D.K., Jackson D.K., Kim C.H. Efficacy of conventional endoscopic disinfection and sterilization methods against Helicobacter pylori contamination. Helicobacter (1999); 4: 198-203.
57. Nurnberg M., Schulz H.J., Ruden H., Vogt K. Do conventional cleaning and disinfection techniques avoid the risk of endoscopic Helicobacter pylori transmission? Endoscopy (2003); 35: 295-299.
58. Buck G.E., Gourley W.K., Lee W.K., Subramanyam K., Latimer J.M., DiNuzzo A.R. Relation of Campylobacter pyloridis to Gastritis and Peptic Ulcer. Journal of Infectious Diseases (1986); 153: 664-669.
59. Polk D.B., Peek R.M. Helicobacter pylori: gastric cancer and beyond. Nat Rev Cancer (2010); 10: 403-414.

60. Moayyedi P., Wason C., Peacock R., Walan A., Bardhan K., Axon A.T.R., et al. Changing Patterns of Helicobacter pylori Gastritis in Long-Standing Acid Suppression. Helicobacter (2000); 5: 206-214.
61. Kapadia C.R. Gastric Atrophy, Metaplasia, and Dysplasia: A Clinical Perspective. J Clin Gastroenterol (2003); 36: S29-S36.
62. Dubois A., Berg D.E., Incecik E.T., Fiala N., Heman-Ackah L.M., Perez-Perez G.I., et al. Transient and persistent experimental infection of nonhuman primates with Helicobacter pylori: implications for human disease. Infect Immun (1996); 64: 2885-2891.
63. Testerman T.L., Morris J. Beyond the stomach: An updated view of pathogenesis, diagnosis, and treatment. World J Gastroenterol (2014); 20: 12781-12808.
64. Peek R.M., Jr., Crabtree J.E. Helicobacter infection and gastric neoplasia. J Pathol (2006); 208: 233-248.
65. Uemura N., Okamoto S., Yamamoto S., Matsumura N., Yamaguchi S., Yamakido M., et al. Helicobacter pylori infection and the development of gastric cancer. N Engl J Med (2001); 345: 784-789.
66. IARC Schistosomes, liver flukes and Helicobacter pylori. IARC Working Group on the Evaluation of Carcinogenic Risks to Humans. Lyon, 7-14 June 1994. IARC Monogr Eval Carcinog Risks Hum (1994); 61: 1-241.
67. El-Omar E.M., Carrington M., Chow W.H., McColl K.E., Bream J.H., Young H.A., et al. Interleukin-1 polymorphisms associated with increased risk of gastric cancer. Nature (2000); 404: 398-402.
68. Machado J.C., Figueiredo C., Canedo P., Pharoah P., Carvalho R., Nabais S., et al. A proinflammatory genetic profile increases the risk for chronic atrophic gastritis and gastric carcinoma. Gastroenterology125: 364-371.
69. Schreiber S., Konradt M., Groll C., Scheid P., Hanauer G., Werling H.O., et al. The spatial orientation of Helicobacter pylori in the gastric mucus. Proc Natl Acad Sci U S A (2004); 101: 5024-5029.
70. Carvalho A.S., Queiroz D.M., Mendes E.N., Rocha G.A., Penna F.J. Diagnosis and distribution of Helicobacter pylori in the gastric mucosa of symptomatic children. Braz J Med Biol Res (1991); 24: 163-166.
71. Bayerdorffer E., Lehn N., Hatz R., Mannes G.A., Oertel H., Sauerbruch T., et al. Difference in expression of Helicobacter pylori gastritis in antrum and body. Gastroenterology (1992); 102: 1575-1582.
72. Genta R.M., Graham D.Y. Comparison of biopsy sites for the histopathologic diagnosis of Helicobacter pylori: a topographic study of H. pylori density and distribution. Gastrointest Endosc (1994); 40: 342-345.
73. Shimizu T., Akamatsu T., Sugiyama A., Ota H., Katsuyama T. Helicobacter pylori and the surface mucous gel layer of the human stomach. Helicobacter (1996); 1: 207-218.

74. Bode G., Malfertheiner P., Ditschuneit H. Invasion of campylobacter-like organisms in the duodenal mucosa in patients with active duodenal ulcer. Klin Wochenschr (1987); 65: 144-146.
75. Papadogiannakis N., Willen R., Carlen B., Sjostedt S., Wadstrom T., Gad A. Modes of adherence of Helicobacter pylori to gastric surface epithelium in gastroduodenal disease: a possible sequence of events leading to internalisation. APMIS (2000); 108: 439-447.
76. Ko G.H., Kang S.M., Kim Y.K., Lee J.H., Park C.K., Youn H.S., et al. Invasiveness of Helicobacter pylori into Human Gastric Mucosa. Helicobacter (1999); 4: 77-81.
77. Hessey S.J., Spencer J., Wyatt J.I., Sobala G., Rathbone B.J., Axon A.T., et al. Bacterial adhesion and disease activity in Helicobacter associated chronic gastritis. Gut (1990); 31: 134-138.
78. Atuma C., Strugala V., Allen A., Holm L. The adherent gastrointestinal mucus gel layer: thickness and physical state in vivo. Am J Physiol Gastrointest Liver Physiol (2001); 280: G922-929.
79. Celli J.P., Turner B.S., Afdhal N.H., Ewoldt R.H., McKinley G.H., Bansil R., et al. Rheology of Gastric Mucin Exhibits a pH-Dependent Sol–Gel Transition. Biomacromolecules (2007); 8: 1580-1586.
80. Celli J.P., Turner B.S., Afdhal N.H., Keates S., Ghiran I., Kelly C.P., et al. Helicobacter pylori moves through mucus by reducing mucin viscoelasticity. Proceedings of the National Academy of Sciences (2009); 106: 14321-14326.
81. Naughton J.A., Marino K., Dolan B., Reid C., Gough R., Gallagher M.E., et al. Divergent mechanisms of interaction of Helicobacter pylori and Campylobacter jejuni with mucus and mucins. Infect Immun (2013); 81: 2838-2850.
82. Clyne M., Drumm B. Adherence of Helicobacter pylori to primary human gastrointestinal cells. Infect Immun (1993); 61: 4051-4057.
83. Keates S., Keates A.C., Katchar K., Peek R.M., Jr., Kelly C.P. Helicobacter pylori induces up-regulation of the epidermal growth factor receptor in AGS gastric epithelial cells. J Infect Dis (2007); 196: 95-103.
84. Steele I.A., Dimaline R., Pritchard D.M., Peek R.M., Jr., Wang T.C., Dockray G.J., et al. Helicobacter and gastrin stimulate Reg1 expression in gastric epithelial cells through distinct promoter elements. Am J Physiol Gastrointest Liver Physiol (2007); 293: G347-354.
85. Tomimori K., Uema E., Teruya H., Ishikawa C., Okudaira T., Senba M., et al. Helicobacter pylori induces CCL20 expression. Infect Immun (2007); 75: 5223-5232.
86. Mangia A., Chiriatti A., Ranieri G., Abbate I., Coviello M., Simone G., et al. H pylori status and angiogenesis factors in human gastric carcinoma. World J Gastroenterol (2006); 12: 5465-5472.

87. Sokolova O., Vieth M., Gnad T., Bozko P.M., Naumann M. Helicobacter pylori promotes eukaryotic protein translation by activating phosphatidylinositol 3 kinase/mTOR. Int J Biochem Cell Biol (2014); 55C: 157-163.
88. Zhuang Y., Cheng P., Liu X.F., Peng L.S., Li B.S., Wang T.T., et al. A pro-inflammatory role for Th22 cells in Helicobacter pylori-associated gastritis. Gut (2014).
89. Hanada K., Uchida T., Tsukamoto Y., Watada M., Yamaguchi N., Yamamoto K., et al. Helicobacter pylori Infection Introduces DNA Double-Strand Breaks in Host Cells. Infect Immun (2014); 82: 4182-4189.
90. Chang H., Kim N., Park J.H., Nam R.H., Choi Y.J., Lee H.S., et al. Different MicroRNA Expression Levels in Gastric Cancer Depending on Helicobacter pylori Infection. Gut Liver (2014).
91. Jurkowska G., Piotrowska-Staworko G., Guzinska-Ustymowicz K., Kemona A., Swidnicka-Siergiejko A., Laszewicz W., et al. The impact of Helicobacter pylori on EGF, EGF receptor, and the c-erb-B2 expression. Adv Med Sci (2014); 59: 221-226.
92. Wen Y., Marcus E.A., Matrubutham U., Gleeson M.A., Scott D.R., Sachs G. Acid-Adaptive Genes of Helicobacter pylori. Infect Immun (2003); 71: 5921-5939.
93. Dunne C., Dolan B., Clyne M. Factors that mediate colonization of the human stomach by Helicobacter pylori. World J Gastroenterol (2014); 20: 5610-5624.
94. Dunn B.E., Campbell G.P., Perez-Perez G.I., Blaser M.J. Purification and characterization of urease from Helicobacter pylori. Journal of Biological Chemistry (1990); 265: 9464-9469.
95. Rektorschek M., Buhmann A., Weeks D., Schwan D., Bensch K.W., Eskandari S., et al. Acid resistance of Helicobacter pylori depends on the UreI membrane protein and an inner membrane proton barrier. Mol Microbiol (2000); 36: 141-152.
96. Marcus E.A., Moshfegh A.P., Sachs G., Scott D.R. The Periplasmic α-Carbonic Anhydrase Activity of Helicobacter pylori Is Essential for Acid Acclimation. J Bacteriol (2005); 187: 729-738.
97. Bury-Mone S., Mendz G.L., Ball G.E., Thibonnier M., Stingl K., Ecobichon C., et al. Roles of alpha and beta carbonic anhydrases of Helicobacter pylori in the urease-dependent response to acidity and in colonization of the murine gastric mucosa. Infect Immun (2008); 76: 497-509.
98. Wroblewski L.E., Peek R.M., Wilson K.T. Helicobacter pylori and Gastric Cancer: Factors That Modulate Disease Risk. Clin Microbiol Rev (2010); 23: 713-739.
99. Backert S., Naumann M. What a disorder: proinflammatory signaling pathways induced by Helicobacter pylori. Trends Microbiol (2010); 18: 479-486.
100. Dossumbekova A., Prinz C., Gerhard M., Brenner L., Backert S., Kusters J.G., et al. Helicobacter pylori outer membrane proteins and gastric inflammation. Gut (2006); 55: 1360-1361; author reply 1361.
101. Roesler B.M., Rabelo-Goncalves E.M., Zeitune J.M. Virulence Factors of Helicobacter pylori: A Review. Clin Med Insights Gastroenterol (2014); 7: 9-17.

102. Figueiredo C., Quint W., Nouhan N., van den Munckhof H., Herbrink P., Scherpenisse J., et al. Assessment of Helicobacter pylori vacA and cagA genotypes and host serological response. J Clin Microbiol (2001); 39: 1339-1344.
103. Yue J.Y., Yue J., Wang M.Y., Song W.C., Gao X.Z. CagA status & genetic characterization of metronidazole resistant strains of H. pylori from: A region at high risk of gastric cancer. Pak J Med Sci (2014); 30: 804-808.
104. Fernandez-Gonzalez E., Backert S. DNA transfer in the gastric pathogen Helicobacter pylori. J Gastroenterol (2014); 49: 594-604.
105. Ki M.R., Hwang M., Kim A.Y., Lee E.M., Lee E.J., Lee M.M., et al. Role of vacuolating cytotoxin VacA and cytotoxin-associated antigen CagA of Helicobacter pylori in the progression of gastric cancer. Mol Cell Biochem (2014).
106. Winter J.A., Letley D.P., Cook K.W., Rhead J.L., Zaitoun A.A., Ingram R.J., et al. A Role for the Vacuolating Cytotoxin, VacA, in Colonization and Helicobacter pylori-Induced Metaplasia in the Stomach. J Infect Dis (2014); 210: 954-963.
107. Cover T.L., Blaser M.J. Purification and characterization of the vacuolating toxin from Helicobacter pylori. J Biol Chem (1992); 267: 10570-10575.
108. Atherton J.C., Sharp P.M., Cover T.L., Gonzalez-Valencia G., Peek R.M., Jr., Thompson S.A., et al. Vacuolating cytotoxin (vacA) alleles of Helicobacter pylori comprise two geographically widespread types, m1 and m2, and have evolved through limited recombination. Curr Microbiol (1999); 39: 211-218.
109. Nogueira C., Figueiredo C., Carneiro F., Taveira Gomes A., Barreira R., Figueira P., et al. Helicobacter pylori Genotypes May Determine Gastric Histopathology. The American Journal of Pathology158: 647-654.
110. Oertli M., Noben M., Engler D.B., Semper R.P., Reuter S., Maxeiner J., et al. Helicobacter pylori γ-glutamyl transpeptidase and vacuolating cytotoxin promote gastric persistence and immune tolerance. Proceedings of the National Academy of Sciences (2013); 110: 3047-3052.
111. Engler D.B., Reuter S., van Wijck Y., Urban S., Kyburz A., Maxeiner J., et al. Effective treatment of allergic airway inflammation with Helicobacter pylori immunomodulators requires BATF3-dependent dendritic cells and IL-10. Proc Natl Acad Sci U S A (2014); 111: 11810-11815.
112. Quine M.A., Bell G.D., McCloy R.F., Charlton J.E., Devlin H.B., Hopkins A. Prospective audit of upper gastrointestinal endoscopy in two regions of England: safety, staffing, and sedation methods. Gut (1995); 36: 462-467.
113. Mitchell H.M., Bohane T.D., Berkowicz J., Hazell S.L., Lee A. Antibody to Campylobacter pylori in families of index children with gastrointestinal illness due to C pylori. Lancet (1987); 2: 681-682.

114. Ekesbo R., Toth E., Fork F.T., Held M., Nilsson I., Wadstrom T., et al. Chronic Helicobacter pylori infection in a population in southern Sweden analysed by histopathology, immunoblot and ELISA serology. Eur J Gastroenterol Hepatol (2006); 18: 589-593.
115. Zuniga-Noriega J.R., Bosques-Padilla F.J., Perez-Perez G.I., Tijerina-Menchaca R., Flores-Gutierrez J.P., Maldonado Garza H.J., et al. Diagnostic utility of invasive tests and serology for the diagnosis of Helicobacter pylori infection in different clinical presentations. Arch Med Res (2006); 37: 123-128.
116. El-Fakhfakh E.A., Montasser I.F., Khalifa R.A. Evaluation of salivary and serum anti-Helicobacter pylori in Egyptian patients with H. pylori related gastric disorders. J Egypt Soc Parasitol (2014); 44: 275-283.
117. Schrier W.H., Schoengold R.J., Baker J.T., Norell J.L., Jaseph C.L., Okin Y., et al. Development of FlexSure HP--an immunochromatographic method to detect antibodies against Helicobacter pylori. Clin Chem (1998); 44: 293-298.
118. Sharma T.K., Young E.L., Miller S., Cutler A.F. Evaluation of a rapid, new method for detecting serum IgG antibodies to Helicobacter pylori. Clin Chem (1997); 43: 832-836.
119. Graham D.Y., Evans D.J., Jr., Peacock J., Baker J.T., Schrier W.H. Comparison of rapid serological tests (FlexSure HP and QuickVue) with conventional ELISA for detection of Helicobacter pylori infection. Am J Gastroenterol (1996); 91: 942-948.
120. Sadowski D., Cohen H., Laine L., Greenberg P., Goldstein J., Mihalov M., et al. Evaluation of the FlexSure HP whole blood antibody test for diagnosis of Helicobacter pylori infection. Am J Gastroenterol (1998); 93: 2119-2123.
121. Hahn M., Fennerty M.B., Corless C.L., Magaret N., Lieberman D.A., Faigel D.O. Noninvasive tests as a substitute for histology in the diagnosis of Helicobacter pylori infection. Gastrointest Endosc (2000); 52: 20-26.
122. Kato S., Ozawa K., Okuda M., Nakayama Y., Yoshimura N., Konno M., et al. Multicenter comparison of rapid lateral flow stool antigen immunoassay and stool antigen enzyme immunoassay for the diagnosis of Helicobacter pylori infection in children. Helicobacter (2004); 9: 669-673.
123. Karakus C., Salih B.A. Comparison of the lateral flow immunoassays (LFIA) for the diagnosis of Helicobacter pylori infection. J Immunol Methods (2013); 396: 8-14.
124. Malfertheiner P M.F.a.O.M.C. Guidelines for the Management of Helicobacter Pylori Infection. BUSINESS BRIEFING: EUROPEAN GASTROENTEROLOGY REVIEW (2005).
125. Megraud F. The most important diagnostic modalities for Helicobacter pylori, now and in the future. Eur J Gastroenterol Hepatol (2012); 9 Suppl 1: S13-15; discussion S15.
126. Choi J., Kim C.H., Kim D., Chung S.J., Song J.H., Kang J.M., et al. Prospective evaluation of a new stool antigen test for the detection of Helicobacter pylori, in comparison with histology, rapid urease test, (13)C-urea breath test, and serology. J Gastroenterol Hepatol (2011); 26: 1053-1059.

127. Kornberg H.L., Davies R.E., Wood D.R. The activity and function of gastric urease in the cat. Biochem J (1954); 56: 363-372.

128. Graham D.Y., Klein P.D., Evans D.J., Jr., Evans D.G., Alpert L.C., Opekun A.R., et al. Campylobacter pylori detected noninvasively by the 13C-urea breath test. Lancet (1987); 1: 1174-1177.

129. Marshall B.J., Surveyor I. Carbon-14 urea breath test for the diagnosis of Campylobacter pylori associated gastritis. J Nucl Med (1988); 29: 11-16.

130. Megraud F., Lehours P. Helicobacter pylori detection and antimicrobial susceptibility testing. Clin Microbiol Rev (2007); 20: 280-322.

131. Mobley H.L., Island M.D., Hausinger R.P. Molecular biology of microbial ureases. Microbiol Rev (1995); 59: 451-480.

132. Pantoflickova D., Scott D.R., Sachs G., Dorta G., Blum A.L. 13C urea breath test (UBT) in the diagnosis of Helicobacter pylori: why does it work better with acid test meals? Gut (2003); 52: 933-937.

133. Shiotani A., Saeed A., Yamaoka Y., Osato M.S., Klein P.D., Graham D.Y. Citric acid-enhanced Helicobacter pylori urease activity in vivo is unrelated to gastric emptying. Aliment Pharmacol Ther (2001); 15: 1763-1767.

134. Slater C., Preston T., Weaver L.T. Is there an advantage in normalising the results of the Helicobacter pylori [13C]urea breath test for CO2 production rate in children? Isotopes Environ Health Stud (2004); 40: 89-98.

135. Logan R.P., Polson R.J., Misiewicz J.J., Rao G., Karim N.Q., Newell D., et al. Simplified single sample 13Carbon urea breath test for Helicobacter pylori: comparison with histology, culture, and ELISA serology. Gut (1991); 32: 1461-1464.

136. Klein P.D., Malaty H.M., Martin R.F., Graham K.S., Genta R.M., Graham D.Y. Noninvasive detection of Helicobacter pylori infection in clinical practice: the 13C urea breath test. Am J Gastroenterol (1996); 91: 690-694.

137. Malfertheiner P., Megraud F., O'Morain C.A., Atherton J., Axon A.T., Bazzoli F., et al. Management of Helicobacter pylori infection--the Maastricht IV/ Florence Consensus Report. Gut (2012); 61: 646-664.

138. Guarner J., Kalach N., Elitsur Y., Koletzko S. Helicobacter pylori diagnostic tests in children: review of the literature from 1999 to 2009. Eur J Pediatr (2010); 169: 15-25.

139. Pathak C.M., Kaur B., Khanduja K.L. 14C-urea breath test is safe for pediatric patients. Nucl Med Commun (2010); 31: 830-835.

140. Bentur Y., Matsui D., Koren G. Safety of 14C-UBT for diagnosis of Helicobacter pylori infection in pregnancy. Can Fam Physician (2009); 55: 479-480.

141. Gisbert J.P., Pajares J.M. Review article: 13C-urea breath test in the diagnosis of Helicobacter pylori infection -- a critical review. Aliment Pharmacol Ther (2004); 20: 1001-1017.

142. Tamadon M.R., Saberi Far M., Soleimani A., Ghorbani R., Semnani V., Malek F., et al. Evaluation of noninvasive tests for diagnosis of Helicobacter pylori infection in hemodialysis patients. J Nephropathol (2013); 2: 249-253.
143. Wardi J., Shalev T., Shevah O., Boaz M., Avni Y., Shirin H. A rapid continuous-real-time 13C-urea breath test for the detection of Helicobacter pylori in patients after partial gastrectomy. J Clin Gastroenterol (2012); 46: 293-296.
144. Hanninen M.L. Sensitivity of Helicobacter pylori to different bile salts. Eur J Clin Microbiol Infect Dis (1991); 10: 515-518.
145. Mapstone N.P., Lynch D.A., Lewis F.A., Axon A.T., Tompkins D.S., Dixon M.F., et al. PCR identification of Helicobacter pylori in faeces from gastritis patients. Lancet (1993); 341: 447.
146. Makristathis A., Pasching E., Schutze K., Wimmer M., Rotter M.L., Hirschl A.M. Detection of Helicobacter pylori in stool specimens by PCR and antigen enzyme immunoassay. J Clin Microbiol (1998); 36: 2772-2774.
147. Vaira D., Malfertheiner P., Megraud F., Axon A.T., Deltenre M., Hirschl A.M., et al. Diagnosis of Helicobacter pylori infection with a new non-invasive antigen-based assay. HpSA European study group. Lancet (1999); 354: 30-33.
148. Chehter E.Z., Bacci M.R., Fonseca F.L., Goncalves J.A., Buchalla G., Shiraichi S.A., et al. Diagnosis of the infection by the Helicobacter pylori through stool examination: method standardization in adults. Clin Biochem (2013); 46: 1622-1624.
149. Cirak M.Y., Akyon Y., Megraud F. Diagnosis of Helicobacter pylori. Helicobacter (2007); 12 Suppl 1: 4-9.
150. Pandya H.B., Patel J.S., Agravat H.H., Singh N.K. Non-Invasive Diagnosis of Helicobacter pylori: Evaluation of Two Enzyme Immunoassays, Testing Serum IgG and IgA Response in the Anand District of Central Gujarat,India. J Clin Diagn Res (2014); 8: DC12-15.
151. Gisbert J.P., Cruzado A.I., Benito L.M., Carpio D., Perez-Poveda J.J., Gonzalez L., et al. Helicobacter pylori "test-and-scope" strategy for dyspeptic patients. Is it useful and safe? Dig Liver Dis (2001); 33: 539-545.
152. Gisbert J.P., Pajares J.M. Diagnosis of Helicobacter pylori infection by stool antigen determination: a systematic review. Am J Gastroenterol (2001); 96: 2829-2838.
153. Sakai Y., Eto R., Kasanuki J., Kondo F., Kato K., Arai M., et al. Chromoendoscopy with indigo carmine dye added to acetic acid in the diagnosis of gastric neoplasia: a prospective comparative study. Gastrointest Endosc (2008); 68: 635-641.
154. Hernandez-Garces H.R., Castellanos-Gonzalez V.V., Gonzalez-Fabian L., Infante-Velazquez M., Pena K., Andrain-Sierra Y. Chromoendoscopy with red phenol in the diagnosis of Helicobacter pylori infection. Rev Esp Enferm Dig (2012); 104: 4-9.
155. Uedo N., Ishihara R., Iishi H., Yamamoto S., Yamada T., Imanaka K., et al. A new method of diagnosing gastric intestinal metaplasia: narrow-band imaging with magnifying endoscopy. Endoscopy (2006); 38: 819-824.

156. Kiesslich R., Burg J., Vieth M., Gnaendiger J., Enders M., Delaney P., et al. Confocal laser endoscopy for diagnosing intraepithelial neoplasias and colorectal cancer in vivo. Gastroenterology (2004); 127: 706-713.
157. Shibuya K., Hoshino H., Chiyo M., Iyoda A., Yoshida S., Sekine Y., et al. High magnification bronchovideoscopy combined with narrow band imaging could detect capillary loops of angiogenic squamous dysplasia in heavy smokers at high risk for lung cancer. Thorax (2003); 58: 989-995.
158. Becker V., Vieth M., Bajbouj M., Schmid R.M., Meining A. Confocal laser scanning fluorescence microscopy for in vivo determination of microvessel density in Barrett's esophagus. Endoscopy (2008); 40: 888-891.
159. Meining A., Saur D., Bajbouj M., Becker V., Peltier E., Höfler H., et al. In Vivo Histopathology for Detection of Gastrointestinal Neoplasia With a Portable, Confocal Miniprobe: An Examiner Blinded Analysis. Clinical Gastroenterology and Hepatology (2007); 5: 1261-1267.
160. Schmidt C., Lautenschlager C., Petzold B., Sakr Y., Marx G., Stallmach A. Confocal laser endomicroscopy reliably detects sepsis-related and treatment-associated changes in intestinal mucosal microcirculation. Br J Anaesth (2013); 111: 996-1003.
161. Liu H., Li Y.Q., Yu T., Zhao Y.A., Zhang J.P., Zhang J.N., et al. Confocal endomicroscopy for in vivo detection of microvascular architecture in normal and malignant lesions of upper gastrointestinal tract. J Gastroenterol Hepatol (2008); 23: 56-61.
162. Hagel S., Bruns T., Stallmach A., Schmidt C. A confocal view of the intestinal microcirculation in a patient with Crohn disease and portal vein thrombosis. Endoscopy (2011); 43 Suppl 2 UCTN: E126-127.
163. Goetz M., Kiesslich R. Confocal Endomicroscopy: In Vivo Diagnosis of Neoplastic Lesions of the Gastrointestinal Tract. Anticancer Res (2008); 28: 353-360.
164. Goetz M., Ziebart A., Foersch S., Vieth M., Waldner M.J., Delaney P., et al. In Vivo Molecular Imaging of Colorectal Cancer With Confocal Endomicroscopy by Targeting Epidermal Growth Factor Receptor. Gastroenterology (2010); 138: 435-446.
165. Hsiung P.L., Hardy J., Friedland S., Soetikno R., Du C.B., Wu A.P., et al. Detection of colonic dysplasia in vivo using a targeted heptapeptide and confocal microendoscopy. Nat Med (2008); 14: 454-458.
166. Hoetker M.S., Kiesslich R., Diken M., Moehler M., Galle P.R., Li Y., et al. Molecular in vivo imaging of gastric cancer in a human-murine xenograft model: targeting epidermal growth factor receptor. Gastrointest Endosc (2012); 76: 612-620.
167. Yserbyt J., Dooms C., Ninane V., Decramer M., Verleden G. Perspectives using probe-based confocal laser endomicroscopy of the respiratory tract. Swiss Med Wkly (2013); 143: w13764.
168. Newton R.C., Kemp S.V., Yang G.Z., Elson D.S., Darzi A., Shah P.L. Imaging parenchymal lung diseases with confocal endomicroscopy. Respir Med (2012); 106: 127-137.

169. Pittayanon R., Rerknimitr R., Wisedopas N., Khemnark S., Thanapirom K., Thienchanachaiya P., et al. The learning curve of gastric intestinal metaplasia interpretation on the images obtained by probe-based confocal laser endomicroscopy. Diagn Ther Endosc (2012); 2012: 278045.

170. Shahid M.W., Buchner A., Gomez V., Krishna M., Woodward T.A., Raimondo M., et al. Diagnostic accuracy of probe-based confocal laser endomicroscopy and narrow band imaging in detection of dysplasia in duodenal polyps. J Clin Gastroenterol (2012); 46: 382-389.

171. Dixon M.F., Genta R.M., Yardley J.H., Correa P. Classification and grading of gastritis. The updated Sydney System. International Workshop on the Histopathology of Gastritis, Houston 1994. Am J Surg Pathol (1996); 20: 1161-1181.

172. Mégraud F., Lehours P. Helicobacter pylori Detection and Antimicrobial Susceptibility Testing. Clinical Microbiology Reviews (2007); 20: 280-322.

173. Garza-Gonzalez E., Perez-Perez G.I., Maldonado-Garza H.J., Bosques-Padilla F.J. A review of Helicobacter pylori diagnosis, treatment, and methods to detect eradication. World J Gastroenterol (2014); 20: 1438-1449.

174. Andersen L.P., Norgaard A., Holck S., Blom J., Elsborg L. Isolation of a "Helicobacter heilmanii"-like organism from the human stomach. Eur J Clin Microbiol Infect Dis (1996); 15: 95-96.

175. Debongnie J.C., Donnay M., Mairesse J. Gastrospirillum hominis ("Helicobacter heilmanii"): a cause of gastritis, sometimes transient, better diagnosed by touch cytology? Am J Gastroenterol (1995); 90: 411-416.

176. Liu C., Smet A., Blaecher C., Flahou B., Ducatelle R., Linden S., et al. Gastric De Novo Muc13 Expression and Spasmolytic Polypeptide-Expressing Metaplasia during Helicobacter heilmannii Infection. Infect Immun (2014); 82: 3227-3239.

177. Morgner A., Lehn N., Andersen L.P., Thiede C., Bennedsen M., Trebesius K., et al. Helicobacter heilmannii-associated primary gastric low-grade MALT lymphoma: complete remission after curing the infection. Gastroenterology (2000); 118: 821-828.

178. El-Zimaity H.M., Graham D.Y. Evaluation of gastric mucosal biopsy site and number for identification of Helicobacter pylori or intestinal metaplasia: role of the Sydney System. Hum Pathol (1999); 30: 72-77.

179. MacOni G., Vago L., Galletta G., Imbesi V., Sangaletti O., Parente F., et al. Is routine histological evaluation an accurate test for Helicobacter pylori infection? Aliment Pharmacol Ther (1999); 13: 327-331.

180. Molyneux A.J., Harris M.D. Helicobacter pylori in gastric biopsies--should you trust the pathology report? J R Coll Physicians Lond (1993); 27: 119-120.

181. Patel S.K., Pratap C.B., Jain A.K., Gulati A.K., Nath G. Diagnosis of : What should be the gold standard? World J Gastroenterol (2014); 20: 12847-12859.

182. Laine L., Sugg J., Suchower L., Neil G. Endoscopic biopsy requirements for post-treatment diagnosis of Helicobacter pylori. Gastrointest Endosc (2000); 51: 664-669.

183. Hirschl A.M., Makristathis A. Methods to detect Helicobacter pylori: from culture to molecular biology. Helicobacter (2007); 12 Suppl 2: 6-11.

184. Perez-Perez G.I. Accurate diagnosis of Helicobacter pylori. Culture, including transport. Gastroenterol Clin North Am (2000); 29: 879-884.

185. Ndip R.N., MacKay W.G., Farthing M.J., Weaver L.T. Culturing Helicobacter pylori from clinical specimens: review of microbiologic methods. J Pediatr Gastroenterol Nutr (2003); 36: 616-622.

186. Glupczynski Y. Microbiological and serological diagnostic tests for Helicobacter pylori: an overview. Br Med Bull (1998); 54: 175-186.

187. Megraud F. How should Helicobacter pylori infection be diagnosed? Gastroenterology (1997); 113: S93-98.

188. Mishra K.K., Srivastava S., Garg A., Ayyagari A. Antibiotic susceptibility of Helicobacter pylori clinical isolates: comparative evaluation of disk-diffusion and E-test methods. Curr Microbiol (2006); 53: 329-334.

189. Osato M.S., Reddy R., Reddy S.G., Penland R.L., Graham D.Y. Comparison of the Etest and the NCCLS-approved agar dilution method to detect metronidazole and clarithromycin resistant Helicobacter pylori. Int J Antimicrob Agents (2001); 17: 39-44.

190. Essa A.S., Kramer J.R., Graham D.Y., Treiber G. Meta-analysis: four-drug, three-antibiotic, non-bismuth-containing "concomitant therapy" versus triple therapy for Helicobacter pylori eradication. Helicobacter (2009); 14: 109-118.

191. Smith S.M., O'Morain C., McNamara D. Antimicrobial susceptibility testing for Helicobacter pylori in times of increasing antibiotic resistance. World J Gastroenterol (2014); 20: 9912-9921.

192. Gisbert J.P. Sequential or Concomitant Therapy for Helicobacter pylori Eradication? J Clin Gastroenterol (2010).

193. Megraud F. Helicobacter pylori and antibiotic resistance. Gut (2007); 56: 1502.

194. Monteiro L., de Mascarel A., Sarrasqueta A.M., Bergey B., Barberis C., Talby P., et al. Diagnosis of Helicobacter pylori infection: noninvasive methods compared to invasive methods and evaluation of two new tests. Am J Gastroenterol (2001); 96: 353-358.

195. Tseng C.A., Wang W.M., Wu D.C. Comparison of the clinical feasibility of three rapid urease tests in the diagnosis of Helicobacter pylori infection. Dig Dis Sci (2005); 50: 449-452.

196. Wong W.M., Wong B.C., Tang V.S., Lai K.C., Yuen S.T., Leung S.Y., et al. An evaluation of the PyloriTek test for the diagnosis of Helicobacter pylori infection in Chinese patients before and after eradication therapy. J Gastroenterol Hepatol (2001); 16: 976-980.

197. Murata H., Kawano S., Tsuji S., Tsujii M., Sawaoka H., Iijima H., et al. Evaluation of the PyloriTek test for detection of Helicobacter pylori infection in cases with and without eradication therapy. Am J Gastroenterol (1998); 93: 2102-2105.

198. Basset C., Holton J., Gatta L., Ricci C., Bernabucci V., Liuzzi G., et al. Helicobacter pylori infection: anything new should we know? Aliment Pharmacol Ther (2004); 20 Suppl 2: 31-41.

199. Clayton C., Kleanthous K., Tabaqchali S. Detection and identification of Helicobacter pylori by the polymerase chain reaction. J Clin Pathol (1991); 44: 515-516.

200. Ho S.A., Hoyle J.A., Lewis F.A., Secker A.D., Cross D., Mapstone N.P., et al. Direct polymerase chain reaction test for detection of Helicobacter pylori in humans and animals. J Clin Microbiol (1991); 29: 2543-2549.

201. De Reuse H., Labigne A., Mengin-Lecreulx D. The Helicobacter pylori ureC gene codes for a phosphoglucosamine mutase. J Bacteriol (1997); 179: 3488-3493.

202. Hoshina S., Kahn S.M., Jiang W., Green P.H., Neu H.C., Chin N., et al. Direct detection and amplification of Helicobacter pylori ribosomal 16S gene segments from gastric endoscopic biopsies. Diagn Microbiol Infect Dis (1990); 13: 473-479.

203. Maeda S., Yoshida H., Ogura K., Kanai F., Shiratori Y., Omata M. Helicobacter pylori specific nested PCR assay for the detection of 23S rRNA mutation associated with clarithromycin resistance. Gut (1998); 43: 317-321.

204. Singh V., Mishra S., Rao G.R., Jain A.K., Dixit V.K., Gulati A.K., et al. Evaluation of nested PCR in detection of Helicobacter pylori targeting a highly conserved gene: HSP60. Helicobacter (2008); 13: 30-34.

205. Ryan K.A., Moran A.P., Little C.L., Glennon M., Smith T., Maher M. Detection and identification of Helicobacter pylori directly from gastric biopsies using polymerase chain reaction. Ir J Med Sci (2002); 171: 117.

206. Xiong L.J., Tong Y., Wang Z., Mao M. Detection of clarithromycin-resistant Helicobacter pylori by stool PCR in children: a comprehensive review of literature. Helicobacter (2013); 18: 89-101.

207. Sen N., Yilmaz O., Simsek I., Kupelioglu A.A., Ellidokuz H. Detection of Helicobacter pylori DNA by a simple stool PCR method in adult dyspeptic patients. Helicobacter (2005); 10: 353-359.

208. Basso D., Navaglia F., Cassaro M., Scrigner M., Toma A., Dal Bo N., et al. Gastric juice polymerase chain reaction: an alternative to histology in the diagnosis of Helicobacter pylori infection. Helicobacter (1996); 1: 159-164.

209. Rimbara E., Sasatsu M., Graham D.Y. PCR detection of Helicobacter pylori in clinical samples. Methods Mol Biol (2013); 943: 279-287.

210. Owen R.J. Molecular testing for antibiotic resistance in Helicobacter pylori. Gut (2002); 50: 285-289.

211. Schmitt B.H., Regner M., Mangold K.A., Thomson R.B., Jr., Kaul K.L. PCR detection of clarithromycin-susceptible and -resistant Helicobacter pylori from formalin-fixed, paraffin-embedded gastric biopsies. Mod Pathol (2013); 26: 1222-1227.

212. Lopes A.I., Vale F.F., Oleastro M. Helicobacter pylori infection - recent developments in diagnosis. World J Gastroenterol (2014); 20: 9299-9313.

213. Miendje Deyi V.Y., Burette A., Bentatou Z., Maaroufi Y., Bontems P., Lepage P., et al. Practical use of GenoType(R) HelicoDR, a molecular test for Helicobacter pylori detection and susceptibility testing. Diagn Microbiol Infect Dis (2011); 70: 557-560.

214. Cambau E., Allerheiligen V., Coulon C., Corbel C., Lascols C., Deforges L., et al. Evaluation of a new test, genotype HelicoDR, for molecular detection of antibiotic resistance in Helicobacter pylori. J Clin Microbiol (2009); 47: 3600-3607.

215. van Doorn L.J., Figueiredo C., Rossau R., Jannes G., van Asbroek M., Sousa J.C., et al. Typing of Helicobacter pylori vacA gene and detection of cagA gene by PCR and reverse hybridization. J Clin Microbiol (1998); 36: 1271-1276.

216. Essawi T., Hammoudeh W., Sabri I., Sweidan W., Farraj M.A. Determination of Helicobacter pylori Virulence Genes in Gastric Biopsies by PCR. ISRN Gastroenterol (2013); 2013: 606258.

217. Ferreira R.M., Machado J.C., Letley D., Atherton J.C., Pardo M.L., Gonzalez C.A., et al. A Novel Method for Genotyping the Helicobacter pylori vacA Intermediate Region Directly in Gastric Biopsy Specimens. J Clin Microbiol (2012); 50: 3983-3989.

218. Gonzalez C.A., Figueiredo C., Lic C.B., Ferreira R.M., Pardo M.L., Ruiz Liso J.M., et al. Helicobacter pylori cagA and vacA genotypes as predictors of progression of gastric preneoplastic lesions: a long-term follow-up in a high-risk area in Spain. Am J Gastroenterol (2011); 106: 867-874.

219. Alaoui Boukhris S., Amarti A., El Rhazi K., El Khadir M., Benajah D.-A., Ibrahimi S.A., et al. *Helicobacter pylori* Genotypes Associated with Gastric Histo-Pathological Damages in a Moroccan Population. PLoS ONE (2013); 8: e82646.

220. Shukla S.K., Prasad K.N., Tripathi A., Ghoshal U.C., Krishnani N., Nuzhat H. Quantitation of Helicobacter pylori ureC gene and its comparison with different diagnostic techniques and gastric histopathology. J Microbiol Methods (2011); 86: 231-237.

221. Linpisarn S., Koosirirat C., Prommuangyong K., Suwan W., Lertprasertsuke N., Phornphutkul K. Use of different PCR primers and gastric biopsy tissue from CLO test for the detection of Helicobacter pylori. Southeast Asian J Trop Med Public Health (2005); 36: 135-140.

222. Di Bonaventura G., Neri M., Angelucci D., Rosini S., Piccolomini M., Piccolomini R. Detection of Helicobacter pylori by PCR on gastric biopsy specimens taken for CP test: comparison with histopathological analysis. Int J Immunopathol Pharmacol (2004); 17: 77-82.

223. Dus I., Dobosz T., Manzin A., Loi G., Serra C., Radwan-Oczko M. Role of PCR in Helicobacter pylori diagnostics and research--new approaches for study of coccoid and spiral forms of the bacteria. Postepy Hig Med Dosw (Online) (2013); 67: 261-268.

224. Thoreson A.C., Borre M., Andersen L.P., Jorgensen F., Kiilerich S., Scheibel J., et al. Helicobacter pylori detection in human biopsies: a competitive PCR assay with internal control reveals false results. FEMS Immunol Med Microbiol (1999); 24: 201-208.

225. Roosendaal R., Kuipers E.J., van den Brule A.J., Pena A.S., Uyterlinde A.M., Walboomers J.M., et al. Importance of the fiberoptic endoscope cleaning procedure for detection of Helicobacter pylori in gastric biopsy specimens by PCR. J Clin Microbiol (1994); 32: 1123-1126.

226. Barrett D.M., Faigel D.O., Metz D.C., Montone K., Furth E.E. In situ hybridization for Helicobacter pylori in gastric mucosal biopsy specimens: quantitative evaluation of test performance in comparison with the CLOtest and thiazine stain. J Clin Lab Anal (1997); 11: 374-379.

227. Can F., Yilmaz Z., Demirbilek M., Bilezikci B., Kunefeci G., Atac F.B., et al. Diagnosis of Helicobacter pylori infection and determination of clarithromycin resistance by fluorescence in situ hybridization from formalin-fixed, paraffin-embedded gastric biopsy specimens. Can J Microbiol (2005); 51: 569-573.

228. Rauws E.A., Langenberg W., Houthoff H.J., Zanen H.C., Tytgat G.N. Campylobacter pyloridis-associated chronic active antral gastritis. A prospective study of its prevalence and the effects of antibacterial and antiulcer treatment. Gastroenterology (1988); 94: 33-40.

229. McNulty C.A., Gearty J.C., Crump B., Davis M., Donovan I.A., Melikian V., et al. Campylobacter pyloridis and associated gastritis: investigator blind, placebo controlled trial of bismuth salicylate and erythromycin ethylsuccinate. Br Med J (Clin Res Ed) (1986); 293: 645-649.

230. Oderda G., Dell'Olio D., Morra I., Ansaldi N. Campylobacter pylori gastritis: long term results of treatment with amoxycillin. Arch Dis Child (1989); 64: 326-329.

231. Graham D.Y., Opekun A.R., Klein P.D. Clarithromycin for the eradication of Helicobacter pylori. J Clin Gastroenterol (1993); 16: 292-294.

232. Prasertpetmanee S., Mahachai V., Vilaichone R.K. Improved efficacy of proton pump inhibitor - amoxicillin - clarithromycin triple therapy for Helicobacter pylori eradication in low clarithromycin resistance areas or for tailored therapy. Helicobacter (2013); 18: 270-273.

233. Chubineh S., Birk J. Proton pump inhibitors: the good, the bad, and the unwanted. South Med J (2012); 105: 613-618.

234. Graham D.Y., Lew G.M., Evans D.G., Evans D.J., Jr., Klein P.D. Effect of triple therapy (antibiotics plus bismuth) on duodenal ulcer healing. A randomized controlled trial. Ann Intern Med (1991); 115: 266-269.

235. Borody T.J., Andrews P., Fracchia G., Brandl S., Shortis N.P., Bae H. Omeprazole enhances efficacy of triple therapy in eradicating Helicobacter pylori. Gut (1995); 37: 477-481.

236. Hosking S.W., Ling T.K., Yung M.Y., Cheng A., Chung S.C., Leung J.W., et al. Randomised controlled trial of short term treatment to eradicate Helicobacter pylori in patients with duodenal ulcer. BMJ (1992); 305: 502-504.

237. Biasco G., Miglioli M., Barbara L., Corinaldesi R., di Febo G. Omeprazole, Helicobacter pylori, gastritis, and duodenal ulcer. Lancet (1989); 2: 1403.

238. Rauws E.A., Langenberg W., Bosma A., Dankert J., Tytgat G.N. Lack of eradication of Helicobacter pylori after omeprazole. Lancet (1991); 337: 1093.

239. Malfertheiner P., Link A., Selgrad M. Helicobacter pylori: perspectives and time trends. Nat Rev Gastroenterol Hepatol (2014); 11: 628-638.

240. Malfertheiner P., Megraud F., O'Morain C., Bell D., Bianchi Porro G., Deltenre M., et al. Current European concepts in the management of Helicobacter pylori infection--the Maastricht Consensus Report. The European Helicobacter Pylori Study Group (EHPSG). Eur J Gastroenterol Hepatol (1997); 9: 1-2.

241. Borody T.J., Brandl S., Andrews P., Ferch N., Jankiewicz E., Hyland L. Use of high efficacy, lower dose triple therapy to reduce side effects of eradicating Helicobacter pylori. Am J Gastroenterol (1994); 89: 33-38.

242. Bazzoli F., Zagari M., Pozzato P., Varoli O., Fossi S., Ricciardiello L., et al. Evaluation of short-term low-dose triple therapy for the eradication of Helicobacter pylori by factorial design in a randomized, double-blind, controlled study. Aliment Pharmacol Ther (1998); 12: 439-445.

243. Zanten S.J., Bradette M., Farley A., Leddin D., Lind T., Unge P., et al. The DU-MACH study: eradication of Helicobacter pylori and ulcer healing in patients with acute duodenal ulcer using omeprazole based triple therapy. Aliment Pharmacol Ther (1999); 13: 289-295.

244. Fischbach L., Evans E.L. Meta-analysis: the effect of antibiotic resistance status on the efficacy of triple and quadruple first-line therapies for Helicobacter pylori. Aliment Pharmacol Ther (2007); 26: 343-357.

245. Wenzhen Y., Yumin L., Quanlin G., Kehu Y., Lei J., Donghai W., et al. Is antimicrobial susceptibility testing necessary before first-line treatment for Helicobacter pylori infection? Meta-analysis of randomized controlled trials. Intern Med (2010); 49: 1103-1109.

246. Chung K.H., Lee D.H., Jin E., Cho Y., Seo J.Y., Kim N., et al. The Efficacy of Moxifloxacin-Containing Triple Therapy after Standard Triple, Sequential, or Concomitant Therapy Failure for Helicobacter pylori Eradication in Korea. Gut Liver (2014); 8: 605-611.

247. Gisbert J.P., Calvet X., O'Connor J.P., Megraud F., O'Morain C.A. The sequential therapy regimen for Helicobacter pylori eradication. Expert Opin Pharmacother (2010); 11: 905-918.

248. Gisbert J.P., Calvet X., O'Connor A., Megraud F., O'Morain C.A. Sequential therapy for Helicobacter pylori eradication: a critical review. J Clin Gastroenterol (2010); 44: 313-325.

249. Vaira D., Zullo A., Vakil N., Gatta L., Ricci C., Perna F., et al. Sequential therapy versus standard triple-drug therapy for Helicobacter pylori eradication: a randomized trial. Ann Intern Med (2007); 146: 556-563.

250. Gisbert J.P., Calvet X. Review article: non-bismuth quadruple (concomitant) therapy for eradication of Helicobater pylori. Aliment Pharmacol Ther (2011); 34: 604-617.

251. Malfertheiner P., Megraud F., O'Morain C.A., Atherton J., Axon A.T., Bazzoli F., et al. Management of Helicobacter pylori infection--the Maastricht IV/ Florence Consensus Report. Gut (2012); 61: 646-664.

252. Pallen M.J., Clayton C.L. Vaccination against Helicobacter pylori urease. Lancet (1990); 336: 186-187.

253. Del Giudice G., Malfertheiner P., Rappuoli R. Development of vaccines against Helicobacter pylori. Expert Rev Vaccines (2009); 8: 1037-1049.

254. Kabir S. The current status of Helicobacter pylori vaccines: a review. Helicobacter (2007); 12: 89-102.

255. Chen M., Lee A., Hazell S. Immunisation against gastric helicobacter infection in a mouse/Helicobacter felis model. Lancet (1992); 339: 1120-1121.

256. Anderl F., Gerhard M. Helicobacter pylori vaccination: is there a path to protection? World J Gastroenterol (2014); 20: 11939-11949.

257. Guo L., Yin R., Liu K., Lv X., Li Y., Duan X., et al. Immunological features and efficacy of a multi-epitope vaccine CTB-UE against H. pylori in BALB/c mice model. Appl Microbiol Biotechnol (2014); 98: 3495-3507.

258. Wang B., Pan X., Wang H., Zhou Y., Zhu J., Yang J., et al. Immunological response of recombinant H. pylori multi-epitope vaccine with different vaccination strategies. Int J Clin Exp Pathol (2014); 7: 6559-6566.

259. Nystrom-Asklin J., Adamsson J., Harandi A.M. The adjuvant effect of CpG oligodeoxynucleotide linked to the non-toxic B subunit of cholera toxin for induction of immunity against H. pylori in mice. Scand J Immunol (2008); 67: 431-440.

260. Aebischer T., Bumann D., Epple H.J., Metzger W., Schneider T., Cherepnev G., et al. Correlation of T cell response and bacterial clearance in human volunteers challenged with Helicobacter pylori revealed by randomised controlled vaccination with Ty21a-based Salmonella vaccines. Gut (2008); 57: 1065-1072.

261. Malfertheiner P., Schultze V., Rosenkranz B., Kaufmann S.H., Ulrichs T., Novicki D., et al. Safety and immunogenicity of an intramuscular Helicobacter pylori vaccine in noninfected volunteers: a phase I study. Gastroenterology (2008); 135: 787-795.

262. DeLong E.F., Wickham G.S., Pace N.R. Phylogenetic stains: ribosomal RNA-based probes for the identification of single cells. Science (1989); 243: 1360-1363.

263. Guimaraes N., Azevedo N.F., Figueiredo C., Keevil C.W., Vieira M.J. Development and application of a novel peptide nucleic acid probe for the specific detection of Helicobacter pylori in gastric biopsies. J ClinMicrobiol (2007).

264. Wagner M., Horn M., Daims H. Fluorescence in situ hybridisation for the identification and characterisation of prokaryotes. Current Opinion in Microbiology (2003); 6: 302-309.

265. Amann R., Fuchs B.M. Single-cell identification in microbial communities by improved fluorescence in situ hybridization techniques. Nat Rev Microbiol (2008); 6: 339-348.

266. Amann R.I., Ludwig W., Schleifer K.H. Phylogenetic identification and in situ detection of individual microbial cells without cultivation. MicrobiolRev (1995); 59: 143-169.

267. Amann R.I., Krumholz L., Stahl D.A. Fluorescent-oligonucleotide probing of whole cells for determinative, phylogenetic, and environmental studies in microbiology. J Bacteriol (1990); 172: 762-770.

268. Makristathis A., Riss S., Hirschl A.M. A novel fluorescence in situ hybridization test for rapid pathogen identification in positive blood cultures. Clinical Microbiology and Infection (2014): n/a-n/a.

269. Harris D.M., Hata D.J. Rapid identification of bacteria and Candida using PNA-FISH from blood and peritoneal fluid cultures: a retrospective clinical study. Ann Clin Microbiol Antimicrob (2013); 12: 2.

270. Vega A.E., Alarcon T., Domingo D., Lopez-Brea M. Detection of clarithromycin-resistant Helicobacter pylori in frozen gastric biopsies from pediatric patients by a commercially available fluorescent in situ hybridization. Diagn Microbiol Infect Dis (2007); 59: 421-423.

271. Cerqueira L., Fernandes R.M., Ferreira R.M., Oleastro M., Carneiro F., Brandao C., et al. Validation of a fluorescence in situ hybridization method using peptide nucleic acid probes for detection of Helicobacter pylori clarithromycin resistance in gastric biopsy specimens. J Clin Microbiol (2013); 51: 1887-1893.

272. Wallner G., Fuchs B., Spring S., Beisker W., Amann R. Flow sorting of microorganisms for molecular analysis. Appl Environ Microbiol (1997); 63: 4223-4231.

273. Lawley B., Tannock G.W. Nucleic acid-based methods to assess the composition and function of the bowel microbiota. Gastroenterol Clin North Am (2012); 41: 855-868.

274. Quast C., Pruesse E., Yilmaz P., Gerken J., Schweer T., Yarza P., et al. The SILVA ribosomal RNA gene database project: improved data processing and web-based tools. Nucleic Acids Res (2013); 41: D590-596.

275. Cole J.R., Wang Q., Fish J.A., Chai B., McGarrell D.M., Sun Y., et al. Ribosomal Database Project: data and tools for high throughput rRNA analysis. Nucleic Acids Res (2014); 42: D633-642.

276. Zhang H. Alignment of BLAST high-scoring segment pairs based on the longest increasing subsequence algorithm. Bioinformatics (2003); 19: 1391-1396.

277. Berlier J.E., Rothe A., Buller G., Bradford J., Gray D.R., Filanoski B.J., et al. Quantitative comparison of long-wavelength Alexa Fluor dyes to Cy dyes: fluorescence of the dyes and their bioconjugates. J Histochem Cytochem (2003); 51: 1699-1712.

278. Hayashi-Takanaka Y., Stasevich T.J., Kurumizaka H., Nozaki N., Kimura H. Evaluation of Chemical Fluorescent Dyes as a Protein Conjugation Partner for Live Cell Imaging. PLoS ONE (2014); 9: e106271.

279. Hugenholtz P., Tyson G.W., Blackall L.L. Design and evaluation of 16S rRNA-targeted oligonucleotide probes for fluorescence in situ hybridization. Methods Mol Biol (2002); 179: 29-42.

280. Behrens S., Fuchs B.M., Mueller F., Amann R. Is the in situ accessibility of the 16S rRNA of Escherichia coli for Cy3-labeled oligonucleotide probes predicted by a three-dimensional structure model of the 30S ribosomal subunit? Appl Environ Microbiol (2003); 69: 4935-4941.

281. Yilmaz L.S., Noguera D.R. Mechanistic approach to the problem of hybridization efficiency in fluorescent in situ hybridization. Appl Environ Microbiol (2004); 70: 7126-7139.

282. Hoshino T., Yilmaz L.S., Noguera D.R., Daims H., Wagner M. Quantification of target molecules needed to detect microorganisms by fluorescence in situ hybridization (FISH) and catalyzed reporter deposition-FISH. Appl Environ Microbiol (2008); 74: 5068-5077.

283. Eltoum I., Fredenburgh, J, Grizzle, WE Advanced concepts in fixation: 1. Effects of fixation on immunohistochemistry, reversibility of fixation and recovery of proteins, nucleic acids, and other molecules from fixed and processed tissues. 2. Developmental methods of fixation. J Histotechnol (2001); 24: 201-210.

284. Rait V.K., Zhang Q., Fabris D., Mason J.T., O'Leary T.J. Conversions of formaldehyde-modified 2'-deoxyadenosine 5'-monophosphate in conditions modeling formalin-fixed tissue dehydration. J Histochem Cytochem (2006); 54: 301-310.

285. Meade A.D., Clarke C., Draux F., Sockalingum G.D., Manfait M., Lyng F.M., et al. Studies of chemical fixation effects in human cell lines using Raman microspectroscopy. Anal Bioanal Chem (2010); 396: 1781-1791.

286. Rhodes A. Fixation of tissues. In: Suvarna KS LC, Bancroft JD., editor. Bancroft's Theory and Practice of Histological Techniques.(2012): Churchill Livingstone.

287. Silverman A.P., Kool E.T. Quenched autoligation probes allow discrimination of live bacterial species by single nucleotide differences in rRNA. Nucleic Acids Res (2005); 33: 4978-4986.

288. Silverman A.P., Abe H., Kool E.T. Quenched autoligation probes. Methods Mol Biol (2008); 429: 161-170.

289. Yilmaz S., Haroon M.F., Rabkin B.A., Tyson G.W., Hugenholtz P. Fixation-free fluorescence in situ hybridization for targeted enrichment of microbial populations. ISME J (2010); 4: 1352-1356.

290. Namimatsu S., Ghazizadeh M., Sugisaki Y. Reversing the effects of formalin fixation with citraconic anhydride and heat: a universal antigen retrieval method. J Histochem Cytochem (2005); 53: 3-11.

291. Roller C., Wagner M., Amann R., Ludwig W., Schleifer K.H. In situ probing of gram-positive bacteria with high DNA G+C content using 23S rRNA-targeted oligonucleotides. Microbiology (1995); 141 (Pt 5): 1267.

292. Friedrich U., Naismith M.M., Altendorf K., Lipski A. Community Analysis of Biofilters Using Fluorescence In Situ Hybridization Including a New Probe for theXanthomonas Branch of the ClassProteobacteria. Appl Environ Microbiol (1999); 65: 3547-3554.

293. Schumann P. E. Stackebrandt and M. Goodfellow (Editors), Nucleic Acid Techniques in Bacterial Systematics (Modern Microbiological Methods). XXIX + 329 S., 46 Abb., 28 Tab. Chichester — New York — Brisbane — Toronto — Singapore 1991. John Wiley & Sons. $ 55.00. ISBN: 0–471–92906–9. Journal of Basic Microbiology (1991); 31: 479-480.

294. Yilmaz L.S., Noguera D.R. Development of thermodynamic models for simulating probe dissociation profiles in fluorescence in situ hybridization. Biotechnol Bioeng (2007); 96: 349-363.

295. Levine L., Gordon J.A., Jencks W.P. The relationship of structure to the effectiveness of denaturing agents for deoxyribonucleic acid. Biochemistry (1963); 2: 168-175.

296. Helmkamp G.K., Ts'O P.O. Secondary structures of nucleic acids in organic solvents. III. Relationship of optical properties to conformation. Biochim Biophys Acta (1962); 55: 601-608.

297. Geiduschek E.P., Herskovits T.T. Nonaqueous solutions of DNA. Reversible and irreversible denaturation in methanol. Arch Biochem Biophys (1961); 95: 114-129.

298. Sander H., Alkemeyer M., Haensel R. [On Solanum dulcamara L. 4. Chemical differentiation of the inner half of the species and isolation of soladulcidine tetraoside]. Arch Pharm (1962); 295/67: 6-12.

299. McConaughy B.L., Laird C.D., McCarthy B.J. Nucleic acid reassociation in formamide. Biochemistry (1969); 8: 3289-3295.

300. Record M.T., Jr. Electrostatic effects on polynucleotide transitions. I. Behavior at neutral pH. Biopolymers (1967); 5: 975-992.

301. Casey J., Davidson N. Rates of formation and thermal stabilities of RNA:DNA and DNA:DNA duplexes at high concentrations of formamide. Nucleic Acids Res (1977); 4: 1539-1552.

302. Hutton J.R. Renaturation kinetics and thermal stability of DNA in aqueous solutions of formamide and urea. Nucleic Acids Res (1977); 4: 3537-3555.

303. Lawson T.S., Connally R.E., Vemulpad S., Piper J.A. Dimethyl formamide-free, urea-NaCl fluorescence in situ hybridization assay for Staphylococcus aureus. Lett Appl Microbiol (2012); 54: 263-266.

304. Schildkraut C. Dependence of the melting temperature of DNA on salt concentration. Biopolymers (1965); 3: 195-208.

305. Bouvier T., Del Giorgio P.A. Factors influencing the detection of bacterial cells using fluorescence in situ hybridization (FISH): A quantitative review of published reports. FEMS Microbiology Ecology (2003); 44: 3-15.

306. Wessendorf M.W., Brelje T.C. Which fluorophore is brightest? A comparison of the staining obtained using fluorescein, tetramethylrhodamine, lissamine rhodamine, Texas red, and cyanine 3.18. Histochemistry (1992); 98: 81-85.

307. Kubota K., Ohashi A., Imachi H., Harada H. Improved in situ hybridization efficiency with locked-nucleic-acid-incorporated DNA probes. Appl Environ Microbiol (2006); 72: 5311-5317.

308. Wilks S.A., Keevil C.W. Targeting Species-Specific Low-Affinity 16S rRNA Binding Sites by Using Peptide Nucleic Acids for Detection of Legionellae in Biofilms. Applied and Environmental Microbiology (2006); 72: 5453-5462.
309. Nakano S., Fujii M., Sugimoto N. Use of nucleic Acid analogs for the study of nucleic Acid interactions. J Nucleic Acids (2011); 2011: 967098.
310. Boutorine A.S., Novopashina D.S., Krasheninina O.A., Nozeret K., Venyaminova A.G. Fluorescent probes for nucleic Acid visualization in fixed and live cells. Molecules (2013); 18: 15357-15397.
311. Pichon C., Goncalves C., Midoux P. Histidine-rich peptides and polymers for nucleic acids delivery. Adv Drug Deliv Rev (2001); 53: 75-94.
312. Hope M.J. Enhancing siRNA delivery by employing lipid nanoparticles. Ther Deliv (2014); 5: 663-673.
313. Kool E.T. Preorganization of DNA: Design Principles for Improving Nucleic Acid Recognition by Synthetic Oligonucleotides. Chem Rev (1997); 97: 1473-1488.
314. Wagner R.W., Matteucci M.D., Lewis J.G., Gutierrez A.J., Moulds C., Froehler B.C. Antisense gene inhibition by oligonucleotides containing C-5 propyne pyrimidines. Science (1993); 260: 1510-1513.
315. Crooke S.T. Therapeutic applications of oligonucleotides. Annu Rev Pharmacol Toxicol (1992); 32: 329-376.
316. Nielsen P.E. DNA Analogues with Nonphosphodiester Backbones. Annual Review of Biophysics and Biomolecular Structure (1995); 24: 167-183.
317. Veedu R.N., Wengel J. Locked nucleic acid nucleoside triphosphates and polymerases: on the way towards evolution of LNAaptamers. Molecular BioSystems (2009); 5: 787-792.
318. Lee Y.S., Park S.M., Kim H.M., Park S.K., Lee K., Lee C.W., et al. C5-Modified nucleosides exhibiting anticancer activity. Bioorg Med Chem Lett (2009); 19: 4688-4691.
319. Lesnik E.A., Guinosso C.J., Kawasaki A.M., Sasmor H., Zounes M., Cummins L.L., et al. Oligodeoxynucleotides containing 2'-O-modified adenosine: synthesis and effects on stability of DNA:RNA duplexes. Biochemistry (1993); 32: 7832-7838.
320. Nielsen C.B., Singh S.K., Wengel J., Jacobsen J.P. The solution structure of a locked nucleic acid (LNA) hybridized to DNA. J Biomol Struct Dyn (1999); 17: 175-191.
321. Egholm M., Buchardt O., Christensen L., Behrens C., Freier S.M., Driver D.A., et al. PNA hybridizes to complementary oligonucleotides obeying the Watson-Crick hydrogen-bonding rules. Nature (1993); 365: 566-568.
322. Jensen T.B., Langkjaer N., Wengel J. Unlocked nucleic acid (UNA) and UNA derivatives: thermal denaturation studies. Nucleic Acids Symp Ser (Oxf) (2008): 133-134.
323. Stein C.A., Tonkinson J.L., Yakubov L. Phosphorothioate oligodeoxynucleotides--anti-sense inhibitors of gene expression? Pharmacol Ther (1991); 52: 365-384.

324. Smith C.D., Ashbolt N.J. The fate of Helicobacter pylori phagocytized by Acanthamoeba polyphaga demonstrated by fluorescent in situ hybridization and quantitative polymerization chain reaction tests. Curr Microbiol (2012); 65: 805-812.

325. Lawson T.S., Connally R.E., Vemulpad S., Piper J.A. Optimization of a two-step permeabilization fluorescence in situ hybridization (FISH) assay for the detection of Staphylococcus aureus. J Clin Lab Anal (2011); 25: 359-365.

326. Roger L.C., McCartney A.L. Longitudinal investigation of the faecal microbiota of healthy full-term infants using fluorescence in situ hybridization and denaturing gradient gel electrophoresis. Microbiology (2010); 156: 3317-3328.

327. Fontenete S., Guimaraes N., Leite M., Figueiredo C., Wengel J., Azevedo N.F. Hybridization-Based Detection of Helicobacter pylori at Human Body Temperature Using Advanced Locked Nucleic Acid (LNA) Probes. PLoS One (2013); 8: e81230.

328. Kumar R., Singh S.K., Koshkin A.A., Rajwanshi V.K., Meldgaard M., Wengel J. The first analogues of LNA (locked nucleic acids): phosphorothioate-LNA and 2'-thio-LNA. Bioorg Med Chem Lett (1998); 8: 2219-2222.

329. Guimaraes N., Azevedo N.F., Figueiredo C., Keevil C.W., Vieira M.J. Development and application of a novel peptide nucleic acid probe for the specific detection of Helicobacter pylori in gastric biopsy specimens. J Clin Microbiol (2007); 45: 3089-3094.

330. Mishra S., Ghosh S., Mukhopadhyay R. Maximizing mismatch discrimination by surface-tethered locked nucleic acid probes via ionic tuning. Anal Chem (2013); 85: 1615-1623.

331. Mishra S., Ghosh S., Mukhopadhyay R. Ordered self-assembled locked nucleic acid (LNA) structures on gold(111) surface with enhanced single base mismatch recognition capability. Langmuir (2012); 28: 4325-4333.

332. Silahtaroglu A., Pfundheller H., Koshkin A., Tommerup N., Kauppinen S. LNA-modified oligonucleotides are highly efficient as FISH probes. Cytogenet Genome Res (2004); 107: 32-37.

333. Robertson K.L., Vora G.J. Locked nucleic acid and flow cytometry-fluorescence in situ hybridization for the detection of bacterial small noncoding RNAs. Appl Environ Microbiol (2012); 78: 14-20.

334. Obika S., Nanbu D., Hari Y., Morio K., In Y., Ishida T., et al. Synthesis of 2'-O,4'-C-methyleneuridine and -cytidine. Novel bicyclic nucleosides having a fixed C-3,-endo sugar puckering. Tetrahedron Letters (1997); 38: 8735-8738.

335. Kierzek E., Ciesielska A., Pasternak K., Mathews D.H., Turner D.H., Kierzek R. The influence of locked nucleic acid residues on the thermodynamic properties of 2'-O-methyl RNA/RNA heteroduplexes. Nucleic Acids Res (2005); 33: 5082-5093.

336. Kierzek E., Pasternak A., Pasternak K., Gdaniec Z., Yildirim I., Turner D.H., et al. Contributions of stacking, preorganization, and hydrogen bonding to the thermodynamic stability of duplexes between RNA and 2'-O-methyl RNA with locked nucleic acids. Biochemistry (2009); 48: 4377-4387.

337. Kurreck J., Wyszko E., Gillen C., Erdmann V.A. Design of antisense oligonucleotides stabilized by locked nucleic acids. Nucleic Acids Res (2002); 30: 1911-1918.

338. Grunweller A., Hartmann R.K. Locked nucleic acid oligonucleotides: the next generation of antisense agents? BioDrugs (2007); 21: 235-243.

339. Vester B., Wengel J. LNA (locked nucleic acid): high-affinity targeting of complementary RNA and DNA. Biochemistry (2004); 43: 13233-13241.

340. Zhang Y., Qu Z., Kim S., Shi V., Liao B., Kraft P., et al. Down-modulation of cancer targets using locked nucleic acid (LNA)-based antisense oligonucleotides without transfection. Gene Ther (2011); 18: 326-333.

341. Castoldi M., Schmidt S., Benes V., Noerholm M., Kulozik A.E., Hentze M.W., et al. A sensitive array for microRNA expression profiling (miChip) based on locked nucleic acids (LNA). RNA (2006); 12: 913-920.

342. Varallyay E., Burgyan J., Havelda Z. MicroRNA detection by northern blotting using locked nucleic acid probes. Nat Protoc (2008); 3: 190-196.

343. Liang R., Kierzek E., Kierzek R., Turner D.H. Comparisons between chemical mapping and binding to isoenergetic oligonucleotide microarrays reveal unexpected patterns of binding to the Bacillus subtilis RNase P RNA specificity domain. Biochemistry (2010); 49: 8155-8168.

344. Kloosterman W.P., Wienholds E., de Bruijn E., Kauppinen S., Plasterk R.H. In situ detection of miRNAs in animal embryos using LNA-modified oligonucleotide probes. Nat Methods (2006); 3: 27-29.

345. Silahtaroglu A.N., Nolting D., Dyrskjot L., Berezikov E., Moller M., Tommerup N., et al. Detection of microRNAs in frozen tissue sections by fluorescence in situ hybridization using locked nucleic acid probes and tyramide signal amplification. Nat Protoc (2007); 2: 2520-2528.

346. Frieden M., Orum H. Locked nucleic acid holds promise in the treatment of cancer. Curr Pharm Des (2008); 14: 1138-1142.

347. Jepsen J.S., Wengel J. LNA-antisense rivals siRNA for gene silencing. Curr Opin Drug Discov Devel (2004); 7: 188-194.

348. Karlsen K.K., Wengel J. Locked nucleic acid and aptamers. Nucleic Acid Ther (2012); 22: 366-370.

349. Kaur H., Babu B.R., Maiti S. Perspectives on chemistry and therapeutic applications of Locked Nucleic Acid (LNA). Chem Rev (2007); 107: 4672-4697.

350. Stenvang J., Silahtaroglu A.N., Lindow M., Elmen J., Kauppinen S. The utility of LNA in microRNA-based cancer diagnostics and therapeutics. Semin Cancer Biol (2008); 18: 89-102.

351. Randazzo A., Esposito V., Ohlenschläger O., Ramachandran R., Mayol L. NMR solution structure of a parallel LNA quadruplex. Nucleic Acids Research (2004); 32: 3083-3092.

352. Piao X., Yan Y., Yan J., Guan Y. Enhanced recognition of non-complementary hybridization by single-LNA-modified oligonucleotide probes. Anal Bioanal Chem (2009); 394: 1637-1643.

353. Kaur H., Arora A., Wengel J., Maiti S. Thermodynamic, counterion, and hydration effects for the incorporation of locked nucleic acid nucleotides into DNA duplexes. Biochemistry (2006); 45: 7347-7355.

354. Owczarzy R., You Y., Groth C.L., Tataurov A.V. Stability and mismatch discrimination of locked nucleic acid-DNA duplexes. Biochemistry (2011); 50: 9352-9367.

355. Umemoto T., Wengel J., Madsen A.S. Functionalization of 2'-amino-LNA with additional nucleobases. Org Biomol Chem (2009); 7: 1793-1797.

356. Inoue H., Hayase Y., Imura A., Iwai S., Miura K., Ohtsuka E. Synthesis and hybridization studies on two complementary nona(2'-O-methyl)ribonucleotides. Nucleic Acids Res (1987); 15: 6131-6148.

357. Molenaar C., Marras S.A., Slats J.C., Truffert J.C., Lemaitre M., Raap A.K., et al. Linear 2' O-Methyl RNA probes for the visualization of RNA in living cells. Nucleic Acids Res (2001); 29: E89-89.

358. Majlessi M., Nelson N.C., Becker M.M. Advantages of 2'-O-methyl oligoribonucleotide probes for detecting RNA targets. Nucleic Acids Res (1998); 26: 2224-2229.

359. Soe M.J., Moller T., Dufva M., Holmstrom K. A sensitive alternative for microRNA in situ hybridizations using probes of 2'-O-methyl RNA + LNA. J Histochem Cytochem (2011); 59: 661-672.

360. Jirka S.M., Heemskerk H., Tanganyika-de Winter C.L., Muilwijk D., Pang K.H., de Visser P.C., et al. Peptide conjugation of 2'-O-methyl phosphorothioate antisense oligonucleotides enhances cardiac uptake and exon skipping in mdx mice. Nucleic Acid Ther (2014); 24: 25-36.

361. Nafee N., Schneider M., Friebel K., Dong M., Schaefer U.F., Murdter T.E., et al. Treatment of lung cancer via telomerase inhibition: self-assembled nanoplexes versus polymeric nanoparticles as vectors for 2'-O-Methyl-RNA. Eur J Pharm Biopharm (2012); 80: 478-489.

362. Wang M., Wu B., Lu P., Tucker J.D., Milazi S., Shah S.N., et al. Pluronic-PEI copolymers enhance exon-skipping of 2'-O-methyl phosphorothioate oligonucleotide in cell culture and dystrophic mdx mice. Gene Ther (2014); 21: 52-59.

363. Dong M., Murdter T.E., Philippi C., Loretz B., Schaefer U.F., Lehr C.M., et al. Pulmonary delivery and tissue distribution of aerosolized antisense 2'-O-Methyl RNA containing nanoplexes in the isolated perfused and ventilated rat lung. Eur J Pharm Biopharm (2012); 81: 478-485.

364. Nafee N., Taetz S., Schneider M., Schaefer U.F., Lehr C.M. Chitosan-coated PLGA nanoparticles for DNA/RNA delivery: effect of the formulation parameters on complexation and transfection of antisense oligonucleotides. Nanomedicine (2007); 3: 173-183.

365. Yoo H., Juliano R.L. Enhanced delivery of antisense oligonucleotides with fluorophore-conjugated PAMAM dendrimers. Nucleic Acids Res (2000); 28: 4225-4231.

366. Pasternak A., Wengel J. Unlocked nucleic acid--an RNA modification with broad potential. Org Biomol Chem (2011); 9: 3591-3597.

367. Pasternak A., Wengel J. Thermodynamics of RNA duplexes modified with unlocked nucleic acid nucleotides. Nucleic Acids Res (2010); 38: 6697-6706.

368. Nielsen P., Dreioe L.H., Wengel J. Synthesis and evaluation of oligodeoxynucleotides containing acyclic nucleosides: introduction of three novel analogues and a summary. Bioorg Med Chem (1995); 3: 19-28.

369. Langkjaer N., Pasternak A., Wengel J. UNA (unlocked nucleic acid): a flexible RNA mimic that allows engineering of nucleic acid duplex stability. Bioorg Med Chem (2009); 17: 5420-5425.

370. Campbell M.A., Wengel J. Locked vs. unlocked nucleic acids (LNA vs. UNA): contrasting structures work towards common therapeutic goals. Chem Soc Rev (2011); 40: 5680-5689.

371. Fluiter K., Mook O.R., Vreijling J., Langkjaer N., Hojland T., Wengel J., et al. Filling the gap in LNA antisense oligo gapmers: the effects of unlocked nucleic acid (UNA) and 4'-C-hydroxymethyl-DNA modifications on RNase H recruitment and efficacy of an LNA gapmer. Mol Biosyst (2009); 5: 838-843.

372. Bramsen J.B., Pakula M.M., Hansen T.B., Bus C., Langkjaer N., Odadzic D., et al. A screen of chemical modifications identifies position-specific modification by UNA to most potently reduce siRNA off-target effects. Nucleic Acids Res (2010); 38: 5761-5773.

373. Karlsen K.K., Pasternak A., Jensen T.B., Wengel J. Pyrene-Modified Unlocked Nucleic Acids: Synthesis, Thermodynamic Studies, and Fluorescent Properties. Chembiochem (2012).

374. Nielsen P.E., Egholm M., Berg R.H., Buchardt O. Sequence-selective recognition of DNA by strand displacement with a thymine-substituted polyamide. Science (1991); 254: 1497-1500.

375. Demidov V.V., Frank-Kamenetskii M.D. Sequence-specific targeting of duplex DNA by peptide nucleic acids via triplex strand invasion. Methods (2001); 23: 108-122.

376. Guo S., Du D., Tang L., Ning Y., Yao Q., Zhang G.J. PNA-assembled graphene oxide for sensitive and selective detection of DNA. Analyst (2013); 138: 3216-3220.

377. Rasmussen H., Kastrup J.S., Nielsen J.N., Nielsen J.M., Nielsen P.E. Crystal structure of a peptide nucleic acid (PNA) duplex at 1.7 A resolution. Nat Struct Biol (1997); 4: 98-101.

378. Seo Y.J., Lim J., Lee E.H., Ok T., Yoon J., Lee J.H., et al. Base pair opening kinetics study of the aegPNA:DNA hydrid duplex containing a site-specific GNA-like chiral PNA monomer. Nucleic Acids Res (2011); 39: 7329-7335.

379. Sen A., Nielsen P.E. Unique properties of purine/pyrimidine asymmetric PNA.DNA duplexes: differential stabilization of PNA.DNA duplexes by purines in the PNA strand. Biophys J (2006); 90: 1329-1337.

380. Demidov V.V., Potaman V.N., Frank-Kamenetskii M.D., Egholm M., Buchard O., Sonnichsen S.H., et al. Stability of peptide nucleic acids in human serum and cellular extracts. Biochem Pharmacol (1994); 48: 1310-1313.

381. Jensen K.K., Orum H., Nielsen P.E., Norden B. Kinetics for hybridization of peptide nucleic acids (PNA) with DNA and RNA studied with the BIAcore technique. Biochemistry (1997); 36: 5072-5077.

382. Giesen U., Kleider W., Berding C., Geiger A., Orum H., Nielsen P.E. A formula for thermal stability (Tm) prediction of PNA/DNA duplexes. Nucleic Acids Res (1998); 26: 5004-5006.

383. Demidov V., Frank-Kamenetskii M.D., Egholm M., Buchardt O., Nielsen P.E. Sequence selective double strand DNA cleavage by peptide nucleic acid (PNA) targeting using nuclease S1. Nucleic Acids Res (1993); 21: 2103-2107.

384. Zhang N., Apella D.H. Advantages of peptide nucleic acids as diagnostic platforms for detection of nucleic acids in resource-limited settings. Journal of Infectious Diseases (2010); 201: S42-S45.

385. Zhang N., Appella D.H. Colorimetric detection of anthrax DNA with a Peptide nucleic acid sandwich-hybridization assay. J Am Chem Soc (2007); 129: 8424-8425.

386. Grossmann T.N., Roglin L., Seitz O. Target-catalyzed transfer reactions for the amplified detection of RNA. Angew Chem Int Ed Engl (2008); 47: 7119-7122.

387. Feriotto G., Corradini R., Sforza S., Bianchi N., Mischiati C., Marchelli R., et al. Peptide nucleic acids and biosensor technology for real-time detection of the cystic fibrosis W1282X mutation by surface plasmon resonance. Lab Invest (2001); 81: 1415-1427.

388. Fazli M., Bjarnsholt T., Hoiby N., Givskov M., Tolker-Nielsen T. PNA-based fluorescence in situ hybridization for identification of bacteria in clinical samples. Methods Mol Biol (2014); 1211: 261-271.

389. Deck M.K., Anderson E.S., Buckner R.J., Colasante G., Davis T.E., Coull J.M., et al. Rapid detection of Enterococcus spp. direct from blood culture bottles using Enterococcus QuickFISH method: a multicenter investigation. Diagn Microbiol Infect Dis (2014); 78: 338-342.

390. Stone N.R., Gorton R.L., Barker K., Ramnarain P., Kibbler C.C. Evaluation of PNA-FISH yeast traffic light for rapid identification of yeast directly from positive blood cultures and assessment of clinical impact. J Clin Microbiol (2013); 51: 1301-1302.

391. Hagiwara T., Hattori J., Kaneda T. PNA-in situ hybridization method for detection of HIV-1 DNA in virus-infected cells and subsequent detection of cellular and viral proteins. Methods Mol Biol (2006); 326: 139-149.

392. Stender H., Lund K., Petersen K.H., Rasmussen O.F., Hongmanee P., Miörner H., et al. Fluorescence In Situ Hybridization Assay Using Peptide Nucleic Acid Probes for Differentiation between Tuberculous and Nontuberculous Mycobacterium Species in Smears of Mycobacterium Cultures. Journal of Clinical Microbiology (1999); 37: 2760-2765.

393. Oliveira K., Procop G.W., Wilson D., Coull J., Stender H. Rapid identification of Staphylococcus aureus directly from blood cultures by fluorescence in situ hybridization with peptide nucleic acid probes. J Clin Microbiol (2002); 40: 247-251.

394. Tinoco Jr I., Bustamante C. How RNA folds. Journal of Molecular Biology (1999); 293: 271-281.

395. Shen Y., Shrestha R., Ibricevic A., Gunsten S.P., Welch M.J., Wooley K.L., et al. Antisense peptide nucleic acid-functionalized cationic nanocomplex for in vivo mRNA detection. Interface Focus (2013); 3: 20120059.

396. Wittung P., Kajanus J., Edwards K., Haaima G., Nielsen P.E., Norden B., et al. Phospholipid membrane permeability of peptide nucleic acid. FEBS Lett (1995); 375: 27-29.

397. Good L., Sandberg R., Larsson O., Nielsen P.E., Wahlestedt C. Antisense PNA effects in Escherichia coli are limited by the outer-membrane LPS layer. Microbiology (2000); 146 (Pt 10): 2665-2670.

398. Püschl A., Sforza S., Haaima G., Dahl O., Nielsen P.E. Peptide nucleic acids (PNAs) with a functional backbone. Tetrahedron Letters (1998); 39: 4707-4710.

399. Winssinger N., Gorska K., Ciobanu M., Daguer J., Barluenga S.Assembly of PNA-Tagged Small Molecules, Peptides, and Carbohydrates onto DNA Templates: Programming the Combinatorial Pairing and Inter-ligand Distance. In: Nielsen PE, Appella DH, editors. Peptide Nucleic Acids. (2014): Humana Press. pp. 95-110.

400. Hensley D.M., Tapia R., Encina Y. An evaluation of the advandx Staphylococcus aureus/CNS PNA FISH assay. Clin Lab Sci (2009); 22: 30-33.

401. Oliveira K., Brecher S.M., Durbin A., Shapiro D.S., Schwartz D.R., De Girolami P.C., et al. Direct identification of Staphylococcus aureus from positive blood culture bottles. J Clin Microbiol (2003); 41: 889-891.

402. Deck M.K., Anderson E.S., Buckner R.J., Colasante G., Coull J.M., Crystal B., et al. Multicenter evaluation of the Staphylococcus QuickFISH method for simultaneous identification of Staphylococcus aureus and coagulase-negative staphylococci directly from blood culture bottles in less than 30 minutes. J Clin Microbiol (2012); 50: 1994-1998.

403. Salimnia H., Fairfax M.R., Lephart P., Morgan M., Gilbreath J.J., Butler-Wu S.M., et al. An International, Prospective, Multi-Center Evaluation of the Combination of the AdvanDx Staphylococcus QuickFISH BC with the mecA XpressFISH for the Detection of Methicillin-Resistant Staphylococcus aureus from Positive Blood Cultures. J Clin Microbiol (2014).

404. Gonzalez V., Padilla E., Gimenez M., Vilaplana C., Perez A., Fernandez G., et al. Rapid diagnosis of Staphylococcus aureus bacteremia using S. aureus PNA FISH. Eur J Clin Microbiol Infect Dis (2004); 23: 396-398.

405. Chapin K., Musgnug M. Evaluation of three rapid methods for the direct identification of Staphylococcus aureus from positive blood cultures. J Clin Microbiol (2003); 41: 4324-4327.

406. Eckstein F. Nucleoside phosphorothioates. J Am Chem Soc (1970); 92: 4718-4723.

407. Guga P., Koziolkiewicz M. Phosphorothioate nucleotides and oligonucleotides - recent progress in synthesis and application. Chem Biodivers (2011); 8: 1642-1681.

408. Lennox K.A., Sabel J.L., Johnson M.J., Moreira B.G., Fletcher C.A., Rose S.D., et al. Characterization of modified antisense oligonucleotides in Xenopus laevis embryos. Oligonucleotides (2006); 16: 26-42.

409. Orr R.M. Technology evaluation: fomivirsen, Isis Pharmaceuticals Inc/CIBA vision. Curr Opin Mol Ther (2001); 3: 288-294.

410. Wong E., Goldberg T. Mipomersen (kynamro): a novel antisense oligonucleotide inhibitor for the management of homozygous familial hypercholesterolemia. P T (2014); 39: 119-122.

411. Raal F.J., Santos R.D., Blom D.J., Marais A.D., Charng M.J., Cromwell W.C., et al. Mipomersen, an apolipoprotein B synthesis inhibitor, for lowering of LDL cholesterol concentrations in patients with homozygous familial hypercholesterolaemia: a randomised, double-blind, placebo-controlled trial. Lancet (2010); 375: 998-1006.

412. Piascik P. Fomiversen sodium approved to treat CMV retinitis. J Am Pharm Assoc (Wash) (1999); 39: 84-85.

413. Caruthers M.H., Beaucage S.L., Becker C., Efcavitch J.W., Fisher E.F., Galluppi G., et al. Deoxyoligonucleotide synthesis via the phosphoramidite method. Gene Amplif Anal (1983); 3: 1-26.

414. Brown T.B.a.T. Solid-phase oligonucleotide synthesis. In: ATDBio, editor. Nucleic Acids Book.(2005). http://www.atdbio.com/: ATDBio.

415. Pon R.T. Solid-phase supports for oligonucleotide synthesis. Curr Protoc Nucleic Acid Chem (2001); Chapter 3: Unit 3 1.

416. Wincott F.E. Strategies for oligoribonucleotide synthesis according to the phosphoramidite method. Curr Protoc Nucleic Acid Chem (2001); Chapter 3: Unit 3 5.

417. Brown T.B.a.T. Nucleic acid analogues. In: ATDBio, editor. Nucleic Acids Book.(2005). http://www.atdbio.com/.

418. Wagner M., Erhart R., Manz W., Amann R., Lemmer H., Wedi D., et al. Development of an Ribosomal-Rna-Targeted Oligonucleotide Probe Specific for the Genus Acinetobacter and Its Application for in-Situ Monitoring in Activated-Sludge. Appl Environ Microbiol (1994); 60: 792-800.

419. Manz W., Amann R., Szewzyk R., Szewzyk U., Stenstrom T.A., Hutzler P., et al. In-Situ Identification of Legionellaceae Using 16s Ribosomal-Rna-Targeted Oligonucleotide Probes and Confocal Laser-Scanning Microscopy. Microbiology-Sgm (1995); 141: 29-39.

420. Neef A., Amann R., Schleifer K.H. Detection of Microbial-Cells in Aerosols Using Nucleic-Acid Probes. Systematic and Applied Microbiology (1995); 18: 113-122.

421. SantaLucia J., Jr., Hicks D. The thermodynamics of DNA structural motifs. Annu Rev Biophys Biomol Struct (2004); 33: 415-440.

422. SantaLucia J., Jr., Allawi H.T., Seneviratne P.A. Improved nearest-neighbor parameters for predicting DNA duplex stability. Biochemistry (1996); 35: 3555-3562.

423. Bloomfield V.A. C.D.M., Tinoco I., , editor Nucleic Acids: Structures, Properties, and Functions. 1 edition ed.(2000); Sausalito, CA: University Science Books. 672 pages p.

424. SantaLucia J., Jr. A unified view of polymer, dumbbell, and oligonucleotide DNA nearest-neighbor thermodynamics. Proc Natl Acad Sci U S A (1998); 95: 1460-1465.

425. McTigue P.M., Peterson R.J., Kahn J.D. Sequence-dependent thermodynamic parameters for locked nucleic acid (LNA)-DNA duplex formation. Biochemistry (2004); 43: 5388-5405.

426. Nakano S.-i., Fujii M., Sugimoto N. Use of Nucleic Acid Analogs for the Study of Nucleic Acid Interactions. Journal of Nucleic Acids (2011); 2011: 11.

427. Karkare S., Bhatnagar D. Promising nucleic acid analogs and mimics: characteristic features and applications of PNA, LNA, and morpholino. Appl Microbiol Biotechnol (2006); 71: 575-586.

428. Veedu R.N., Wengel J. Locked Nucleic Acids: Promising Nucleic Acid Analogs for Therapeutic Applications. Chemistry & Biodiversity (2010); 7: 536-542.

Chapter II

Application of locked nucleic acid-based probes in fluorescence in situ hybridization

Application of locked nucleic acid-based probes in fluorescence *in situ* hybridization

Sílvia Fontenete[1,2,3,4,5], Daniel Carvalho[1], Nuno Guimarães[1,2,3,4], Pedro Madureira [2,5,6], Céu Figueiredo[2,3,7], Jesper Wengel[4], Nuno Filipe Azevedo[1].

[1] LEPABE , Laboratory for Process Engineering, Environment, Biotechnology and Energy, Faculty of Engineering, University of Porto, Porto, Portugal; [2] i3S, Instituto de Investigação e Inovação em Saúde, Universidade do Porto, Porto, Portugal. [3]IPATIMUP, Institute of Molecular Pathology and Immunology of the University of Porto, Porto, Portugal; [4] Nucleic Acid Center, Department of Physics, Chemistry and Pharmacy, University of Southern Denmark, Odense M, Denmark; [5] ICBAS, Institute of Biomedical Sciences Abel Salazar, University of Porto, Porto, Portugal; [6] IBMC, Institute for Molecular Biology and Cell Biology, Porto, Portugal; [7] FMUP, Faculty of Medicine of the University of Porto University, Porto, Portugal;

Abstract

Aim: Fluorescence *in situ* hybridization (FISH) employing nucleic acid mimics is becoming an emerging molecular tool in the microbiology area for the detection and visualization of microorganisms. However, the impact of using locked nucleic acid (LNA) and 2'-*O*-methyl RNA (2'OMe) modifications in the FISH procedure is unknown.

Methods: In this study we compared melting and hybridization efficiency properties of 18 different probes in regards to their use in FISH for the detection of the 16S rRNA of *Helicobacter pylori*.

Results: For the same sequence and target, the probe length and the type of nucleic acid mimics used as mixmers in LNA-based probes strongly influences the efficiency of detection. LNA probes with 10 to 15 mers showed the highest efficiency. Additionally, the combination of 2'OMe RNA with LNA allowed an increase on the fluorescence intensities of the probes.

Conclusion: Overall, these results have significant implications for the design and applications of LNA probes for the detection of microorganisms.

Keywords: FISH, Locked nucleic acids, urea, bacteria

2.1. Introduction

FISH is a technique commonly used for the identification of bacteria and other microorganisms [1]. One of the challenges in FISH is the design of adequate probes, that provide high hybridization efficiency [2]. As a way to overcome those challenges, probes modified with conformationally-restricted nucleotides such as LNA monomers have been used [3-5]. LNA probes can be designed jointly with DNA monomers or other types of chemical modifications, such as 2'-*O*-methyl RNA (2'OMe). Recent studies appear to indicate that the substitution of DNA monomers by 2'OMe monomers leads to superior hybridization efficiency in FISH [3,6]. Other types of modifications can be also added to LNA probes, such as the substitution of the regular PO backbone by PS. In a PS backbone, a sulfur atom substitutes one of the non-bridging oxygen atoms in the internucleoside linkages of a probe. This modification increases the resistance of a probe to nuclease degradation [7], and allows its application in therapeutic approaches [8,9]. However, the use of PS probes in FISH has not been systematically studied in the microbiology area.

In this paper we analyse the ability of different probes consisting of LNA/DNA and LNA/2'OMe and with different backbones (PO and PS) to target both naked RNA and the intracellular rRNA of *H. pylori*. We also compared the different types of FISH methodologies in attached and suspended bacteria. The efficiency of the probes was quantitatively evaluated using image analysis and flow cytometry (Figure 2.1).

2.2. Materials and Methods

2.2.1. Bacterial strains and culture conditions

H. pylori 26695 obtained from the American Type Culture Collection (ATCC 700392, VA, USA) was maintained on trypticase soy agar (TSA) supplemented with 5% (v/v) sheep blood (Becton Dickinson GmbH, Germany). Single colonies were streaked onto fresh media every 48 hours and the plates were incubated at 37 °C under microaerobic conditions. After the incubation time, biomass was scraped from the plate and suspended in water or saline (0.90% w/v of NaCl). Bacterial density was determined by the dilution of this initial culture to 1x 10^6 bacteria and the absorbance was measured at 600 nm.

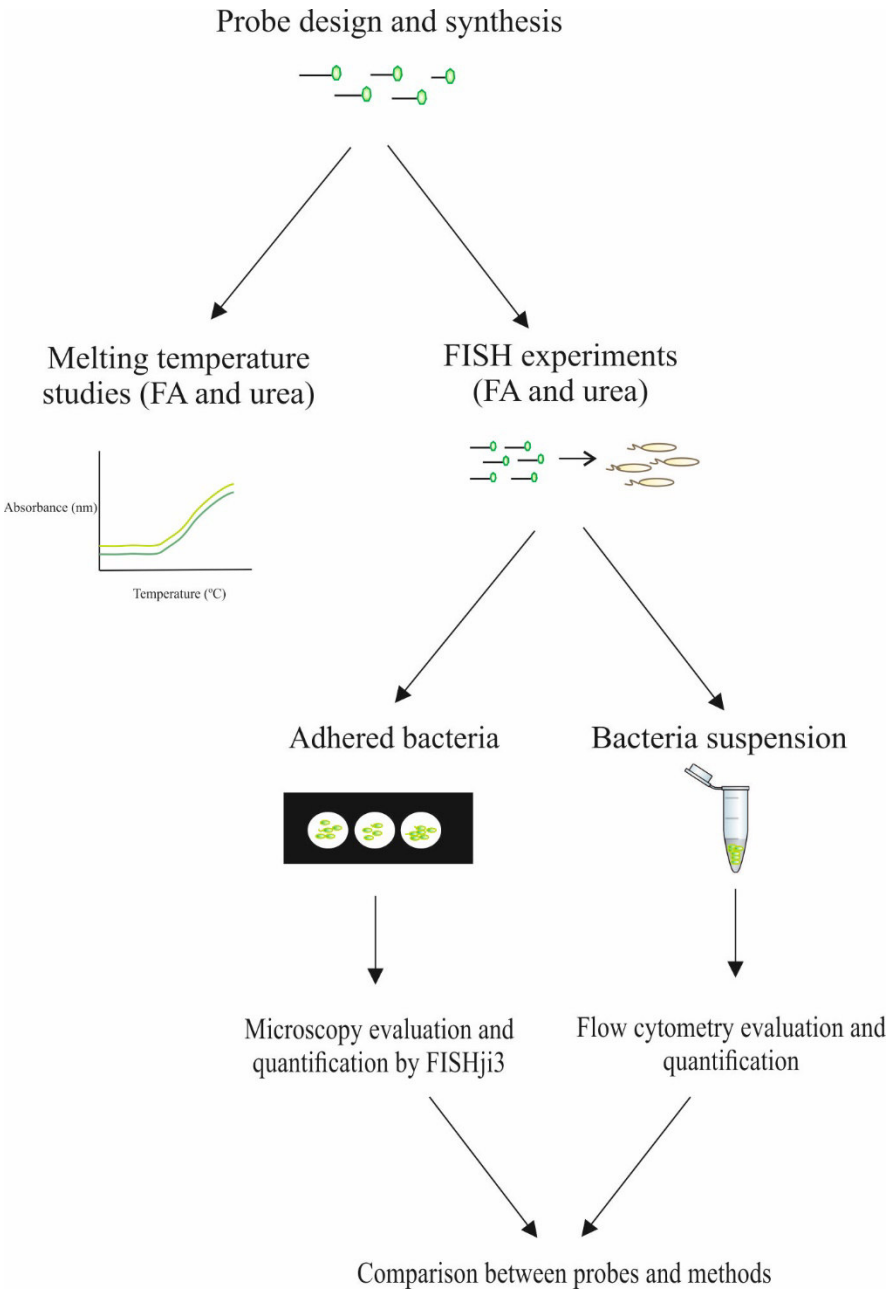

Figure 2.1 - Experimental flowchart for this study. The first step in this study was probe design using bioinformatics tools followed by thermodynamic analysis. Then, LNA advanced probes were synthetized based on standard phosphoramidite chemistry. The following step was to determine experimental melting temperature (T_m) of each probe using different buffers and denaturants (formamide, FA, and urea). FISH experiments using the same denaturants were also performed in pure cultures of *H. pylori* 26695. In these studies both attached bacteria and bacterial suspensions were used which were analysed by microscopy and flow cytometry, respectively. Finally, data from fluorescence intensities obtained from these two methods were compared.

2.2.2. Probe design and synthesis

The 16S rRNA target region for the probes was selected based on previous results from our group [10]. LNA-based probes (DNA/LNA and LNA/2'-OMe chimeras) of different lengths (Table 2.1) were designed based on previous reports [11-13]. Since LNA and 2'OMe substitutions are expected to increase duplex stability comparatively to LNA and DNA [14,15], and because LNA and 2'OMe probes can be designed to be shorter than unmodified DNA or RNA probes, we therefore tested probes with 10 to 18 monomers based on the indications obtained from thermodynamic parameters egg. free Gibbs energy [16]. The binding affinity towards RNA of LNA/2'OMe probes is expected to increase when compared to LNA/DNA. An optimal design is also expected to include LNA monomers alternated with other monomers as opposed to being sequential [13].

Probe sequences were compared against sequences of *H. pylori* and closely-related microorganisms using the freely available 16S rRNA database of the Ribosomal Database Project II (RDP-II), version 10 [17] to analyse the theoretical specificity and sensitivity of each individual probe, as described in Almeida *et al*. [18]. Only high-quality sequences with **≥** 1200 bp were used to perform this analysis [17]. All probes selected differed by at least two mismatches from non-*H. pylori* species. Probes were synthesized as described in [3] using a PerSpective Biosystems Expedite 8909 (Applied Biosystems, USA) nucleic acid synthesizer. The 5'-end of each probe was labelled by a fluorescein (FAM) phosphoramidite building block. LNA and 2'OMe phosphoramidite monomers were purchased from Exiqon (Copenhagen, Denmark) and Ribotask (Langeskov, Denmark), respectively.

Unmodified DNA and RNA sequences used in melting temperature (T_m) studies were obtained from Sigma-Aldrich (St. Louis, USA) and Integrated DNA Technologies (Leuven, Belgium), respectively.

2.2.3. Melting temperature (T_m) studies

The T_m values for duplexes involving RNA complementary strands were determined on PerkinElmer Lambda 35 UV/VIS spectrometer equipment with PTP 6 (Peltier Temperature Programmer). These studies were performed in different types of buffers; medium salt buffer with 110 mM Na^+ (100 mM NaCl, 10 mM NaH_2PO_4 and 0.1 mM EDTA, pH 7.0), medium salt buffer with 30% (v/v) formamide (FA), a low salt buffer of 10 mM Na^+ (10 mM NaCl, 0.5 mM EDTA, 5 mM Tris-HCl and 30% (v/v) FA, pH 7.5) and a high salt buffer of 900 mM Na^+ (900 mM NaCl, 5mM EDTA and 50 mM Tris, pH 7.5) and with 4M urea.

One µM of each probe and RNA complementary strand were mixed and denaturation at 85 °C for 5 min was performed followed by cooling to 15 °C prior to measurements.

Table 2.1 - Sequences of probes used in this study. Designs of the probes represented were based on thermodynamic parameters. All the probes were synthetised by *phosphoramidite chemistry*. LNA nucleotide monomers are represented with L superscript, 2'-OMe-RNA monomers in boldface letters, DNA nucleotides in capital letters, and phosphorothioate linkages by the symbol*

Probes analysed	Sequence
HP_18LNA_PO	5'- FAM GA^{L}GA^{L}CT^{L}AA^{L}GC^{L}CC^{L}TC^{L}CA^{L}AC^{L} -3'
HP_18LNA_PS	5'- FAM G*A^{L*}G*A^{L*}C*T^{L*}A*A^{L*}G*C^{L*}C*C^{L}*T*C^{L}*C*A^{L}*A*C^{L} -3'
HP_18LNA/2OMe_PO	5'- FAM G^{L}**AG**A^{L} **CU**A ^{L}**AG** C^{L}**CC**T^{L}**CC**A^{L}**AC** -3'
HP_ 18LNA/2OMe _PS	5'- FAM G^{L}*__A__*G*A^{L}*__C__*__U__*A^{L}*__A__*__G__*C^{L}*__C__*__C__*T^{L}*__C__*__C__*A^{L}*__A__*__C__ -3'
HP_15LNA_PO	5'- FAM GA^{L}GA^{L}CT^{L}AA^{L}GC^{L}CC^{L}TC^{L}C -3'
HP_15LNA_PO_2	5'- FAM GA^{L}GACT^{L}AAGC^{L}CCTC^{L}C -3'
HP_15LNA_PS	5'- FAM G*A^{L*}G*A^{L*}C*T^{L*}A*A^{L*}G*C^{L*}C*C^{L}*T*C^{L}C-3'
HP_15LNA_PS_2	5'- FAM G*A^{L}*G*A*C*T^{L}*A*A*G*C^{L}*C*C*T*C^{L}*C-3'
HP_15LNA/2OMe_PO	5'- FAM G^{L}**AG**A^{L} **CU**A ^{L}**AG** C^{L}**CC**T^{L}**CC**-3'
HP_ 15LNA/2OMe _PS	5'- FAM G^{L}*__A__*__G__*A^{L}*__C__*__U__*A^{L}*__A__*__G__*C^{L}*__C__*__C__*T^{L}*__C__*__C__-3'
HP_12LNA_PO	5'- FAM GA^{L}GA^{L}CT^{L}AA^{L}GC^{L}CC^{L}-3'
HP_12LNA_PS	5'- FAM G*A^{L*}G*A^{L*}C*T^{L*}A*A^{L*}G*C^{L*}C*C^{L}-3'
HP_12LNA/2OMe_PO	5'- FAM G^{L}**AG**A^{L} **CU**A ^{L}**AG** C^{L}**CC**-3'
HP_ 12LNA/2OMe _PS	5'- FAM G*A^{L*}G*A^{L*}C*T^{L*}A*A^{L*}G*C^{L*}C*C^{L}-3'
HP_10LNA_PO	5'- FAM GA^{L}GA^{L}CT^{L}AA^{L}GC^{L}-3'
HP_10LNA_PS	5'- FAM G*A^{L*}G*A^{L*}C*T^{L*}A*A^{L*}G*C^{L}-3'
HP_10LNA/2OMe_PO	5'- FAM G^{L}**AG**A^{L} **CU**A ^{L}**AG** C^{L}-3'
HP_ 10LNA/2OMe _PS	5'- FAM G^{L}*__A__*__G__*A^{L}*__C__*__U__*A^{L}*__A__*__G__*C^{L}-3'

Absorbance versus temperature melting temperatures were measured at 260 or 270 nm depending on the buffer in solution [19] (A_{260} vs. temperature for medium salt buffer and for high salt buffer; A_{270} vs. temperature for medium salt buffer with 30% (v/v) FA and for low salt buffer with 30% FA). A heating rate of 1.0 ºC/min from 15 °C to 85 °C was used. The T_m values provided in Table 2 and S1 were obtained from the maxima of the first derivatives of the melting curves and determined as an average of two measurements within ± 0.5 °C.

2.2.4. Hybridization procedure on slides

FISH on attached *bacteria* was performed as described in our previous study [3] with some modifications. After fixation and permeabilization of the smears with 4% (v/v) paraformaldehyde (15 min) and 50% (v/v) ethanol (15 min), the hybridization step was performed using 200 nM of each probe diluted in two different types of buffer. Because one of the goals of this study was to evaluate if the substitution of FA by urea was not detrimental, one of the buffers contained 50% (v/v) FA (Across Organic, New Jersey, US) and the other 4 M of urea (VWR BHD Prolabo, Haasrode, Belgium). The other reagents were common to both buffers: 10% (v/v) dextran sulphate (Fisher Scientific, MA, US), 0.1% (v/v) Triton-X (Panreac, Barcelona, Spain), 5 mM of EDTA disodium salt 2-hydrate (Panreac), 50 mM Tris-HCl (Fisher Scientific, New Jersey, US) and 900 mM NaCl (Panreac). The following steps were performed as previously described by Fontenete *et al.,* [3]. Samples were covered by coverslips, place in moist chamber in an incubator at the temperature in study and incubated during 90 minutes. After hybridization, the coverslips were removed and the slide were submerged in washing solution containing 5 mM Tris Base (Fisher Scientific), 15 mM NaCl (Panreac) and 1% Triton X (Panreac), for 30 min at same hybridization temperature (T_H). Finally removed from the incubator and the slides were allowed to air dry. For each experiment a negative control was performed simultaneously, following all the steps for standard hybridization but without the addition of the probe to the hybridization solution. All slides were analysed immediately after the experiment by microscopy. All experiments were performed in triplicate.

2.2.5. Hybridization in suspension

The hybridization method was based on procedures described in Fontenete *et al.* [3] with small modifications. Cells for flow cytometry analysis were fixed in 400 µL of 4% (v/v) paraformaldehyde for 1 hour at room temperature, the pellet was then resuspended in 500 µL of 50% (v/v) ethanol and incubated at -20 °C for at least 30 min. Cells were subjected to sonication for 12 min (Transsonic 420, Elma, Germany), followed by filtration through a sterile 10 µm pore-size filter (CellTrics®,Görliz, Germany) to avoid bacterial aggregates in the final suspension. The hybridization step was then performed, using 100 µL of fixed cells and 100 µL of hybridization solution (with FA and urea) at different temperatures for 90 min. The pellet was washed in 500 µL of washing solution and incubated at the respective temperature for 30 min. The pellet was resuspended in 100 µL of saline and a sterile filter with 10 µm pore size (CellTrics®) was used to remove cellular aggregates. Cells were stored at 4 °C until flow cytometry analysis. Similarly to the hybridization

procedure on slides, a negative control was performed for each experiment. For each protocol all probes were tested simultaneously at the same temperature to minimize intra-experimental errors. All experiments were performed in triplicate.

2.2.6. Microscopy evaluation and image analysis

Samples were observed using a Leica DM LB2 epifluorescent microscope (Leica Microsystems GmbHy, Germany) equipped with adequate filters. For image acquisition, a DFC300 FX camera (Leica) was used and the exposure time, gain and saturation values were fixed for all preparations. Fluorescence intensities were quantified by using an open source image-processing ImageJ software (version 1.49o) [20] though a semi-automatic method developed by us designated FISHji3 This method is consist in three steps: optimization (selection of regions of interest), segmentation (removal of artefacts in the image) and analysis (mean of fluorescence intensity of each image).

2.2.7. Flow cytometry analysis

H. pylori suspensions stained with FAM-labeled LNA probes, and the respective unstained negative controls, were analysed in an EPICS XL flow cytometer using the EXPO32ADC software (Beckman Coulter, Brea, USA) equipped with a 488 nm laser. For each sample, 20.000 events were collected. All experiments were repeated in triplicate and unstained negative controls were included for each type of protocol in every analysis.

2.2.8. Statistical analysis

Results were compared using One-way analysis of variance (ANOVA) by applying Tukey multiple-comparisons test, using GraphPad Prism version 5 software (GraphPad Sofware, San Diego, USA). A confidence level of 95% was employed for all statistical analysis.

2.3. Results

2.3.1. Melting temperature studies

The initial purpose of this study was to understand the efficiency of the hybridization using different designs of LNA probes. Different properties such as ionic strength play an important role for the stability of nucleic acid duplexes [21]. Therefore, to study the stability of these LNA probes coupled to the target sequence, we performed measurements of T_m in different types of buffers (Table 2.2 and S1). These buffers differ in salt concentration and presence of denaturants (FA or urea). For the high salt buffer with urea it was not

possible to exactly determine any T_m as they were all higher than 85 °C (the maximum temperature that could be assessed) for the RNA target.

2.3.2. FISH detection of H. pylori by fluorescence microscopy and flow cytometry

To analyse if the microbial detection by FISH is dependent on the type of FISH technique, the probes were evaluated through two different FISH methodologies: by fluorescent microscopy on slides in attached *bacteria* and by cytometry in bacterial suspensions. The use of two FISH methodologies allowed us to analyse if the practical procedure could affect the final results. This study was also very important to determine the robustness of the probes. To compare both protocols, we determined the optimal TH in both methodologies as the higher value of fluorescence intensities obtained by quantification by FISHji (Chapter III) and flow cytometry data. Different hybridization temperatures, between 37 °C and 65 °C, were tested. We observed that for both methods the same optimal T_H, i.e., the temperature at which the fluorescence signal was highest, was obtained for all probes (Table 2.2). Therefore we showed that both methods can be used, thus demonstrating a high correlation (Figure S1). It was also observed that the optimal hybridization temperature for each probe was independent of the denaturing agent used at the specific concentrations tested.

The correlation between T_m and T_H is not entirely clear [16]. Therefore, we analysed the correlation between the T_m using the medium buffer with FA with naked RNA for each type of probe, and the optimal hybridization temperature obtained *in vitro* (Figure 2.2). We observed a moderate level of correlation when these temperatures are compared under similar ionic strength conditions and in the presence of denaturant (Figure 2.2A). The difference between T_m and T_H was also studied and showed to be similar to the value previously calculated in the literature (LNA ref) (Figure 2.2B).

Table 2.2 - Results of thermal denaturation experiments in different types of buffers for different types of probes and optimal hybridization temperatures (T_H) obtained by FISH (attached and suspension) for each probe in study. The RNA complementary oligonucleotide has the following sequence: 5'-UUGGAGGGCUUAGUCUCUCCAG-3'. The DNA reference ("HP_21DNA_PO") has the following sequence: 5'- CTGGAGAGACTAAGCCCTCCAA-3'

	Melting temperatures			**Optimal hybridization temperature**
	Medium salt buffer	Medium salt buffer with FA	Low salt buffer with FA	High salt buffer with urea/FA
Oligonucleotide analysed	RNA complement T_m (°C)	RNA complement T_m (°C)	RNA complement T_m (°C)	16rRNA T_H (°C)
HP_21DNA_PO	64	69	68	-
HP_18LNA_PO	>85 °C	>85 °C	>85 °C	57
HP_18LNA_PS	>85 °C	79	78	57
HP_18LNA/2OMe_PO	>85 °C	>85 °C	>85 °C	58
HP_ 18LNA/2OMe _PS	>85 °C	>85 °C	>85 °C	58
HP_15LNA_PO	>85 °C	85	78	55
HP_15LNA_PO_2	76	66	65	47
HP_15LNA_PS	>85 °C	75	74	43
HP_15LNA_PS_2	77	68	67	45
HP_15LNA/2OMe_PO	>85 °C	>85 °C	78	55
HP_ 15LNA/2OMe _PS	>85 °C	75	72	55
HP_12LNA_PO	85	76	71	43
HP_12LNA_PS	77	67	67	45
HP_12LNA/2OMe_PO	85	70	68	55
HP_ 12LNA/2OMe _PS	77	68	66	58
HP_10LNA_PO	78	69	67	55
HP_10LNA_PS	77	68	66	58
HP_10LNA/2OMe_PO	79	66	67	37
HP_ 10LNA/2OMe _PS	78	63	66	37

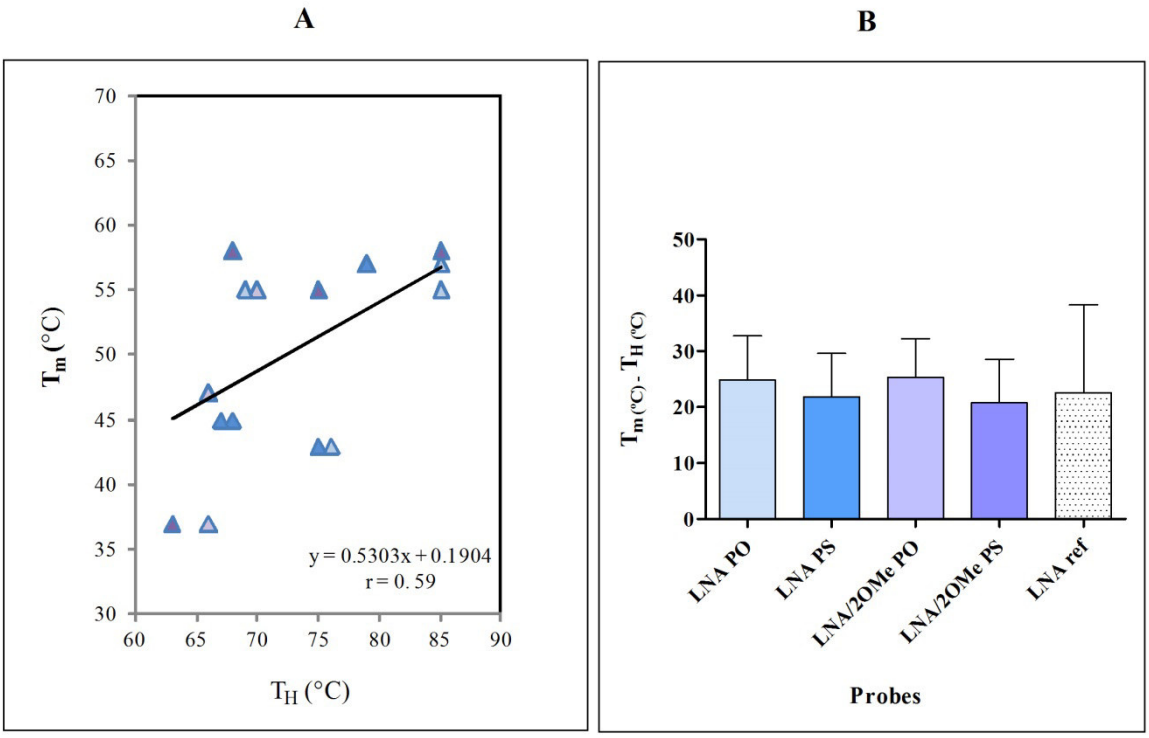

Figure 2.2 - Comparison between hybridization temperature (T_H) and melting temperature (T_m) obtained from the LNA advanced probes studied in this work. A. Representation of the linear regression equations and correlations values of T_H *vs* and experimental T_m for all LNA advanced probes. The T_H for each probe corresponds to the optimal T_H obtained *in vitro*. The T_m used in this correlation was obtained using the medium salt buffer with FA. Data are means of two independent experiments. B. Difference between T_m and T_H for the different types of LNA advanced probes used in this study and a value described in the literature for other studies (LNA ref). Data collected in this work represent the means of two independent experiments and error bars represent standard deviation.

2.3.3. Effect of the denaturant on hybridization

The effect of urea instead of FA in the hybridization solutions at the optimal temperatures (defined in Table 2.1) was analysed for all the different probes designed. In average, hybridizations with urea allowed higher fluorescence intensities compared to those using with FA (Figure 2.3) as evaluated by both flow cytometry analysis and microscopy. However, these results were very dependent of the length and nature of the probe.

A more detailed analysis of the fluorescence intensities obtained by flow cytometry showed that in some probe designs (HP_12LNA_PS, HP_15LNA/2OMe_PO, HP_12LNA_PO, HP_10LNA_PO, HP_10LNA/2OMe_PO, HP_10LNA/2OMe_PS) the use of urea led to higher fluorescence values (p<0.05) compared to those obtained when FA was used (Figure S2A). Nevertheless, when the efficiency of the probe is low this improvement is not so evident. In a few cases, such as HP_12LNA/2OMe _PS, FA leads

to higher fluorescence intensities than urea. However, for all cases where FA provides better results than urea, differences are not statistically significant (p>0.05). This analysis was also performed for the results obtained by microscopy in attached *cells.* The beneficial effect of urea in the hybridization is not so obvious with this methodology. Statistically significant differences for HP_15LNA/2OMe_PO and HP_10LNA/2OMe_PS (p<0.05) were observed, but for most probes the increase in fluorescence intensity was not statistically significant (Figure S2B).

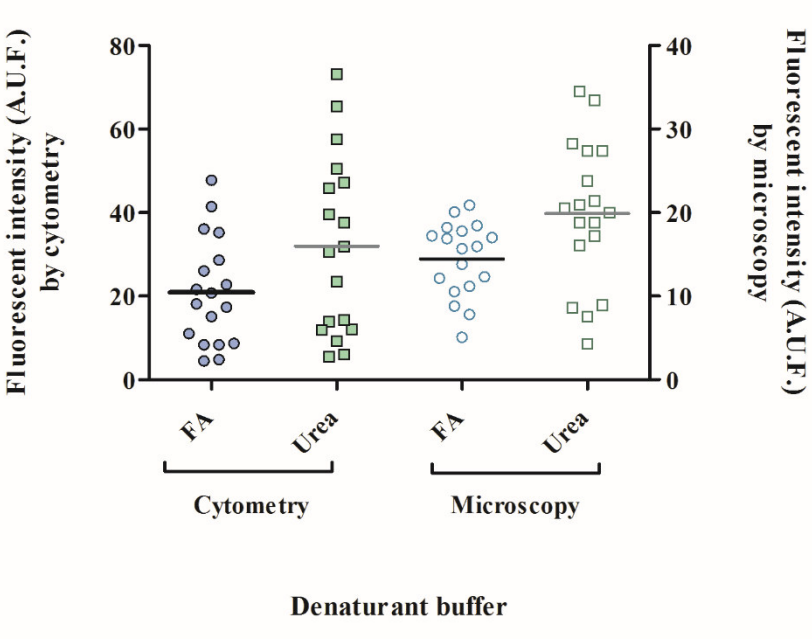

Figure 2.3 - Analysis of fluorescence intensity in LNA advanced probes using cytometry and microscopy. The circles filled in blue and the squares filled in green represent the values of fluorescence intensity for each individual probe using the protocol for cells in suspension analysed by cytometry. The white circles and squares represent the values of fluorescence intensity for each individual probe using the protocol for attached cells analysed by ImageJ.A.U.F: Arbitrary Units of Fluorescence.

2.3.4. Effect of length on hybridization

The analysis of the efficiency using different combinations of nucleic acid monomers showed some differences between the lengths of the oligonucleotides (Figure 2.4).

In general, short probes provide higher fluorescence intensities compared to 18 mer probes in both flow cytometry and microscopy analysis (Figure 2.4A and 4B). Additionally, if all the conditions were combined the results showed a statistically significant difference between 10 and 18 mers ($p \leq 0.05$) (Figure S3).

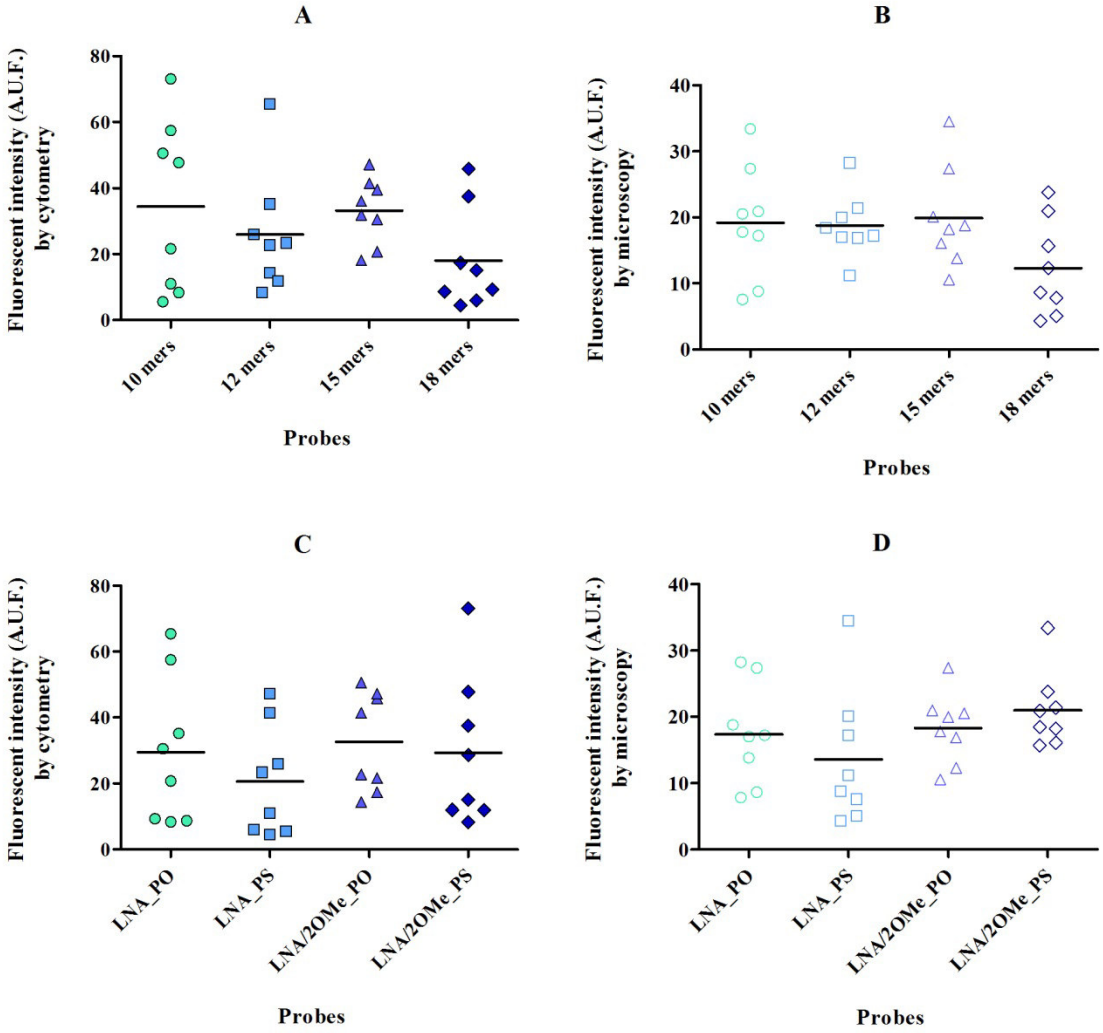

Figure 2.4 - Analysis of fluorescence intensities obtained by flow cytometry and microscopy analysis using urea and FA buffer in LNA advanced probes. A and B. Analysis of fluorescence intensities for probes of different length, obtained by flow cytometry (A) and microscopy (B). C-D. Analysis of fluorescence intensities for probes of different nucleic acid mimics, obtained by flow cytometry (C) and microscopy (D). Data are means of two independent experiments. A.U.F: arbitrary units of fluorescence.

In LNA designs it was observed a statistically significant difference between 12 and 18 mers ($p \leq 0.05$) (Figure S4A). Contrarily, for LNA/2'OMe designs no statistically significant difference was observed ($p \geq 0.05$) (Figure S4B).

2.3.5. Effect of chemical modifications on hybridization

The use of different chemical modifications showed to have implications on the efficiencies of LNA probes (Figure 2.4C-D). The use of different backbones linkages showed differences depending of the nucleic acid composition of the probes. For LNA

probes, PO oligonucleotides had higher fluorescence intensity relative to PS oligonucleotides in both techniques (flow cytometry and microscopy, Figure 2.4C and 2.4D, respectively). In the case of LNA/2'OMe, PO and PS probes the backbones linkages, the results showed to be similar (Figure2. 4C and 2.4D).

LNA/2'OMe design allow a similar or increase of fluorescence intensities comparatively to LNA design (Figure 2.4C and 2.4D). This difference is more evident when individual probes were studied. For example in FA, 18 LNA/2'OMe_PO probe showed higher fluorescence intensities comparatively to the 18 LNA probes ($p \leq 0.001$) (Figure S2A). In the same buffer, 10_ LNA/2'OMe_PS probe also obtained higher efficiency relatively to 10_ LNA_PS ($p \leq 0.05$).

In order to analyse the effect of the number of LNA monomers in probes of the same length, we designed two different 15 mers probes, LNA_PO_2 and LNA_PS_2. It was observed that the design LNA_PO2 or LNA_PS_2 had lower fluorescence intensities compared with the designs with higher number of LNA monomers ($p \leq 0.05$) (Figure 2.5).

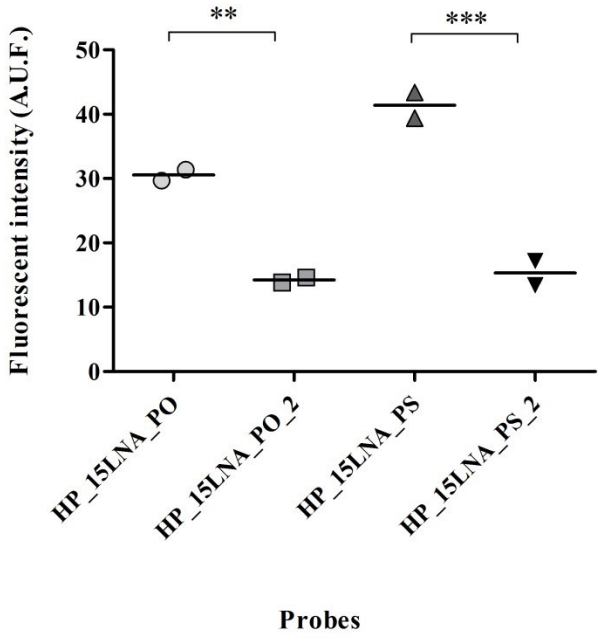

Figure 2.5 - Analysis of fluorescence intensities obtained by flow cytometry analysis using urea buffer, using LNA/DNA 15 mers. Data are means of two independent experiments. ** $p \leq 0.01$; *** $p \leq 0.001$.

2.4. Discussion

Despite an increasing number of successful applications of LNA probes in FISH [22-24], there is an absence of studies that have analysed the impact of different LNA probe designs in this methodology. The design of probes containing LNA have been extensively

optimized to be used in the antisense area [25-28], but only a few studies have used LNA for the detection of microorganisms by FISH [29]. Furthermore, the impact of the design of chimeric LNA probes on detection of bacteria by FISH has not yet been investigated.

Different types of designs were studied: i) LNA/DNA and LNA/2'OMe chimeric probes; ii) phosphorodiester and phosphorothioates backbones; and iii) probes of different length (18, 15, 12 and 10 mers). Five main points were addressed: i) how does the targeting capability of LNA probes change in buffers generally used *in vitro* in FISH experiments (T_m studies); ii) how do the methodological protocols affect the final results; iii) what type of denaturant should be used in LNA FISH protocols; iv) what is the appropriate length of LNA advanced probes for the detection of microorganisms and v) how does the FISH detection efficiency change as a result of chemical modifications of the probes.

We first analysed the RNA targeting capability of LNA probes by thermal studies. It was previously shown that the introduction of LNA increases duplex stabilities due to, for example, increased base stacking [25,30,31]. Several studies have shown that the addition of LNA raises the T_m by 1 to 8 °C against DNA and by 2 to 10 °C against RNA [32,33]. In our study we observed a similar increase in the T_m for LNA/DNA probes (Table 2.1 and S1). For LNA/2'OMe probes we observed that a single LNA substitution is generally more stabilizing than within DNA strands, which is in agreement with other studies [13].

To study the changes in T_m in similar conditions as used *in vitro* we used the most common denaturants in FISH experiments, FA and urea. Previous studies showed that the effect of FA on the stability of duplexes is mediated through a weakening of the hydrogen bonds [24,34], thus leading to a drop in T_m [35]. The use of FA in medium salt buffer showed a decrease of 9 °C to 16 °C in T_m, values that are relatively close to the ones described in the literature (18 °C). The lower values obtained are probably due to a specific effect of the LNA monomers in the probes rather than DNA monomers as used in these previous studies. Contrarily, the use of urea did not as strongly interfere with T_m as FA did. It has been described that urea leads to a decrease of more than 2 °C in T_m per molar concentration increase of urea [36]. Similarly, we observed an increase in the range of 3 °C to 9 °C in T_m for DNA (Table S1). For the RNA target it was not possible to determine this effect because all the T_m were above the upper limit of detection (Table 2.1).

The importance of T_m determination in FISH studies has previously been discussed by Fontenete *et al*. [16]. In this study we proved a moderate correlation between T_m and optimal T_H when similar conditions are used (r=0.59). This value can be explained since it

was not possible to determine T_m values for the same ionic strength of the *in vitro* studies in bacteria (values exceed the upper limit of detection). However, the average difference for the different probes (T_m-T_H) was 23.1±7.34 and if each type of probe was analysed (Figure 2.2B) this values is also correlated well with the values obtained in the study of Fontenete *et al.* [16] (Figure 2.2B).

Secondly, the efficiency of LNA probes was analysed through the intensity of fluorescence in FISH detection of *H. pylori*. We performed this study using two different FISH methodologies to understand if the probe efficiencies depend of the type of protocol used. Our findings for LNA probes design are supported by both methods and therefore we can argue that these oligonucleotide designs are robust and reliable. In *in vitro* experiments, the salt concentration used was based on the T_m stability studies and the low background normally obtained with this type of buffers [37]. We tested FA and urea as denaturant in the hybridization solution. FA has been the preferred solvent to lower the melting point and T_H in FISH [38-40]. However, previous studies showed that urea could substitute FA in FISH methodology [6,41]. Nevertheless, these studies did not test different LNA probes designs. Consequently we intended to study if this effect embraced all types of probe designs. In general, urea showed a tendency to increase the efficiency of hybridization (Figure 2.3), and the use of urea in FISH protocols allows a non-toxic approach and an expected increase in efficiency. Additionally, studies have also showed that the use of urea does not compromise the specificity and sensitivity of the probes [3,6,28]. Moreover, Matthiesen *et al.* has proposed that FA can compete with hydrogen donors and delay the hybridization, affecting the signal of hybridization [42] .

The optimal T_H (higher intensity fluorescence) obtained depended strongly on the length of probes (Figure 2.4A-B). Small probes were more efficient. However, the designs used in this study were specific for *H. pylori* and were limited to defined lengths and nucleotide combinations. Consequently the data obtained are not sufficient to formulate a complete model for the design of LNA/DNA or LNA/2'OMe chimeras. Broader studies applied to different types of microorganisms using different chemical modifications of probes would be useful.

The change in efficiency when PS substitutes PO backbones in FISH probes showed to be dependent of the length of the oligonucleotide. In this specific sequence the use of PS appeared to decrease signal intensity in some cases (Figure 2.4C-D). In urea buffer this backbone modification only showed positive influence ($p< 0.05$) in 15 mer LNA probes and 10 mer LNA/2'OMe mixmers (Figure S2), thereby confirming our earlier results [3]. In fact, the main advantage of this type of chemical modification is the reduced susceptibility

to degradation by serum nucleases and improvement in the efficiency of inhibition in antisense studies in animal cells [43-45]. In the microbiology area, this is the first extensive study which combines and analyses different designs of LNA probes with the 2'-OMe type of chemical modification.

We have further compared the different designs of probes. The use of 2'OMe monomers generally showed to increase the efficiency of hybridization for small probes (Figure 2.4D-C). It was already proven that LNA substitutions are additive when LNA nucleotide are spaced by at least two 2'OMe nucleotides [13]. However, for LNA/DNA probes the design is not so established. Therefore we analysed different designs for 15 mer LNA/DNA probes. In this specific sequence we observed that LNA and DNA nucleotides should be alternating (Figure 2.5). The difference between the efficiency of these probes in *H. pylori* detection could be explained by the differences observed in the hybridization affinity (Table 2.1).

2.5. Conclusions

This study presents some start points for the design of LNA probes for microbiology use. We demonstrated that LNA probes can be used in FISH protocols for suspended or attached bacteria with similar levels of efficiency. Small LNA probes with 10 mers with 2'OMe or PS backbones displayed high performance under the conditions tested.

In conclusion, this study suggests some important indications for the design of LNA probes for FISH applications that can be used to help others authors to start other works in microbiology research field.

2.6. References

1. Amann R.I., Krumholz L., Stahl D.A. Fluorescent-oligonucleotide probing of whole cells for determinative, phylogenetic, and environmental studies in microbiology. J Bacteriol (1990); 172: 762-770.
2. Wright E.S., Yilmaz L.S., Corcoran A.M., Ökten H.E., Noguera D.R. Automated Design of Probes for rRNA-Targeted Fluorescence In Situ Hybridization Reveals the Advantages of Using Dual Probes for Accurate Identification. Applied and Environmental Microbiology (2014); 80: 5124-5133.
3. Fontenete S., Guimaraes N., Leite M., Figueiredo C., Wengel J., Filipe Azevedo N. Hybridization-based detection of Helicobacter pylori at human body temperature using advanced locked nucleic acid (LNA) probes. PloS one (2013); 8: e81230.
4. Sempere L.F., Korc M. A method for conducting highly sensitive microRNA in situ hybridization and immunohistochemical analysis in pancreatic cancer. Methods Mol Biol (2013); 980: 43-59.
5. Priya N.G., Pandey N., Rajagopal R. LNA probes substantially improve the detection of bacterial endosymbionts in whole mount of insects by fluorescent in-situ hybridization. BMC Microbiol (2012); 12: 81.
6. Soe M.J., Moller T., Dufva M., Holmstrom K. A sensitive alternative for microRNA in situ hybridizations using probes of 2'-O-methyl RNA + LNA. J Histochem Cytochem (2011); 59: 661-672.
7. Eckstein F., Gish G. Phosphorothioates in molecular biology. Trends Biochem Sci (1989); 14: 97-100.
8. Tanganyika-de Winter C.L., Heemskerk H., Karnaoukh T.G., van Putten M., de Kimpe S.J., van Deutekom J., et al. Long-term Exon Skipping Studies With 2'-O-Methyl Phosphorothioate Antisense Oligonucleotides in Dystrophic Mouse Models. Mol Ther Nucleic Acids (2012); 1: e44.
9. Heemskerk H.A., de Winter C.L., de Kimpe S.J., van Kuik-Romeijn P., Heuvelmans N., Platenburg G.J., et al. In vivo comparison of 2'-O-methyl phosphorothioate and morpholino antisense oligonucleotides for Duchenne muscular dystrophy exon skipping. J Gene Med (2009); 11: 257-266.
10. Guimaraes N., Azevedo N.F., Figueiredo C., Keevil C.W., Vieira M.J. Development and application of a novel peptide nucleic acid probe for the specific detection of Helicobacter pylori in gastric biopsy specimens. J Clin Microbiol (2007); 45: 3089-3094.
11. Kumar R., Singh S.K., Koshkin A.A., Rajwanshi V.K., Meldgaard M., Wengel J. The first analogues of LNA (locked nucleic acids): phosphorothioate-LNA and 2'-thio-LNA. Bioorg Med Chem Lett (1998); 8: 2219-2222.
12. You Y., Moreira B.G., Behlke M.A., Owczarzy R. Design of LNA probes that improve mismatch discrimination. Nucleic Acids Res (2006); 34: e60.

13. Kierzek E., Ciesielska A., Pasternak K., Mathews D.H., Turner D.H., Kierzek R. The influence of locked nucleic acid residues on the thermodynamic properties of 2'-O-methyl RNA/RNA heteroduplexes. Nucleic Acids Res (2005); 33: 5082-5093.
14. Yan Y., Yan J., Piao X., Zhang T., Guan Y. Effect of LNA- and OMeN-modified oligonucleotide probes on the stability and discrimination of mismatched base pairs of duplexes. J Biosci (2012); 37: 233-241.
15. Maciaszek A., Krakowiak A., Janicka M., Tomaszewska-Antczak A., Sobczak M., Mikolajczyk B., et al. LNA units present in the (2'-OMe)-RNA strand stabilize parallel duplexes (2'-OMe)-RNA/[All-RP-PS]-DNA and parallel triplexes (2'-OMe)-RNA/[All-RP-PS]-DNA/RNA. An improved tool for the inhibition of reverse transcription. Org Biomol Chem (2015); 13: 2375-2384.
16. Fontenete S., Guimarães N., Wengel J., Azevedo N.F. Prediction of melting temperatures in fluorescence in situ hybridization (FISH) procedures using thermodynamic models. Critical Reviews in Biotechnology0: 1-12.
17. Cole J.R., Chai B., Farris R.J., Wang Q., Kulam S.A., McGarrell D.M., et al. The Ribosomal Database Project (RDP-II): sequences and tools for high-throughput rRNA analysis. Nucleic Acids Res (2005); 33: D294-296.
18. Almeida C., Sousa J.M., Rocha R., Cerqueira L., Fanning S., Azevedo N.F., et al. Detection of Escherichia coli O157 by Peptide Nucleic Acid Fluorescence In Situ Hybridization (PNA-FISH) and Comparison to a Standard Culture Method. Applied and Environmental Microbiology (2013); 79: 6293-6300.
19. Sadhu C D.S., Gopinathan KP Influence of Formamide on the Thermal-Stability of DNA. J Bioscience (1984); 6: 817-821.
20. Collins T.J. ImageJ for microscopy. Biotechniques (2007); 43: 25-30.
21. Tan Z.J., Chen S.J. Nucleic acid helix stability: effects of salt concentration, cation valence and size, and chain length. Biophys J (2006); 90: 1175-1190.
22. Silahtaroglu A.N., Tommerup N., Vissing H. FISHing with locked nucleic acids (LNA): evaluation of different LNA/DNA mixmers. Mol Cell Probes (2003); 17: 165-169.
23. Robertson K.L., Thach D.C. LNA flow-FISH: a flow cytometry-fluorescence in situ hybridization method to detect messenger RNA using locked nucleic acid probes. Anal Biochem (2009); 390: 109-114.
24. Robertson K.L., Vora G.J. Locked nucleic acid flow cytometry-fluorescence in situ hybridization (LNA flow-FISH): a method for bacterial small RNA detection. J Vis Exp (2012): e3655.
25. Kurreck J., Wyszko E., Gillen C., Erdmann V.A. Design of antisense oligonucleotides stabilized by locked nucleic acids. Nucleic Acids Res (2002); 30: 1911-1918.
26. Yoo B., Ghosh S.K., Kumar M., Moore A., Yigit M.V., Medarova Z. Design of nanodrugs for miRNA targeting in tumor cells. J Biomed Nanotechnol (2014); 10: 1114-1122.

27. Shimo T., Tachibana K., Saito K., Yoshida T., Tomita E., Waki R., et al. Design and evaluation of locked nucleic acid-based splice-switching oligonucleotides in vitro. Nucleic Acids Res (2014).
28. Wahlestedt C., Salmi P., Good L., Kela J., Johnsson T., Hokfelt T., et al. Potent and nontoxic antisense oligonucleotides containing locked nucleic acids. Proc Natl Acad Sci U S A (2000); 97: 5633-5638.
29. Kubota K., Ohashi A., Imachi H., Harada H. Improved in situ hybridization efficiency with locked-nucleic-acid-incorporated DNA probes. Appl Environ Microbiol (2006); 72: 5311-5317.
30. Kaur H., Wengel J., Maiti S. Thermodynamics of DNA-RNA heteroduplex formation: effects of locked nucleic acid nucleotides incorporated into the DNA strand. Biochemistry (2008); 47: 1218-1227.
31. McTigue P.M., Peterson R.J., Kahn J.D. Sequence-dependent thermodynamic parameters for locked nucleic acid (LNA)-DNA duplex formation. Biochemistry (2004); 43: 5388-5405.
32. Braasch D.A., Corey D.R. Locked nucleic acid (LNA): fine-tuning the recognition of DNA and RNA. Chem Biol (2001); 8: 1-7.
33. Kvaerno L., Kumar R., Dahl B.M., Olsen C.E., Wengel J. Synthesis of abasic locked nucleic acid and two seco-LNA derivatives and evaluation of their hybridization properties compared with their more flexible DNA counterparts. J Org Chem (2000); 65: 5167-5176.
34. Bottari B. E.D., Gatti M., Neviani E. FISH in Food Microbiology. In: Liehr T, editor.(2009). Berling: Springer-Verlag.
35. Sadhu C. S.D., Gopinathan K.P. Influence of formamide on the thermal stability of DNA. Journal of Biosciences (1984); 6: 817-821.
36. Hutton J.R. Renaturation kinetics and thermal stability of DNA in aqueous solutions of formamide and urea. Nucleic Acids Res (1977); 4: 3537-3555.
37. Rose K., Mason J.O., Lathe R. Hybridization parameters revisited: solutions containing SDS. Biotechniques (2002); 33: 54-56, 58.
38. Bisha B., Kim H.J., Brehm-Stecher B.F. Improved DNA-FISH for cytometric detection of Candida spp. J Appl Microbiol (2011).
39. McConaughy B.L., Laird C.D., McCarthy B.J. Nucleic acid reassociation in formamide. Biochemistry (1969); 8: 3289-3295.
40. Blake R.D., Delcourt S.G. Thermodynamic effects of formamide on DNA stability. Nucleic Acids Res (1996); 24: 2095-2103.
41. Lawson T.S., Connally R.E., Vemulpad S., Piper J.A. Dimethyl formamide-free, urea-NaCl fluorescence in situ hybridization assay for Staphylococcus aureus. Lett Appl Microbiol (2012); 54: 263-266.
42. Matthiesen S.H., Hansen C.M. Fast and non-toxic in situ hybridization without blocking of repetitive sequences. PLoS One (2012); 7: e40675.

43. Behlke M.A. Chemical modification of siRNAs for in vivo use. Oligonucleotides (2008); 18: 305-319.
44. Monia B.P., Johnston J.F., Sasmor H., Cummins L.L. Nuclease resistance and antisense activity of modified oligonucleotides targeted to Ha-ras. J Biol Chem (1996); 271: 14533-14540.
45. Adams A.M., Harding P.L., Iversen P.L., Coleman C., Fletcher S., Wilton S.D. Antisense oligonucleotide induced exon skipping and the dystrophin gene transcript: cocktails and chemistries. BMC Mol Biol (2007); 8: 57.

Chapter III

FISHJi: new ImageJ macros for the quantification of epifluorescence images

FISHji: new ImageJ macros for the quantification of fluorescence in epifluorescence images

Sílvia Fontenete[1,2,3,4,5], Daniel Carvalho[1], Anália Lourenço, Nuno Guimarães[1,2,3,4], Pedro Madureira [2,5,8], Céu Figueiredo[2,3,9], Nuno Filipe Azevedo[1].

[1]LEPABE, Laboratory for Process Engineering, Environment, Biotechnology and Energy, Faculty of Engineering, University of Porto, Porto, Portugal; [2] i3S, Instituto de Investigação e Inovação em Saúde, Universidade do Porto, Portugal, Porto, Portugal; [3]IPATIMUP, Instituto of Molecular Pathology and Immunology, University of Porto; [4]Nucleic Acid Center, Department of Physics, Chemistry and Pharmacy, University of Southern Denmark, Odense M, Denmark; [5] ICBAS, Institute of Biomedical Sciences Abel Salazar ,University of Porto, Porto, Portugal; [6]ESEI, Escuela Superior de Ingeniería Informática, Universidad de Vigo, Ourense, Spain; [7]Centre of Biological Engineering, University of Minho, Braga, Portugal, [8] IBMC, Institute for Molecular Biology and Cell Biology, Porto, Portugal; [9] FMUP, Faculty of Medicine of the University of Porto, Porto, Portugal .

Abstract

In biological sciences, fluorescence is crucial to study, analyse or diagnose pathologies. Several techniques, such as fluorescence *in situ* hybridization (FISH) use fluorescence staining dyes, however frequently the images obtained in the microscope cannot be quantified with accuracy by the researcher. The development of innovative digital image processing programs and tools has been trying to overcome this problem, however the determination of fluorescent intensity in microscope images still has issues due to the lack of precision in the results.

This work presents FISHji, a set of new ImageJ methods for quantification of fluorescence in images obtained by epifluorescence microscopy. As a case study, we used 18 FISH probes containing locked nucleic acids (LNA) and 2'-O-methly RNA (2'OMe) or deoxyribonucleic acid (DNA), with phosphate and phosphorothioate backbones, in regards to detect 16S rRNA in bacteria (*Helicobacter pylori*). These probes were used to perform FISH in a range of temperatures, in attached and suspension of *H. pylori* samples. The captured images of attached bacteria were analyzed by epifluorescence microscopy and the fluorescence intensities were quantified through three semi-automated (FISHji 1,2,3) and two automated (FISHji 4,5) tools. The results were then compared using flow cytometry from bacteria suspension. The results from FISHji3, 4 and 5 were analogous in terms of accuracy, specifically the mean correlation between these methods and flow cytometry data was high and significant.

Hopefully, FISHji will be of broad utility for biologists as well as clinical scientists. FISHji software, comprehensive documentation of the functionalities, and usage examples, are freely available for non-commercial use at http://paginas.fe.up.pt/~nazevedo/.

Keywords: FISH, Locked nucleic acids, image analysis, computational image processing, ImageJ

3.1. Introduction

In science, digital images are a crucial piece of information. The ability to process and analyze the large volume of images produced by the plethora of microscopy techniques available raises the need for specialized software tools [1]. Images should be processed in a systematic and standardized way, such that results are comprehensible and reproducible. There are a number of commercial and open source image processing tools available, and the range of implemented functionalities is significant [2-10]. However, the general purpose of most of these tools hampers domain or application-specific use by laymen, i.e. it is not straightforward for a researcher to use such general software to analyze biological images, without understanding the specifics of the image processing and analysis algorithms. As such, the development of end-user biological image analysis tools is considered useful, essentially for analyzing fluorescence results obtained by diagnostic methodologies for microorganisms. These methodologies or techniques use staining with fluorescent binding dyes which are then visualized using fluorescence microscopy. In order to have a quantitative analysis of the results, the fluorescence intensity needs to be accurately measured.

FISH is one of the methodologies in which a quantitative validation of results is required. This technique has been used as a molecular tool for the analysis and detection of microorganisms [11]. Since the first application in 1989 by Delong and coworkers [12], this method has undergone several improvements in order to overcome limitations, such as low fluorescence intensity [13,14]. This evolution of the method has led to the use of new types of nucleic acids such as locked nucleic acids (LNA) and 2'-O-methyl RNA (2'OMe) [14,15]. Other chemical modifications within nucleobases, ribose or deoxyribose and within phosphate moieties have been also introduced to improve the resistance to nucleases present in the cells or body fluids [16-18]. In FISH experiments, the evaluation of the results is based on microscopy, which the quantitative assessment is performed by the researcher, and is dependent of the observer interpretation [19], or on flow cytometry. Flow cytometry provides an automated quantitative assessment but requires the use of expensive equipment and is only applicable for cells in suspension. Therefore, computerized image processing tools offer the most promising and versatile approach to minimize costs and overcome the variability of human microscope analysis. Daims *et al.,* developed a digital image analysis program (DAIME) especially used for microbial ecology [20]. Although, DAIME has different features such as analyzing 2D and 3D microscopy datasets of microorganisms stained by FISH, this program is complex, is generally used for environmental bacteria [21-23] and no validation studies against flow

cytometry have been made so for. ImageJ is another well-known and publicly available image processing tool (http://rsbweb.nih.gov/ij/). It has released many plugins and macros useful to biomedical image processing [24], however, also in this case there are no comparative studies against flow cytometry to confirm the use of this software in fluorescence quantification of microscopic images.

This article describes five different methods for the quantification of fluorescent intensity in microscopic images (named FISHji). As a case study, LNA probes were applied in different hybridization conditions, and evaluated by microscopy and cytometry approaches. The biological goal was the detection of 16S rRNA in the clinically relevant bacterium, *Helicobacter pylori*. The developed methods are freely available and integrated in the ImageJ software package.

3.2. Materials and methods

3.2.1. Workflow of FISHji methods and validation

In this work, three semi-automatic and two automatic FISHji methods were created (Figure 3.1). To validate these methods, the FISH procedure was performed both in bacterial suspensions and in attached bacteria. Eighteen LNA probes specifically designed for *H. pylori* were used at different temperatures, in order to obtain a large range of fluorescence intensities. All images obtained by microscopy (attached bacteria) were analyzed by the five FISHji methods and these results were compared with cytometry data (bacterial suspensions) hybridized under the same conditions (temperature and buffer). Afterwards, all results were statistically analyzed and the correlation between each FISHji method and flow cytometry was performed. Finally, an extra validation was then performed using another fluorescence staining procedure (propidium iodide) for the FISHji methods.

3.2.2. Fluorescence analysis and FISHji architecture

In terms of operational mode, there are three semi-automatic (FISHji1, FISHji2 and FISHji3) and two automatic approaches (FISHji4, and FISHji5) (Figure 3.2). For all methods, the channels of the original RGB (red, green, and blue light) images were separated in order to analyse the channel where fluorescence is emitted.

The methods consist of three sequential steps: optimization, segmentation and analysis, and measurement steps. In the optimization module, pixel-based treatments are performed in order to highlight the regions of interest (ROIs) and allow the removal of

artefacts. In the segmentation module a default black and white threshold supports cell segmentation. The ROIs are outlined and artefacts are discarded by the command "Analyse Particles". The mean fluorescence intensity (MFI) is then calculated as the average of each ROI (Figure 3.2).

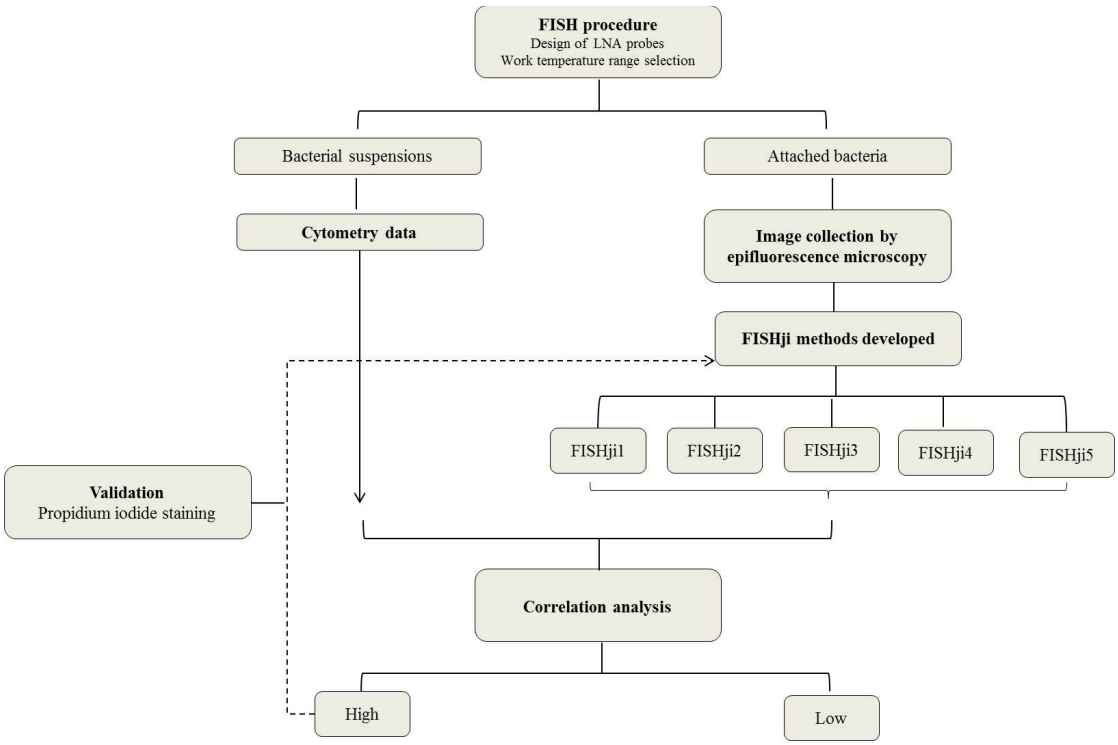

Figure 3.1 - A general view of this study. Firstly 18 LNA probes were designed and synthesised. FISH was then performed using these probes in different hybridization temperatures, in attached and suspended bacteria. The images obtained by microscopy from attached bacteria were analysed and quantified by four FISHji methods. Subsequently, these results were statistically compared with the data obtained by flow cytometry from bacteria in suspension. The FISHji methods that obtained high correlation values were then validated using a standard staining procedure (propidium iodide).

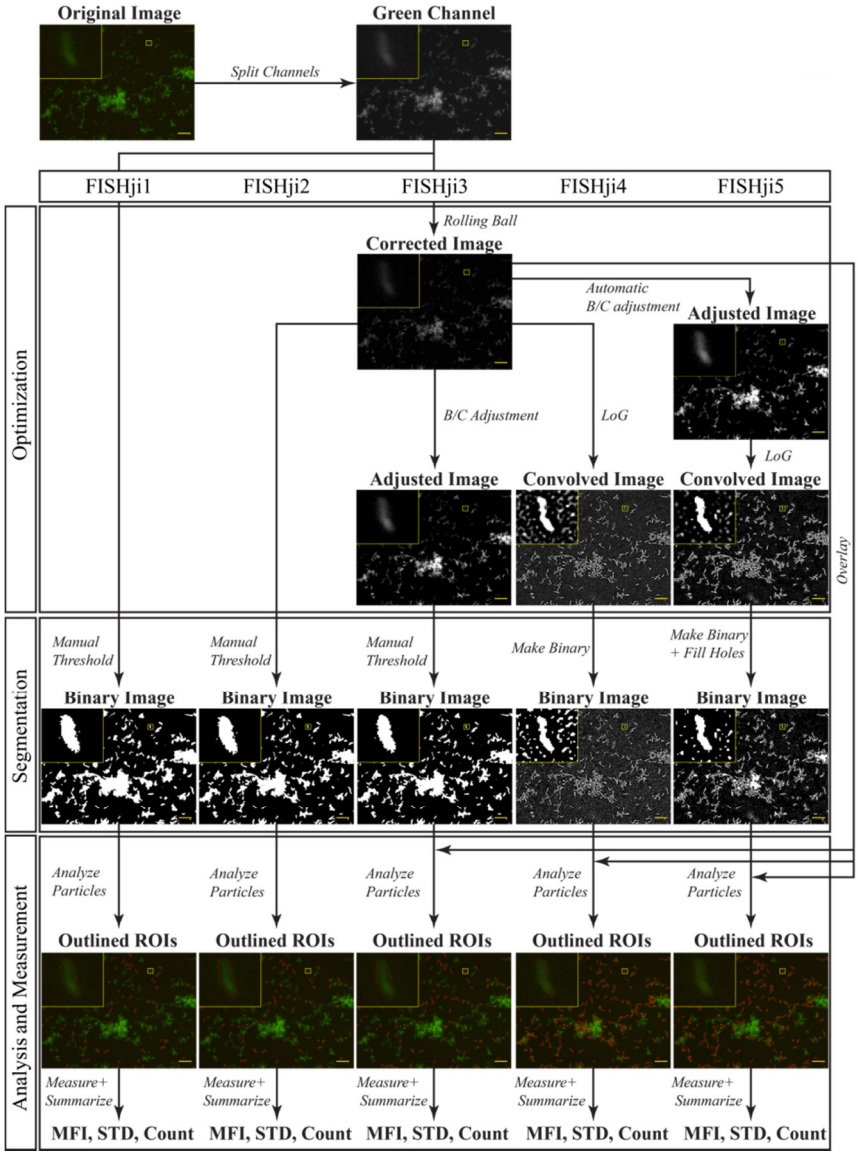

Figure 3.2 - The schematic workflow of FISHji methods. After microscopic acquisition of the fluorescent images, the green channel (the wavelength at which the probe fluoresces) was obtained and further analyzed in order to obtain the MFI. The FISHji methods consist of three steps, optimization, segmentation and analysis and measurements.

Optimization step: optimization treatments were applied to eliminate possible background defects or/and to adjust the brightness and contrast features of the corrected image. Segmentation step: for FISHji1,2,3, the ROIs were segmented from the background by manual default black and white threshold, whereas for FISHji4,5 an automatic threshold was applied by the "Make Binary" option. Analysis and Measurement step: after segmentation, the ROIs were outlined by the command "Analyze Particles". Finally, the fluorescence intensity of each ROI was provided by the option "Measure" in the ROI interface and then the average value was determined by the "Summarize" command as well as the STD. It should be noted that the overlay of the ROIs with the original image represented by the "Outlined ROIs" images is only to demonstrate the efficiency of the ROI definition. In real action, this overlay is not necessary. B/C - Brightness and Contrast; LoG - Laplacian of Gaussian; ROI - region of interest; MFI - mean fluorescence intensity; STD - standard deviation.

Figure 3.2 (continuation) - For FISHji1, optimization treatments are not applied. In the FISHji2 and FISHji3, a background subtraction based on the "rolling ball" algorithm (radius = 80 pixels) is performed to the green channel in order to reduce background heterogeneity and the presence of artefacts [25]. In the FISHji2 method, the obtained image is segmented and further analysed to determine the MFI of the image. In FISHji3, the brightness and contrast features of the corrected image are manually adjusted using the "B/C Adjustment" (Brightness and Contrast) tool to further enhance the foreground. Subsequently, the adjusted image is thresholded and a binary mask is created. The ROIs present in the mask are redirected to the corrected image and MFI is quantified by the ROI manager interface.

In the automatic FISHji4 and FISHji5 methods, the corrected image is convoluted using a Laplacian of Gaussian (LoG) filter (9x9 kernel) [26]. In the FISHji5 method, an automatic B/C adjustment of the corrected image is performed before the convolution. First, a B/C adjustment based on the image's histogram is automatically applied and then the convolution step was performed. In addition, the binary operation "Fill Holes" is applied to fill intra-aggregate spaces and maintain ROI integrity, providing an optimal binary mask.These optimization steps (except "Rolling Ball") change the real pixel values of the image, including the ROIs. So, a duplicated image is taken from the corrected image in order to allow enhancement of foreground pixels without compromising MFI quantification. After segmentation, the ROIs defined by the binary mask are redirected to the duplicated image, and only then the MFI is calculated. Thus, the MFI is determined from the real pixel values of the Corrected Image, outlined by the binary mask overlay.
All FISHji methods were implemented as macros in ImageJ (version 1.49o or higher). The analysis parameters were set as 100-600 pixels for the minimum and maximum valid object size (i.e. pixel^2) and 0.1-0.7 for the range of circularity (i.e. 4*pi*(area/perimeter^2). These values were established by experimental trials, and taking into account the real size and shape of the bacterium. Images were not calibrated since all had the same resolution (1392x1040 cm). FISHji4 and FISHji5 macro can be found on the webpage: http://paginas.fe.up.pt/~nazevedo/

3.2.3. Overlap index

Overlap index Ω is a measure of activating regions' spatial overlap and symmetry. This value was determined using two different edges (image processing technique for finding the boundaries of cells within images detecting discontinuities in brightness): the defined by the ImageJ method and the manual one as the ground truth [27]. After obtaining the binary images of each ROI using ImageJ, a Matlab® script (data not shown) was

developed to overlap the images and subsequently to calculate the overlap index Ω according to the following equation [28]:

$$\Omega = \frac{\mathrm{TP}}{\mathrm{TP+FP+FN}} \quad (1)$$

where TP is the true positive area, FP is the false positive area of the ROI and FN is the false negative area or background of the ROI.

3.2.4. Oligonucleotide probe design and synthesis

LNA oligonucleotides (DNA/LNA and LNA/2'-OMe RNA chimeras with phosphates (PO) or phosphorothioates (PS) backbones (Table 3.1) were designed based on previous reports [29,30]. Oligonucleotides were prepared as described previously [31]. LNA and 2'OMe monomers were purchased from Exiqon (Copenhagen, Denmark) and Ribotask (Langeskov, Denmark), respectively.

Table 3.1 - Probe sequences used in this study. LNA nucleotide monomers are represented with L superscript, 2'-OMe-RNA monomers in boldface letters, DNA nucleotides in capital letters, and phosphorothioate linkages by the symbol*

Probes analysed	Sequence (5'-FAM-3')
HP_18LNA_PO	GA^{L}GA^{L}CT^{L}AA^{L}GC^{L}CC^{L}TC^{L}CT^{L}CC^{L}
HP_18LNA_PS	G*A^{L*}G*A^{L*}C*T^{L*}A*A^{L*}G*C^{L*}C*C^{L*}T*C^{L*}C*T^{L*}C*C^{L}
HP_18LNA/2OMe_PO	G^{L}**AG**A^{L} **CU**A ^{L}**AG** C^{L}**CC**T^{L}**CC**T^{L}**CC**
HP_ 18LNA/2OMe _PS	G^{L*}**A*G***A^{L*}**C*U***A^{L*}**A*G***C^{L*}**C*C***T^{L*}**C*C***T^{L*}**C*C**
HP_15LNA_PO	GA^{L}GA^{L}CT^{L}AA^{L}GC^{L}CC^{L}TC^{L}C
HP_15LNA_PO_2	GA^{L}GACT^{L}AAGC^{L}CCTC^{L}C
HP_15LNA_PS	G*A^{L*}G*A^{L*}C*T^{L*}A*A^{L*}G*C^{L*}C*C^{L*}T*C^{L}C
HP_15LNA_PS_2	G*A^{L*}G*A*C*T^{L*}A*A*G*C^{L*}C*C*T*C^{L*}C
HP_15LNA/2OMe_PO	G^{L}**AG**A^{L} **CU**A ^{L}**AG** C^{L}**CC**T^{L}**CC**
HP_ 15LNA/2OMe _PS	G^{L*}**A*G***A^{L*}**C*U***A^{L*}**A*G***C^{L*}**C*C***T^{L*}**C*C**
HP_12LNA_PO	GA^{L}GA^{L}CT^{L}AA^{L}GC^{L}CC^{L}
HP_12LNA_PS	G*A^{L*}G*A^{L*}C*T^{L*}A*A^{L*}G*C^{L*}C*C^{L}
HP_12LNA/2OMe_PO	G^{L}**AG**A^{L} **CU**A ^{L}**AG** C^{L}**CC**
HP_ 12LNA/2OMe _PS	G*A^{L*}G*A^{L*}C*T^{L*}A*A^{L*}G*C^{L*}C*C^{L}
HP_10LNA_PO	GA^{L}GA^{L}CT^{L}AA^{L}GC^{L}
HP_10LNA_PS	G*A^{L*}G*A^{L*}C*T^{L*}A*A^{L*}G*C^{L}
HP_10LNA/2OMe_PO	G^{L}**AG**A^{L} **CU**A ^{L}**AG** C^{L}
HP_ 10LNA/2OMe _PS	G^{L*}**A*G***A^{L*}**C*U***A^{L*}**A*G***C^{L}

3.2.5. Bacterial strains and culture conditions

H. pylori strain 26695 obtained from the American Type Culture Collection (ATCC 700392, VA USA) was maintained on trypticase soy agar (TSA) supplemented with 5% (v/v) sheep blood (Becton Dickinson GmbH, Germany). Single colonies were streaked onto fresh media every 48 hours and the plates were incubated at 37 °C under microaerobic conditions. Bacterial density was determined by the dilution of initial culture in water or saline and the absorbance was measured at 600 nm. All experiments were performed using bacteria in the same growth phase to avoid differences associated to cell permeabilization [32].

3.2.6. Hybridization conditions on slides and in suspension by FISH

To validate the FISHji methods, hybridization was assessed by fluorescent microscopy on slides in *attached bacteria* and by flow cytometry in bacterial suspensions. All probes from Table 3.1 were tested at temperatures between 37 °C and 65 °C and the fluorescence signal was quantified by both cytometry and FISHji methods. For both methodologies triplicate samples were used. In FISHji measurements we have also analysed nine images for each sample in order to study the entire sample. FISH in *attached and suspended bacteria* was performed as described in a previous study [31]. The cells were left at 4 °C until being analysed by cytometry. Probes were tested simultaneously at the same temperature in both samples types (attached and suspension bacteria), to minimize experimental variations between both methods (cytometry and FISHij).

3.2.7. Propidium iodide (PI)

Increasing concentrations of bacteria suspension (500 µL) were mixed with propidium iodide (PI) (Invitrogen, Eugene, USA) at a concentration of 50 ug/mL. For each concentration four samples were stained. Bacteria were incubated with PI for 10 minutes at room temperature. Afterwards, the samples were centrifuged during 5 minutes at 14 000 rpm and the supernatant was discarded. Then, two of the pellets were resuspended in water and analysed by microscopy and the other two were resuspended in saline and analysed by flow cytometry.

3.2.8. Microscope evaluation and quantitative analysis of fluorescence intensity

The slides with *attached bacteria* were evaluated on a Leica DM LB2 epifluorescent microscope. For image acquisition, a Leica DFC300 FX camera (Leica Microsystems

GmbHy, Germany) was used and the exposure time, gain and saturation values were fixed for all preparations. For image capture, Leica IM50 Image Manager, Image Processing and Archiving software was used. All experiments were performed in triplicate.

3.2.9. Flow cytometry and data analysis

The analysis of fluorescence intensities obtained by FISH in suspension was performed by flow cytometry. Flow cytometry analysis was performed using a Beckman Coulter Epics XL (Brea, USA) using the EXPO32ADC software (Beckman Coulter, Brea, USA) equipped with a low-power air-cooled 15 mW blue (488 nm) argon laser. For each sample, 20.000 events were collected. All the experiments were performed in triplicate and negative controls were included for each temperature in every analysis. Flow cytometric analyses of samples were performed based on forward scatter, side scatter and FL-1. Fluorescence was detected on the FL1 channel (BP: 530/30). Amplification was carried out using logarithmical scales.

3.2.10. Statistical and correlation analysis

Results are compared using one-way analysis of variance (ANOVA) by applying Tukey multiple-comparisons test, using GraphPad Prism version 5 software (GraphPad Sofware, San Diego, USA). All tests were performed with a confidence level of 95%.

3.3. Results and Discussion

3.3.1. Comparison between FISHji measurements and quantification by cytometry

In this paper we developed and validated five semi-automatic or automatic fluorescent intensity quantification methods, called FISHji, capable of quantifying the MFI. The settings and characteristics of each FISHji method developed are described in Table 3.2. As ground truth, the MFI of the hybridization experiments was also quantified using flow cytometry (gold standard method in fluorescence quantification) at the same temperature as the hybridizations performed in *attached* bacteria.

Table 3.2 - Comparisons between the five FISHji methods. The different methods were compared relatively to these general features

General features	FISHji1	FISHji 2	FISHji3	FISHji4	FISHji5
Operational mode	Semi-automatic	Semi-automatic	Semi-automatic	Automatic	Automatic
Image for analysis	Single image	Single image	Single image	Multiple images	Multiple images
Analysis speed per image	~50s	~50s	~ 1min20s	4s	4s
Cell segmentation	Manual Threshold	Manual Threshold	Manual Threshold	Automatic threshold	-
Rolling Ball	-	+	+	+	+
Manual B/C	-	-	+	+	-
B/C auto	-	-	-	-	+
LoG	-	-	-	+	+
Fill Holes	-	-	-	-	+
Analysed image	Original	Corrected	Corrected	Corrected	Corrected

In order to assess which FISHji method provide MFI values closer to the ones obtained by cytometry, the correlation between results from each FISHji (semi-automatic and automatic methods) and cytometry was calculated (Table 3.3). The three semi-automatic methods (FISHji 1, FISHji 2 and FISHji 3) present different results when compared to the cytometry. FISHji1 showed the lowest correlation with flow cytometry (Table 3.3). FISHji 2 showed a better correlation than FISHji 1, which suggests that, the performance of the optimization steps improved MFI quantification efficiency. The FISHji3 revealed to be the best semi-automatic method demonstrating that the application of a B/C adjustment after subtraction of the background contributed to a more effective MFI quantification.

Nevertheless, semi-automatic methods showed to be very time-consuming when a large number of samples have to be processed (Table 3.1), and since a routine protocol to perform fluorescence quantification should be fast and easy to work with, the need for an automatic method becomes clear. The automatic threshold definition is much more difficult to perform since one image is never equal to the other. Hence, has emerged the need for a more suitable and automatic segmentation technique. Previous studies have used LoG convolution to automatically enhance ROIs from the background with good outcomes [33]. Herein, FISHji4 was designed in which this approach was used to do both smoothing and edge detection. A high correlation between our plugin results and flow

cytometry analysis for the automatic FISHji4 was observed (Table 3.3). However the correlation factor is lower comparatively to the semi-automatic FISHji3. This result might have been influenced by cells from aggregates that were selected and subsequently counted due to the elevated sensibility of the convolution (Figure 3.2). Further, artifacts are not possible to discard in the ROI manager.

Table 3.3 - Comparison between each FISHji method values and flow cytometry data.

Measurements	FISHji 1	FISHji 2	FISHji 3	FISHji 4	FISHji 5
Ω	0.46	0.51	0.54	0.63	0.62
Correlation coefficient (p-value) *	0.456(<0.0001)	0.751(<0.0001)	0.819(<0.0001)	0.723(<0.0001)	0.717(<0.0001)

*Flow cytometry is used as a ground truth for calculating the correlation coefficient and the p-value

In an attempt to increase the automatic performance, a fifth method was designed (FISHji5) specifically to blurred regions after subtracted background, thereby connecting nearby cells (i.e. belonging to aggregates) and subsequently impairing the aforementioned problem. A high correlation between FISHji 5 and flow cytometry was also observed (Table 3.3). Contrary to expected, no significant differences emerged between both automatic methods. Visual image analysis allowed to conclude that the influence of aggregates in the present study was overestimated and auto B/C adjustment in ROIs with high fluorescence intensity increased the area of analysis, selecting false positive regions.
The results obtained for the correlation coefficient for FISHji 3, 4 and 5 are shown in detail in Figure 3.3. The average Pearson product moment correlation coefficient from all our biological repeats show a high level of correlation between the FISHji results and cytometry analysis, r=0.819 (0.733-0.880) in FISHji3.
One of the main factors that is influencing the results is the implementation of optimization steps that reflects on the efficiency of the definition of the edges of the ROI. In order to verify this influence in the MFI quantification, we calculated the overlap index Ω, as a measurement of the overlap performance between the edges defined by the implemented methods and the ground truth. This analysis is a commonly used method in several processing image studies, however it can suffer different adaptations depending on the purpose of the analysis [34,35]. FISHj1 showed the lowest mean Ω, indicating that the application of optimization steps before image segmentation improved the definition of the cell. In general, the overlapping results were congruent with the correlation factors for each method, indicating that the cell definition contributes largely to the MFI quantification.

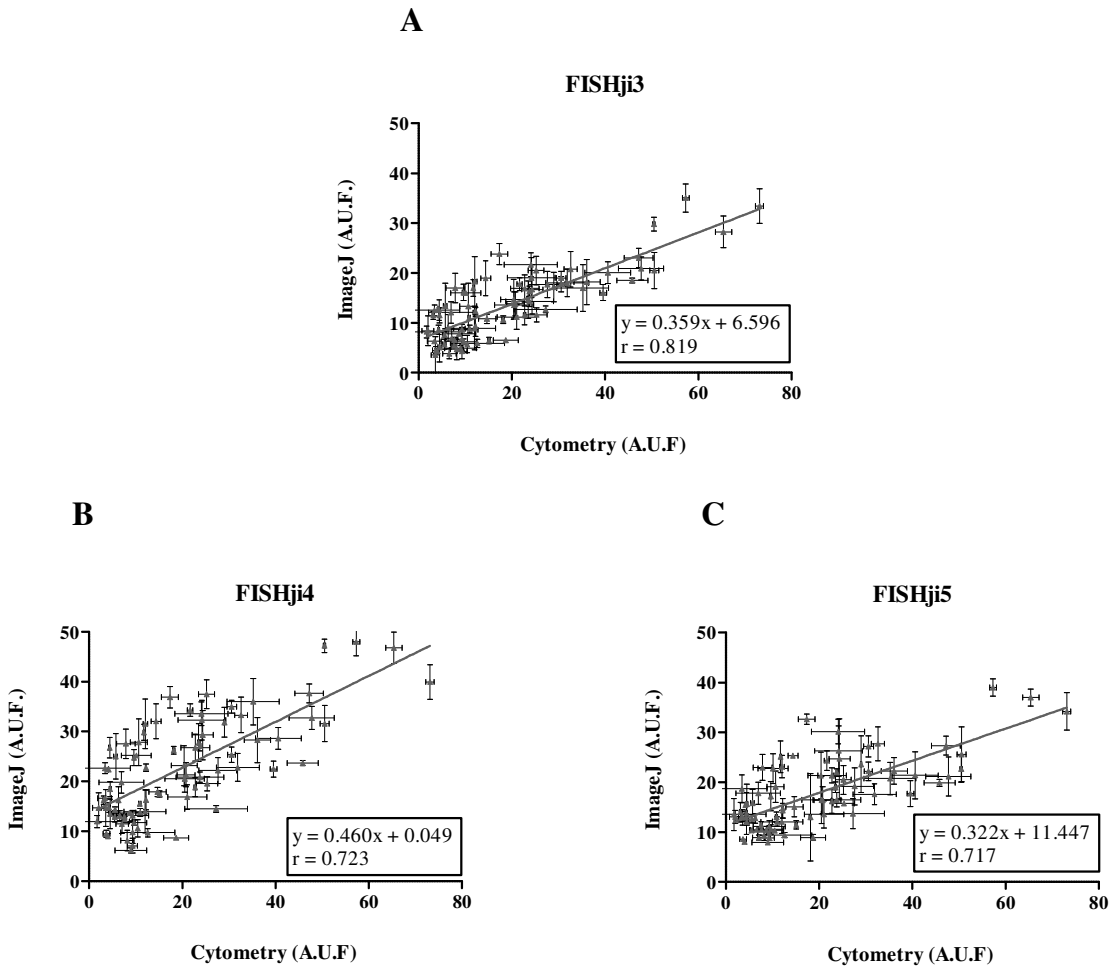

Figure 3.3 - Correlation analysis between fluorescence intensity (A.U.F) of LNA FISH obtained by ImageJ method and flow cytometry. A. FISHji 3; B. FISHji4; C. FISHji5. Regression lines are drawn and a high correlation between both methods was observed for semi and automatic methods in this study. Each data point consists of two parameters: the X-axis values corresponds to the mean of fluorescence intensity obtained by cytometry with a specific probe and temperature and the Y-axis values represent the mean value of fluorescence intensity obtained by FISHji in the same conditions

To evaluate whether the choice of the optimization steps and the consequent image analysed had influence in the MFI quantification, FISH images were re-analysed by the FISHji4 and FISHji5 methods, however now redirecting the binary mask to the original image instead of the corrected one. The low correlation coefficients obtained (r= 0.317 and r= 0.231, for FISHji4 and FISHji5, respectively) showed that the use of corrected images (after optimization steps) is essential in these analysis. Additionally, the original images can contain many different artefacts and autofluorescence signals that may blur or omit the real fluorescence value of the cell. The application of the "rolling ball" algorithm to the original green channel can correct background heterogeneity and eliminate some

artifacts, contributing to a more realistic MFI quantification when compared to the cytometry. Therefore, the choice of the analyzed image showed to be a major point in the MFI quantification, whereas the application of optimization steps before thresholding takes a relevant part in the efficiency of the definition of the cell, contributing in a smaller scale to the MFI quantification performance.

We also evaluated the influence of hybridization temperature in FISHji methods. Although there were differences between different hybridization temperatures, overall, the correlation coefficients were higher than those in the global analysis. As an example, we showed in Figure 3.4 the results for hybridization performed at 45 °C and 55 °C for FISHji3. In both cases we observed a high correlation r= 0.990 (0.724-0.990) for 45 °C and r= 0.907(0.647-0.978) for 55 °C. This suggests that the lower correlation values obtained for the FISHji3 using the entire set of data might also be due to some experimental variation.

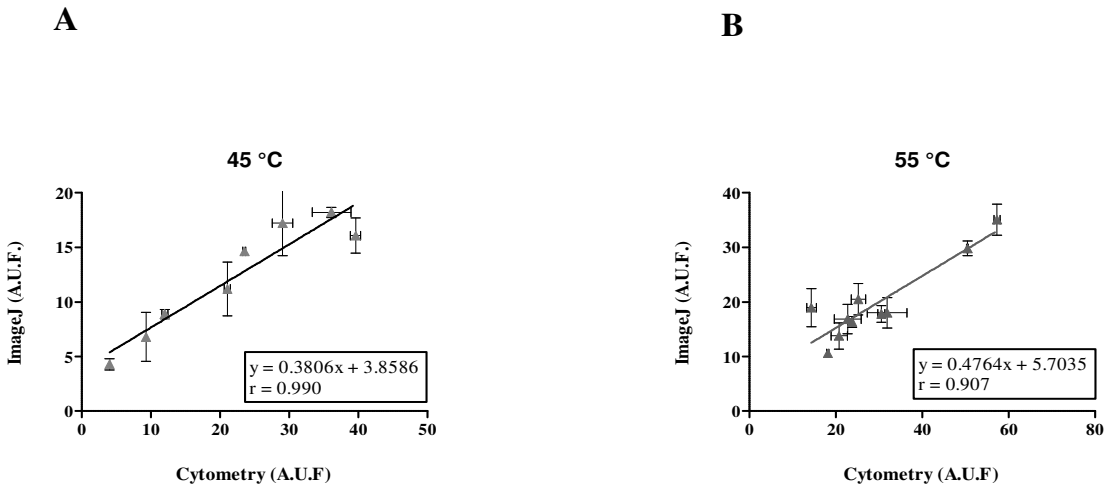

Figure 3.4 - Analysis of correction between fluorescence intensity (A.U.F.) obtained by FISHji3 method against fluorescence intensity (A.U.F.) obtained by flow cytometry, using hybridization temperatures. A. 45 °C; B. 55 °C. Regression lines are drawn and the r is displayed for each data comparison.

Because FISHji3 is a semi-automatic method, it requires manual definition of a threshold by the operator. In order to evaluate the influence of different operators in MFI quantification, two different operators have quantified the MFI of the same images. Our results (Figure 3.5) did not show statistically significance differences between the MFI values determined by each operator (p>0.05). The same results were obtained for FISHji1 and FISHji2 (Figure S5).

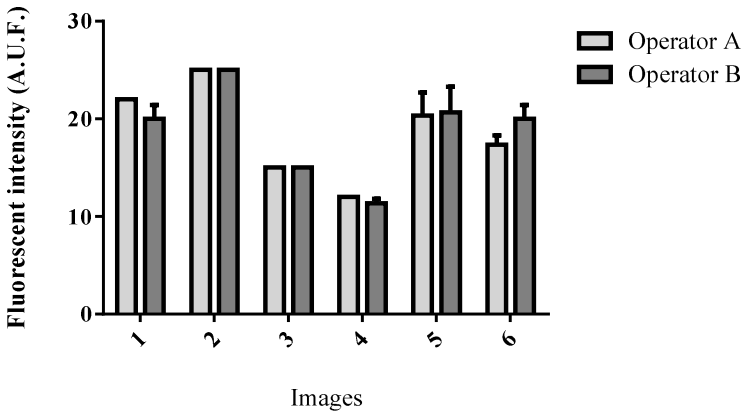

Figure 3.5 - Variability test between operators in FISHji 3.Fluorescence intensity was quantified for 6 images from 6 different experiments. Each image was independently analysed by each operator. Differences were observed between operators A and B were statistically non-significant ($p \geq 0.05$). A.U.F.: Arbitrary units of fluorescence.

While FISHji3 shows higher correlation with cytometer and is operator-independent for threshold, automatic methods FISHji4 or FISHji5 could be the key to development of a routine analysis for multiple FISH images. In this sense, automatic quantification without the need of expensive equipment (such as cytometer) would be recommended. Comparisons between FISHji3, FISHji4 and FISHji5 showed high levels of correlation in both cases (Figure 3.6), suggestion that both FISHji4 and FISHji5 offer the ability to automatically analyze considerable amounts of image data.

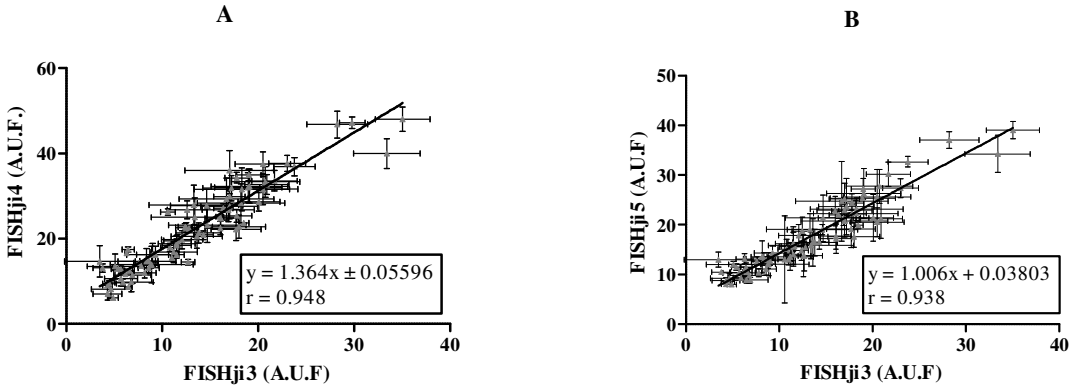

Figure 3.6 - Correlation between fluorescence intensity obtained by the best semi-automatic method (FISHji3) against fluorescence intensity (A.U.F.) obtained with automatic methods FISHji4 (A) and FISHji5 (B). A.U.F.: Arbitrary units of fluorescence.

In the present study, the main cornerstone of fluorescence intensity quantification was cell segmentation (i.e. definition of the ROIs). Indeed, segmentation can be very difficult due to the complexity of original images, represented by combination of different features like (1) autofluorescence; (2) background heterogeneity; (3) presence of non-cell objects and aggregates (herein considered as artifacts). Therefore, a very important issue to take in consideration when using this tool is the high dependence on image quality [3]. There are several factors which may interfere with the quality of the images, such as the numeral aperture (NA) of the objective, filed illumination of the lens, the refractive index of the embedding medium, use of coverslip, stability of the light source, the ratio between emission and excitation wavelength, amongst others [36]. Therefore, we always used the same settings in the microscope for every experiment to minimize these factors. Although all parameters associated with the image collection were kept constant, such as exposures times, illumination and focus, it was impossible to guarantee that the fluorescent lamp would produce the same light intensity during the whole of the experiments.

3.3.2. Correlation between FISHji measurements and quantification by cytometry using PI staining

In order to address the use of FISHji methods in measuring fluorescence obtained by means other than FISH, we performed the staining of *H. pylori* samples with PI. Therefore, we analysed the same sample by microscopy (and consequently the fluorescence intensity by FISHji 3, 4 and 5 methods) and cytometry. All the parameters were maintained in relation to the previous study. Our results (Figure 3.7) showed that there is a high correlation with the FISHji3 method r=0.981(0.8690 to 0.9972), with high significance ($p < 0.0001$). The analysis with the automatic methods also showed high correlation r=0.934(0.6137 to 0.9906) and r=0.902(0.4650 to 0.9856) for FISHji4 and FISHji5, respectively.

These results prove that FISHji could be used for any type of fluorescence procedures and that the correlation coefficients can be even higher for more reproducible experimental procedures. For that reason, we can conclude that a higher correlation relatively to the FISH experiments was probably due to several factors which interfere with signal fluorescence in this type of technique. It is already know that fluorescence is a complex phenomenon controlled by many external factors [37]. In fact, small FISH variations could happen during the experimental procedures which cannot be controlled.

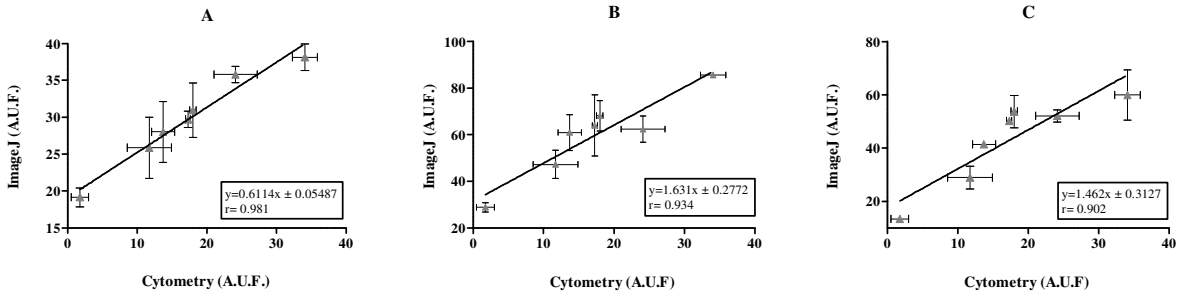

Figure 3.7- Correlation between FISHji measurements with quantification by cytometry using propidium iodide (PI) staining. Fluorescence quantification was performed in the red channel. A: FISHji3; B: FISHji4; C: FISHji5. A.U.F.: Arbitrary units of fluorescence.

3.4. Conclusion

Here we present FISHji methods to quantify fluorescence in images from biological samples obtained by microscopy.

We show that the semi-automatic FISHji3 and automatic FISHji4 and FISHji5 have high accuracy in different settings such as FISH and PI staining.

Since automated methods are able to simultaneously analyse multiple images and are faster, we provide an easy and freely available access to FISHji4 or FISHji5 for non-commercial use at http://paginas.fe.up.pt/~nazevedo/.

3.5. References

1. Wiesmann V., Franz D., Held C., Munzenmayer C., Palmisano R., Wittenberg T. Review of free software tools for image analysis of fluorescence cell micrographs. J Microsc (2015); 257: 39-53.
2. Collins T.J. ImageJ for microscopy. Biotechniques (2007); 43: 25-30.
3. Hartig S.M. Basic image analysis and manipulation in ImageJ. Curr Protoc Mol Biol (2013); Chapter 14: Unit14 15.
4. Shivanandan A., Radenovic A., Sbalzarini I.F. MosaicIA: an ImageJ/Fiji plugin for spatial pattern and interaction analysis. BMC Bioinformatics (2013); 14: 349.
5. Winter P.W., Shroff H. Faster fluorescence microscopy: advances in high speed biological imaging. Current Opinion in Chemical Biology (2014); 20: 46-53.
6. Cordelières F.P., Bolte S.Chapter 21 - Experimenters' guide to colocalization studies: Finding a way through indicators and quantifiers, in practice. In: Jennifer CW, Torsten W, editors. Methods in Cell Biology. (2014): Academic Press. pp. 395-408.
7. Winter P.W., Shroff H. Faster fluorescence microscopy: advances in high speed biological imaging. Curr Opin Chem Biol (2014); 20: 46-53.
8. Dorn J.F., Danuser G., Yang G.Computational Processing and Analysis of Dynamic Fluorescence Image Data. In: Kevin FS, editor. Methods in Cell Biology. (2008): Academic Press. pp. 497-538.
9. Cohen A.R. Extracting meaning from biological imaging data. Molecular Biology of the Cell (2014); 25: 3470-3473.
10. van Teeffelen S., Shaevitz J.W., Gitai Z. Image analysis in fluorescence microscopy: Bacterial dynamics as a case study. BioEssays (2012); 34: 427-436.
11. Amann R.I., Krumholz L., Stahl D.A. Fluorescent-oligonucleotide probing of whole cells for determinative, phylogenetic, and environmental studies in microbiology. J Bacteriol (1990); 172: 762-770.
12. DeLong E.F., Wickham G.S., Pace N.R. Phylogenetic stains: ribosomal RNA-based probes for the identification of single cells. Science (1989); 243: 1360-1363.
13. Amann R.I., Ludwig W., Schleifer K.H. Phylogenetic identification and in situ detection of individual microbial cells without cultivation. Microbiol Rev (1995); 59: 143-169.
14. Kubota K., Ohashi A., Imachi H., Harada H. Improved in situ hybridization efficiency with locked-nucleic-acid-incorporated DNA probes. Appl Environ Microbiol (2006); 72: 5311-5317.
15. Cerqueira L., Fernandes R.M., Ferreira R.M., Carneiro F., Dinis-Ribeiro M., Figueiredo C., et al. PNA-FISH as a new diagnostic method for the determination of clarithromycin resistance of Helicobacter pylori. BMC Microbiol (2011); 11: 101.
16. Yamamoto T., Nakatani M., Narukawa K., Obika S. Antisense drug discovery and development. Future Med Chem (2011); 3: 339-365.

17. Elayadi A.N., Braasch D.A., Corey D.R. Implications of high-affinity hybridization by locked nucleic acid oligomers for inhibition of human telomerase. Biochemistry (2002); 41: 9973-9981.
18. Bell N.M., Micklefield J. Chemical modification of oligonucleotides for therapeutic, bioanalytical and other applications. Chembiochem (2009); 10: 2691-2703.
19. Konsti J., Lundin J., Jumppanen M., Lundin M., Viitanen A., Isola J. A public-domain image processing tool for automated quantification of fluorescence in situ hybridisation signals. J Clin Pathol (2008); 61: 278-282.
20. Daims H., Lucker S., Wagner M. daime, a novel image analysis program for microbial ecology and biofilm research. Environ Microbiol (2006); 8: 200-213.
21. Stoecker K., Dorninger C., Daims H., Wagner M. Double labeling of oligonucleotide probes for fluorescence in situ hybridization (DOPE-FISH) improves signal intensity and increases rRNA accessibility. Appl Environ Microbiol (2010); 76: 922-926.
22. Hatzenpichler R., Lebedeva E.V., Spieck E., Stoecker K., Richter A., Daims H., et al. A moderately thermophilic ammonia-oxidizing crenarchaeote from a hot spring. Proc Natl Acad Sci U S A (2008); 105: 2134-2139.
23. Weber S.D., Ludwig W., Schleifer K.H., Fried J. Microbial composition and structure of aerobic granular sewage biofilms. Appl Environ Microbiol (2007); 73: 6233-6240.
24. Schneider C.A., Rasband W.S., Eliceiri K.W. NIH Image to ImageJ: 25 years of image analysis. Nat Methods (2012); 9: 671-675.
25. Sternberg S.R. Biomedical Image Processing. Computer (1983); 16: 22-34.
26. Chen J.S., Huertas A., Medioni G. Fast Convolution with Laplacian-of-Gaussian Masks. IEEE Trans Pattern Anal Mach Intell (1987); 9: 584-590.
27. Hogeweg L., Sánchez C.I., de Jong P.A., Maduskar P., van Ginneken B. Clavicle segmentation in chest radiographs. Medical Image Analysis (2012); 16: 1490-1502.
28. Gerig G., Jomier M., Chakos M.Valmet: A New Validation Tool for Assessing and Improving 3D Object Segmentation. In: Niessen W, Viergever M, editors. Medical Image Computing and Computer-Assisted Intervention – MICCAI 2001. (2001): Springer Berlin Heidelberg. pp. 516-523.
29. Kumar R., Singh S.K., Koshkin A.A., Rajwanshi V.K., Meldgaard M., Wengel J. The first analogues of LNA (locked nucleic acids): phosphorothioate-LNA and 2'-thio-LNA. Bioorg Med Chem Lett (1998); 8: 2219-2222.
30. You Y., Moreira B.G., Behlke M.A., Owczarzy R. Design of LNA probes that improve mismatch discrimination. Nucleic Acids Res (2006); 34: e60.
31. Fontenete S., Guimaraes N., Leite M., Figueiredo C., Wengel J., Filipe Azevedo N. Hybridization-based detection of Helicobacter pylori at human body temperature using advanced locked nucleic acid (LNA) probes. PloS one (2013); 8: e81230.
32. Bottari B. E.D., Gatti M., Neviani E. FISH in Food Microbiology. In: Liehr T, editor.(2009). Berling: Springer-Verlag.

33. Haidekker M. Advanced Biomedical Image Analysis.(2010): Wiley. pp. 528.
34. Zaidi H., Abdoli M., Fuentes C.L., El Naqa I.M. Comparative methods for PET image segmentation in pharyngolaryngeal squamous cell carcinoma. Eur J Nucl Med Mol Imaging (2012); 39: 881-891.
35. Zou K.H., Warfield S.K., Bharatha A., Tempany C.M., Kaus M.R., Haker S.J., et al. Statistical validation of image segmentation quality based on a spatial overlap index. Acad Radiol (2004); 11: 178-189.
36. Kumar G. Z.R.M. Fluorescence In Situ Hybridization (FISH) Imaging. In: Dako, editor. Immunohistochemical Staining Methods Education Guide.(2013).
37. Tanke H.Fluorescence microscopy for quantitative fluorescence in situ hybridization analysis. In: Andreeff M. PD, editor. Introduction to Fluorescence In Situ Hybridization: Principles and Clinical Applications. (1999): Wiley-Liss

Chapter IV

Mismatch discrimination in Fluorescent in situ hybridization using different types of nucleic acids

Appl Microbiol Biotechnol (2015) 99:3961–3969
DOI 10.1007/s00253-015-6389-4

APPLIED GENETICS AND MOLECULAR BIOTECHNOLOGY

Mismatch discrimination in fluorescent in situ hybridization using different types of nucleic acids

Silvia Fontenete[1,2,3,4] · **Joana Barros**[1,5] · **Pedro Madureira**[4,6] · **Céu Figueiredo**[2,7] · **Jesper Wengel**[3] · **Nuno Filipe Azevedo**[1]

Received: 20 August 2014 / Revised: 7 November 2014 / Accepted: 8 November 2014 / Published online: 21 January 2015

ABSTRACT

In the past few years, several researchers have focused their attention on nucleic acid mimics due to the increasing necessity of developing a more robust recognition of DNA or RNA sequences. Fluorescence *in situ* hybridization (FISH) is an example of a method where the use of these novel nucleic acid monomers might be crucial to the success of the analysis. To achieve the expected accuracy in detection, FISH probes should have high binding affinity towards their complementary strands and discriminate effectively the non-complementary strands.

In this study, we investigate the effect of different chemical modifications in fluorescent probes on their ability to successfully detect the complementary target and discriminate the mismatched base pairs by FISH. To our knowledge, this paper presents the first study where this analysis is performed with different types of FISH probes directly in biological targets, *Helicobacter pylori* and *Helicobacter acinonychis*. This is also the first study where unlocked nucleic acids (UNA) were used as chemistry modification in probes for FISH methodologies.

The effectiveness in detecting the specific target and in mismatch discrimination appears to be improved using locked nucleic acids (LNA)/2'-O-methyl RNA (2'OMe) or peptide nucleic acid (PNA) in comparison to LNA/DNA, LNA/UNA or DNA probes. Further, the use of LNA modifications together with 2'OMe monomers allowed the use of shorter fluorescent probes and increased the range of hybridization temperatures at which FISH would work.

Keywords: FISH, probes, nucleic acids, microbiology, mismatch discrimination

4.1. Introduction

It has been shown that fluorescent *in situ* hybridization (FISH) is a very sensitive and specific method for microbial identification in clinical, industrial and environmental samples [1-3]. The success of this methodology relies on the specificity of oligonucleotide sequences to their complementary target. Ideally, oligonucleotides should hybridize with fully-complementary DNA or RNA sequences and fail to hybridize with sequences that contain one or more mismatches [4]. However, it has been shown that for DNA sequences this discrimination is often difficult to achieve [5]. More recently, other types of synthetic nucleic acids such as peptide nucleic acid (PNA) and locked nucleic acids (LNA) have been used in FISH with very promising results [6-11]. To understand the specificity of these novel molecules towards DNA and RNA, several thermal dissociation studies have been conducted to analyze the effects of mismatches on duplex stability [4,12,13]. However, this type of analysis has always been performed with naked DNA in standard chemical solutions. Therefore it is not necessarily predictive of what occurs during a FISH procedure in which a chemically modified probe hybridizes to rRNA within a cellular microenvironment [14].

In here, we evaluate the mismatch discrimination potential of different types of DNA/RNA mimics used frequently in the literature for FISH, such as PNA, LNA and 2'-O-methyl RNA (2'OMe), and also of a molecule that has not been previously used in FISH, named unlocked nucleic acids (UNA). Mismatch discrimination was assessed both by thermal dissociation studies and in FISH experiments. As a case study, we tested the discrimination of the sequences for two closely-related *Helicobacter* spp., *Helicobacter pylori* and *Helicobacter acinonychis* [15,16]. In fact, our group has been focused on the development of several FISH methodologies to detect *Helicobacter* species, namely using peptide nucleic acids (PNA) [7,9,17], locked nucleic acids (LNA) and 2'-O-methyl RNAs (2'OMe) [18]. The novel probes were purposely designed for a specific and conservative region in the 16S rRNA of *H. pylori* that is also present, with a single mismatch, in *Helicobacter acinonychis* (*H. acinonychis*). Therefore, we evaluate how a single mismatch in the DNA or RNA target influences the hybridization stability and also report on the ability of different probes to discriminate between *H. pylori* and *H. acinonychis,* at a large range of temperatures.

4.2. Materials and methods

4.2.1 Probe design

For mismatch discrimination, it was necessary to find a sequence which was identical within the two *Helicobacter species* with the exception of a single nucleotide. The 16S rRNA target region was selected based on a search conducted at the 16S rRNA database of the Ribosomal Database Project II (RDP-II), version 10 (http://rdp.cme.msu.edu/) The ribosomal sequence *5'-ATTACTGGAGAGACTAAGC-3'*, which allowed the detection of *H. pylori*, was selected. The 16S sequence of *H. acinonychis* is similar except for the G (underlined) that in *H. acinonychis* is an A**.** We used different types of nucleic acids targeting *H. pylori*: LNA, 2'OMe, unlocked nucleic acid (UNA), PNA and DNA (Table 4.1). Different designs of oligonucleotide probes were tested to find the best discrimination possible based on earlier published criteria to improve mismatch discrimination [13,19-23]. As DNA has a restricted flexibility of oligonucleotide design, only one probe was designed (Table 4.1). The length of this probe was selected based on the analysis of the Gibbs free energy (Δ*G*°), which, according to Yilmaz *et al*. [24], must be lower than -13.5 kcal/mol. The probe used in this study has a Δ*G*° of -16.63 kcal/mol. Similarly, PNA also has a restricted flexibility of probe design as PNA cannot be mixed with nucleotide monomers like DNA, LNA or UNA. In this case, and because there are no guidelines related to the minimum Δ*G*°, we based our design on our extensive experience in working with these probes [7,9,17]. In contrast, LNA, 2'OMe and UNA bases can be positioned anywhere within an oligonucleotide sequence, which means that the design is much more flexible and that probe fine-tuning is possible [22]. As a general rule, these probes were designed with a triplet of LNA-modified nucleotides positioned at the center of the mismatch site to improve the discrimination [13,22]. The use of a higher density of LNA residues in each probe is another important parameter to improve mismatch discrimination [22]. In the case of HyP_LNA/2'OMe probes (1 and 2) (Table 4.1), every second base was LNA-modified as previously reported [25].

Table 4.1 - Sequence of the different oligonucleotide probes used in the present study. LNA nucleotide monomers are represented with L superscript, 2'-OMe-RNA monomers are represented with m superscript, DNA monomers are represented with italic and with *d*, and UNA monomers are represented with u and in boldface letters

Name	*Sequence (5'FAM-3')*
HyP_DNA	*d*(TTACTGGAGAGACTAAG)
HyP_PNA	CTGGAGAGACT
HyP_LNA/UNA1	$T^{L}G^{L}$**uG**$A^{L}G^{L}A$**uG**$A^{L}C^{L}$
HyP_LNA/UNA2	$C^{L}T^{L}$**uG**$G^{L}A^{L}G^{L}A^{L}G$**uA**$C^{L}T^{L}$
HyP_LNA/UNA3	$C^{L}T^{L}G$**uG**$A^{L}G^{L}A$**uG**$A^{L}C^{L}T^{L}$
HyP_LNA/2'OMe1	$U^{m}G^{L}G^{m}A^{m}G^{L}A^{m}G^{L}A^{m}C^{m}$
HyP_LNA/2'OMe2	$C^{m}U^{L}G^{m}G^{m}A^{L}G^{m}A^{m}G^{L}A^{m}C^{m}U^{m}$
HyP_LNA/DNA1	T^{L}*d*GG^{L}*dA*G^{L}*d*AG^{L}*d*AC^{L}
HyP_LNA/DNA2	C^{L}*d*T*d*G*d*G$A^{L}G^{L}A^{L}$*d*G*d*A*d*CT^{L}

4.2.2 Probes synthesis and purification

The DNA oligonucleotide (HyP_DNA) attached to fluorescein phosphoramidite (FAM) was purchased from Sigma-Aldrich (St. Louis, USA). The PNA (HyP-PNA) probe was synthesized by Panagene (Daejeon, South Korea) and the probe N terminus was attached to an FAM molecule via a double 8-amino-3,6-diaxaoctanoic acid (AEEA) linker. Both probes were HPLC purified to reach a purity of >90%.

The remaining probes were synthesized on an Expedite DNA synthesizer (PerSpective Biosystems Expedite 8909 instrument) using standard phosphoramidite chemistry in 1.0 µmoL scale. The synthesized probes were deprotected and cleaved from the solid support by treatment with 32% (v/v) aqueous ammonia solution for 12h at 55 °C (UNA1_HPy, UNA2_HPy, UNA3_HPy, LNA1_HPy and LNA2_HPy probes) or with 98% (v/v) aqueous methanol/ammonia solution 7 N in methanol (1:1) for 2 h at RT, followed by an incubation with 32% (v/v) aqueous ammonia solution for 12 h at 55 °C (2'OMe1_HPy and 2'OMe2_HPy probes). DNA and LNA monomers are commercially available from Proligo Reagents and Exiqon (Copenhagen, Denmark), respectively. UNA and 2'OMe monomers are commercially available from Ribotask (Langeskov, Denmark). All probes were purified by reversed phase HPLC (RP-HPLC) and characterized by IonExchange HPLC conditions (IE-HPLC) on a Dionex system HPLC and matrix-assisted laser desorption ionization time-of-flight mass spectrometry (MALDI-TOF). The purified probes were precipitated by acetone and their purity (>90%) and composition were verified by IE-HPLC and MALDI-TOF analysis, respectively.

For thermal denaturation studies, unmodified DNA [HyP_DNA_Target: 5'-d(GCTTAGTCTCTCCAGTAAT)-3'] and RNA oligonucleotides [HyP_RNA_Target: 5'-r(GCUUAGUCUCUCCAGUAAU)-3'] were purchased from Sigma-Aldrich and Integrated DNA technologies (Leuven, Belgium), respectively. Also, the DNA sequence 5'-d(ATTACTGGAGAGACTAAGC)-3' (HyP_DNA_Ref), that was used as a reference in thermal denaturation studies, was purchased from Sigma-Aldrich.

4.2.3 Thermal denaturation studies

The thermal denaturation studies were performed following published protocols [26,27]. Melting curves of fully-complementary and of one-mismatch containing oligonucleotide duplexes were recorded on a Perkin Elmer Lambda 35 UV/VIS spectrometer equipment with a PTP 6 (Peltier Temperature Programmer) element (Massachusetts, USA). One µM of each strand was used in different types of melting buffers: medium salt buffer with 110 mM Na^+ (100 mM NaCl, 10 mM NaH_2PO_4 and 0.1 mM EDTA, pH 7.0); low salt buffer with 30% formamide and 10 mM Na^+ (10 mM NaCl, 5 mM EDTA, 50 mM Tris-HCl and 30% (v/v) formamide, pH 7.5); and a high salt buffer with 4 M of urea and 900 mM Na^+ (900 mM NaCl, 5 mM EDTA, 50 mM Tris-HCl and 4 M of urea, pH 7.5). The medium buffer is a standard buffer used in this type of studies. The low and the high salt buffers were used to mimic the buffers used in FISH experiments with bacterial cells. Each sample was mixed and the resulting complexes denatured by heating to 85 °C during 5 min; samples were then cooled to the starting temperature of the experiment. Quartz optimal cells with a path length of 1.0 cm were used. Melting temperatures (T_m values) were determined as the maximum of the first derivative of the thermal denaturation curve (A_{260} vs. temperature for medium salt buffer and high salt buffer with 4 M urea and A_{270} vs. temperature low salt buffer with 30% (v/v) formamide). Absorbance was monitored at 270 nm in the low salt buffer because of the inherent absorbance of formamide at 260 nm [28]. A temperature range from 13-15 °C to 80-85 °C and a ramp of 1.0 °C/min were used. Reported T_m values are an average of two measurements within ± 0.5 °C.

4.2.4 Bacterial strains and culture conditions

H. pylori 26695, obtained from the American Type Culture Collection (ATCC 700392, VA USA) and *H. acinonychis* strain 90-119, obtained from the Health Protection Agency Culture Collections (HPA Culture Collections 12686, Salisbury, UK), were subcultured every 48 h in trypticase soy agar (TSA) supplemented with 5% (v/v) sheep blood (Becton Dickinson GmbH, Germany) and incubated at 37 °C under microaerobic conditions using

a GENbox microaer (bioMérieux, Marcy l'Étoile, France). Cell concentration was obtained by optical density (O.D.) and each initial culture was diluted in saline buffer in order to obtain a final concentration of 10^6 total cells/mL.

4.2.5 Optimization of probe hybridization conditions

Different hybridization conditions were used, depending on the nucleic acid composition, length and chemical nature of each probe. Therefore, we studied a large temperature range of 25-70 °C in pure cultures of *H. pylori*. For specificity analysis we tested these probes for mismatch discrimination using *H. acinonychis* at temperatures for which probes showed higher sensitivity. All probes were optimized in FISH standard conditions (hybridization temperature, salt concentration, pH and formamide/urea concentration). To optimize the DNA-FISH protocol we used different types of model protocols for DNA-FISH [29,30] and we performed several adjustments for all steps. After fixation and cell disaggregation of each suspension (as previously described [18]), an extra permeabilization step was performed by adding 30 µL lyzozyme (2 mg/mL in 10 mM Tris/HCl (pH 8)) during 1 h at 37 °C. The fixed cells (100 µL) were resuspended in equal volume of the hybridization solution (0.9 M NaCl, 20 mM Tris-HCl [pH 7.5], 0.001% (v/v) SDS, 30% (v/v) formamide and 400 nM of probe) and incubated at different temperatures for 90 min. Samples were centrifuged at 14000 rpm for 5 min, resuspended in 500 µL of washing solution (0.64 M NaCl, 5 mM Tris-HCl [pH 7.5], 0.01% (v/v) SDS, pH 7) and incubated at the same temperature of hybridization for 20 min. Samples were again centrifuged at 14000 rpm for 5 min and resuspended in saline buffer. To remove aggregates, samples were filtered by a sterile filter with 10 µm pore size (CellTrics®) and were directly analyzed using flow cytometry.

The hybridization procedure for the PNA probe was similar to that used for the LNA probes [9,18] however using a different type of hybridization buffer as described in Table 4.2. The hybridization method in suspension for LNA probes (LNA+DNA, LNA+2'OMe and LNA+UNA) was based on procedures described by Fontenete *et al.* [18].

The ability of the probes to discriminate the mismatch base pairs was then assessed by fluorescence intensity quantification studies (flow cytometry).

Table 4.2 - Differences between hybridization buffers used for each type of probe. FA: formamide

Probe	Denaturant	[NA^+]	Tris-HCl	Others reagents
HyP_DNA	30% (v/v) FA 0.001% (v/v) SDS	900 mM	20 mM	-
HyP_PNA	30% (v/v) FA	10 mM	50 mM	0.1%(v/v) Triton-x 10% (v/v) dextran sulphate 5 mM of EDTA
HyP_LNA	4 M urea	900 mM	50 mM	

4.2.6 Evaluation of rRNA level

To confirm if the percentage of rRNA is similar in both of *Helicobacter* species an universal PNA EUB338 probe (5'Alexa fluor 488-TGCCTCCCGTAGGA-3') which recognized a conserved region of the 16S rRNA in the domain Bacteria [31] was used as a model probe . FISH experiments were performed as described above for PNA probes at 57 °C. Each experiment was performed in triplicate.

4.2.7 Flow Cytometry and data analysis

Flow cytometry analysis was performed using an EPICS XL flow cytometer containing a low-power air-cooled 15 mW blue (488 nm) argon laser. Data analysis was performed with the EXPO32ADC software (Beckman Coulter, Brea, USA). For each sample, 20 000 events were collected. All experiments were repeated in two runs (using three biological replicates of cultures for each run) and negative controls without probe were included for each type of protocol in every analysis. Flow cytometric analyses of samples were performed based on both scattering signals (forward scatter and side scatter) and FL-1. FAM fluorescence was detected on the FL1 channel (BP 530/30). For all detected parameters, amplification was carried out using logarithmical scales.

4.2.8 Statistical analysis

Statistical significance was determined by One-way analysis of variance (ANOVA) by applying the Tukey multiple-comparisons test, using SPSS® statistics 17.0 (SPSS, Statistical Package for the Social Sciences, Chicago, USA) or Microsoft Office Excel® (Microsoft Corporation, Redmond, USA). Results were expressed as mean values. Differences were considered significant when $p<0.05$.

4.3. Results

4.3.1 Melting temperature analysis

The T_m values for the probes bound to fully-complementary and single-mismatched targets are shown in Table 4.3 for the DNA target and in Table 4.4 for the RNA target. Because FISH hybridizations are performed in buffers of various compositions, we used different types of buffers with different ionic environments (different salt concentrations) and denaturing agents. In general, we observed an increase of T_m at higher salt concentrated solutions and destabilization in the duplex strands when FA was used. For probes of similar lengths, LNA/ 2'OMe displayed the highest thermal stability in all buffers studied. LNA/DNA probes also allowed the formation of relatively stable duplexes. The PNA oligonucleotide also showed a high stability in all buffers. The use of UNA monomers affected negatively the stability of the duplexes, and as such the lowest melting temperatures in all buffers were obtained for these probes (Table 4.4).

The specificity of the LNA and PNA probes was confirmed by testing their ability to discriminate against mismatches in single-mismatch DNA and RNA strands (Table 4.3 and 4.4, respectively). Modified probes exhibited better mismatch discrimination than the DNA oligomers, as confirmed by the higher ΔT_m values. HyP_UNA/LNA probes showed a high capacity of mismatch discrimination in medium salt buffer (110 mM), and in some cases no hybridization in the buffers with FA and urea was found with the single-mismatch strand. LNA/2'OMe probes had the highest discrimination capacity in the high salt buffer with 4M of urea, even though HyP_LNA/DNA and PNA probes also presented a strong specificity for this sequence.

Table 4.3 - Melting temperatures, T_m (°C) and mismatch (C>T/U) discrimination temperature difference. ΔT_m in different buffers for DNA complementary target in 110 mM Na^+ buffer, 10 mM Na^+ buffer with 30% (v/v) formamide and 900 mM Na^+ buffer with 4 M urea

	T_m at total [Na^+] indicated					
	110 mM		10 mM		900 mM	
Name	T_m	ΔT_m	T_m	ΔT_m	T_m	ΔT_m
Reference	52.3	**6.9**	37.4	**1.3**	56.6	**8.2**
HyP_DNA	48.9	**8.4**	33.5	**6.9**	51.5	**8.9**
HyP_PNA	64.6	**15.3**	42.7	**16.5**	60.9	**17.2**
HyP_LNA/UNA1	17.4	***nb***	15.3	***nb***	42.1	***nb***
HyP_LNA/UNA2	38.5	**17.9**	21.8	**9.7**	41.6	**21.3**
HyP_LNA/UNA3	35.5	**14.2**	20.5	***nb***	34.2	**14.9**
HyP_LNA/2'OMe1	59.1	**12.1**	47.6	**17.3**	70.8	**10.2**
HyP_LNA/2'OMe2	63.51	**12.2**	51.7	**15.5**	78.3	**13.1**
HyP_LNA/DNA1	57.5	**20.3**	44.6	**17.3**	60.7	**13.2**
HyP_LNA/DNA2	53.2	**15.0**	44.2	**21.2**	62.0	**14.1**

nb: no binding could be detected

Table 4.4 - Melting temperatures, T_m (°C), mismatch (C>T/U) discrimination temperature difference (ΔT_m) and hybridization temperatures T_H (°C) at which each probe had highest sensitivity and specificity. ΔTm in different buffers for RNA complementary oligonucleotide: 110 mM Na^+ buffer[a], 10 mM Na^+ buffer with 30% (v/v) formamide and 900 mM Na^+ buffer with 4 M urea

	T_m at total [Na^+] indicated						Hybridization Temperature
	110 mM		10 mM		900 mM		900 mM
Name	T_m	ΔT_m	T_m	ΔT_m	T_m	ΔT_m	T_H
Reference	49.3	**3.3**	35.2	**5.1**	52.6	**9.1**	-
HyP_DNA	44.5	**10.0**	30.2	**9.35**	46.6	**9.9**	70
HyP_PNA	67.6	**13.2**	44.6	**15.6**	62.4	**11.4**	45
HyP_LNA/UNA1	32.4	***nb***	32.1	***nb***	35.9	**16.8**	53
HyP_LNA/UNA2	53.7	**13.8**	38.1	**15.3**	59.6	**13.3**	53
HyP_LNA/UNA3	50.7	**12.9**	36.1	**14.9**	54.9	**13.4**	48
HyP_LNA/2'OMe1	69.4	**13.3**	57.8	**15.9**	78.9	**18.1**	60
HyP_LNA/2'OMe2	75.4	**12.8**	62.3	**13.2**	78.2	**17.6**	65
HyP_LNA/DNA1	66.4	**13.5**	54.2	**14.1**	71.4	**11.5**	43
HyP_LNA/DNA2	62.1	**12.8**	47.9	**14.4**	67.4	**13.9**	40

Nb: no binding could be detected

4.3.2 Mismatch discrimination analysis in bacteria by flow cytometry studies

To analyze the efficiency of the probes in bacterial cells, we tested each probe in a range of temperatures between 25 and 70 °C measuring the fluorescence signal by flow cytometry. All FISH conditions used were the standard for each type of oligonucleotide, therefore we used different buffers depending on whether we were using DNA, PNA or LNA probes.

The hybridization experiments were first performed with *H. pylori* as a target, in order to understand at which temperatures we could obtain a more efficient detection. The optimal hybridization temperature for each probe was considered as the temperature at which the hybridization with the microorganism of interest provided the strongest fluorescent signal and more specificity (weakest signal for the microorganism with the mismatch).

The subsequent experiments analyzed the capacity of mismatch discrimination. As a result, we performed FISH experiments with each probe in *H. acinonychis*, which had a single mismatch in the rRNA comparatively to *H. pylori*. As an example, Figure 4.1 shows the results obtained for HyP_LNA/2_OMe1 for both microorganisms at different temperatures. From Figure 4.1 we conclude that the hybridization temperature where the fluorescence intensity is higher for *H. pylori* is 45 °C, whereas this hybridization temperature for *H. acinonychis* is 30 ºC. This appears to indicate a ΔT_m for this probe of 15 °C, which compares with the ΔT_m of 18.1 °C obtained in the thermal dissociation studies for the buffer used for LNA probes (900 mM Na+ buffer with 4 M urea). While these values are not very different, further studies would have to be performed to confirm that thermal dissociation studies provide an acceptable prediction of differences in hybridization temperatures between fully-complementary and single-mismatch targets in FISH experiments.

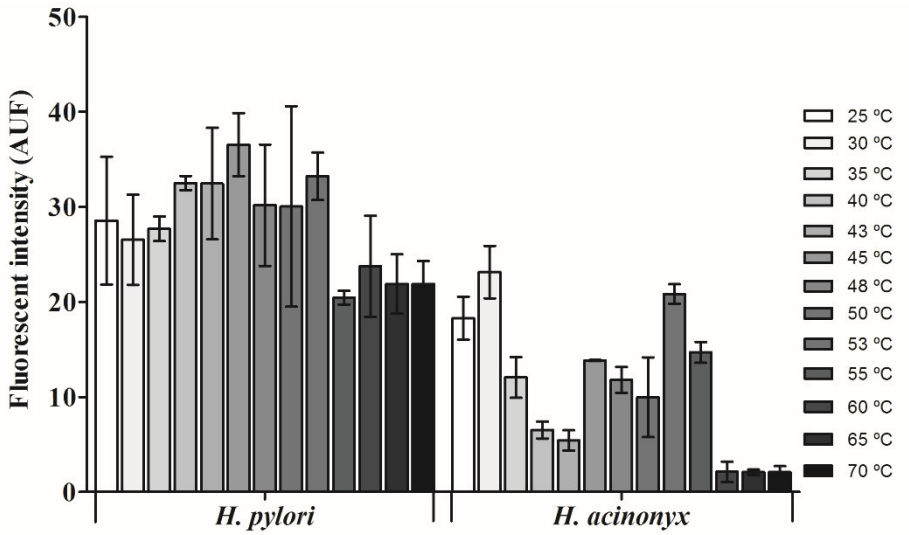

Figure 4.1 - The effect of the temperature on the specificity of HyP_LNA/2_OMe1 probe. Histogram showing the distribution of fluorescence intensity with the temperature in *H. pylori* and *H. acinonychis*.

The results of the FISH experiments for the optimal hybridization temperatures of *H. pylori* using the different probes can be analyzed in Figure 4.2. The fluorescence intensity of the HyP_LNA/2'OMe1 and HyP_LNA/2'OMe2 probes is significantly higher in *H. pylori* than in *H. acinonychis* (p=0.028 and p=0.00, respectively). The difference between the detection in *H. pylori* than *H. acinonychis* is also statistically significant in HyP_PNA (p=0.001). On the other hand, no statistically significant differences were observed in terms of fluorescence intensity between the bacteria in study with HP_DNA probe, HyP_LNA/UNA probes and HyP_LNA/DNA probes (p>0.05).

In the specific conditions used for each experiment, LNA/2'OMe probes showed the highest fluorescence signal of the probes analyzed. The difference in fluorescence intensity is statistically significant (p<0.05) between these probes and HyP_LNA/UNA and HyP_LNA/DNA2 probes. However, the PNA probe represents a good alternative for these types of studies, since it showed a higher sensitivity and specificity at lower hybridization temperatures. LNA/DNA probes showed distinct results, which were dependent on the length of the probe. The shorter probe had similar results to the PNA oligonucleotide in terms of fluorescent intensity; however, the 11 mer oligonucleotide showed a very low capacity of hybridization with the target. Although the data from the melting behavior of this probe was very similar to those of the 9 mer LNA/DNA probe, the hybridization in the bacteria revealed very different results. The same behavior was observed for the HyP_DNA probe.

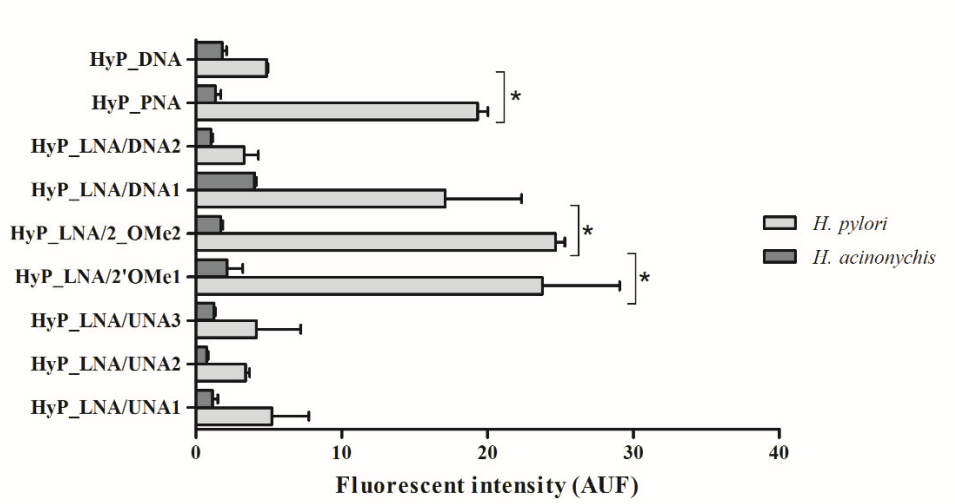

Figure 4.2 - FISH detection of *H. pylori* and *H. acinonychis* by cytometry at the optimal hybridization temperature. Quantification of the mean fluorescence intensity of each probe in two independent experiments. The optimal hybridization temperature for each probe is described in Table 4.4. The fluorescent signal intensity is expressed in arbitrary fluorescent units (AUF). * Difference between *H. pylori* and *H. acinonychis is* statistically significant (p<0.05).

For the evaluation of the rRNA level of each species of *Helicobacter*, we used EUB338 probe which target both species. It was observed similar gates (percentage of cells identified by EUB338 probe) and comparable AUF for both bacteria (47.9±9.8 and 45.8±5.3 for *H. pylori* and *H. acinonychis*, respectively). Therefore, there are not significant differences in rRNA levels between these bacteria.

4.4 Discussion

The detection of microorganisms by FISH has significantly changed with the introduction of several types of synthetic probes that possess a higher capacity of discrimination and affinity towards complementary sequences [9,32-36]. Therefore, it is very important to discuss which type of nucleic acid mimics is more suitable for each specific situation, such as the recognition of mismatches. To tackle this issue, in this study we analyzed the performance of different types of probes to discriminate mismatches, not only by thermal melting analysis of naked nucleic acids, but also for specifically targeting bacterial cells with a FISH methodology.

To analyze the relationship between different types of probes and specificity we performed melting studies for all probes with DNA and RNA targets. The use of different targets is important because even though the FISH methodology is more frequently described for RNA targets, there are also several studies using modified probes which use

DNA as a target e.g.[37,38]. In accordance with the literature, a higher T_m was observed at higher salt concentrated solutions [39]. Higher concentrations of NaCl allow the repulsion between the negatively charged probes to be increasingly compensated by the positive counterions. However, this effect is smaller in one-mismatch duplexes because the two strands are further apart [40]. On the other hand, the use of FA and urea was expected to allow for the destabilization in the duplex strands leading to lower melting temperatures [41]. However, this destabilization did not decrease the Tm to the same extent in the high salt buffer (Table 4.4). As expected, we observed a large difference in Tm for all probes bound to fully-complementary oligonucleotides versus oligonucleotides containing one mismatch. The difference between the Tm values for each oligonucleotide was in agreement with results published earlier [20,42,43]. LNA/ 2'OMe and PNA showed high stability in all buffers, comparatively to LNA/DNA probes. It has already been demonstrated that LNA and 2'OMe have different impact on duplex stability, in spite of sharing a *C3'*-endo sugar pucker conformation [4]. In general we observed an increase of thermal duplex stability in the following order: HyP_LNA/UNA probes<DNA probe<HyP_LNA/DNA probes < HyP_PNA = HyP_LNA/2' OMe probes (Table 4.4).

Usually T_m is used as an indication for the hybridization temperature because it is at this temperature half of the nucleic-acid strands are forming a duplex and the other half are single stranded [44]. However, the hybridization temperature determined by experimental procedures *in vitro* is dependent of all biological parameters and chemical compounds involved in the hybridization step of a FISH procedure. These factors can be a cause for the absence of a pattern between these temperatures [45]. In fact, when we compare the discrimination temperature difference obtained by thermal studies with FISH under the same buffer conditions (Table 4.4), we can observe that statistically significant differences may arise (p<0.05). Actually, it is highly unpredictable how each probe will hybridize in experiments with bacteria, because there are several factors that can affect the efficiency of the hybridization [14]. For instance, the diffusion through the extracellular membrane can be different for each probe [46]. Therefore, we used the same standard parameters for all studied probes and the experiments were performed under presumed optimal conditions. We have also assessed for the first time the use of HyP_LNA/UNA probes in FISH experiments. However, our results show that the use of UNA leads to a large destabilization in the duplex which affects the hybridization in bacteria (Table 4.4 and Figure 4.2). Therefore the use of UNA modifications in FISH probes may require the use of longer probes.

In general, nucleic acid mimics can indeed provide better mismatch discrimination than standard DNA probes in FISH, as it has been suggested previously [9,40,47,48]. PNA with a low number of bases can broadly provide a good discrimination. Some studies have shown that LNA can increase single base mismatch discrimination in bulk solutions [22]. However, the design flexibility in LNA and 2'OMe oligonucleotides appears to indicate that the better performance should typically be obtained with these probes.

In this study we showed that, the analysis of probes using native targets allows a more realistic approach as it accounts for all variables that can interfere during the hybridization process. Methods that use only naked DNA for studying or comparing probes do not analyze the factors inside the cells that can interfere with the hybridization, e.g. molecular crowding and the presence of several solutes. As such, when several probes are compared it is fundamental to analyze this behavior in terms of permeabilization or access to the target. For example, a molecule can have adequate thermodynamics parameters but its chemistry may not be compatible with its use in a biological target. Therefore, approaches that combine naked and native target contribute for a more complete and realistic study.

4.5 Conclusions

As a final conclusion, both LNA/2'OMe and PNA probes are able to discriminate mismatches with a high signal-to-noise ratio, but LNA/2'OMe probes allow for a greater flexibility in probe design. Nonetheless, as probe design and optimum hybridization conditions varies for each type of probe, it is impossible to have an absolute certainty on which type of nucleic acid is better for mismatch discrimination. As such, for each specific sequence and mismatch, testing many possible probe designs and hybridization conditions with probes consisting of PNA and LNA/2'OMe is still advisable. Future work will focus on reassessing the impact of mismatches in a larger number of microorganisms which contain different types of cell wall, like Gram positive bacteria and yeast cells.

4.6 References

1. Kempf V.A.J., Trebesius K., Autenrieth I.B. Fluorescent In Situ Hybridization Allows Rapid Identification of Microorganisms in Blood Cultures. J Clin Microbiol (2000); 38: 830-838.
2. Sekiguchi Y., Kamagata Y., Nakamura K., Ohashi A., Harada H. Fluorescence In Situ Hybridization Using 16S rRNA-Targeted Oligonucleotides Reveals Localization of Methanogens and Selected Uncultured Bacteria in Mesophilic and Thermophilic Sludge Granules. Appl Environ Microbiol (1999); 65: 1280-1288.
3. DeLong E.F., Wickham G.S., Pace N.R. Phylogenetic stains: ribosomal RNA-based probes for the identification of single cells. Science (1989); 243: 1360-1363.
4. Yan Y., Yan J., Piao X., Zhang T., Guan Y. Effect of LNA- and OMeN-modified oligonucleotide probes on the stability and discrimination of mismatched base pairs of duplexes. J Biosci (2012); 37: 233-241.
5. Kubota K., Ohashi A., Imachi H., Harada H. Improved in situ hybridization efficiency with locked-nucleic-acid-incorporated DNA probes. Appl Environ Microbiol (2006); 72: 5311-5317.
6. Mook O.R., Baas F., de Wissel M.B., Fluiter K. Evaluation of locked nucleic acid-modified small interfering RNA in vitro and in vivo. Mol Cancer Ther (2007); 6: 833-843.
7. Cerqueira L., Fernandes R.M., Ferreira R.M., Oleastro M., Carneiro F., Brandao C., et al. Validation of a fluorescence in situ hybridization method using peptide nucleic acid probes for detection of Helicobacter pylori clarithromycin resistance in gastric biopsy specimens. J Clin Microbiol (2013); 51: 1887-1893.
8. Almeida C., Azevedo N.F., Bento J.C., Cerca N., Ramos H., Vieira M.J., et al. Rapid detection of urinary tract infections caused by Proteus spp. using PNA-FISH. Eur J Clin Microbiol Infect Dis (2013); 32: 781-786.
9. Guimaraes N., Azevedo N.F., Figueiredo C., Keevil C.W., Vieira M.J. Development and application of a novel peptide nucleic acid probe for the specific detection of Helicobacter pylori in gastric biopsy specimens. J Clin Microbiol (2007); 45: 3089-3094.
10. Campbell M.A., Wengel J. Locked vs. unlocked nucleic acids (LNA vs. UNA): contrasting structures work towards common therapeutic goals. Chem Soc Rev (2011); 40: 5680-5689.
11. Tavares A., Inacio J., Melo-Cristino J., Couto I. Use of fluorescence in situ hybridization for rapid identification of staphylococci in blood culture samples collected in a Portuguese hospital. J Clin Microbiol (2008); 46: 3097-3100.
12. Matsumoto K., Nakata E., Tamura T., Saito I., Aizawa Y., Morii T. A peptide nucleic acid (PNA) heteroduplex probe containing an inosine-cytosine base pair discriminates a single-nucleotide difference in RNA. Chemistry (2013); 19: 5034-5040.
13. Owczarzy R., You Y., Groth C.L., Tataurov A.V. Stability and mismatch discrimination of locked nucleic acid-DNA duplexes. Biochemistry (2011); 50: 9352-9367.

14. Cerqueira L., Azevedo N.F., Almeida C., Jardim T., Keevil C.W., Vieira M.J. DNA mimics for the rapid identification of microorganisms by fluorescence in situ hybridization (FISH). Int J Mol Sci (2008); 9: 1944-1960.
15. Marshall B R.H., Annear DI, Goodwin CS, Pearman JW, Warren JR, Armstrong JA. Original isolation of Campylobacter pyloridis from human gastric mucosa. Microbiol Lett (1984); 25: 83-88.
16. Eaton K.A., Dewhirst F.E., Radin M.J., Fox J.G., Paster B.J., Krakowka S., et al. Helicobacter acinonyx sp. nov., isolated from cheetahs with gastritis. Int J Syst Bacteriol (1993); 43: 99-106.
17. Cerqueira L., Fernandes R.M., Ferreira R.M., Carneiro F., Dinis-Ribeiro M., Figueiredo C., et al. PNA-FISH as a new diagnostic method for the determination of clarithromycin resistance of Helicobacter pylori. BMC Microbiol (2011); 11: 101.
18. Fontenete S., Guimaraes N., Leite M., Figueiredo C., Wengel J., Filipe Azevedo N. Hybridization-based detection of Helicobacter pylori at human body temperature using advanced locked nucleic acid (LNA) probes. PloS one (2013); 8: e81230.
19. Langkjaer N., Pasternak A., Wengel J. UNA (unlocked nucleic acid): a flexible RNA mimic that allows engineering of nucleic acid duplex stability. Bioorg Med Chem (2009); 17: 5420-5425.
20. Pasternak A., Wengel J. Thermodynamics of RNA duplexes modified with unlocked nucleic acid nucleotides. Nucleic Acids Res (2010); 38: 6697-6706.
21. Pasternak A., Wengel J. Unlocked nucleic acid--an RNA modification with broad potential. Org Biomol Chem (2011); 9: 3591-3597.
22. You Y., Moreira B.G., Behlke M.A., Owczarzy R. Design of LNA probes that improve mismatch discrimination. Nucleic Acids Res (2006); 34: e60.
23. Kumar R., Singh S.K., Koshkin A.A., Rajwanshi V.K., Meldgaard M., Wengel J. The first analogues of LNA (locked nucleic acids): phosphorothioate-LNA and 2'-thio-LNA. Bioorg Med Chem Lett (1998); 8: 2219-2222.
24. Yilmaz L.S., Okten H.E., Noguera D.R. Making all parts of the 16S rRNA of Escherichia coli accessible in situ to single DNA oligonucleotides. Appl Environ Microbiol (2006); 72: 733-744.
25. Kierzek E., Ciesielska A., Pasternak K., Mathews D.H., Turner D.H., Kierzek R. The influence of locked nucleic acid residues on the thermodynamic properties of 2'-O-methyl RNA/RNA heteroduplexes. Nucleic Acids Res (2005); 33: 5082-5093.
26. Christensen U., Jacobsen N., Rajwanshi V.K., Wengel J., Koch T. Stopped-flow kinetics of locked nucleic acid (LNA)-oligonucleotide duplex formation: studies of LNA-DNA and DNA-DNA interactions. Biochem J (2001); 354: 481-484.
27. Perlikova P., Karlsen K.K., Pedersen E.B., Wengel J. Unlocked nucleic acids with a pyrene-modified uracil: synthesis, hybridization studies, fluorescent properties and i-motif stability. Chembiochem (2014); 15: 146-156.

28. Sadhu C., Dutta S., Gopinathan K.P. Influence of Formamide on the Thermal-Stability of DNA. J Biosci (1984); 6: 817-821.
29. Krimmer V., Merkert H., von Eiff C., Frosch M., Eulert J., Lohr J.F., et al. Detection of Staphylococcus aureus and Staphylococcus epidermidis in clinical samples by 16S rRNA-directed in situ hybridization. J Clin Microbiol (1999); 37: 2667-2673.
30. Moreno Y., Ferrus M.A., Alonso J.L., Jimenez A., Hernandez J. Use of fluorescent in situ hybridization to evidence the presence of Helicobacter pylori in water. Water Res (2003); 37: 2251-2256.
31. Amann R.I., Binder B.J., Olson R.J., Chisholm S.W., Devereux R., Stahl D.A. Combination of 16S rRNA-targeted oligonucleotide probes with flow cytometry for analyzing mixed microbial populations. Appl Environ Microbiol (1990); 56: 1919-1925.
32. Koshkin A.A., Singh S.K., Nielsen P., Rajwanshi V.K., Kumar R., Meldgaard M., et al. LNA (Locked Nucleic Acids): Synthesis of the adenine, cytosine, guanine, 5-methylcytosine, thymine and uracil bicyclonucleoside monomers, oligomerisation, and unprecedented nucleic acid recognition. Tetrahedron (1998); 54: 3607-3630.
33. Buchardt O., Egholm M., Berg R.H., Nielsen P.E. Peptide nucleic acids and their potential applications in biotechnology. Trends Biotechnol (1993); 11: 384-386.
34. Majlessi M., Nelson N.C., Becker M.M. Advantages of 2'-O-methyl oligoribonucleotide probes for detecting RNA targets. Nucleic Acids Res (1998); 26: 2224-2229.
35. Guga P., Koziolkiewicz M. Phosphorothioate nucleotides and oligonucleotides - recent progress in synthesis and application. Chem Biodivers (2011); 8: 1642-1681.
36. Obika S., Nanbu D., Hari Y., Morio K.-i., In Y., Ishida T., et al. Synthesis of 2′-O,4′-C-methyleneuridine and -cytidine. Novel bicyclic nucleosides having a fixed C3, -endo sugar puckering. Tetrahedron Lett (1997); 38: 8735-8738.
37. Matthiesen S.H., Hansen C.M. Fast and Non-Toxic In Situ Hybridization without Blocking of Repetitive Sequences. PloS one (2012); 7: e40675.
38. Celeda D., Aldinger K., Haar F.M., Hausmann M., Durm M., Ludwig H., et al. Rapid fluorescence in situ hybridization with repetitive DNA probes: quantification by digital image analysis. Cytometry (1994); 17: 13-25.
39. Owczarzy R., You Y., Moreira B.G., Manthey J.A., Huang L., Behlke M.A., et al. Effects of sodium ions on DNA duplex oligomers: improved predictions of melting temperatures. Biochemistry (2004); 43: 3537-3554.
40. Mishra S., Ghosh S., Mukhopadhyay R. Maximizing mismatch discrimination by surface-tethered locked nucleic acid probes via ionic tuning. Anal Chem (2013); 85: 1615-1623.
41. Yilmaz L.S., Noguera D.R. Development of thermodynamic models for simulating probe dissociation profiles in fluorescence in situ hybridization. Biotechnol Bioeng (2007); 96: 349-363.

42. Kaur H., Wengel J., Maiti S. Thermodynamics of DNA-RNA heteroduplex formation: effects of locked nucleic acid nucleotides incorporated into the DNA strand. Biochemistry (2008); 47: 1218-1227.
43. Filichev V.V., Christensen U.B., Pedersen E.B., Babu B.R., Wengel J. Locked nucleic acids and intercalating nucleic acids in the design of easily denaturing nucleic acids: thermal stability studies. Chembiochem (2004); 5: 1673-1679.
44. SantaLucia J., Jr., Allawi H.T., Seneviratne P.A. Improved nearest-neighbor parameters for predicting DNA duplex stability. Biochemistry (1996); 35: 3555-3562.
45. Fontenete S., Guimaraes N., Wengel J., Azevedo N.F. Prediction of melting temperatures in fluorescence in situ hybridization (FISH) procedures using thermodynamic models. Crit Rev Biotechnol (2015): 1-12.
46. Politz J.C., Browne E.S., Wolf D.E., Pederson T. Intranuclear diffusion and hybridization state of oligonucleotides measured by fluorescence correlation spectroscopy in living cells. Proc Natl Acad Sci U S A (1998); 95: 6043-6048.
47. Mishra S., Ghosh S., Mukhopadhyay R. Ordered self-assembled locked nucleic acid (LNA) structures on gold(111) surface with enhanced single base mismatch recognition capability. Langmuir (2012); 28: 4325-4333.
48. Stender H., Fiandaca M., Hyldig-Nielsen J.J., Coull J. PNA for rapid microbiology. J Microbiol Methods (2002); 48: 1-17.

Chapter V

Hybridization-based detection of Helicobacter pylori at human body temperature using advanced Locked Nucleic Acid (LNA) probes

OPEN ACCESS Freely available online

PLOS ONE

Hybridization-Based Detection of *Helicobacter pylori* at Human Body Temperature Using Advanced Locked Nucleic Acid (LNA) Probes

Sílvia Fontenete[1,2,3,4], Nuno Guimarães[1,2,3], Marina Leite[2], Céu Figueiredo[2,5], Jesper Wengel[3], Nuno Filipe Azevedo[1*]

1 LEPABE, Laboratory for Process Engineering, Environment, Biotechnology and Energy, Department of Chemical Engineering, Faculty of Engineering, University of Porto, Porto, Portugal, **2** IPATIMUP, Institute of Molecular Pathology and Immunology of the University of Porto, Porto, Portugal, **3** Nucleic Acid Center, Department of Physics, Chemistry and Pharmacy, University of Southern Denmark, Odense M, Denmark, **4** ICBAS, Institute of Biomedical Sciences Abel Salazar, University of Porto, Porto, Portugal, **5** FMUP, Faculty of Medicine of the University of Porto, Porto, Portugal

ABSTRACT

The understanding of the human microbiome and its influence upon human life has long been a subject of study. Hence, methods that allow the direct detection and visualization of microorganisms and microbial consortia (e.g. biofilms) within the human body would be invaluable. In here, we assessed the possibility of developing a variant of fluorescence in situ hybridization (FISH), named fluorescence *in vivo* hybridization (FIVH), for the detection of *Helicobacter pylori*. Using oligonucleotide variations comprising locked nucleic acids (LNA) and 2'-O-methyl RNAs (2'OMe) with two types of backbone linkages (phosphate or phosphorothioate), we were able to successfully identify two probes that hybridize at 37 °C with high specificity and sensitivity for *H. pylori*, both in pure cultures and in gastric biopsies. Furthermore, the use of this type of probes implied that toxic compounds typically used in FISH were either found to be unnecessary or could be replaced by a non-toxic substitute. We show here for the first time that the use of advanced LNA probes in FIVH conditions provides an accurate, simple and fast method for *H. pylori* detection and location, which could be used in the future for potential *in vivo* applications either for this microorganism or for others.

Keywords: FISH, Nucleic Acid Analogs, LNA, *Helicobacter pylori*

5.1. Introduction

The human microbiome has long been studied for a better understanding of its influence upon human development, physiology, immunity, and nutrition [1]. In most of these studies, microbial identification methods rely on sample collection followed by DNA isolation and sequencing [2,3]. Despite providing important information on the communities that inhabit the human body, these methods disrupt the spatial structure of the sample, meaning that important information about human/microorganism or microorganism/microorganism interactions might be lost. In addition, the time needed to process a sample is quite long, making these methods less suitable as a diagnostic routine. Hence, novel methods which are able to address those shortcomings, by allowing the direct visualization of microorganisms and microbial consortia (e.g. biofilms) within the human body and in a short period of time, would be invaluable.

Fluorescent in situ hybridization (FISH) using DNA probes has long been used to rapidly detect and localize microbial cells in human clinical samples [4,5]. Nonetheless, this method was never employed to detect microorganisms within the human body (or other higher-order animals). The emergence of a new variant of FISH, here named as fluorescence *in vivo* hybridization of microorganisms (FIVH), has mainly been hindered by two factors. The first was the lack of suitable systems that were able to detect fluorescence signals within the human body. This issue has been recently overcome, with the arrival of medical devices with built-in advanced imaging systems, such as the confocal endomicroscope that allows an in depth analysis of the mucosa of the stomach [6] or colon [7]. So far, this device has only successfully allowed the detection of microorganisms in the human gastrointestinal-tract using non-specific staining methods [6,8]. The second factor is the lack of control over the FIVH process, as it has to be carried out under the conditions imposed by the microenvironment where the microorganism is to be found. For microorganisms present in the mucosa of the human stomach, for instance, the method would have to be carried out at 37 ℃ and low pH. Adding to that, DNA probes would have to resist degradation by nucleases [9].

The above-mentioned reasons make it very unlikely for a DNA FIVH method to work, but the evolution of nucleic acid chemistry allowed the development of chemical variations (of the nucleobase, sugar and/or phosphate backbones) of nucleic acids that can replace the DNA as a probe. In fact modified oligonucleotides, such as locked nucleic acids (LNA) or 2'-O-methyl RNA (2'OMe), have been proven to hybridize *in vivo* with native nucleic acids with low toxic effects [10-14], and are hence good candidates to develop a successful FIVH method.

LNA is a nucleic acid analogue with binding sensitivity and specificity towards complementary DNA or RNA targets [15]. LNA contains a ribose ring locked by a O2'-C4'-methylene linkage resulting in a N-type (3-endo) conformation (Figure 5.1) [16,17]. LNA hybridizes with high affinity toward RNA (and DNA) complementary sequences according to Watson-Crick base-pairing rules, has high resistance to nuclease degradation (high bio-stability), is fully soluble in water, and display low general toxicity in animals [13,15,17]. 2'-O-Methyl-RNA based oligoribonucleotides (2'OMe) (Figure 5.1) constitute another nucleic acid analogue that is being used as a diagnostic probe in animal cells [18-20]. The 2'OMe group induces relatively high affinity towards an RNA target likely due to the C_3'-endo conformation adopted by 2'OMe ribose sugars [21]. The use of 2'OMe monomers increases probe's biostability, improves the specificity and the kinetics of hybridization, and allows targeting under conditions where DNA probes would normally not hybridize [21]. The introduction of LNA monomers into 2'OMe probes increases the target affinity even further due to an additive effect on the melting temperature (T_m) which has been shown to improve the overall detection yield of an experiment [18,22].

Other types of modifications may also be incorporated to improve the target's applicability. For instance, the use of phosphorothioate (PS) oligonucleotides presented some particularly interesting results in the case of human clinical trials as therapeutic agents for the treatment of viral infections and cancer [23,24]. The PS monomers include replacement of one of the two non-bridging oxygen atoms by a sulfur atom at each internucleotide linkage (Figure 5.1) [25]. These types of oligonucleotides have an increased resistance to exo- and endonucleases when compared to phosphodiester oligonucleotides (PO) [26,27], and are particularly suitable for *in vivo* applications due to their longer elimination half-life [28].

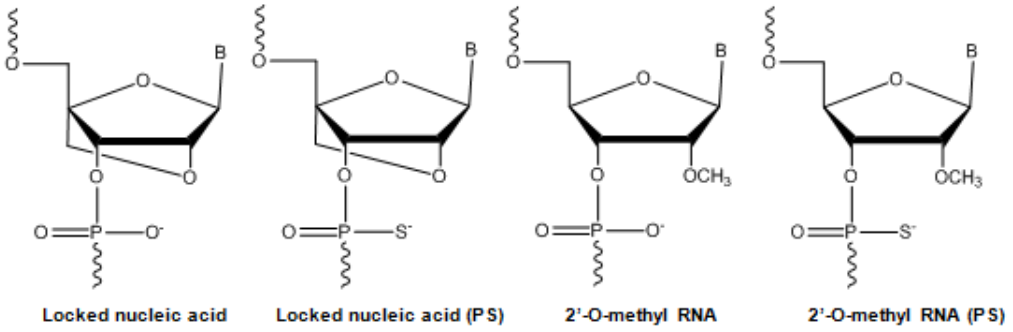

Figure 5.1 - Structures of LNA and 2' O-methyl RNA monomers (phosphate and phosphorothioate structures) used.

Taking advantage of recent progress in DNA mimics, the main objective of this work is the development of a FIVH method for the detection of microorganisms at the human body temperature (normothermia) using these novel nucleic acid molecules. As a target microorganism we selected *Helicobacter pylori* (*H. pylori*), a Gram-negative and microaerophilic bacterium that colonizes the stomach of almost half of the human population and is a major risk factor associated with gastric cancer, the second deadliest cancer worldwide [29,30].

5.2. Materials and methods

5.2.1. Bacterial strains and culture conditions

All bacterial cultures were grown in trypticase soy agar (TSA) supplemented with 5% (vol/vol) sheep blood (Becton Dickinson GmbH, Germany) and incubated for 48 hours at 37 °C under microaerobic conditions. Bacterial density was determined by the dilution of initial culture in water or saline and the absorbance was measured at 600 nm. Initial protocol optimization was performed with *H. pylori* strain 26695, obtained from the American Type Culture Collection (ATCC 700392, VA USA). For testing the specificity and sensitivity of the probes, other *H. pylori* strains and Helicobacter *spp.* were used (Table 5.1).

5.2.2. Oligonucleotide probe design

The 16S rRNA target region was selected based on a previous study [31]. The probe sequences were designed following guidelines for FISH-probes, including limitation of purine content to 60% and restriction of self-complementarity to 3 base pairs. Different types of modified nucleotide monomers were used in the probes (Figure 5.1). The position and the number of LNA and 2'OMe substitutions used in each probe were based on previous reports [32,33]. At the moment, a specific and reliable thermodynamic model to predict the hybridization temperature is still absent for LNA and 2'OMe-RNA. However is possible to study theoretical melting temperature of each probe through a 2'OMeRNA/Calculator online (http://rnachemlab.ibch.poznan.pl/calculator1.php). As such, it has designed several probes with different sizes to increase the chances of finding one or more probe(s) working at human body conditions (37 °C). Once the probes were selected, a search was conducted at the available 16S rRNA databases of Ribosomal Database Project II (RDP-II), version 10 (http://rdp.cme.msu.edu/) to confirm the

theoretical specificity and sensitivity of the probe against other microorganisms. For this analysis, only high quality sequences with more than 1200 bp were selected [34]. It was found that all probes differed by at least two bases (two mismatches) from non-*H. pylori* species.

Table 5.1 - Helicobacter strains tested in this study

Helicobacter spp.
H. pylori strains
26695 (ATCC 700392)
G27 (NCTC 13282)
H. pylori CI-31[a]
H. pylori CI-116[a]
Non-pylori Helicobacter strains
H. cinaedi 33221-1.2[b]
H. mustelae 2H1[b]
H. salomanis[b]
H. muridarum 2A5+[c]
H. pametensis[c]
H. bilis[b]
H. canis CIP104753[b]

[a] - Own isolates
[b] - Isolate provided by Francis Megraud.
[c] - Isolate provided by Jay Solnick

5.2.3. Oligonucleotides synthesis and purification

Oligonucleotides were synthesized under anhydrous conditions using standard phosphoramidite chemistry using an automated nucleic acid synthesizer (PerSpective Biosystems Expedite 8909 instrument). LNA and 2'OMe monomers were commercially available from Exiqon and Ribotask, respectively. The syntheses were performed in 1.0 µmol scale using a universal polystyrene-based support. The synthesis conditions used for the incorporation of LNA and 2'OMe monomers were as follows: trichloroacetic acid in CH_2Cl_2 (3:97) as detritylation reagent; 0.25 M 4,5-dicyanoimidazole (DCI) in CH_3CN as activator; acetic anhydride in THF (9:91, v/v) as cap A solution; *N*-methylimidazole in THF (1:9, v/v) as cap B solution. As an oxidizing solution 0.02 M iodine in H_2O/pyridine/THF was used for phosphate oligonucleotides. As a thiolation solution 0.0225 M xanthan hydrate in pyridine/CH_3CN (20:90, v/v) was used for phosphorothioate

oligonucleotides. Coupling time was 4.6 min for both monomers. Fluorescein phosphoramidite, FAM (Glen Research, VA, USA) was added in anhydrous acetonitrile (0.1 M) and activated by tetrazole with a 20 min coupling time. The stepwise coupling yields (95-99% per step) were based on the absorbance of the dimethoxytrityl cations (DMT^+) released after each coupling step. The cleavage from the support was carried out by using 98% aqueous methanol/ammonia solution 7 N in methanol (1:1), 2 h at room temperature followed by 32% aqueous ammonia solution, 12 h at 55℃.

All oligonucleotides were purified by reversed phase HPLC (RP-HPLC) using a Waters 600 system equipped with an XBridge OST C18 (2.5 µm, 19×100 mm) column and an XBridge Prep C18 (5 µm, 10×10 mm) precolumn. After removal of the DMT-group, oligonucleotides were characterized by ionexchange HPLC (IE-HPLC) using a Dionex system HPLC (VWR) and by matrix-assisted laser desorption ionization time-of-flight mass spectrometry (MALDI-TOF) using a Microflex Maldi (Bruker instruments, Leipzig, Germany). The purified oligonucleotides were precipitated by acetone and their purity (>90%) and compositions were verified by IE-HPLC and MALDI-TOF analysis, respectively.

Because the probes will target the rRNA of *H. pylori*, the melting temperature of the synthetic oligonucleotides was assessed using non-modified oligonucleotides consisting only of RNA (HP_RNA_Target), fully complementary to the probes designed here (purchased from Integrated DNA Technologies). A DNA probe to serve as a reference probe (HP_DNA_Ref) with a higher number of bases than the LNA and 2'-OMe probes was purchased from Sigma-Aldrich (MO, USA).

5.2.4. Melting temperature studies

From each strand, 1.0 µM was used in the following buffers: a medium salt buffer with 220 mM Na^+ (200 mM NaCl, 20 mM NaH_2PO_4 and 0.2 mM EDTA, pH 7.0), a medium salt buffer with 30% (vol/vol) formamide and a low salt buffer with 30% (vol/vol) formamide with 110 mM Na^+ (110 mM NaCl, 5 mM EDTA, 50 mM Tris-HCl and 30% (v/v) formamide, pH 7.5). After mixing each sample and denaturing the complex by heating up to 85 °C during 5 min, samples were cooled to the starting temperature of the experiment. Quartz optimal cells with a path length of 1.0 cm were used. Melting temperatures (T_m values/ °C) were measured on Perkin Elmer Lambda 35 UV/VIS spectrometer equipment with a PTP 6 (Peltier Temperature Programmer) and determined as the maximum of the first derivative of the thermal denaturation curve (A_{260} vs. temperature for medium salt buffer).

A temperature range from 13-15 °C to 80-85 °C and a ramp of 1.0 °C/min were used. Reported Tm values are an average of two measurements within ± 1 °C.

5.2.5. Optimization of probe hybridization conditions on slides and in suspension

The hybridization procedures developed to detect *H. pylori* were performed by FISH and evaluated by two independent techniques: by fluorescent microscopy on slides (to obtain a faster but qualitative assessment of the fluorescence signal) and by imaging flow cytometry sorting in bacterial suspensions (to obtain a quantitative assessment). Detection of 16S rRNA in slides by FISH was performed mostly as described in Azevedo *et al.* [35], with a few modifications. For fixation on glass slides, smears of each species/strain were immersed in 4% (v/v) paraformaldehyde for 15 min at room temperature, followed by a treatment of 50% (vol/vol) ethanol for 10 min and allowed to air dry. The hybridization was performed using 20 µl of hybridization buffer with 200 nM of the respective probe, which covered each smear individually. Two different types of hybridization buffer (pH 7.5) were tested: one containing 50% (vol/vol) formamide (Across Organic, New Jersey, US) and the other 4 M of urea (VWR BHD Prolabo, Haasrode, Belgium). The following reagents were common to both buffers: 10% (vol/vol) dextran sulphate (Fisher Scientific, MA, US), 0.1% (vol/vol) Triton-X (Panreac, Barcelona, Spain), 5 mM of EDTA disodium salt 2-hydrate (Panreac), 50 mM Tris-HCl (Fisher Scientificm New Jersey, US), 900 mM NaCl (Panreac). Samples were covered with coverslips and incubated for 90 min at 37 °C. Slides were subsequently washed in a prewarmed solution (pH 10), containing 5 mM Tris Base (Fisher Scientific), 15 mM NaCl (Panreac) and 1% Triton X (Panreac), for 30 min at 37 °C and then, the slides were allowed to air dry. All experiments were performed in triplicate and for each experiment a negative control (same hybridization conditions, but without a probe in the hybridization solution) was included. Slides were stored in the dark before microscopy analysis. For image acquisition a Leica 2000 epifluorescence microscope (Leica Microsystems GmbH, Wetzlar, Germany) was used. FAM-labeling was excited by using a 488 nm laser; the exposure time was fixed for all preparations. The fluorescence intensity of each probe and sample was quantified in the microscopy images using the ImageJ software (http://rsbweb.nih.gov/ij/index.html) and FISHji3 (Chapter III).

The hybridization method in suspension was based on procedures described by Almeida *et al.* [36], with slight modifications. Each type of bacterium was collected from one TSA plate with 1 mL of saline and centrifuged at 14 000 x *g* for 15 min. The pellet was resuspended in 400 µL of 4% (v/v) paraformaldehyde for 1 hour, followed by

centrifugation at 14 000 x *g* for 5 min. The fixed cells were resuspended in 500 µL of 50% (vol/vol) ethanol and incubated at -20 °C for at least 30 min. For bacteria disaggregation the samples were subjected to sonication by ultrasounds (Transsonic 420, Elma, Germany) for 12 min, followed by a filtration through a sterile 10 µm pore-size filter (CellTrics®,Görliz, Germany). Afterwards, 100 µL of fixed cells were resuspended in 100 µL of hybridization solution (as previously described) with 200 nM of probe and incubated at 37 °C for 90 min. After hybridization the samples were centrifuged at 14,000 rpm for 5 min, resuspended in 500 µL of washing solution (as described above) and incubated at 37 °C for 30 min. The cells were again centrifuged at 14 000 x *g* for 5 min and resuspended in 100 µL of saline. To remove aggregates samples were filtered by a sterile filter with 10 µm pore size (CellTrics®). Samples were used directly for imaging flow cytometry analysis.

5.2.6. Image Quantification

Using the ImageJ program (National Institutes of Health Software), each image obtained by microscopy was analysed for the mean fluorescence intensity (FISHji3). Background values were obtained by measuring a blank region from each image and these were removed from the test frames. Data was plotted as mean of arbitrary fluorescence units (AFU) which represented the mean fluorescence intensity minus background intensities.

5.2.7. Imaging flow cytometry and data analysis

H. pylori bacterial cell suspensions stained with FAM-labeled LNA probes, and the respective unstained negative controls, were analysed in an ImageStream$^{X®}$ (Amnis Corporation, Seattle WA, USA) imaging flow cytometer equipped with two lasers (488 nm and 785 nm), a 40x magnification objective of 0.75 N.A, and one CDD camera. Images acquired using the INSPIRE^{TM} software included a brightfield image (Channel 1, 430-480 nm), and a green fluorescence image (Channel 2, 480-560 nm). During the sample acquisition, the area feature was used as cell classifier, in the brightfield channel, with a lower limit of 2, to exclude debris, and an upper limit of 20, to exclude bacterial aggregates and thus minimize the error in the fluorescence signal intensity that bacterial aggregates would represent in the data analysis. For each sample, 50,000 events were collected and two independent experiments were performed. All imagery data was analysed using the algorithms of IDEAS® v4.0 software (Amnis Corporation). Hierarchical gating schemes were used to further eliminate bacterial aggregates and to determine the spot count and the mean fluorescence signal intensity of each bacterial sample.

5.2.8. Hybridization in gastric biopsies

Formalin-fixed paraffin-embedded biopsies of gastric tissue sections from one patient infected with *H. pylori* were used. The use of the biopsy for research purposes was previously approved by the ethics committee of the Portuguese Institute of Oncology (IPO) in Porto, and informed written consent was obtained from the patient. Sections were cut to 3 µm thickness, and mounted on microscope glass slides and stored at 4 °C until use. Slides were immersed twice in xylol for 15 min each time, and then subjected to rehydration by decreasing concentrations of ethanol (100%, 95%, 80%, 70% and 50%) for 5 min each time. Finally, slides were washed with distilled water for 10 min and allowed to air dry. Subsequently, the hybridization procedure in slides was used as previously described using both buffers.

5.2.9. Statistical Analysis

Statistical significance was determined by One-way analysis of variance (ANOVA) by applying the Tukey multiple-comparisons test, using SPSS statistics 17.0 (SPSS, Statistical Package for the Social Sciences, Chicago, USA) or Microsoft Office Excel (Microsoft Corporation, Redmond, CA). Differences in data values were considered significant at values lower than 0.05.

5.3. Results

5.3.1. Melting temperature behaviour

The initial purpose of this work was to find a type of synthetic oligonucleotide that would be capable of efficiently hybridizing in a bacterium at human body temperature (37 °C). A first screening was performed to determine the melting temperature of 18 synthesized probes (Chapter II). The hybridization temperature is not only affected by the type of probe, size and sequence, but also by the amount and type of other substances present in the hybridization solution. For this reason UV thermal denaturation studies were carried out in solutions containing not only the probes, but also different salt concentrations and a denaturing compound (formamide; FA).

After a biophysics analysis comparing melting and hybridization temperatures of the LNA probes (with different lengths), it was concluded that the hybridization temperature should be between 15-30 °C lower than the melting temperature measured under similar conditions (i.e. in the presence of salt and FA) (Chapter II). Based on this criterion, four

candidate probes, with melting temperatures ranging between 60-70 °C were selected for further studies (Table 5.2).

Table 5.2 - Results of thermal denaturation experiments in different types of buffers for different types of oligoribonucleotides. The DNA oligonucleotide probe reference (Ref) has the following sequence: 5'-CTGGAGAGACTAAGCCCTCCAA-3'. The RNA complementary oligonucleotide has the following sequence: 5'-UUGGAGGGCUUAGUCUCUCCAG-3'. LNA nucleotide monomers are represented with L superscript, 2'-OMe-RNA monomers in boldface letters, DNA nucleotides in capital letters, and phosphorothioate linkages by the symbol*

		Medium salt buffer	Medium salt buffer with FA	Low salt buffer with FA
Probes analysed	Sequence	RNA complement T_m (°C)	RNA complement T_m (°C)	RNA complement T_m (°C)
Ref	5'-CTGGAGAGACTAAGCCCTCCAA-3'	64	69	68
HP_LNA_PO	5'-FAM $GA^{L}CT^{L}AA^{L}GC^{L}CC^{L}$ -3'	78	69	67
HP_LNA_PS	5'-FAM $G*A^{L*}C*T^{L*}A*A^{L*}G*C^{L*}C*C^{L}$ -3'	77	68	66
HP_LNA/2OMe_PO	5'- FAM $G^{L}ACT^{L}AAG^{L}CCC^{L}$-3'	79	66	67
HP_ LNA/2OMe _PS	5'- FAM $G^{L*}A*C*T^{L*}A*A*G^{L*}C*C*C^{L*}$-3'	78	63	66

Thermodynamically, similar results were observed for the phosphate (HP_LNA_PO and HP_LNA/2OMe_PO) and phosphorothioate (HP_LNA_PS and HP_LNA/2OMe_PS) probes. Phosphorothioate probes (HP_LNA_PS and HP_LNA/2OMe_PS) showed only small differences (only 1°C variation in Tm values) when compared to the respective phosphate probes, with the exception of HP_LNA/2OMe_PS in the medium salt with FA. Although the number of LNA is higher in HP_LNA_PO and HP_LNA_PS probes (5 LNA monomers) than in HP_LNA/2OMe_PO and HP_LNA/2OMe_PS probes (4 LNA monomers) the only significant differences were observed in the melting temperatures when medium buffer with FA was used. It should be noted that the different salt concentration of the salt buffers did not significantly impact the Tm.

5.3.2. FISH detection of H. pylori by fluorescence microscopy

The ability of the selected candidate probes (Table 5.2) to hybridize at human body temperature (37 °C) was then tested using the FISH method in glass slides. In spite of having being designed to work at similar melting temperatures, microscopy results have shown that only the HP_LNA/2OMe_PO and HP_LNA/2OMe_PS probes were able to hybridize at 37 °C (Figure 5.2A). Because HP_LNA_PO and HP_LNA_PS probes were only able to hybridize at temperatures higher than 40 °C (as shown in Chapter II), they were not considered for further evaluation. One of the components of the hybridization

solution is FA that acts as a denaturing or destabilizing agent allowing the hybridizations to be carried out at lower temperatures. However, it is not possible to use FA *in vivo* due to its toxic nature to human cells [37]. Therefore, we have tested urea at a 4 M concentration as a suitable non-toxic alternative. The hybridization efficiency of the HP_LNA/2OMe_PS probe was higher than that of the HP_LNA/2OMe_PO probe in both FA and urea buffers, as it can be observed by the high fluorescence signal (Figure 5.2A). Because fluorescence microscopy only provides qualitative results, we determined the average fluorescence intensity of each sample using ImageJ software (Figure 5.2B).

The results obtained by ImageJ confirmed that the HP_LNA/2OMe_PS probe presents higher fluorescence intensities than the HP_LNA/2OMe_PO probe, irrespectively of the buffer used. The fluorescence intensity of the HP_LNA/2OMe_PS probe is significantly higher in the urea buffer than in the FA buffer (p=0.006). The difference between HP_LNA/2OMe_PS urea and the other analysed conditions is statistically significant (p<0.05). No statistically significant differences were observed in fluorescence intensity between the HP_LNA/2OMe_PS probe in FA and the HP_LNA/2OMe_PO in both buffer (p>0.05). As expected, control experiments (without probe) showed low levels of fluorescence; this very faint background was likely due to the presence of autofluorescence substances in bacterial cells could be sometimes observed (Figure 5.2B).

Sensitivity and specificity of the probes are two important factors for the success of a FISH method. Because low hybridization temperatures can influence these two factors, after optimization of the hybridization conditions it has tested the sensitivity and specificity of the candidate probes against the panel of strains presented in Table 5.1 and in Figure S6. The candidate probes were able to detect *H. pylori* reference strains and *H. pylori* clinical isolates, while no fluorescent signal was detected for the non-*pylori Helicobacter* strains tested. These results showed that 2'-*O*-methyl/LNA-modified probes were both specific and sensitive for *H. pylori* strains, even when the hybridization is carried out at 37 °C in the presence of urea as a denaturing agent. A central parameter for a future FIVH application in the human stomach is the optimization of the FISH technique at low pH. As such, preliminary tests using HP_LNA/2OMe_PS analysed in this study have been performed at pH 4 with positive results (which will be discussed in Chapter VI).

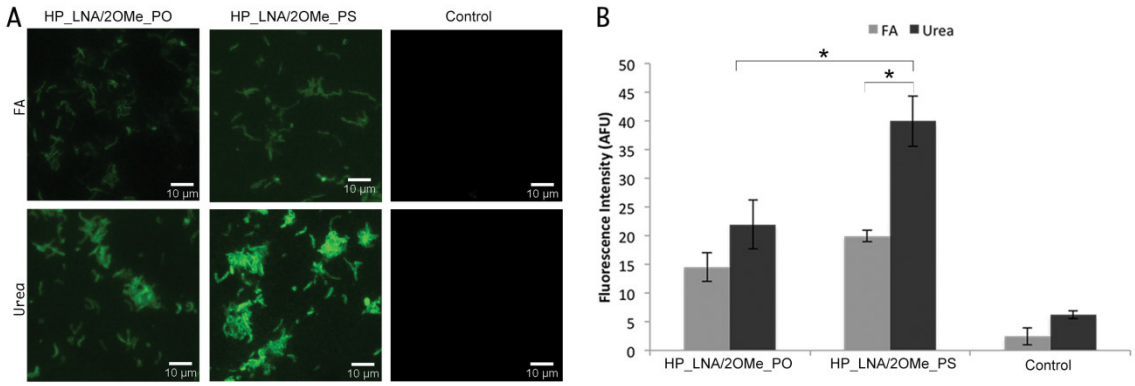

Figure 5.2 - FISH detection of *H. pylori* 26695 strain (ATCC 700392) using FAM- HP_LNA/2OMe_PO and HP_LNA/2OMe_PS probes. FISH analysis was performed by epifluorescent microscopy in smears, using either 50% (vol/vol) formamide and 4 M urea as denaturing agents in the hybridization buffer. Smears without probe were used as negative control (Control) (2A). (2B) Average fluorescence intensity from each probe in 4 M urea and 50% formamide (v/v) buffers; fluorescent signal intensity is expressed in arbitrary fluorescent units (AFU) and was quantified using ImageJ software. All images were acquired at equal exposure conditions. Original magnification: 1000x.

5.3.3. FISH detection of H.pylori by imaging flow cytometry

After optimization of the method on slides, it has applied the FISH procedure to *H. pylori* suspensions for imaging flow cytometry analysis. The mean fluorescence intensity of each sample was assessed and the overall results were similar to the ones determined by ImageJ for FISH application on slides (Figure 5.3). The HP_LNA/2OMe_PS probe in urea buffer hybridized with a significantly higher efficiency than that of HP_LNA/2Ome_PS in FA, and HP_LNA/2OMe_PO probe in both buffers (p<0.05), showed by the higher mean fluorescence intensity. Both probes hybridized more efficiently in the 4 M urea buffer than in the FA buffer when compared with the control without probe (Figure 5.3A and 5.3B). On the other hand, the both probes in the FA buffer did not show significant differences to the respective control (p>0.05) (Figure 5.3A and 5.3B). Under these conditions, using imaging flow cytometry, all different morphological types of *H. pylori* cells (spiral, coccoid and U-shaped) emitted a bright green fluorescence (Figure 5.3C).

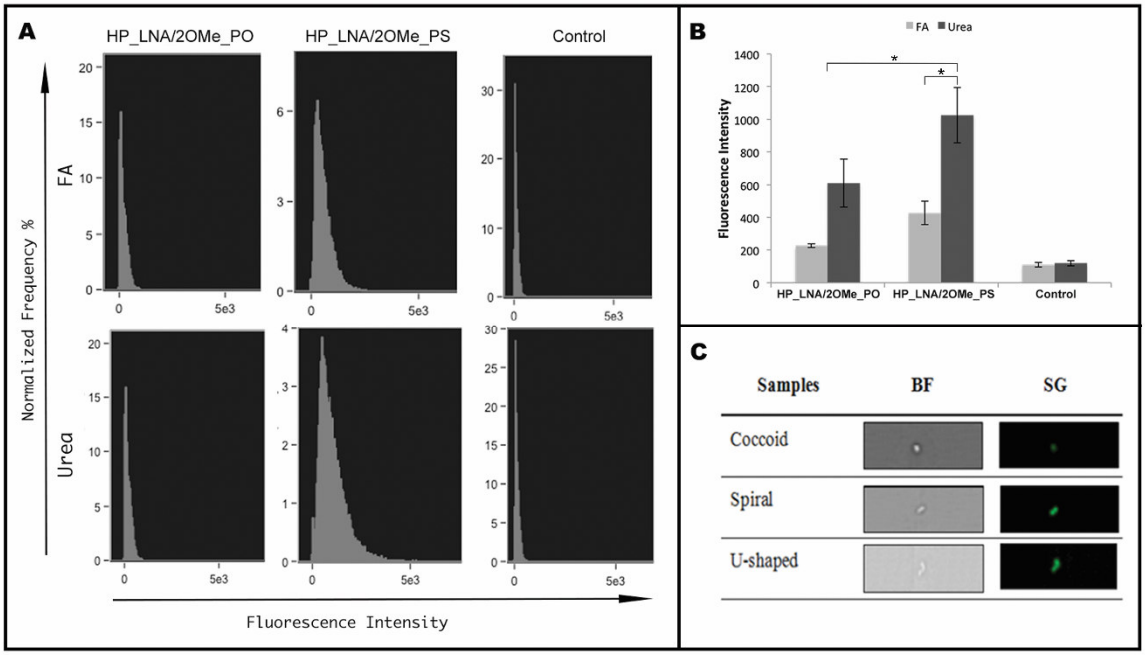

Figure 5.3 - FISH detection of *H.pylori* by imaging flow cytometry. FAM labeled 2OMe/LNA probes were analysed in 50% (v/v) formamide buffer and in 4M buffer. A) Representative histograms of the green fluorescence intensity of FAM-labeled HP_LNA/2OMe_PO, HP_LNA/2OMe_PS probes and controls. B) Quantification of the mean fluorescence intensity of each probe in two independent experiments obtained by flow cytometry. C) Representative images of individual *H. pylori* with different morphologies. The population identified as individual *H. pylori* bacterium by FISH analysis was manually examined and individual cell events were identified. Individual bacterial cells, shown by brightfield images (BF, left column) and green fluorescence images (SG, right column).

5.3.4. Gastric biopsy hybridization analysis

Considering the application of 2'-O-methyl/LNA in clinical settings, the identification of *H. pylori* strains was performed in histological slides of gastric biopsy samples from patients infected with this bacterium. In all paraffin sections, bacterial rRNA was detected using FAM labeled HP_LNA/2OMe_PO and HP_LNA/2OMe_PS probes. However, the analysis of gastric biopsies using HP_LNA/2OMe_PS showed more fluorescence intensity of *H. pylori* than in the same conditions with HP_LNA/2OMe_PO. Negative controls confirmed the lack of autofluorescence from non-labeled *H. pylori* cells (Figure 5.4B). Therefore, using hybridization conditions similar to FIVH it is possible to identify and locate the bacteria in the gastric mucosal surface.

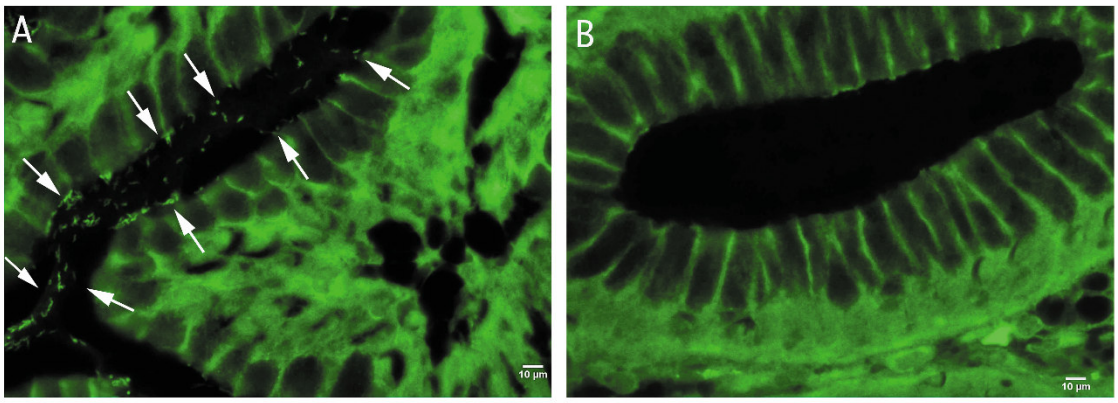

Figure 5.4- FISH detection of *H.pylori* in paraffin-embedded sections of gastric biopsies, using 2'-O-methyl/LNA FISH detection conditions. (A) Detection of *H. pylori* using the HP_LNA/2OMe_PS probe in a histological slide of a gastric biopsy specimen of an infected patient; (B) Experiment control performed in parallel using the HP_LNA/2OMe_PS probe in a histological slide of a gastric biopsy specimen of an non infected patient . Arrows indicate the presence of *H. pylori* infecting the gastric mucosa. All images were taken at equal exposure times Scale bars: 10 µm. Original magnification of ×1000.

5.4. Discussion

This work presents the first approach to obtain a method for the detection of *H. pylori* under *in vivo* mimicking conditions. Taking advantage of the evolution of nucleic acid chemistry, we have synthesized a set of LNA and/or 2'-O-Methyl RNA probes using the standard phosphodiester and the synthetic phosphorothiate backbones and have evaluated their suitability to hybridize at 37 °C.

The hybridization assays showed that only HP_LNA/2OMe_PS and HP_LNA/2OMe_PO probes were able to emit fluorescence at 37 °C. These results suggest that the substitution of DNA for 2'-O-Methyl-RNA nucleotides in LNA probes allows the hybridization to occur at lower temperatures, as long as a shorter LNA/2'-OMe-RNA sequence is used when compared to the corresponding DNA probe. It is furthermore expected that the introduction of 2'OMe monomers into LNA probes will increase probe's biostability, specificity and kinetics of hybridization, and allows targeting under conditions where DNA/LNA probes do not hybridize, an observation that has been corroborated by others [18,21,22]. We have shown that both HP_LNA/2OMe_PS and HP_LNA/2OMe_PO probes are able to successfully hybridize with *H. pylori* RNA at 37 °C. The HP_LNA/2OMe_PS probe yield higher fluorescence intensities in slides and in suspensions of *H. pylori,* as well as in the gastric biopsies, which appears to indicate that phosphorothioate probes are the best candidates to be used as probes in this type of experiments.

Taking in mind the future application of this method to *in vivo* conditions, and since the FISH procedure includes solutions that are toxic, we have successfully replaced FA by urea. In fact, FA, used as a destabilizing agent of nucleic acid duplexes, is one of the most hazardous chemicals present in the hybridization solution and the use of urea as a substitute has already been suggested by other authors [37]. The replacement of the common 50% (v/v) FA by 4M urea led to a 40% increase in the signal intensity, in both probes analysed (Figure 5.3), which could be explained by the additional permeabilization role of urea [38]. More importantly, the use of warmed urea-containing buffer did not affect the renaturation kinetics of the reaction.

Although different studies have performed the hybridization step of a FISH process at 37 ℃, these typically use a previous denaturation step and a washing step performed at higher temperatures [10,39] or long periods of incubation [40]. Furthermore, some of these studies used DNA probes, and as such the hybridization step alone lasted at least for 8 hours, which is undesirable for the final purpose of FIVH. Moreover, these experiments have only been performed in animal cells, where nucleic acids are able to diffuse more freely into the cell due to the lack of a cell wall. The present study is the first to perform the detection of a bacterium by FISH at human body temperature used for all steps of the hybridization procedure. The only study that used the designation of FIVH and that was performed in live animal cells [41], applies hybridization in an *ex vivo* culture environment and as such is not a true FIVH. To the best of our knowledge, the few studies that were performed *in vivo* in animal cells used fluorescently-labelled small peptides as probes instead of nucleic acids [7]. Another issue observed in this study was the autofluorescence of the tissues in the biopsy. Non-specific fluorescence agents, such as fluorescein, have been used in several studies with endomicroscopy analysis [42]. The sensitivity of this technique allowed for the visualization of small cellular structures such as capillaries and inflammatory cells [43]. Therefore, although autofluorescence is present in the analysed tissues (Figure 5.4), published works showed that it is possible to discriminate small fluorescence signals *in vivo* [44,45]. There are also imaging analysis methods which allow the reduction of autofluorescent signatures from image data mathematically [46,47]. Another possible approach is the use of a different exogenous fluorophores with a different spectral region where tissue autofluorescence cannot be observed [48]. Therefore, if the presence of autofluorescence in fluorescent images becomes a problem in *in vivo* analysis, there still exist different types of strategies that might allow to overcome this issue.

While significant steps have been taken in here to successfully achieve FIVH in the future, there is still much work to be carried out. For instance, other components employed in the hybridization solutions, such as dextran sulphate and Triton X will have to be substituted or have their concentrations decreased for FIVH application due to their toxicity [49,50]. Dextran sulphate is used as an hybridization rate accelerator [51], whereas Triton X acts as a detergent and prevents non-specific binding. A balance in the concentration of these reagents simultaneously with the concentration of added urea that will ensure reasonable kinetics and specificity of hybridization while keeping acceptable levels of toxicity will have to be accomplished. The exposure time of the probe to the respective target is also one of the most important factors for FIVH success. In fact, the decrease of the time-course of each experiment (30 min) has already been done in our lab for PNA probes [52]. Matthiesen and Hansen also tried to reduce the required hybridization time using DNA probes, however, the best results were observed only with one hour of hybridization [53]. Therefore, future studies will be also focused on decreasing the exposure time of the HP_LNA/2OMe_PS probe.

A suitable detection system that is able to detect the fluorescence signal inside the human body to assess the efficiency of hybridization is available to FIVH, using a computer connected to a confocal laser endomicroscope [42]. This equipment has been shown to be useful for *in vivo* diagnosis of precancerous conditions and gastric cancer, and has also allowed direct, nonspecific *in vivo* identification of *H. pylori* [54]. Therefore, it could be used to detect the fluorescence signal of the HP_LNA/2OMe_PS probe *in vivo*, possibly allowing acquisition of real time high resolution images of this bacterium during ongoing endoscopy. Another important advantage of this method is that it should be easily adapted to detect the resistance of *H. pylori* to clarithromycin, by a simple redesign of the probes [55]. This would imply that by the end of an endomicroscopy, the gastroenterologist would not only know about the presence of *H. pylori*, but also have information about the best therapy that should be prescribed to the patient.

In this study, the fluorescence intensity was used as a parameter of probe hybridization efficiency in slides and in suspension. The quantification of fluorescence was performed both by the ImageJ software and by flow cytometry. One of the reasons why the quantification of fluorescence was performed by two methods was that when using flow cytometry it is possible to analyze each cell as an independent observation and therefore stronger statistical data is obtained (Figure 5.3). The other reason was that, within the human body, not all the microbial cells are adhered to a surface. For instance, when microbial infections of the blood occur, microorganisms such as *Candida spp.*,

Staphylococcus aureus and many others can be found in the bloodstream [56,57]. Because one of the goals of this study was to establish a framework for other FIVH methods, we considered it relevant to assess if differences in the hybridization performance could also be observed between hybridization in slides and in suspension. As this was not the case, FIVH might also be applicable in the future as a diagnostic method to detect the causative agent of a septicaemia, pending on the development of suitable technologies to detect the fluorescent signal of the probe.

5.5. Conclusions

Specific and sensitive detection by FISH of a microorganism under human normothermia conditions is reported herein for the first time. More importantly, the study also lays the foundation for other projects that aim to develop methods for *in vivo* detection of other microorganisms using FIVH. For instance, the remarkable properties of LNA in terms of hybridization affinity and specificity were essential for the obtained results. Furthermore, phosphorothioate internucleoside linkages coupled with the introduction of 2'OMe residues proved to be the most suitable probes. As the FIVH process is mostly controlled by the thermodynamics of hybridization of nucleic acids, it is suggested that works targeting other microorganisms should employ LNA/2OMe with PS linkage-based probes.
Future research should be focussed in three main directions: 1) decrease of the time of a standard FISH procedure; 2) evaluation of the cytotoxicity of all compounds used in this process, and 3) assessment of the ability of confocal endomicroscopy to detect the fluorescent signal emitted by the fluorochrome attached to the cells.

5.6. References

1. Woese C.R. Bacterial evolution. Microbiol Rev (1987); 51: 221-271.
2. Bik E.M., Eckburg P.B., Gill S.R., Nelson K.E., Purdom E.A., Francois F., et al. Molecular analysis of the bacterial microbiota in the human stomach. Proc Natl Acad Sci U S A (2006); 103: 732-737.
3. Theves C., Senescau A., Vanin S., Keyser C., Ricaut F.X., Alekseev A.N., et al. Molecular identification of bacteria by total sequence screening: determining the cause of death in ancient human subjects. PLoS One (2011); 6: e21733.
4. Robertson K.L., Vora G.J. Locked nucleic acid flow cytometry-fluorescence in situ hybridization (LNA flow-FISH): a method for bacterial small RNA detection. J Vis Exp (2012): e3655.
5. Malic S., Hill K.E., Hayes A., Percival S.L., Thomas D.W., Williams D.W. Detection and identification of specific bacteria in wound biofilms using peptide nucleic acid fluorescent in situ hybridization (PNA FISH). Microbiology (2009); 155: 2603-2611.
6. Ji R., Li Y.Q., Gu X.M., Yu T., Zuo X.L., Zhou C.J. Confocal laser endomicroscopy for diagnosis of Helicobacter pylori infection: a prospective study. J Gastroenterol Hepatol (2010); 25: 700-705.
7. Miller S.J., Joshi B.P., Feng Y., Gaustad A., Fearon E.R., Wang T.D. In vivo fluorescence-based endoscopic detection of colon dysplasia in the mouse using a novel peptide probe. PLoS One (2011); 6: e17384.
8. Polglase A.L., McLaren W.J., Skinner S.A., Kiesslich R., Neurath M.F., Delaney P.M. A fluorescence confocal endomicroscope for in vivo microscopy of the upper- and the lower-GI tract. Gastrointest Endosc (2005); 62: 686-695.
9. Amann R.I., Ludwig W., Schleifer K.H. Phylogenetic identification and in situ detection of individual microbial cells without cultivation. Microbiol Rev (1995); 59: 143-169.
10. Silahtaroglu A.N., Tommerup N., Vissing H. FISHing with locked nucleic acids (LNA): evaluation of different LNA/DNA mixmers. Mol Cell Probes (2003); 17: 165-169.
11. Kubota K., Ohashi A., Imachi H., Harada H. Improved in situ hybridization efficiency with locked-nucleic-acid-incorporated DNA probes. Appl Environ Microbiol (2006); 72: 5311-5317.
12. Silahtaroglu A., Pfundheller H., Koshkin A., Tommerup N., Kauppinen S. LNA-modified oligonucleotides are highly efficient as FISH probes. Cytogenet Genome Res (2004); 107: 32-37.
13. Robertson K.L., Thach D.C. LNA flow-FISH: a flow cytometry-fluorescence in situ hybridization method to detect messenger RNA using locked nucleic acid probes. Anal Biochem (2009); 390: 109-114.
14. Maruo R., Yamada H., Watanabe M., Hidaka Y., Iwatani Y., Takano T. mRNA quantification after fluorescence activated cell sorting using locked nucleic acid probes. Mol Biotechnol (2011); 49: 42-47.

15. Veedu R.N., Wengel J. Locked nucleic acid as a novel class of therapeutic agents. RNA Biol (2009); 6: 321-323.
16. Singh S.K. K.A.A., Wengel J and Nielsen P. LNA (locked nucleic acids): synthesis and high-affinity nucleic acid recognition. Chem Commun (1998): 455-456.
17. Koshkin AA S.S., Nielsen P, Rajwanshi VK, Kumar R, Meldgaard M, Olsen CE, Wengel J LNA (Locked Nucleic Acids): Synthesis of the adenine, cytosine, guanine, 5-methylcytosine, thymine and uracil bicyclonucleoside monomers, oligomerisation, and unprecedented nucleic acid recognition. Tetrahedron (1998): 3607-3630.
18. Soe M.J., Moller T., Dufva M., Holmstrom K. A sensitive alternative for microRNA in situ hybridizations using probes of 2'-O-methyl RNA + LNA. J Histochem Cytochem (2011); 59: 661-672.
19. Molenaar C., Marras S.A., Slats J.C., Truffert J.C., Lemaitre M., Raap A.K., et al. Linear 2' O-Methyl RNA probes for the visualization of RNA in living cells. Nucleic Acids Res (2001); 29: E89-89.
20. Aronica E., Fluiter K., Iyer A., Zurolo E., Vreijling J., van Vliet E.A., et al. Expression pattern of miR-146a, an inflammation-associated microRNA, in experimental and human temporal lobe epilepsy. Eur J Neurosci (2010); 31: 1100-1107.
21. Majlessi M., Nelson N.C., Becker M.M. Advantages of 2'-O-methyl oligoribonucleotide probes for detecting RNA targets. Nucleic Acids Res (1998); 26: 2224-2229.
22. Kierzek E., Ciesielska A., Pasternak K., Mathews D.H., Turner D.H., Kierzek R. The influence of locked nucleic acid residues on the thermodynamic properties of 2'-O-methyl RNA/RNA heteroduplexes. Nucleic Acids Res (2005); 33: 5082-5093.
23. Matsukura M., Koike K., Zon G. Antisense phosphorothioates as antivirals against human immunodeficiency virus (HIV) and hepatitis B virus (HBV). Toxicol Lett (1995); 82-83: 435-438.
24. Dias N., Stein C.A. Antisense oligonucleotides: basic concepts and mechanisms. Mol Cancer Ther (2002); 1: 347-355.
25. Guga P., Koziolkiewicz M. Phosphorothioate nucleotides and oligonucleotides - recent progress in synthesis and application. Chem Biodivers (2011); 8: 1642-1681.
26. Hoke G.D., Draper K., Freier S.M., Gonzalez C., Driver V.B., Zounes M.C., et al. Effects of phosphorothioate capping on antisense oligonucleotide stability, hybridization and antiviral efficacy versus herpes simplex virus infection. Nucleic Acids Res (1991); 19: 5743-5748.
27. Stein C.A., Mori K., Loke S.L., Subasinghe C., Shinozuka K., Cohen J.S., et al. Phosphorothioate and normal oligodeoxyribonucleotides with 5'-linked acridine: characterization and preliminary kinetics of cellular uptake. Gene (1988); 72: 333-341.
28. Woolf T.M., Jennings C.G., Rebagliati M., Melton D.A. The stability, toxicity and effectiveness of unmodified and phosphorothioate antisense oligodeoxynucleotides in Xenopus oocytes and embryos. Nucleic Acids Res (1990); 18: 1763-1769.

29. Belair C., Darfeuille F., Staedel C. Helicobacter pylori and gastric cancer: possible role of microRNAs in this intimate relationship. Clin Microbiol Infect (2009); 15: 806-812.
30. Resende C., Thiel A., Machado J.C., Ristimaki A. Gastric cancer: basic aspects. Helicobacter (2011); 16 Suppl 1: 38-44.
31. Guimaraes N., Azevedo N.F., Figueiredo C., Keevil C.W., Vieira M.J. Development and application of a novel peptide nucleic acid probe for the specific detection of Helicobacter pylori in gastric biopsy specimens. J Clin Microbiol (2007); 45: 3089-3094.
32. Kumar R., Singh S.K., Koshkin A.A., Rajwanshi V.K., Meldgaard M., Wengel J. The first analogues of LNA (locked nucleic acids): phosphorothioate-LNA and 2'-thio-LNA. Bioorg Med Chem Lett (1998); 8: 2219-2222.
33. You Y., Moreira B.G., Behlke M.A., Owczarzy R. Design of LNA probes that improve mismatch discrimination. Nucleic Acids Res (2006); 34: e60.
34. Cole J.R., Chai B., Farris R.J., Wang Q., Kulam S.A., McGarrell D.M., et al. The Ribosomal Database Project (RDP-II): sequences and tools for high-throughput rRNA analysis. Nucleic Acids Res (2005); 33: D294-296.
35. Azevedo N., Vieira MJ., Keevil CW.Development of peptide nucleic acid probes to detect Helicobacter pylori in diverse species potable water biofilms. In: McBain A. AD, Brading M., Rickard A., Verran J. , Walker J. , editor. Biofilm Communities: Order from Chaos? (2003): BioLine. pp. 105-112.
36. Almeida C., Azevedo N.F., Fernandes R.M., Keevil C.W., Vieira M.J. Fluorescence in situ hybridization method using a peptide nucleic acid probe for identification of Salmonella spp. in a broad spectrum of samples. Appl Environ Microbiol (2010); 76: 4476-4485.
37. Simard C., Lemieux R., Cote S. Urea substitutes toxic formamide as destabilizing agent in nucleic acid hybridizations with RNA probes. Electrophoresis (2001); 22: 2679-2683.
38. Huang E., Talukder S., Hughes T.R., Curk T., Zupan B., Shaulsky G., et al. BzpF is a CREB-like transcription factor that regulates spore maturation and stability in Dictyostelium. Dev Biol (2011); 358: 137-146.
39. Dewald G.W., Smyrk T.C., Thorland E.C., McWilliams R.R., Van Dyke D.L., Keefe J.G., et al. Fluorescence in situ hybridization to visualize genetic abnormalities in interphase cells of acinar cell carcinoma, ductal adenocarcinoma, and islet cell carcinoma of the pancreas. Mayo Clin Proc (2009); 84: 801-810.
40. Garcia-Hernandez J., Moreno Y., Amorocho C.M., Hernandez M. A combination of direct viable count and fluorescence in situ hybridization for specific enumeration of viable Lactobacillus delbrueckii subsp. bulgaricus and Streptococcus thermophilus. Lett Appl Microbiol (2012).
41. Wiegant J., Brouwer A.K., Tanke H.J., Dirks R.W. Visualizing nucleic acids in living cells by fluorescence in vivo hybridization. Methods Mol Biol (2010); 659: 239-246.
42. Neumann H., Kiesslich R., Wallace M.B., Neurath M.F. Confocal laser endomicroscopy: technical advances and clinical applications. Gastroenterology (2010); 139: 388-392, 392 e381-382.

43. Neumann H., Neurath M.F., Mudter J. New endoscopic approaches in IBD. World J Gastroenterol (2011); 17: 63-68.
44. Shukla R., Abidi W.M., Richards-Kortum R., Anandasabapathy S. Endoscopic imaging: How far are we from real-time histology? World J Gastrointest Endosc (2011); 3: 183-194.
45. Krauss E., Agaimy A., Douplik A., Albrecht H., Neumann H., Hartmann A., et al. Normalized autofluorescence imaging diagnostics in upper GI tract: a new method to improve specificity in neoplasia detection. Int J Clin Exp Pathol (2012); 5: 956-964.
46. Szollosi J., Lockett S.J., Balazs M., Waldman F.M. Autofluorescence correction for fluorescence in situ hybridization. Cytometry (1995); 20: 356-361.
47. Bingham E., Hyvarinen A. A fast fixed-point algorithm for independent component analysis of complex valued signals. Int J Neural Syst (2000); 10: 1-8.
48. Borisova E. V.B., Avramov L. 5-ALAMediated Fluorescence Detection of Gastrointestinal Tumors. Advances in Optical Technologies (2008).
49. Flexner C., Barditch-Crovo P.A., Kornhauser D.M., Farzadegan H., Nerhood L.J., Chaisson R.E., et al. Pharmacokinetics, toxicity, and activity of intravenous dextran sulfate in human immunodeficiency virus infection. Antimicrob Agents Chemother (1991); 35: 2544-2550.
50. Koley D., Bard A.J. Triton X-100 concentration effects on membrane permeability of a single HeLa cell by scanning electrochemical microscopy (SECM). Proc Natl Acad Sci U S A (2010); 107: 16783-16787.
51. Englert H.a. Nucleic Acid Hybridization. In: A.S. G, editor. Molecular Biology Problem Solver: A Laboratory Guide.(2001): John Wiley and Sons.
52. Santos R.S., Guimaraes N., Madureira P., Azevedo N.F. Optimization of a peptide nucleic acid fluorescence in situ hybridization (PNA-FISH) method for the detection of bacteria and disclosure of a formamide effect. J Biotechnol (2014); 187: 16-24.
53. Matthiesen S.H., Hansen C.M. Fast and non-toxic in situ hybridization without blocking of repetitive sequences. PLoS One (2012); 7: e40675.
54. Kiesslich R., Goetz M., Burg J., Stolte M., Siegel E., Maeurer M.J., et al. Diagnosing Helicobacter pylori in vivo by confocal laser endoscopy. Gastroenterology (2005); 128: 2119-2123.
55. Cerqueira L., Fernandes R.M., Ferreira R.M., Carneiro F., Dinis-Ribeiro M., Figueiredo C., et al. PNA-FISH as a new diagnostic method for the determination of clarithromycin resistance of Helicobacter pylori. BMC Microbiol (2011); 11: 101.
56. Ngo J.T., Parkins M.D., Gregson D.B., Pitout J.D., Ross T., Church D.L., et al. Population-based assessment of the incidence, risk factors, and outcomes of anaerobic bloodstream infections. Infection (2013); 41: 41-48.
57. Erdem I., Ozgultekin A., Inan A.S., Ozturk Engin D., Senbayrak Akcay S., Turan G., et al. Bloodstream infections in a medical-surgical intensive care unit: incidence, aetiology, antimicrobial resistance patterns of Gram-positive and Gram-negative bacteria. Clin Microbiol Infect (2009); 15: 943-946.

Chapter VI

Towards fluorescence in vivo hybridization (FIVH) detection of H. pylori in gastric mucosa using advanced LNA probes

PLOS ONE

RESEARCH ARTICLE

Towards Fluorescence *In Vivo* Hybridization (FIVH) Detection of *H. pylori* in Gastric Mucosa Using Advanced LNA Probes

Sílvia Fontenete[1,2,3,4,5]*, Marina Leite[2,3], Nuno Guimarães[1,2,3,4], Pedro Madureira[2,5,6], Rui Manuel Ferreira[2,3], Céu Figueiredo[2,3,7], Jesper Wengel[3], Nuno Filipe Azevedo[1]

1 LEPABE, Laboratory for Process Engineering, Environment, Biotechnology and Energy, Faculty of Engineering, University of Porto, Porto, Portugal, **2** Instituto de Investigação e Inovação em Saúde, Universidade do Porto, Porto, Portugal, **3** IPATIMUP, Institute of Molecular Pathology and Immunology of the University of Porto, Porto, Portugal, **4** Nucleic Acid Center, Department of Physics, Chemistry and Pharmacy, University of Southern Denmark, Odense M, Denmark, **5** ICBAS, Institute of Biomedical Sciences Abel Salazar, University of Porto, Porto, Portugal, **6** IBMC, Institute for Molecular Biology and Cell Biology, Porto, Portugal, **7** FMUP, Faculty of Medicine of Porto University, Porto, Portugal

* sfontenete@fe.up.pt

ABSTRACT

In recent years, there have been several attempts to improve the diagnosis of infection caused by *Helicobacter pylori*. Fluorescence *in situ* hybridization (FISH) is a commonly used technique to detect *H. pylori* infection but it requires biopsies from the stomach. Thus, the development of an *in vivo* FISH-based method (FIVH) that directly detects and allows the visualization of the bacterium within the human body, would significantly reduce the time of analysis, allowing the diagnosis to be performed during endoscopy. In a previous study it was designed and synthesized a phosphorothioate locked nucleic acid (LNA)/ 2' O-methyl RNA (2'OMe) probe using standard phosphoramidite chemistry and then FISH hybridization it was successfully performed both on attached and suspended bacteria at 37 °C. In this work it was simplified, shortened and adapted FISH to work at gastric pH values, meaning that the hybridization step now takes only 30 minutes and, in addition to the buffer, uses only urea and probe at non-toxic concentrations. Importantly, the sensitivity and specificity of the FISH method was maintained in the range of conditions tested, even at low stringency conditions (e.g. low pH). In conclusion, this methodology is a promising approach that might be used *in vivo* in the future in combination with a confocal laser endomicroscope for *H. pylori* visualization.

Keywords: FISH, Nucleic Acid Analogs, LNA, *Helicobacter pylori*

6.1. Introduction

Microbial communities coexisting within the human host are known as the human microbiome. Under normal circumstances, there is a very high number of microorganisms that protect the human body, however the shift from a normal to an abnormal microbiome may predispose the individual to several diseases [1]. *Helicobacter pylori* is part of the Gram-negative bacterial flora that colonizes the human gastric mucosa and establishes a persistent infection [2]. *H. pylori* causes chronic gastritis, which may progress to gastric or duodenal ulcers, gastric atrophy, mucosa-associated lymphoid tissue lymphoma and adenocarcinoma [3]. This bacterium is thus one of the most important pathogens and is responsible for at least half a millions deaths per year [4]. *H. pylori* can be detected by invasive methods which include endoscopy, where a biopsy is removed and further used for histopathological examination, rapid urease test, PCR or bacterial culturing [5,6]. High-definition endoscopy offers a potential to improve diagnostic accuracy, allowing a real-time decision-making. Recently, a new endoscope imaging technology was developed, the confocal laser endomicroscopy [7], enabling real time *in vivo* detection during ongoing endoscopy [8,9]. This equipment is based on the excitation of a fluorochrome through a laser which provides a clear two-dimensional image of the tissue [10,11]. It includes a powerful microscope that allows clinicians to view bacteria in real time and contains a water jet nozzle which could be used to inject a solution into the gastric mucosa [12]. Confocal laser endomicroscopy can be in theory combined with fluorescent *in situ* hybridization (FISH) for the identification of microorganisms. The high sensitivity and specificity of FISH and the speed at which the assays can be performed have made FISH an important methodology in clinical microbiology [13,14]. Another advantage is the direct visualization of the bacterium within the sample [15]. Because the fluorescent signal generated by FISH has a strong signal-to-noise ratio, automated image analysis is possible to be implemented [16]. However, the development of FISH methods allowing the detection of specific microorganism in living cells (called FIVH, fluorescence *in vivo* hybridization) has proved to be a challenge [17] as many technical issues have to be overcome. For instance, to perform FIVH in the human gastric stomach it would be necessary for the method to work in very acidic conditions. Consequently, only a highly acid-resistant and efficient oligonucleotide will allow such detection. In recent years, a variety of modified oligonucleotides have been developed to increase not only the stability in biological media but also the ability to bind specifically to a target [18]. Oligonucleotides containing locked nucleic acid (LNA) and 2'-*O*-Methyl-RNA (2'OMe) nucleotide monomers are examples of such oligonucleotides. Both LNA and 2'OMe can be considered as RNA mimics and have shown biological stability, lack of detectable toxicity and potent biological

activities [18-23]. Many variations of backbone modifications, most notably the phosphorothioate (PS) backbone, have also evolved and even advanced to the level of clinical trials. [24,25]. PS oligonucleotides containing LNA monomers thus improve target affinity and display significant nuclease resistance [26,27].

In Chapter V, the use of one probe composed of a mixture of LNA and 2'OMe nucleotides (LNA/2'OMe) with a PS backbone modification were shown to have an excellent performance at 37 °C, displaying higher affinity, increased specificity, faster hybridization kinetics, and superior ability to hybridize to the target [17]. However, current FISH protocols have not been optimized for *in vivo* use. Most, if not all, hybridization buffers are toxic and/or require incubation times that are too long to be used in FIVH. Additionally, FISH protocols are performed at physiological pH (pH 7.0-7.5), and no studies are known which analyzed the behavior of oligonucleotides for FISH under acidic pH conditions.

In order to address these questions, herein it has tested the chemical stability and efficiency of hybridization of the HP_ LNA/2OMe _PS probe in a range of pH values and in the presence of pepsin. Then, it was evaluated the specificity and toxicity of this probe in a human gastric epithelial cell line.

6.2. Materials and methods

6.2.1. Oligonucleotide synthesis

The sequence of the probe was selected based on the parameters described in Chapter V [17] (Table 6.1). The oligonucleotides were synthesized using an automated DNA synthesizer using standard phosphoramidite chemistry at 1.0 µmol scale. Two different probes were synthesized using the same sequence but with two different fluorescent labels: fluorescein (FAM) and cyanine 3 (Cy3). Probes were purified by reverse phase HPLC (RP-HPLC) and characterized by IonExchange HPLC conditions (IE-HPLC) using a Dionex system HPLC (VWR) and matrix-assisted laser desorption ionization time-of-flight mass spectrometry (MALDI-TOF) on a Microflex Maldi (Bruker Instruments, Leipzig, Germany). The purified oligonucleotides were precipitated by acetone and their purity (>90%) and composition was verified by IE-HPLC and MALDI-TOF analysis. The probes were resuspended in different hybridization buffers as described in the following sections.

Table 6.1 - Designation and sequence of the probes containing locked nucleic acid (LNA; with L superscript) and 2'-O-methyl RNA (2'-OMe; in Boldface) nucleotide monomers. HP_ LNA/2OMe _PS is a phosphorothioate oligomer (PS backbones) labeled with either FAM (Fluorescein) or Cy3 (Cyanine)

Designation	Sequence (10-mer)
FAM HP_ LNA/2OMe _PS	5'- FAM G^{L}**AC**T^{L}**AA**G^{L}**CC**C^{L}-3'
Cy3 HP_ LNA/2OMe _PS	5'- Cy3 G^{L}**AC**T^{L}**AA**G^{L}**CC**C^{L}-3'

6.2.2. Analysis of probe integrity at low pH by analytical chemistry

To determine if the integrity of the fluorochrome-labeled HP_ LNA/2OMe _PS probe was maintained at low pH and in the buffer used in FISH, the probe was exposed to pH 2 and pH 4 (using a 0.5M urea and 900 mM NaCl buffer) in the same buffer for 3 hours at 37 °C. To correctly perform the characterization, the salts in the solution were removed using illustra^{TM} NAP-10 columns (GeHealthcare, UK). Afterwards, whilst the probe was submersed in different buffers, it was characterized by ion exchange HPLC (IE-HPLC) on a Dionex system HPLC (VWR) using a Dionex DNAPac PA-100, 9*x*250mm analytical column, and by matrix-assisted laser desorption ionization time-of-flight mass spectrometry (MALDI-TOF) using a Microflex Maldi (Bruker Instruments, Leipzig, Germany). As a control, the same characterization was performed in parallel for a suspension of the HP_ LNA/2OMe _PS probe that was not exposed to acidic conditions.

6.2.3. Bacterial strains and culture conditions

All bacterial cultures were grown in trypticase soy agar (TSA) supplemented with 5% (v/v) sheep blood (Becton Dickinson GmbH, Germany) and incubated for 48 hours at 37 °C under microaerobic conditions using a GENbox microaer (bioMérieux, Marcy l'Étoile, France). Bacteria were collected from TSA plates using water or saline (microscopy or cytometry analysis, respectively). The bacterial density was determined by the dilution of initial culture in water or saline and the absorbance was measured at 600 nm. *H. pylori* 26695 was used for the optimization of probe hybridization conditions, whereas other bacteria, either *Helicobacter spp.* or the non-*Helicobacter spp.*, were used for the analysis of probe specificity and sensitivity. All bacteria used in this study are listed in Table 6.2.

Table 6.2 - *Helicobacter* and non-*Helicobacter* bacterial strains included in this study

Helicobacter spp.		
***H. pylori* strains**	***Non-pylori Helicobacter strains***	***Non-Helicobacter spp.***
26695 (ATCC® 700392™)	*H. cinaedi* 33221-1.2[b]	*Staphylococcus epidermidis* (ATCC® RP602A™)
G27 (NCTC 13282)	*H. mustelae* 2H1[b]	*Staphylococcus* aureus (ATCC® 25923™)
60190 (*ATCC®* 49503™)	*H. salomonis*[b]	*Pseudomonas fluorescens* (ATCC® 13525™)
84-183(ATCC® 53726™)	*H. muridarum 2*A5+[c]	*Escherichia coli* (CECT 434)
H. pylori CI-31[a]	*H. pametensis*[c]	*Campylobacter jejuni*
H. pylori CI-116[a]	*H. bilis*[b]	*Campylobacter coli*
	H. canis CIP104753	
	H. canadensis [b]	
	H. acinonychis (ATCC® 51101™)	

Legend: *Helicobacter* clinical isolates provided by: [a] Céu Figueiredo [28] ; [b] Francis Megraud, and [c] Jay Solnick

6.2.4. Analysis of probe behavior in a pH range

In the Chapter V, it was shown that the FAM HP_LNA/2OMe_PS probe is able to efficiently detect *H. pylori* at the human body temperature (37 °C) [17]. Here, it was further evaluate if this probe efficiently hybridize under conditions similar to those of the human stomach, particularly the acidic pH. Therefore, the first analysis encompassed the evaluation of the performance of this probe at a range of pH values using different hybridization times applying the FISH protocol in suspension, as previously described [17]. For this analysis, it was used the response surface methodology (RSM) [29,30] to quantify the relationship between the response (or output variable, i.e. fluorescence intensity upon probe hybridization) and the independent variable (input variable, i.e. pH and time). Having used the central compose design, formulated through the statistical software package Design Expert® 9.0.3 (StatEase Inc., Minneapolis, USA), it was analysed the variation of fluorescence intensity as a function of pH change and time of hybridization. This design was built in a quadratic surface, where all experiments were conducted in 14 runs, and in which six of them were center points. Each experiment was carried out in duplicate. The levels of the independent variables in pH *versus* time are presented in Table 6.3. The levels selected for the time and pH variables (corresponding to -1, 0 and 1 in coded units) were based on the hybridization time described for FISH

experiments [17,31,32] and to cover the range of physiological conditions of the human stomach [33], respectively. Therefore, the fluorescence intensity (arbitrary units of fluorescence, AUF) was taken as a response to derive the model.

Table 6.3 - Experimental levels of variables tested for fluorescence intensity, using the response surface methodology

Variables	Range and level				
	-α	**-1**	**0**	**+1**	**+α**
Time (min)	0.07	15.5	52.7	90	105.4
pH	0.96	2	4.5	7	8.04

6.2.5. Optimization of probe hybridization conditions in bacterial suspensions

6.2.5.1. Optimization of the washing step

To confirm the results obtained by RSM, it was studied the probe's performance at pH 2, 4 or 7, the three most relevant ranges of pH in the human stomach corresponding to the pH of the lumen, mucus, and epithelial layer, respectively. Moreover, for each pH value it was tested different incubation times with washing buffer ranging from 0, 5 and 15 min and different washing buffers. The performance of the probe was compared in the standard FISH washing buffer [pre-warmed solution (pH 10), containing 5 mM Tris Base (Fisher Scientific), 15 mM NaCl (Panreac) and 1% Triton X (Panreac)] and in a non-toxic washing buffer (aqueous solution at the pH under study). All FISH experiments were performed in suspension using the protocol described in Chapter V [17], with the exception of the time and pH parameters referred above.

6.2.5.2. Optimization of the hybridization step

Since the aim of this work it was adapt the FISH methodology to be used *in vivo* directly in the gastric mucosa, it has tested a short hybridization time period aiming to reduce the overall time of the hybridization step (the standard time currently used is 90 minutes) [15,17,31]. Therefore, using the optimized washing step described above the hybridization step at 30 and 90 minutes was tested. Following this, specificity and sensitivity analysis was performed with the reduced time using other *H. pylori* 26695 and G27 strains and *Helicobacter spp* (*H. cinaedi, H. mustelae, H. salomanis, H. muridarum, H. pametensis, H. bilis and H. canis*).

It was optimized the probe with a buffer containing urea to substitute formamide in the Chapter V [17]. However, in order to use a completely non-toxic buffer, a larger number of

experiments were performed to remove some of the toxic compounds that are normally present in the washing and hybridization buffer, such as dextran sulphate, Triton-X and ethylenediaminetetraacetate (EDTA) disodium salt 2-hydrate. Therefore, it was tested a hybridization buffer containing 4M urea (VWR BHD Prolabo, Haasrode, Belgium), 900 mM NaCl (Panreac) and different buffer solutions to keep the desired pH (pH2:KCl-HCl, pH4:phosphate-citrate, pH7:Tris-HCl buffer). The following procedure aimed at reducing the concentration of urea and we therefore tested 2M and 0.5M of urea in the same conditions. Thus, in the final optimized protocol, 100 µL of fixed cells (50% ethanol during 15 minutes) were resuspended in 100 µL of hybridization solution (0.5M of urea, 900 mM NaCl and pH buffer solution) with 400 nM probe, and the resulting mixture was incubated at 37℃ for 30 min. After hybridization, samples were centrifuged at 14.000 rpm for 5 min, resuspended in 500 µL of washing solution (buffer solution diluted in MiliQ water) and incubated at 37 °C for 15 min. The cells were again centrifuged at 14 000 rpm for 5 min and resuspended in 100 µL of saline. To remove aggregates, samples were filtered by a sterile filter (0.22 µm filter, Frilabo). A specificity and sensitivity analysis of the probe in optimized conditions was performed using other *H. pylori* 26695 and G27 strains and *Helicobacter spp* (as above).

FISH in slides was performed as previously reported in Chapter V, with a few modifications [17,34]. For permeabilization on glass slides, smears of each species/strain were immersed in 50% (v/v) ethanol for 10 min and allowed to air dry. The hybridization was performed using 20 µl of hybridization buffer with 200 nM probe, such that the resulting mixture was covering each smear individually. Samples were covered with coverslips and incubated for 30 min at 37 °C. Slides were subsequently washed in a preheated aqueous acid solution for 15 min at 37 °C whereupon the slides were allowed to air dry. All experiments were performed in triplicate and for each experiment a negative control (same hybridization conditions, but without a probe in the hybridization mixture) was included. Slides were stored in the dark before microscopy analysis.

6.2.5.3. Optimization of the permeabilization step

Most FISH protocols include a fixative/permeabilization step where toxic compounds such *as* paraformaldehyde (PF) are used. Since PF is toxic for cells, it was compared the efficiency of probe hybridization under conditions with (normal protocol) and without PF in the FISH protocol.

6.2.5.4. Optimization of FISH protocol in conditions similar to gastric juice

Since human gastric mucosa is covered by gastric juice, the washing step in FIVH could be considered the gastric juice. Therefore, the standard washing buffer in the FISH protocol was substituted by a gastric simulated juice that contains pepsin [35]. The hybridization step was performed in *H. pylori* 26695 bacterial suspension, using 0.5M urea buffer at different pH values (2, 4 and 7). Afterwards specificity and sensitivity analysis was performed with the bacteria described in Table 6.2.

6.2.6. Cytometry analysis

H. pylori bacteria cell suspensions stained with Cy3-labeled or FAM-labeled HP_ LNA/2OMe _PS probes, and the respective unstained negative controls, were analyzed in a Beckman Coulter Epics XL flow cytometer (Brea, USA) equipped with a 488 nm laser. For each sample, 20 000 events were collected. All the experiments were repeated in triplicate.

6.2.7. Microscope evaluation

Bacteria images were acquired with a Carl Zeiss Apotome Axiovert 200M Fluorescence Microscope (Carl Zeiss, Jena, Germany). Images were taken with an Axiocam HRm camera and processed with Zeiss Axion Vision 4.8 software. All the experiments were performed in triplicate.

AGS (gastric adenocarcinoma) cells were analyzed on an inverted epi-fluorescence microscope, (Axiovert 200M, Zeiss,Germany). Images were acquired with a Leica TCP SP2 AOBS camera and processed LAS AF using Lite software (Leica Microsystems CMS GmbH).

6.2.8. Cell culture conditions and infection with H. pylori

Human gastric epithelial cell line AGS (ATCC® CRL-1739) was maintained at 37 °C under 5% CO_2 humidified air, in RPMI medium 1640 Glutamax I (Gibco, Invitrogen, Grand Island, NY, USA) supplemented with 10% (v/v) fetal bovine serum (FBS) and 1% (v/v) Penicillin/Streptomycin (complete medium). Culture medium was replaced every two days. For infection experiments, AGS cells were seeded in a 6-well culture plate and grown in antibiotic-free medium until reach the desired confluence. AGS cells were infected with *H. pylori* at a multiplicity of infection (MOI) of 100, for 3 hours. Controls without infection were also seeded in the same conditions. In order to evaluate the specificity of Cy3 HP_

LNA/2OMe _PS, FISH was performed with different concentrations of probe and the fluorescence signal was studied by confocal microscopy.

6.2.9. Cell proliferation assay

AGS cells were seeded in 96-well plates with a final volume of 200 µL of complete medium per well and grown to 50% and 100% confluence. Upon reaching the desired confluence, AGS cells were incubated with 200 nM of Cy3_ HP_ LNA/2OMe _PS diluted in hybridization buffer [0.5 M urea and 900 mM NaCl; 1% (v/v) or 5% (v/v)] or in complete medium (untreated control) for 24 hours. At the end of the incubation period, the cell viability was evaluated using CellTilter 96® Aqueous One Solution Cell Proliferation Assay (Promega Corporation, Madison, WI), according to the manufacturer's instructions. Absorbance at 490 and 630 nm was measured using a microplate reader (Biotek Instruments Inc. Synergy MX, USA). Background absorbance values were subtracted from the absorbance values generated with MTS assay. The values from treated cells were compared with the values generated from untreated control cells and reported as percent viability. All experiments were performed in triplicate.

6.2.10. Cell death analysis in AGS cells

The caspase 3/7 activity in AGS cells treated with probe was analysed using the luminometric Caspase-Glo™ assay (Promega, Madison USA), according to manufacturer's instructions. AGS cell were plated in 96 well solid white bottom plates in 200 µL of complete medium. When AGS cells reached 50% confluence, they were treated with 200 nM of Cy3 HP_ LNA/2OMe _PS diluted in a hybridization buffer (vehicle) or complete media (untreated control) and cells were incubated for 24 hours. The plates were then incubated with 100 µL of Caspase-Glo reagent at room temperature for 30 minutes. The luminescence of each sample was measured in a plate-reading luminometer (Biotek Instruments Inc. Synergy MX, USA). The experiments were performed in triplicate and repeated on three separately-initiated cultures.

Evaluation of apoptosis was performing using the Cell Death Detection ELISA^{PLUS} kit (Roche Applied Science, Germany) according to the manufacturer's protocol. The principle of this assay is the detection of mono- and oligonucleosomes in the cell lysates using biotinylated anti-histone and peroxidase-coupled anti-DNA antibodies. The amount of peroxidase retained in the immunocomplex was photometrically determined with 2,2′-azino-bis-(3-ethylbenzthiazoline-6-sulfonic acid) as the substrate through the absorbance quantification quantified at 405 nm. Data are expressed as mean of three independent

experiments. In a separate experiment, AGS (4 x10^4 cells/mL) were treated for 24 h with 200 nM of Cy3_HP_ LNA/2OMe _PS or vehicle (hybridization buffer) [in 1% (v/v) or in 5% (v/v)]. Wells with serum free medium were used as negative controls. Briefly, cells were lysed by adding lysis buffer to each well and incubating for 30 min at 20 °C, 300 rpm. Each plate was centrifuged at 200 x *g* for 10 min, and 20 µL of each supernatant was transferred to streptavidin-coated wells. The wells were treated with anti-histone and anti-DNA-containing immune-reagent, incubated for 2h at 25 °C, 250 rpm, washed three times, and treated with peroxidase substrate 2,2'-azino-di-(3-ethyl-benzthiazoline sulfonate). Absorption at 405 nm and 490 nm was measured using a spectrophotometer (Biotek Instruments Inc. Synergy MX, USA). All experiments were repeated three times.

6.2.11. Statistical analysis

Statistical significance was determined by One-way analysis of variance (ANOVA) by applying the Tukey multiple-comparisons test, using SPSS statistics 17.0 (SPSS, Statistical Package for the Social Sciences, Chicago, USA). Results were expressed as mean values±SD. Differences were considered to be statistically significant when $p<0.05$.

6.3. Results

6.3.1. Analytical chemistry of HP_LNA/2OMe_PS at low pH and high salt concentrations

Although the most commonly used dye in FISH is FAM, this dye has been described as sensitive to pH [36]. Therefore, it was tested the integrity of the probe and fluorochrome conjugate at pH values of 2 and 4. The analytical spectra obtained by IC-HPLC and MALDI showed that most of the FAM-labeled HP_ LNA/2OMe _PS was intact. The spectra obtained by IC-HPLC were very similar in all conditions with identical retention time (~21.8 min) for the oligonucleotide not subjected to acidic conditions and after exposure to pH 2 or pH 4 conditions (Figure S7 A). This analytical analysis allowed to verify the presence of the dye and to confirm the purity of the sample even after exposure to strongly acidic conditions. Similarly, the molar mass of the probe was analysed and confirmed to be the same under all conditions studied (MALDI-TOF spectrum; Figure S7 B). In the mass spectrum of the FAM_HP_ LNA/2OMe _PS, there was no significant change in the molar mass (MW = 4002.003) (Figure S7 B). Therefore, the integrity of the probe is maintained at low pH and high salt concentration. The results clearly show that the FAM_ HP_ LNA/2OMe _PS is in principle suitable for applications in the low pH environment of the human stomach.

6.3.2. Central composite design, pH versus time

In the present study the RSM was employed to identify the interactions between variable pH and hybridization time. Fluorescence intensity values were determined by flow cytometry and corresponded to the average of duplicates. The design matrix and the matching observed responses are shown in Table S2. The table shows fluorescent intensities corresponding to the combined effect of the studied variables in their specific ranges.

The central composite design with two variables, including six replicates at the central point and one response, was used for fitting a quadratic response surface. A regression analysis was performed to fit the response function with the experimental data. The statistical significance of the linear model equation was checked by ANOVA and the data are shown in Table S3.

The results obtained were subjected to analysis of variance with the inverse square root model observed in Figure 6.1. Interaction effects and optimal variable levels were determined by plotting the response surface. The contour plot shows the behavior of response (fluorescence intensity) with respect to simultaneous change in the two variables under study (time and pH).

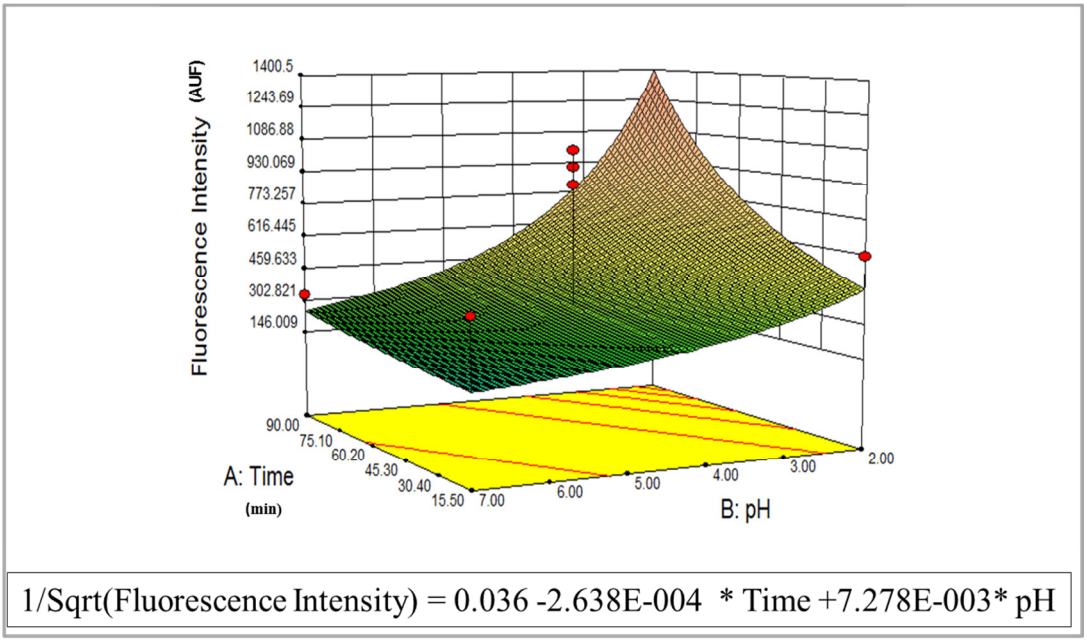

Figure 6.1 - Analysis of FAM HP_LNA/2OMe_PS probe performance using the response surface methodology (RSM). Three dimensional surface plot showing the variation of *H. pylori* fluorescence intensity as a function of model terms. The model graphs are represented in gradient color shading. The surface is red at higher response levels and blue at lower ones.

Although the model was significant for only one of the variables (pH), it helped to understand that the probe could work at a large range of pH values, particularly at low pH. Therefore, after performed this analysis it was carried out experiments without using RSM as a strategy to compare and confirm the model.

6.3.3. Optimization of washing and probe hybridization conditions

Specificity of probe binding to the target typically depends on the washing conditions. The washing step serves mainly to rinse off excess probe molecules at conditions that prevent unspecific binding [37]. Usually, the washing buffer includes detergents and a salt and the washing procedure takes around 30 minutes. However, in FIVH this type of protocol is not possible; therefore, it was tested the use of an aqueous buffer (water with buffer solution) at shorter periods of time (5 to 15 minutes). It was observed that it is possible to use aqueous buffer during 15 minutes in the range of pH in study (Figure S8A). A desirable feature of any diagnostic test is that it should achieve results in the shortest possible time. The alternative approach presented showed that the hybridization process can be performed in 30 minutes in bacteria, obtaining similar results (Figure S8B).

Several studies use complex hybridization buffers in FISH methodologies containing toxic compounds. Most of them have not been proved to be always necessary to improve the yield of a hybridization reaction involving LNA probes (e.g. EDTA and dextran sulfate). In these experiments at pH 7, no effect in the hybridization efficiency was observed after the elimination of these chemicals from the hybridization solution (Figure S8C). In many FISH protocols, increasing stringency improves specificity with a corresponding loss in sensitivity. The use of denaturants is essential to lower the Tm of the hybrids and increase the stringency of the probe to target binding. Therefore, the use of urea has a crucial role in the hybridization to the target. In these experiments it was reduced the quantity of this denaturant from 4 M to 0.5 M which, despite the significant large reduction in concentration, led to no significant decrease observed in fluorescence quantification (Figure S8C).

When performing FIVH the use of toxic compounds such as the fixative buffer is not possible. Consequently, it was optimized the permeabilization step by replacing PF for 50% (v/v) ethanol. Unlike in other studies [38,39], no significant differences were observed in the fluorescent signal intensity with this replacement (Figure 28D). It was further observed that when the permeabilization step with ethanol was not performed in suspended bacteria, the obtained fluorescence intensity was very weak for all of pH values studied. Nevertheless, in attached bacteria, high fluorescence was obtained with a non-fixative protocol (Figure S9).

While acidity profiles in the human stomach can vary extensively [33], the three profiles tested were carefully selected to be representative of the conditions in all groups of patients. It was maintained a denaturant, urea, and sodium chloride in the hybridization buffer since these compounds are essential not only for the high efficiency of the FISH methodology but also to adjust the stringency conditions of the hybridization [40].

After all protocol optimizations, FISH in pure cultures of *H. pylori* was performed, in attached and in suspended bacteria, and evaluation was performed by microscopy (Figure 6.2A-F) and flow cytometry (Figure 6.2G-I). The probe was tested in attached bacteria once *H. pylori* has colonized the gastric mucosa by adhering to the mucus layer that lining the gastric epithelium [41]. It is already known that adhesion to epithelial cells is essential for the infection step [42]. The FISH performed in attached bacteria showed to be efficient for all pH values (Figure 6.2). However, at pH 4 it was observed a higher fluorescent intensity. The control without probe showed a low background in the optimized hybridization buffer (Figure 6.2D-F).

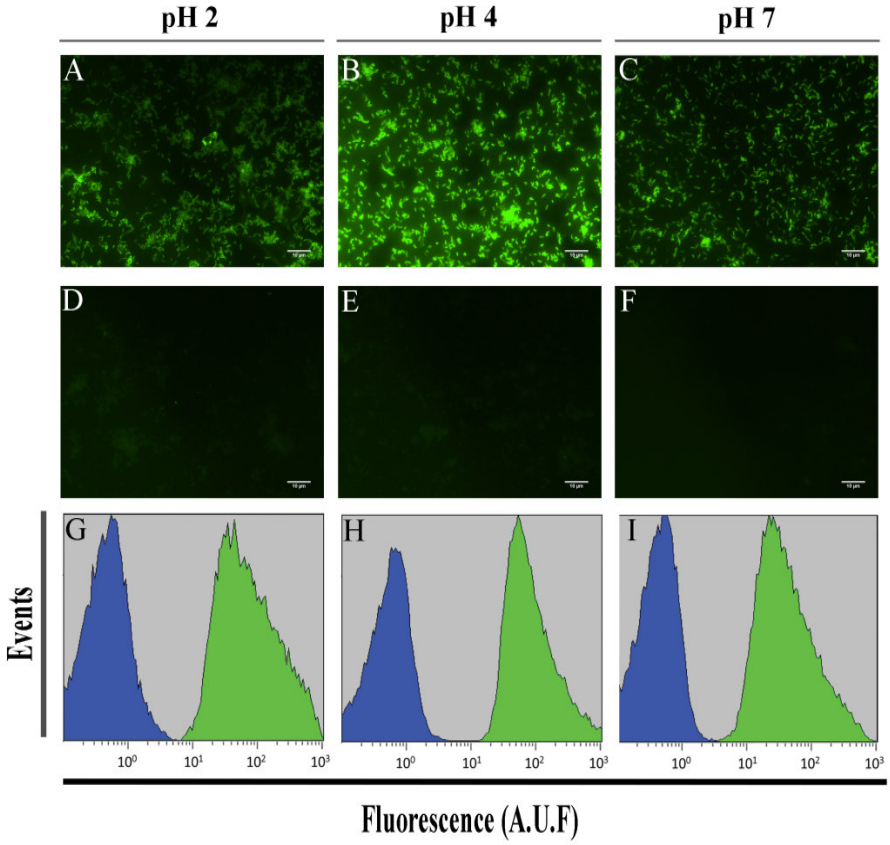

Figure 6.2 - Detection of *H. pylori* in slides, by epifluorescent microscopy (A-F), and in suspension, by flow cytometry (H-J), using the FAM HP_ LNA/2OMe _PS probe at different pH values. A - F Smear of pure culture of *H. pylori* strain 26695 observed by epifluorescent microscopy. A-C. Experiment using 200 nM of the probe. D-F. Smears without probe were used as negative control. All images were taken at equal exposure times. G-I. Relative fluorescence histograms of LNA-FISH targeting *H .pylori* in different pH for two different assays – Blue: negative control with no probe; Green: positive sample. Scale bar = 10 µm.

The results obtained by flow cytometry also showed high fluorescence intensities at all pH values and a low background (Figure 6.2G-I). This analysis was also performed using the Cy3-labelled HP_ LNA/2OMe _PS and the results showed significantly brighter staining (Figure S10) probably due to higher resistance of the fluorochrome Cy3 to photobleaching [40,43].

The sensitivity studies (Figure 6.3) were performed with the FAM HP_ LNA/2OMe _PS probe and showed that this probe is able to detect both *H. pylori* reference strains and *H. pylori* clinical isolates (Figure 6.3A), while no fluorescent signal was detected for the non-*pylori Helicobacter* strains tested (Figure 6.3B). These results also showed that this probe was specific and sensitive for *H. pylori* strains, even when the hybridization is carried out under low stringency conditions (low temperature, short hybridization time and low pH).

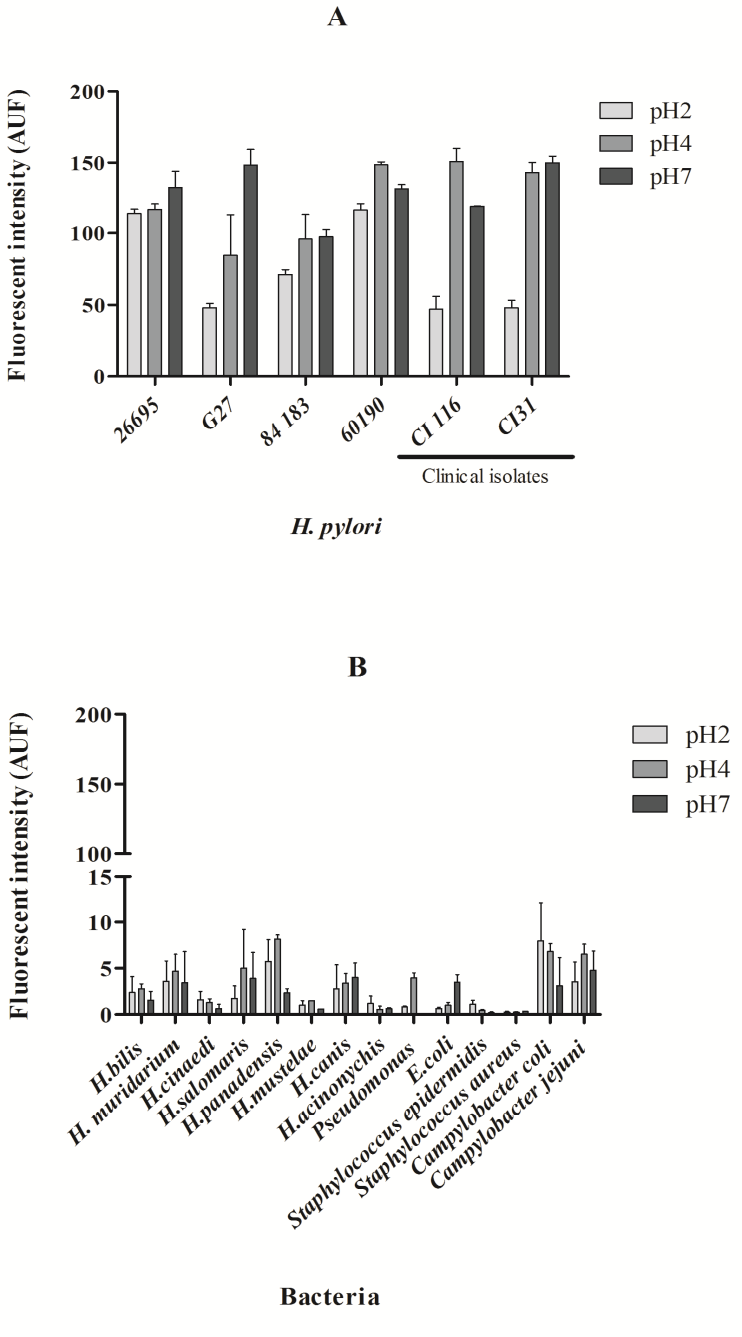

Figure 6.3 - Sensitivity and specificity studies performed with the HP_ LNA/2OMe _PS probe at different pH values evaluated by flow cytometry. A. Sensitivity test using different strains and clinical isolates of *H. pylori*. C. Analysis of the probe in clinical isolates of *H. pylori*. B. Specificity test using different species of Helicobacter and other bacteria.

To mimic the human gastric mucosa, the water in the washing step of the FISH protocol was replaced with simulated gastric juice. It was observed that the signal of the FAM_ HP_ LNA/2OMe _PS be was decreased in the presence of this solution (Figure S11). Therefore, an analytical study to understand if the FAM is functional in this acid solution was performed (Figure S11). Using this acid solution low fluorescence intensity was observed. A possible explanation is that when the dye oligonucleotide conjugates are subjected to acid conditions, protonation or deprotonation of the dye units can alter their electronic structure which can then affect the ability to fluoresce [44]. A protonation of neighboring nucleobases can also alter their electron-donating properties and therefore determine their quenching abilities with consequent loss of fluorescence [45]. On the other hand, the Cy3-labelled HP_ LNA/2OMe _PS still had a strong signal for all hybridization conditions in the simulated juice (Figure 6.4).

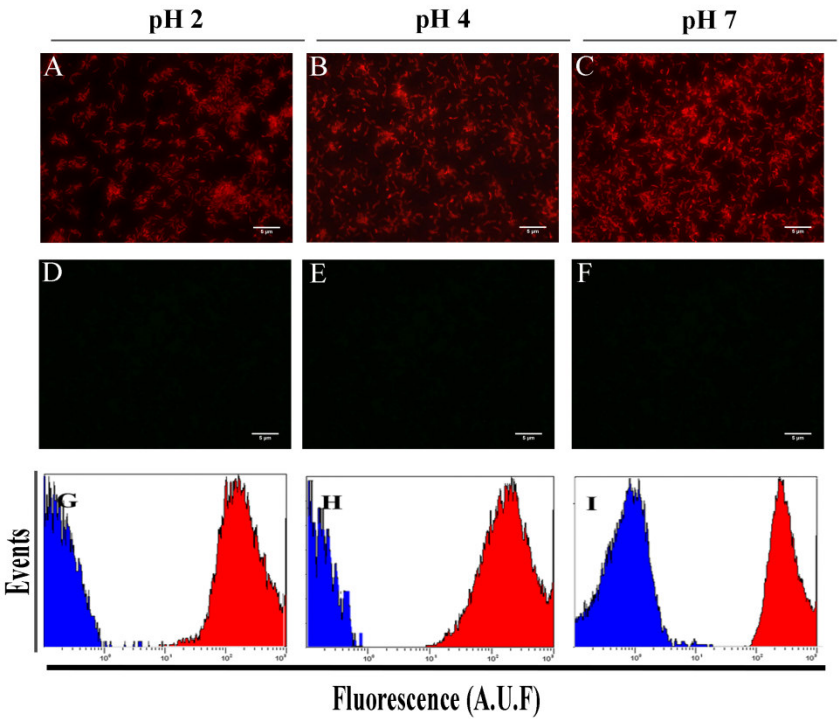

Figure 6.4 - Detection of *H. pylori* using the Cy3 HP_ LNA/2OMe _PS oligonucleotide probe in a smear of pure culture of *H. pylori* strain 26695 using simulated gastric juice by epifluorescent microscopy. A-F Smear of pure culture of *H. pylori* strain 26695 (ATCC 700392) observed by epifluorescent microscopy. A-C Experiment using 200 nM of Cy3 HP_ LNA/2OMe _PS oligonucleotide probe. D-F. Smears without probe were used as negative control. All images were taken at equal exposure times. Original magnification: 1000x**.** G-I. Relative fluorescence histograms of LNA-FISH targeting *H. pylori* in different pH for two different assays – Blue: negative control with no oligonucleotide probe; Red: sample. Scale bar = 5 µm.

All sensitivity and specificity studies demonstrated that the gastric juice does not interfere with the hybridization efficiency of the Cy3_HP_ LNA/2OMe _PS (Figure 6.5).

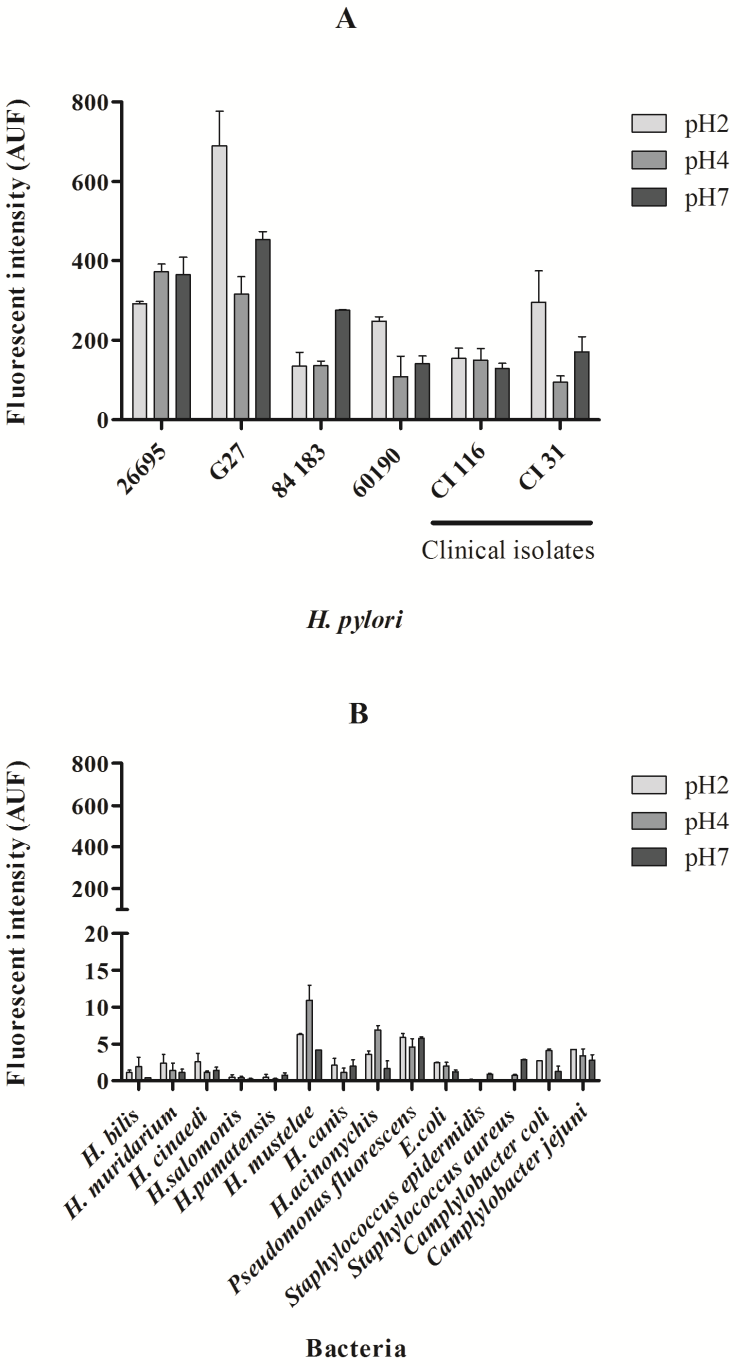

Figure 6.5 - Sensitivity and specificity studies performed with the HP_ LNA/2OMe _PS oligonucleotide probe using simulated gastric juice. A. Sensitivity test using different strains and clinical isolates of *H. pylori*. B. Specificity test using different species of Helicobacter and other bacteria.

6.3.4. Detection of H. pylori in infected gastric AGS cell line

In vivo H. pylori is found free in the gastric mucus, and also in close contact with epithelial cells [46,47]. A few *in vitro* studies have showed that *H. pylori* can be invasive and reside within the cytoplasmic vacuole of the infected cells [48-50]. Therefore, the hybridization of the Cy3_HP_ LNA/2OMe _PS probe was tested in AGS cells infected with *H. pylori* by confocal microscopy. The analysis of the confocal showed that the probe can still hybridize to *H. pylori* when it is adhered to the gastric cells, and even when a high concentration of bacteria is present (Figure 6.6A). It was also observed a low background of the confocal images obtained (Figure 6.6B) which is a fundamental feature in this type of studies, since background fluorescence emission is a significant drawback in *in vivo* assays [51]. In these studies, it was not observed any unspecific binding signal as observed in the control samples (only AGS cells) (Figure 6.6C).

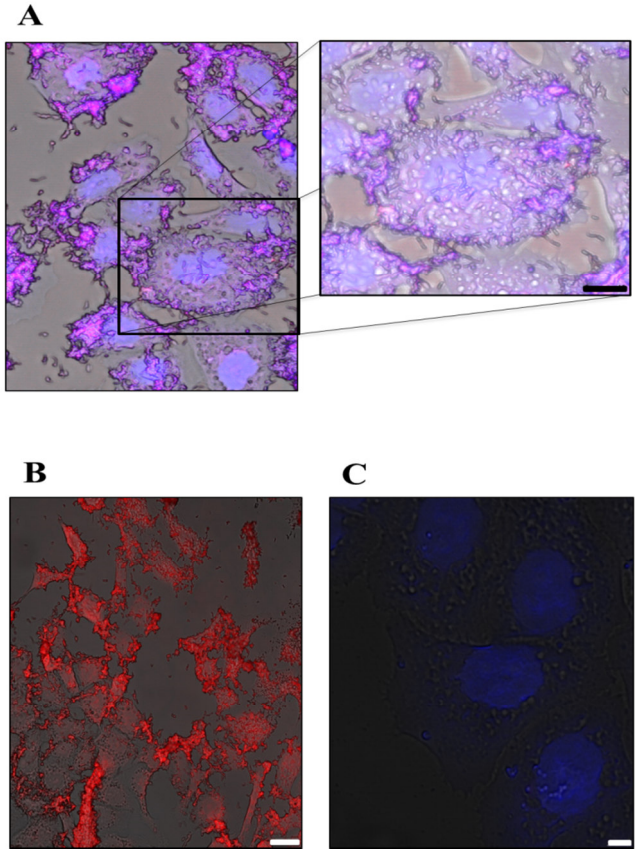

Figure 6. 6 - Confocal microscopy images of AGS cells infected with *H. pylori* 26695 strain. A. Detection of *H. pylori* by the Cy3_ HP_ LNA/2OMe _PS _oligonucleotide probe in infected epithelial cells. Channel red, DAPI and bright field were overlapping. Scale bar = 10µm B. Detection of *H. pylori* by Cy3_ HP_ LNA/2OMe _PS _oligonucleotide probe in co-infected cells and isolates bacteria. Channel red, and bright field were overlapping. Scale bar = 25µm C. Uninfected AGS cells stained with Cy3_ HP_ LNA/2OMe _PS _oligonucleotide probe and DAPI. Channel red, and bright field and DAPI were overlapping. Scale bar = 5µmRed: Cy3 fluorescence. Blue: DAPI staining to counterstain nuclei.

6.3.5. Toxicity studies

Although LNA modified oligonucleotides offer advantages for improved target specificity they can be hampered by toxicity in non-clinical studies [52,53]. Burdick *et al*. [54] have demonstrated that this toxicity is associated with some sequence motifs. Therefore, it has evaluated if the Cy3_HP_ LNA/2OMe _PS induces toxicity to gastric epithelial cells through viability and apoptosis assays.

The MTS assay was used to investigate the effect of the Cy3_ HP_ LNA/2OMe _PS on AGS cell viability at different confluences (50% and 100%). Treatment of AGS cells with the Cy3_ HP_ LNA/2OMe _PS at 200 nM did not result in a statistically significant decrease in proliferation for any of the confluences (Figure 6.7A). It was also tested the effect of the probe vehicle (hybridization buffer) on cell proliferation, and again no statistically significant differences were observed ($p>0.05$) relatively to the untreated cells.

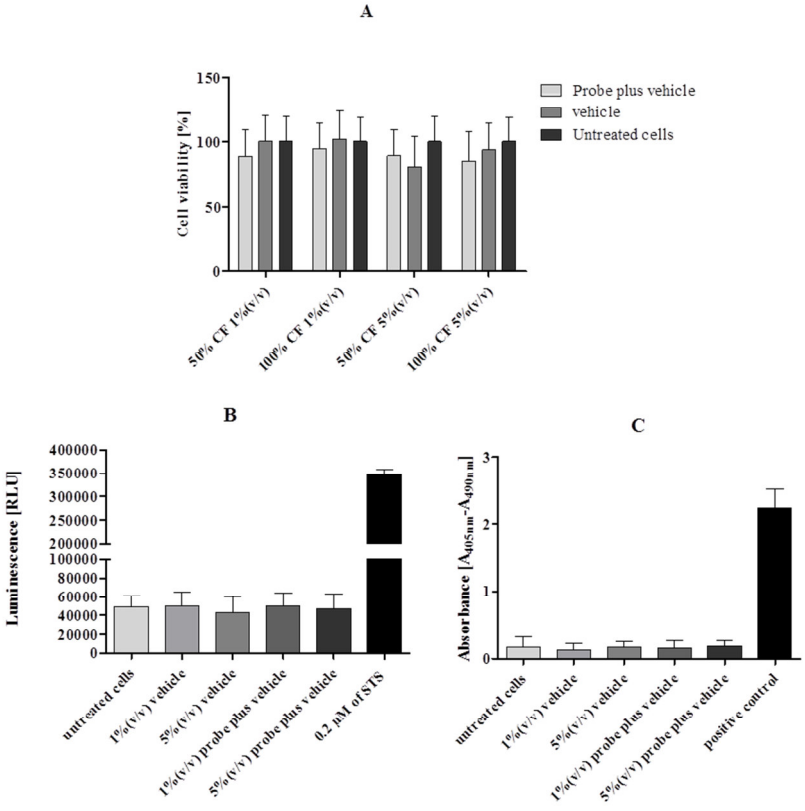

Figure 6.7 - Effect of the Cy3_ HP_ LNA/2OMe _PS oligonucleotide probe on viability (MTS assay, A) and cell death (apoptosis, B and C) of AGS cells. AGS cells were treated with 200 nM of Cy3_ HP_ LNA/2OMe _PS oligonucleotide probe for 24h. The results are the mean ± SEM of three independent experiments; *$p<0.05$ *vs* untreated cells by ANOVA. A) Cell viability was measured using MTS assay. B) Analysis of caspase-3/7 activity in AGS cells treated with Cy3_ HP_ LNA/2OMe _PS oligonucleotide probe. Staurosporine, STS, was a positive control of cell death. C) Effect of Cy3_ HP_ LNA/2OMe _PS oligonucleotide probe on the amount of DNA fragmentation in the cultured gastric cell line AGS. The level of apoptosis occurring with each treatment was determined by cell death ELISA^{Plus} kit.

Apoptosis is a natural form of cell death that induces condensation of the nucleoplasm and cytoplasm, blebbing of cytoplasmic membranes and fragmentation of the cell into apoptotic bodies that are recognized and eliminated by adjacent cells [55]. Since apoptosis is ultimately mediated by caspase 3 and caspase 7, a Caspase-Glo 3/7 Assay was conducted to determine whether the Cy3_ HP_ LNA/2OMe _PS activates the apoptotic pathway in probe-treated gastric cells. As depicted in Figure 6.7B, no statistically significant differences regarding activation of caspase 3 and 7 were observed between untreated cells and Cy3_ HP_ LNA/2OMe _PS-treated cells (24 h at 200 nM); the same was found for the vehicle in both volumes tested, which contrasts with staurosporine treatment (positive control for cell death) that induces activation of caspases 3 and 7. The Cell Death Detection^{Plus} system (Roche) was used as another technique to confirm these results (Figure 6.7C). Cy3_ HP_ LNA/2OMe _PS treatment of AGS cells did not induce cell death, as no significant increase in the ratio of DNA fragmentation was found in comparison to untreated cells. Additionally, no significant differences were observed between the vehicle (hybridization buffer) and untreated cells regarding the induction of DNA fragmentation.

6.4. Discussion

In this study it has tested a LNA probe using a non-toxic and simple FISH protocol as a potential novel technique for *in vivo* diagnosis of *H. pylori* infection. The presence of *H. pylori* was detected by FISH using *ex vivo* experiments with a specific molecular probe in conditions that mimic gastric environment. It was optimized a fast, simple and non-toxic FISH protocol and analyzed the efficiency, sensitivity and specificity of the probe in a range of pH and using a gastric simulated juice. An *in vitro* analysis of the probe toxicity in a gastric cell line was also performed. The main objective of this work is to build the knowledge and the necessary tools to detect *H. pylori* by FIVH which could provide spatial information on the localization of *H. pylori*. Such information is important in the clinic in order to perform a correct and fast diagnosis and to decide the best treatment for the infection.

The pH within the human stomach lumen varies between 1 to neutral after a meal, although in adults the luminal pH rarely exceeds 5.5 [56]. *H. pylori* uses this transmucus pH gradient for spatial mobility and orientation to reach zones where the pH is near neutral [57,58]. Therefore, pH conditions in the stomach may have a strong effect on the number of *H. pylori* cells present in the mucus layers *in vivo*. It was initially studied the behavior of the probe in a range of pH values using RSM as an experiment tool designer. The RSM approach has been used to determine the best conditions for a study

comprising two or more variables by calculating the combined effect of selected variables [59,60]. In Figure 6.1, the response surface shows the effect of the time of hybridization and pH on the fluorescence intensity. The result demonstrates that the response surface has a maximum point at a very low pH and around 50 min of hybridization. However, because the time component was not statistically significant ($p>0.05$), it can only prove that this probe can work effectively in an acid range of pH values. To the best of our knowledge, this is the first study where FISH is performed under extremely acid conditions. In the majority of the studies, experiments at pH values of 6.5–7.5 or even higher have been applied to obtain more stringent hybridization conditions [15,31].

Conventional hybridization time in FISH performed in bacteria requires 1.5 hours incubation with oligonucleotide probes [15,31]. The decrease of hybridization time has already been described for FISH in mammalian cells or at higher hybridization temperatures [32,61]. Here, it was showed that a 30 min hybridization step followed by a 15 min washing step could be used to obtain higher fluorescence intensities while maintaining the specificity and sensitivity desired (Figure 6.3 and 6.5).

The use of toxic and complex buffers is recurrent in FISH protocols. Although there are some studies which explore novel non-toxic hybridization buffers, some of the toxic reagents have not been removed [32,62,63]. PF is the most commonly used fixative in FISH experiments, however its well described toxicity and carcinogenic proprieties make it impossible to use in FIVH [64]. Some concerns also exist in terms of the effect of the cross-links created by PF with respect to the ability of the probes to recognize their targets [39,65]. In addition, it has been suggested that the RNA target may be degraded during the fixation process [66]. Even though it was able to remove PF from the permeabilization step, the presence of ethanol was shown to be essential for bacteria in suspension (Figure S2D) but not for attached bacteria (Figure S3). Because *H. pylori* in the human stomach can be found either adhered to the gastric epithelial cells [67] or in suspension in the gastric juice or mucus [68], permeabilization using ethanol was maintained in the protocol.

Other types of toxic compounds currently used in the hybridization buffer in FISH protocols are ion chelators, such as EDTA, which should be used in hybridization experiments with low salt buffers. In the case of high salt conditions, the need of using chelators has not been proven. [69]. It has also been reported that dextran sulfate (the exclusion agent most commonly used in FISH protocols) has only a minor, or no effect at all, in hybridization reactions with short probes [70]. However, the use of denaturant and salt is essential in FISH in order to obtain an efficient and specific hybridization reaction. The replacement of formamide by urea has been reported in some studies [17,62,63]. In

these results it was showed that the reduction of the concentration of urea in the hybridization solution from 4 M to 0.5 M does not affect the efficiency of the reaction (Figure S2C). The substitution of the salt solution used in the washing step by an aqueous buffer (Figure 6.2) or gastric juice (Figure 6.4) also had a positive outcome in the protocol. One possible reason could be the low stringency conditions that we used (low hybridization temperature and high salt concentration). It has generally been accepted that low-stringency hybridization corresponds to a stronger binding of probes to the targeted rRNA sites [71]. Therefore, higher temperatures appear to be less suitable for FISH in terms of obtaining a satisfactory fluorescence signal [38]. However, the absence of an washing step in the reaction leads to the decrease of the oligonucleotide probe specificity [37]. Specificity is one of the most important parameters in FISH methodology and is an essential property of nucleic acids [72]. In our studies we observed that the HP_ LNA/2OMe _PS has higher specificity when used with hybridization buffer (NaCl and urea). Some authors have reported that 2′OMe/LNA PS oligonucleotides have low specificity [73], but in our hands this probe presented very low or no binding to non-pylori bacteria and no binding to AGS cells under the conditions tested. These differences may be explained by the experimental conditions selected in each study.

Although it is already known that FAM is sensitive to low pH conditions [36,65], it was performed a chemical analysis after acid buffer treatments (HCl buffer, pH2 or pH4) and proved that this is not always true. However, when we use simulated gastric juice, the FISH results showed a huge decrease in the fluorescence intensity (Figure S5). Therefore, we can argue that the fluorescence of this fluorochrome could be rapidly quenched in the presence of pepsin. As a member of the aspartic protease family, pepsin has a significant role in drug research and in pharmacological studies [74], and we therefore can propose that this quenching mechanism could be the key to the decrease of fluorescence of the FAM_2′OMe/LNA PS in simulated gastric juice.

It is also known that oligonucleotides can have significant toxic effects in mammalian cells. Some of these effects can be related with certain chemical modifications or with the reagents used as vehicles of probe in the experiments [73]. For the following step in this study, it was investigated whether the Cy3_ HP_ LNA/2OMe _PS would induce toxicity in a gastric cell line, AGS, through viability and apoptosis analysis. Although it has been reported, in some studies, that all-phosphorothioate probes can induce toxicity [75], it was observed no significant toxicity under the conditions used (Figure 6.7). The HP_ LNA/2OMe _PS contains 2'OMe, which is a non-toxic, naturally occurring nucleic acid [76], and therefore it could reduce the toxicity of the probe. Other authors have reported minimal LNA toxicity in their studies [19,73,77]. Hepatoxicity is also reported in animals for

some LNA oligonucleotides [52,78], however, recently, Burdick *et al*., refers that the hepatoxicity of LNA oligonucleotides is associated with specific motifs [54]. LNA-based oligonucleotides have in fact advanced into phase 1 and 2 clinical studies, which also demonstrates the non-toxic character of some sequences [77,79].

In order to establish FIVH in the routine practice of clinical laboratories, several limitations have to be overcome in the future. First, although it was reduced the time needed to perform some of the FISH steps, the duration of the entire protocol is still too long. In fact, for FIVH in diagnosis, a further decrease in hybridization time may be beneficial for the patient. Therefore, a new system capable of delivering directly the probe, avoiding the permeabilization step and speeding up the hybridization period, might be useful. Second, FIVH is only possible if confocal laser endomicroscopy is used, and is hence limited to certain areas of the human body. However, despite of the difficulties which have to be overcome, this study provides a technological advance not only for current FISH methodologies but also towards the development of FIVH for the diagnosis of pathogens and to assess disturbances in the microbiome.

6.5. Conclusion

In this study it was developed a FISH protocol that might be used directly in gastric human mucosa using a *H. pylori* specific LNA-based oligonucleotide probe that has an excellent performance at 37 ℃ as demonstrated in the Chapter V. Therefore, it was reported the development of a FISH-based method that can be carried out at 37 ℃ and at a large range of pH (2-7), using only ethanol as a fixative agent for 15 min, and a hybridization solution consisting of 0.9 M NaCl and 0.5 M urea. In this method, the washing step can be performed by the gastric mucus that is naturally present in the stomach. This final method proved to be non-toxic, while retaining the specificity and sensitivity towards *H. pylori*.

This promising new method can be used *in vivo* in future clinical applications, in combination with a confocal laser endomicroscope for *H. pylori* detection. It also provides a powerful new approach for the diagnosis of microorganisms in general. Future work will focus on using animal models as an *in vivo* proof-of-concept for FIVH.

6.6. References

1. Khan A.A., Shrivastava A., Khurshid M. Normal to cancer microbiome transformation and its implication in cancer diagnosis. Biochim Biophys Acta (2012); 1826: 331-337.
2. Olfat F.O., Naslund E., Freedman J., Boren T., Engstrand L. Cultured human gastric explants: a model for studies of bacteria-host interaction during conditions of experimental Helicobacter pylori infection. J Infect Dis (2002); 186: 423-427.
3. Suerbaum S., Michetti P. Helicobacter pylori infection. N Engl J Med (2002); 347: 1175-1186.
4. Forman D. The prevalence of Helicobacter pylori infection in gastric cancer. Aliment Pharmacol Ther (1995); 9 Suppl 2: 71-76.
5. Yilmaz O., Demiray E. Clinical role and importance of fluorescence in situ hybridization method in diagnosis of H pylori infection and determination of clarithromycin resistance in H pylori eradication therapy. World J Gastroenterol (2007); 13: 671-675.
6. Vinette K.M., Gibney K.M., Proujansky R., Fawcett P.T. Comparison of PCR and clinical laboratory tests for diagnosing H. pylori infection in pediatric patients. BMC Microbiol (2004); 4: 5.
7. Shukla R., Abidi W.M., Richards-Kortum R., Anandasabapathy S. Endoscopic imaging: How far are we from real-time histology? World J Gastrointest Endosc (2011); 3: 183-194.
8. McNulty C.A., Lehours P., Megraud F. Diagnosis of Helicobacter pylori Infection. Helicobacter (2011); 16 Suppl 1: 10-18.
9. Karstensen J.G., Klausen P.H., Saftoiu A., Vilmann P. Molecular confocal laser endomicroscopy: A novel technique for cellular characterization of gastrointestinal lesions. World J Gastroenterol (2014); 20: 7794-7800.
10. Neumann H., Kiesslich R., Wallace M.B., Neurath M.F. Confocal laser endomicroscopy: technical advances and clinical applications. Gastroenterology (2010); 139: 388-392, 392 e381-382.
11. Wong Kee Song L.M., Wilson B.C. Endoscopic detection of early upper GI cancers. Best Pract Res Clin Gastroenterol (2005); 19: 833-856.
12. Kiesslich R., Neurath M.F. Endoscopic confocal imaging. Clin Gastroenterol Hepatol (2005); 3: S58-60.
13. Gozzetti A., Le Beau M.M. Fluorescence in situ hybridization: uses and limitations. Semin Hematol (2000); 37: 320-333.
14. Cerqueira L., Fernandes R.M., Ferreira R.M., Oleastro M., Carneiro F., Brandão C., et al. Validation of a Fluorescence In Situ Hybridization Method Using Peptide Nucleic Acid Probes for Detection of Helicobacter pylori Clarithromycin Resistance in Gastric Biopsy Specimens. Journal of Clinical Microbiology (2013); 51: 1887-1893.
15. Almeida C., Azevedo N.F., Fernandes R.M., Keevil C.W., Vieira M.J. Fluorescence In Situ Hybridization Method Using a Peptide Nucleic Acid Probe for Identification of Salmonella spp. in a Broad Spectrum of Samples. Applied and Environmental Microbiology (2010); 76: 4476-4485.

16. Bergman J.J., Tytgat G.N. New developments in the endoscopic surveillance of Barrett's oesophagus. Gut (2005); 54 Suppl 1: i38-42.
17. Fontenete S., Guimaraes N., Leite M., Figueiredo C., Wengel J., Azevedo N.F. Hybridization-Based Detection of Helicobacter pylori at Human Body Temperature Using Advanced Locked Nucleic Acid (LNA) Probes. PLoS One (2013); 8: e81230.
18. Kurreck J., Wyszko E., Gillen C., Erdmann V.A. Design of antisense oligonucleotides stabilized by locked nucleic acids. Nucleic Acids Res (2002); 30: 1911-1918.
19. Wahlestedt C., Salmi P., Good L., Kela J., Johnsson T., Hokfelt T., et al. Potent and nontoxic antisense oligonucleotides containing locked nucleic acids. Proc Natl Acad Sci U S A (2000); 97: 5633-5638.
20. Crinelli R., Bianchi M., Gentilini L., Magnani M. Design and characterization of decoy oligonucleotides containing locked nucleic acids. Nucleic Acids Res (2002); 30: 2435-2443.
21. Crinelli R., Bianchi M., Gentilini L., Palma L., Magnani M. Locked nucleic acids (LNA): versatile tools for designing oligonucleotide decoys with high stability and affinity. Curr Drug Targets (2004); 5: 745-752.
22. Sun Z., Xiang W., Guo Y., Chen Z., Liu W., Lu D. Inhibition of hepatitis B virus (HBV) by LNA-mediated nuclear interference with HBV DNA transcription. Biochem Biophys Res Commun (2011); 409: 430-435.
23. Majlessi M., Nelson N.C., Becker M.M. Advantages of 2'-O-methyl oligoribonucleotide probes for detecting RNA targets. Nucleic Acids Res (1998); 26: 2224-2229.
24. Finotto S., Buerke M., Lingnau K., Schmitt E., Galle P.R., Neurath M.F. Local administration of antisense phosphorothioate oligonucleotides to the c-kit ligand, stem cell factor, suppresses airway inflammation and IL-4 production in a murine model of asthma. J Allergy Clin Immunol (2001); 107: 279-286.
25. Hildner K.M., Schirmacher P., Atreya I., Dittmayer M., Bartsch B., Galle P.R., et al. Targeting of the transcription factor STAT4 by antisense phosphorothioate oligonucleotides suppresses collagen-induced arthritis. J Immunol (2007); 178: 3427-3436.
26. Guga P., Koziolkiewicz M. Phosphorothioate nucleotides and oligonucleotides - recent progress in synthesis and application. Chem Biodivers (2011); 8: 1642-1681.
27. Heemskerk H.A., de Winter C.L., de Kimpe S.J., van Kuik-Romeijn P., Heuvelmans N., Platenburg G.J., et al. In vivo comparison of 2'-O-methyl phosphorothioate and morpholino antisense oligonucleotides for Duchenne muscular dystrophy exon skipping. J Gene Med (2009); 11: 257-266.
28. Ferreira R.M., Machado J.C., Letley D., Atherton J.C., Pardo M.L., Gonzalez C.A., et al. A novel method for genotyping the Helicobacter pylori vacA intermediate region directly in gastric biopsy specimens. J Clin Microbiol (2012); 50: 3983-3989.
29. Myers R. H. M.D.C., Anderson-Cook C. M. Response Surface Methodology: Process and Product Optimization Using Designed Experiments, 3rd Edition(2009); Statistics WSiPa, editor. Wiley.

30. Santos R.S., Guimarães N., Madureira P., Azevedo N.F. Optimization of a peptide nucleic acid fluorescence in situ hybridization (PNA-FISH) method for the detection of bacteria and disclosure of a formamide effect. Journal of Biotechnology (2014); 187: 16-24.
31. Guimaraes N., Azevedo N.F., Figueiredo C., Keevil C.W., Vieira M.J. Development and application of a novel peptide nucleic acid probe for the specific detection of Helicobacter pylori in gastric biopsy specimens. J Clin Microbiol (2007); 45: 3089-3094.
32. Matthiesen S.H., Hansen C.M. Fast and Non-Toxic *In Situ* Hybridization without Blocking of Repetitive Sequences. PLoS One (2012); 7: e40675.
33. Bucker R., Azevedo-Vethacke M., Groll C., Garten D., Josenhans C., Suerbaum S., et al. Helicobacter pylori colonization critically depends on postprandial gastric conditions. Sci Rep (2012); 2: 994.
34. Azevedo N., Vieira MJ., Keevil CW.Development of peptide nucleic acid probes to detect Helicobacter pylori in diverse species potable water biofilms. In: McBain A. AD, Brading M., Rickard A., Verran J. , Walker J. , editor. Biofilm Communities: Order from Chaos? (2003): BioLine. pp. 105-112.
35. Ezzat K., Zaghloul E.M., El Andaloussi S., Lehto T., El-Sayed R., Magdy T., et al. Solid formulation of cell-penetrating peptide nanocomplexes with siRNA and their stability in simulated gastric conditions. J Control Release (2012); 162: 1-8.
36. Kenzaka T., Yamaguchi N., Tani K., Nasu M. rRNA-targeted fluorescent in situ hybridization analysis of bacterial community structure in river water. Microbiology (1998); 144 (Pt 8): 2085-2093.
37. Pernthaler J., Glöckner F.-O., Schönhuber W., Amann R.Fluorescence in situ hybridization (FISH) with rRNA-targeted oligonucleotide probes. In: John HP, editor. Methods in Microbiology. (2001): Academic Press. pp. 207-226.
38. Tang Y.Z., Gin K.Y., Lim T.H. High-temperature fluorescent in situ hybridization for detecting Escherichia coli in seawater samples, using rRNA-targeted oligonucleotide probes and flow cytometry. Appl Environ Microbiol (2005); 71: 8157-8164.
39. Shaffer S.M., Wu M.T., Levesque M.J., Raj A. Turbo FISH: a method for rapid single molecule RNA FISH. PLoS One (2013); 8: e75120.
40. Bouvier T., Del Giorgio P.A. Factors influencing the detection of bacterial cells using fluorescence in situ hybridization (FISH): A quantitative review of published reports. FEMS Microbiol Ecol (2003); 44: 3-15.
41. Magalhaes A., Reis C.A. Helicobacter pylori adhesion to gastric epithelial cells is mediated by glycan receptors. Braz J Med Biol Res (2010); 43: 611-618.
42. Wadstrom T., Hirmo S., Nilsson B. Biochemical aspects of H. pylori adhesion. J Physiol Pharmacol (1997); 48: 325-331.
43. Wessendorf M.W., Brelje T.C. Which Fluorophore Is Brightest - a Comparison of the Staining Obtained Using Fluorescein, Tetramethylrhodamine, Lissamine Rhodamine, Texas Red, and Cyanine 3.18. Histochemistry (1992); 98: 81-85.

44. You Y., Tataurov A.V., Owczarzy R. Measuring thermodynamic details of DNA hybridization using fluorescence. Biopolymers (2011); 95: 472-486.
45. Seidel C.A.M., Schulz A., Sauer M.H.M. Nucleobase-Specific Quenching of Fluorescent Dyes. 1. Nucleobase One-Electron Redox Potentials and Their Correlation with Static and Dynamic Quenching Efficiencies. The Journal of Physical Chemistry (1996); 100: 5541-5553.
46. Chung H.J., Reiner T., Budin G., Min C., Liong M., Issadore D., et al. Ubiquitous detection of gram-positive bacteria with bioorthogonal magnetofluorescent nanoparticles. ACS Nano (2011); 5: 8834-8841.
47. Noach L.A., Rolf T.M., Tytgat G.N. Electron microscopic study of association between Helicobacter pylori and gastric and duodenal mucosa. J Clin Pathol (1994); 47: 699-704.
48. Chu Y.T., Wang Y.H., Wu J.J., Lei H.Y. Invasion and multiplication of Helicobacter pylori in gastric epithelial cells and implications for antibiotic resistance. Infect Immun (2010); 78: 4157-4165.
49. Amieva M.R., Salama N.R., Tompkins L.S., Falkow S. Helicobacter pylori enter and survive within multivesicular vacuoles of epithelial cells. Cell Microbiol (2002); 4: 677-690.
50. Dubois A., Boren T. Helicobacter pylori is invasive and it may be a facultative intracellular organism. Cell Microbiol (2007); 9: 1108-1116.
51. Okamoto A. ECHO probes: a concept of fluorescence control for practical nucleic acid sensing. Chem Soc Rev (2011); 40: 5815-5828.
52. Swayze E.E., Siwkowski A.M., Wancewicz E.V., Migawa M.T., Wyrzykiewicz T.K., Hung G., et al. Antisense oligonucleotides containing locked nucleic acid improve potency but cause significant hepatotoxicity in animals. Nucleic Acids Res (2007); 35: 687-700.
53. Hagedorn P.H., Yakimov V., Ottosen S., Kammler S., Nielsen N.F., Hog A.M., et al. Hepatotoxic potential of therapeutic oligonucleotides can be predicted from their sequence and modification pattern. Nucleic Acid Ther (2013); 23: 302-310.
54. Burdick A.D., Sciabola S., Mantena S.R., Hollingshead B.D., Stanton R., Warneke J.A., et al. Sequence motifs associated with hepatotoxicity of locked nucleic acid--modified antisense oligonucleotides. Nucleic Acids Res (2014); 42: 4882-4891.
55. Alberts B. J.A., Lewis J., Raff M., Roberts K., Walter P. Molecular Biology of the Cell. 4th edition. Programmed Cell Death (Apoptosis).(2002): New York:: Garland Science.
56. Fimmel C.J., Etienne A., Cilluffo T., von Ritter C., Gasser T., Rey J.P., et al. Long-term ambulatory gastric pH monitoring: validation of a new method and effect of H2-antagonists. Gastroenterology (1985); 88: 1842-1851.
57. Schreiber S., Konradt M., Groll C., Scheid P., Hanauer G., Werling H.O., et al. The spatial orientation of Helicobacter pylori in the gastric mucus. Proc Natl Acad Sci U S A (2004); 101: 5024-5029.
58. Schreiber S., Bucker R., Groll C., Azevedo-Vethacke M., Garten D., Scheid P., et al. Rapid loss of motility of Helicobacter pylori in the gastric lumen in vivo. Infect Immun (2005); 73: 1584-1589.

59. Farooq Anjum M., Tasadduq I., Al-Sultan K. Response surface methodology: A neural network approach. European Journal of Operational Research (1997); 101: 65-73.
60. Myers RH M.D., Anderson-Cook CM Response surface methodology: Process and product optimization using designed experiments(2009): Wiley.
61. Markey F.B., Ruezinsky W., Tyagi S., Batish M. Fusion FISH imaging: single-molecule detection of gene fusion transcripts in situ. PLoS One (2014); 9: e93488.
62. Lawson T.S., Connally R.E., Vemulpad S., Piper J.A. Dimethyl formamide-free, urea-NaCl fluorescence in situ hybridization assay for Staphylococcus aureus. Lett Appl Microbiol (2012); 54: 263-266.
63. Soe M.J., Moller T., Dufva M., Holmstrom K. A sensitive alternative for microRNA in situ hybridizations using probes of 2'-O-methyl RNA + LNA. J Histochem Cytochem (2011); 59: 661-672.
64. de Groot A., Geier J., Flyvholm M.A., Lensen G., Coenraads P.J. Formaldehyde-releasers: relationship to formaldehyde contact allergy. Metalworking fluids and remainder. Part 1. Contact Dermatitis (2010); 63: 117-128.
65. Moralli D., Monaco Z.L. Simultaneous Detection of FISH Signals and Bromo-Deoxyuridine Incorporation in Fixed Tissue Cultured Cells. PLoS One (2009); 4: e4483.
66. Masuda N., Ohnishi T., Kawamoto S., Monden M., Okubo K. Analysis of chemical modification of RNA from formalin-fixed samples and optimization of molecular biology applications for such samples. Nucleic Acids Res (1999); 27: 4436-4443.
67. Backert S., Clyne M., Tegtmeyer N. Molecular mechanisms of gastric epithelial cell adhesion and injection of CagA by Helicobacter pylori. Cell Commun Signal (2011); 9: 28.
68. Celli J.P., Turner B.S., Afdhal N.H., Keates S., Ghiran I., Kelly C.P., et al. Helicobacter pylori moves through mucus by reducing mucin viscoelasticity. Proc Natl Acad Sci U S A (2009); 106: 14321-14326.
69. Wetmur J.G. Hybridization and renaturation kinetics of nucleic acids. Annu Rev Biophys Bioeng (1976); 5: 337-361.
70. Meinkoth J., Wahl G. Hybridization of nucleic acids immobilized on solid supports. Anal Biochem (1984); 138: 267-284.
71. Fuchs B.M., Wallner G., Beisker W., Schwippl I., Ludwig W., Amann R. Flow cytometric analysis of the in situ accessibility of Escherichia coli 16S rRNA for fluorescently labeled oligonucleotide probes. Appl Environ Microbiol (1998); 64: 4973-4982.
72. Zhang D.Y., Chen S.X., Yin P. Optimizing the specificity of nucleic acid hybridization. Nat Chem (2012); 4: 208-214.
73. Lennox K.A., Owczarzy R., Thomas D.M., Walder J.A., Behlke M.A. Improved Performance of Anti-miRNA Oligonucleotides Using a Novel Non-Nucleotide Modifier. Mol Ther Nucleic Acids (2013); 2: e117.
74. Lian S., Wang G., Zhou L., Yang D. Fluorescence spectroscopic analysis on interaction of fleroxacin with pepsin. Luminescence (2013); 28: 967-972.

75. Levin A.A. A review of the issues in the pharmacokinetics and toxicology of phosphorothioate antisense oligonucleotides. Biochim Biophys Acta (1999); 1489: 69-84.
76. Behlke M.A. Chemical modification of siRNAs for in vivo use. Oligonucleotides (2008); 18: 305-319.
77. Hildebrandt-Eriksen E.S., Aarup V., Persson R., Hansen H.F., Munk M.E., Orum H. A locked nucleic acid oligonucleotide targeting microRNA 122 is well-tolerated in cynomolgus monkeys. Nucleic Acid Ther (2012); 22: 152-161.
78. Stanton R., Sciabola S., Salatto C., Weng Y., Moshinsky D., Little J., et al. Chemical modification study of antisense gapmers. Nucleic Acid Ther (2012); 22: 344-359.
79. Lanford R.E., Hildebrandt-Eriksen E.S., Petri A., Persson R., Lindow M., Munk M.E., et al. Therapeutic silencing of microRNA-122 in primates with chronic hepatitis C virus infection. Science (2010); 327: 198-201.

Chapter VII

Fluorescence in vivo hybridization (FIVH) for detection of Helicobacter pylori infection in a C57BL/6 mouse model

Fluorescence *in vivo* hybridization (FIVH) for detection of Helicobacter pylori infection in a C57BL/6 mouse model

Fontenete S.[1,2,3,4,5*], Leite M.[2,3],Cappoen D.[6], Santos R[1,2,3]., Figueiredo C.[2,3,7], Wengel J.[4], Cos P.[6], Azevedo N.F.[1]

[1] LEPABE , Laboratory for Process Engineering, Environment, Biotechnology and Energy, Faculty of Engineering, University of Porto, Porto, Portugal; [2] i3S, Instituto de Investigação e Inovação em Saúde, Universidade do Porto, Porto, Portugal , [3] IPATIMUP, Institute of Molecular Pathology and Immunology of the University of Porto, Porto, Portugal; [4] Nucleic Acid Center, Department of Physics, Chemistry and Pharmacy, University of Southern Denmark, Odense M, Denmark;[5] ICBAS, Institute of Biomedical Sciences Abel Salazar, University of Porto, Porto, Portugal; [6] Laboratory of Microbiology, Parasitology and Hygiene (LMPH), Faculty of Pharmaceutical, Biomedical and Veterinary Sciences, University of Antwerp, Antwerp, Belgium; [7] FMUP, Faculty of Medicine of the University of Porto University, Porto, Portugal.

Abstract

Purpose: *Helicobacter pylori* (*H. pylori*) are gram negative bacteria that chronically infect the human stomach of approximately 50% of the human population. *H. pylori* detection is usually based on invasive methods that include endoscopy for collection of a biopsy that is further used for histopathological examination, culture, or polymerase chain reaction (PCR)-based detection. In this study, we applied fluorescence *in vivo* hybridization (FIVH) using locked nucleic acid (LNA) probes targeting the bacterial ribosomal RNA (rRNA) gene for *in vivo* detection of *H. pylori* infecting the C57BL/6 mouse model. This pilot study sets the ground for the use of FIVH for *in vivo* detection of *H. pylori* in infected individuals.
Procedures: A previously designed Cy3_HP_LNA/2OMe_PS probe, complementary to a sequence of the *H. pylori* 16S rRNA gene, was used to perform FIVH in C57BL/6 mice infected with *H. pylori* SS1. First, the potential cytotoxicity and genotoxicity of the probe was assessed by commercial assays. Further, the performance of the probe for detecting *H. pylori* at different pH conditions was tested *in vitro*, using FISH. Finally, the efficiency of FIVH to detect *H. pylori* SS1 strain in C57BL/6 infected mice was evaluated *ex vivo* in mucus samples, and in cryosections and paraffin-embedded sections of the mice glandular stomach by epifluorescence and confocal microscopy.
Results: *H. pylori SS1* strain infecting C57BL/6 mice was successful detected by the Cy3_HP_LNA/2OMe_PS probe in the mucus, attached to gastric epithelial cells and colonizing the gastric pits. The specificity of the probe for *H. pylori* was confirmed by microscopy. Nonspecific binding was not observed in the control non-infected mice groups.
Conclusions: In the future this methodology can be used in combination with a confocal laser endomicroscope for *in vivo* diagnosis of *H. pylori* infection using fluorescent LNA probes, which would be helpful to obtain an immediate diagnosis.

Keywords: Fluorescence *in vivo* hybridization (FIVH), locked nucleic acid, *Helicobacter pylori*, *in vivo* diagnostics.

7.1. Introduction

Helicobacter pylori (*H. pylori*) colonizes the human gastric epithelium, representing the most common infection worldwide [1]. This infection increases the risk for peptic ulcer disease, distal gastric adenocarcinoma and mucosa-associated lymphoid tissue lymphoma [1,2]. Due to its important role in gastric cancer development, *H. pylori* was recognised as a carcinogen (class 1) by the World Health Organization [3]. Therefore, a rapid, accurate and early diagnosis of *H. pylori* infection is crucial not only for individual patient management but also to identify individuals at high risk of developing gastric cancer. Currently, a number of diagnostic methods are available to detect *H. pylori* [4]. Upper endoscopy allows the collection of gastric biopsy specimens used to identify *H. pylori* by histology, culture, rapid urease tests, and PCR-based methods [3]. Therefore, and with the exception of rapid urease tests, the diagnostic result is not immediately obtained after endoscopy, requiring time and an experienced laboratory.

Confocal laser endomicroscopy (CLE) allows *in vivo* visualization and analysis of epithelial mucosa using 1000x magnification [5]. Some studies have suggested that CLE images of colonic mucosa have the potential to substitute conventional histological diagnostics [5-7]. However, only unspecific stains, such as fluorescein sodium and acriflavine have been used for *in vivo* histology of the mucosal layer [8-10]. For this reason, only indirect evidence of the presence of *H. pylori* infection can be observed [11]. Consequently, a precise and specific identification of this bacterium is not yet possible using this method.

Fluorescence *in vivo* hybridization (FIVH) can be applied in detecting DNA or RNA sequences in living eukaryotic cells [12]. Nevertheless, to the best of our knowledge this method was never employed to detect microorganisms directly in the human body, possibly due to the peptidoglycan cell wall of the microorganisms that hinders the entry of the probes into the cell. Nucleic acid mimics such as peptide nucleic acid (PNA), locked nucleic acid (LNA) and 2'-O-methly-RNA (2OMe) have been studied as diagnostic probes of infectious diseases and are capable of replacing conventional DNA or RNA probes [13]. The key advantages of these mimics are the higher stability *in vivo* [14-16] and the more favorable diffusion and hybridization properties than the corresponding unmodified DNA or RNA probes [17,18]. However, the unsolved question of how these types of probes can be used to detect clinically relevant bacteria remains. The different approaches that have been undertaken to develop *in vivo* diagnostic methods mostly rely on the use of non-specific stains or label oligonucleotides with radioactive isotopes such as halogens [19-21].

In Chapter V and VI, it was reported the development of an LNA probe (HP_LNA/2OMe_PS) that specifically detects *H. pylori* in biopsies of infected patients, and

in experimental conditions of extreme acid pH and at 37 °C [22,23]. Still, the performance of this probe for *H. pylori in vivo* detection remained unknown.

In this Chapter, it is provided the first FIVH protocol applied to an experimental mouse model of *H. pylori* infection, that successfully enables the detection of both free-swimming bacteria in the protective mucus layer that overlays the stomach surface and bacteria colonizing gastric epithelial cells.

7.2. Materials and Methods

7.2.1. Oligonucleotide synthesis

The sequence of the probe was selected and synthesized based on the parameters described in our previous studies [22,23] (Table 7.1).

Table 7.1 - Designation and sequence of probe containing locked nucleic acid (LNA; with L superscript) and 2'-O-methyl-RNA (2'-OMe; in boldface) nucleotide monomers. Cy3_HP_LNA/2OMe_PS is a phosphorothioate oligomer (PS backbones), Cy3 (Cyanine)

Designation	**Sequence (10-mer)**
Cy3 HP_ LNA/2OMe _PS	5'- Cy3 G^{L}**AC**T^{L}**AA**G^{L}**CC**C^{L}-3'

7.2.2. Cell proliferation assay

The human gastric epithelial cell line AGS (ATCC® CRL-1739) was cultured in RPMI medium 1640 Glutamax I (Gibco, Invitrogen, Grand Island, NY, USA) supplemented with 10% (v/v) fetal bovine serum (FBS, HyClone, Thermo Fisher Scientific, Inc, UK) and 1% (v/v) Penicillin/Streptomycin (Gibco) at 37 °C in a humidified 5% CO_2 atmosphere. Cells were seeded at 1.6 x 10^5 cells/well in a 96-well plate. After overnight culture, media was changed and cells were incubated with predetermined concentrations (0.4 µM to 2 µM) of Cy3_HP_ LNA/2OMe _PS probe diluted in vehicle (0.5 M urea and 900 mM NaCl) or only with the vehicle, for 24 h. Cell viability was assessed by CellTilter 96® Aqueous One Solution Cell Proliferation Assay (Promega Corporation, Madison, WI), according to the manufacturer's instructions. Untreated cells served as a negative control. The experiments were performed in triplicate.

7.2.3. VITOTOX® Assay

Briefly, the VITOTOX® model from gentaur makes use of two recombinant *Salmonella typhymurium* reporter strains, the TA104 recN2-4 (Genox strain) and TA104 pr1 (Cytox strain). The Cytox strain expresses bacterial luciferase from Vibrio fischeri, encoded episomal. A reduction in the signal/noise of the luminescent signal indicates cytotoxicity and an increase indicates interferences of the compound with the luminescent signal itself. The Genox strain carries an integrated lux operon from Vibrio fischeri under transcriptional control of the recN promoter. When a compound is genotoxic, transcription of the DNA repair mechanism will lead to an increase of the luminescent signal. Addition of rat liver S9 fraction is used to mimic the mammalian metabolic conditions so that the mutagenic potential of metabolites formed by a parent compound in the hepatic system can be assessed [24-26]. The luminescence is measured for 4 hours with a 5 minute interval period in a plate-reading GloMax® Discover System GM3000 luminometer (Promega, Madison, USA) and generally, when the signal to noise ratio in the cytox strain model is reduced below 0.8, the compound is regarded as cytotoxic for *S. typhymurium* and the genotoxicity cannot be studied. When the signal to noise ratio in the genox strain model is above 1.5, the DNA repair mechanism is activated by the cell as an early respons to genotoxicity by the compound. The concentrations of Cy3 HP_LNA/2OMe_PS probe tested in this assay were of 0.04, 0.08, 0.2, 0.4, 1 and 2 µM. The compound 4-nitroquinoline-oxide (4-NQO) (a direct acting base-altering mutagen) and benzo(α)pyrene (BaP) (indirect mutagen which requires metabolic activation by S9 mix), were used as positive controls. The experiments were performed in triplicate.

7.2.4. Bacteria and growth conditions

The mouse-adapted *Helicobacter pylori* Sydney strain 1 (SS1), originally described by Lee *et al.*, [27], was kindly provided by Sara Lindén (Gothenburg University, Sweden). *H. pylori* SS1 was routinely cultured for 48 hours on Tryptic Soy Agar (TSA) plates (Lab M Limited, Lancashire, UK) medium, supplemented with 5% sheep blood (Oxoid, Cambridge, UK) at 37 °C under micro-aerophilic conditions (5% O_2, 10% CO_2, 85% N_2), generated by Whitley H35 Hypoxystation (Don Whitley, West Yorkshire, UK). For liquid cultures, bacteria were resuspended in Tryptic Soy Broth (TSB) (Lab M Limited, Lancashire, UK) containing 10% of fetal calf serum (FCS) (Invitrogen, Ghent, Belgium) and grown overnight at 37 °C, with shaking under microaerophilic conditions.

7.2.5. Fluorescence in situ hybridization on slides

To determine if the probe Cy3-labeled HP_LNA/2OMe_PS detect the *H. pylori* SS1 strain, a theoretical evaluation was performed against the 16 S rRNA from this bacterial strain, using BLAST software (http://blast.ncbi.nlm.nih.gov/Blast.cgi). Then, the hybridization of the Cy3 HP_LNA/2OMe_PS against *H. pylori SS1* was studied using LNA-FISH protocol on glass slides as previously described in Chapter VI, with few modifications. Briefly, 20 µL of *H. pylori SS1* liquid cultures were spread onto glass slides and the smears were allowed to air dry. The hybridization was performed using 20 µL of hybridization buffer with 0.2 µM of the probe, which covered each smear individually. Three different hybridization buffers were tested at different pH (2, 4, and 7), containing 0.5M urea (BHD Prolabo, Haasrode, Belgium), 900 mM NaCl (Panreac, Illinois, USA) and different buffer solutions to keep the desired pH (pH2:KCl-HCl, pH4:phosphate-citrate, pH7:Tris-HCl buffer). Smears were covered with coverslips and incubated for 30 min at 37 °C. Slides were subsequently washed in a gastric simulated juice that contains pepsin for 15 min at 37 °C and then, the slides were allowed to air dry. All experiments were performed in triplicate and for each experiment a negative control (without a probe) was included. For image acquisition a Carl Zeiss inverted Axiovert fluorescence microscope (Carl Zeiss, Jena, Germany) was used. Cy3-labeling was excited by using a 565 nm laser; the exposure time was fixed for all preparations.

7.2.6. Animals

Female specific-pathogen-free (SPF) from the inbred C57BL/6 (C57BL/6JRj strain) mice (n=24) were purchased from Janvier LABS (Le Genest-St-Isle, France). Animals were housed in 332 × 150 × 130 cm (3 mice) or 382 × 220 × 150 cm (6 mice) autoclaved Micro-Isolater clear plastic cages, with a ventilation rate of 10 to 15 air changes per hour (ACH), at 20 °C, 50% humidity and under a light/dark cycle of 12/12 hours, with free access to standard rodent food pellets (Carfil Quality, Turnhout, Belgium) and water. Cages were lined with B 8/20 chips for bedding material, and with cardboard tubes and shredded paper as nesting material for environmental enrichment. Animals were handled by trained and experienced personnel for routine maintenance and experimental procedures to reduce stress. To minimize variation in the gut microflora, all animals within an experimental cohort were bred in the same room and housed on the same rack in a specific pathogen-free barrier facility. All animal experimentation was performed according to institutional guidelines and with approval of the local institute review board, in accordance to the European Directive 2010/63/EU regulations.

7.2.7. Infection of mice with H. pylori SS1

Female SPF C57BL/6 mice were randomly allocated to 6 groups of 3 to 6 animals (Figure 7.1A). Mice were inoculated intragastrically with two doses of 0.1 mL TSB containing $1x10^9$ H. pylori CFU/mL by oral gavage (with polyethylene catheters attached to 1 mL disposable syringes, Biotrol, Paris, France). The administration was performed at two time points, with an interval of one hour, in two consecutive days. In the control groups, mice were given TSB alone. Mice were fasted from 4 hours before infection until four hours after oral gavage. Mice were sacrificed by cervical dislocation, 2 weeks post-infection for collection of stomach and detection of H. pylori by FIVH.

7.2.8. FIVH procedure and assessment in mice

FIVH procedure was performed 15 days post-infection (Figure 7.1A). Cy3-labeled HyP_LNA/2'OMe probe, diluted in an adjuvant buffer contained 0.5M urea and 900 mM NaCl), was given by oral gavage at 0.5 µM (group I and group V) or 2 µM concentration (group II and group VI) (Figure 7.1B). After 30 min, animals were sacrificed by cervical dislocation (Figure 7.1A). The stomach of each animal was removed in aseptic conditions and opened along the greater curvature.

The stomach contents were removed and samples of the mucus were recovered in coverslips. After that, the glandular stomachs were washed in physiological buffered saline and divided into tissue fragments representing cardia, body and antrum. Half of the stomach was used for *H. pylori* culture. The remaining half of the glandular stomach was equally divided in two parts. One part was rinsed in PBS with 0.01% NaN_3 and immediately frozen in liquid nitrogen in Optimal Cutting Temperature compound (OCT; Sakura FInetek, USA) for histopathological examination and analysis of fluorescence. Tissue cryosections (10 µm) were prepared. The other part of the stomach was fixed in 4% paraformaldehyde (PAF, Sigma-Aldrich), for 1 hour, at room temperature. Afterwards, the tissue was rinsed 3 times for PBS and stored in PBS with 0.01% NaN_3 at 4 °C, before being processed and embedded in paraffin. Tissue sections with 3 µm were obtained.

The detection of FIVH signal was performed *ex vivo* in mucus samples, paraffin-embedded sections and cryosections. Mucus and cryosections were evaluated using a Carl Zeiss inverted Axiovert fluorescence microscope. Paraffin-embedded sections were evaluated using a Nikon Eclipse Ti-E inverted microscope attached to a microlens-enhanced dual spinning disk confocal system (UltraVIEW VoX; PerkinElmer, Seer Green, UK) equipped with 405, 488 and 561 nm diode lasers for excitation of blue, green and red

fluorophores, respectively. Images were acquired and processed using Volocity image analysis software (Improvision, PerkinElmer, Waltham, USA).

A

Groups	Conditions				
	Infection	[0.5 µM] of probe	[2 µM] of probe	vehicle	water
I	✓	✗	✗	✓	✗
II	✓	✗	✗	✗	✓
III	✗	✓	✗	✓	✗
IV	✗	✗	✓	✓	✗
V	✓	✓	✗	✓	✗
VI	✓	✗	✓	✓	✗

B

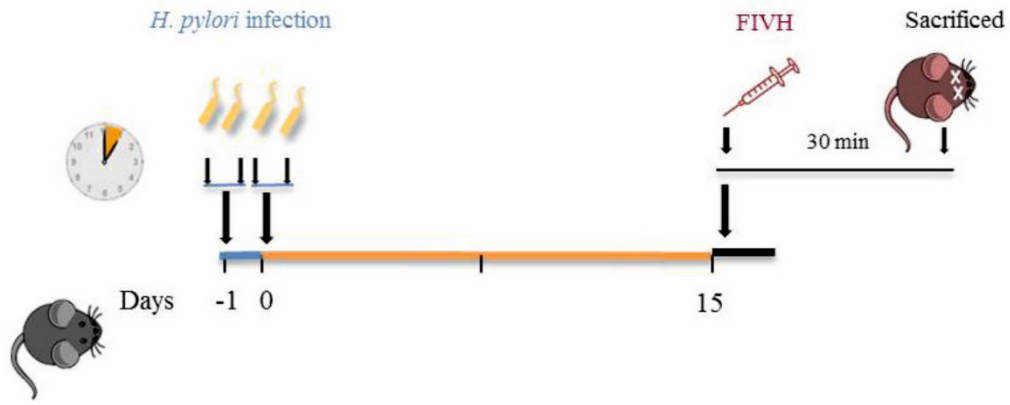

Figure 7.1 – FIVH scheme used for detecting *H. pylori* in C57BL/6 mice. A. Four control groups with *n*=3 (group I to IV) were used to evaluate the background of the vehicle (group I) and tissue (group II) and the specificity of the Cy3_HyP_LNA/2'OMe probe (groups III and IV). Two tests groups (*n*=6, each group) were used with different probe concentrations, 0.5 µM (group V) and 2 µM (group VII). B. Animal study protocol depicting *H. pylori* inoculation, time of infection in C57BL/6 mice, and FIVH after 15 days post-infection.

7.2.9. Retention of Cy3 HP_LNA/2OMe_PS probe in the mouse stomach

To evaluate the retention of the probe in the gastric mucosa, an extra experiment was performed using a group of mice with a period of 5 days post-infection. The infection procedure was performed as described in section 7.2.7. Each mouse in the group was

administered 2 µM of Cy3_HyP_LNA/2'OMe probe through oral gavage. Mice were killed after 24 hours and the stomach were processed and analysed as previously described.

7.2.10. Evaluation of H. pylori colonization in infected mice

The presence of *H. pylori* infection was determined by viable bacterial counts (CFU, colony forming units) and histopathological evaluation. To quantify bacteria on stomachs samples, as a measure of the colonization level, tissues fragments were mechanically homogenized in 1 mL TSB (TissueRuptor, QIAgen). The homogenates were serially diluted and then plated in duplicate onto TSA plates, supplemented with 5% sheep blood, vancomycin (10 µg/mL), trimethroprim (5 µg/mL), amphotericin (5 µg/mL) and cefsulodin (10 µg/mL) (all purchased from Sigma-Aldrich) and incubated at 37 °C under microaerophilic conditions. After 5 days of incubation, *H. pylori* colonies were identified and enumerated as CFU per gram of stomach.

7.2.11. Statistical analysis

Statistical significance was determined by One-way analysis of variance (ANOVA) using GraphPad PRISM 5 software (GraphPad Software, San Diego, USA). Results were expressed as mean ± SD. Differences were considered to be statistically significant when $p < 0.05$.

7.3. Results

7.3.1. HyP_LNA/2'OMe probe in vitro toxicity study

To address if the Cy3-labelled HP_LNA/2OMe_PS probe affects gastric cell viability, a gastric epithelial cell line, AGS, was incubated with different concentrations of the probe and evaluated cell viability using the MTS assay. The range of concentrations of the Cy3_HyP_LNA/2'OMe probe tested on AGS cells, between 0.4 µM and 2 µM did not affect cell viability, since no statistically significant differences were found for any of the concentrations tested ($p > 0.05$) relatively to the untreated cells (Figure 7.2).

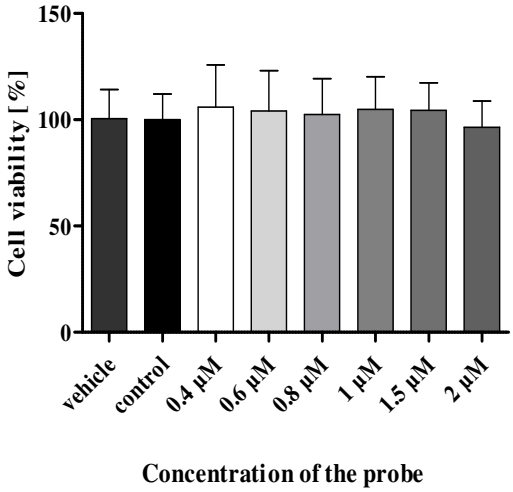

Figure 7.2 - Effect of the Cy3_HP_LNA/2OMe_PS probe on viability of AGS gastric epithelial cells using the MTS assay. AGS cells were treated with a range of concentrations of the Cy3_HP_LNA/2OMe_PS probe for 24h (0.4 µM to 2 µM). Results are expressed as the mean ± SEM of three independent experiments, performed in triplicate; No statistical significant differences were found regarding probe-treated *vs* untreated control cells (*p>0.05* by ANOVA).

7.3.2. Evaluation of genotoxicity of the HyP_LNA/2'OMe probe by VITOTOX® Assay

The possibility of genotoxicity caused by the Cy3_HyP_LNA/2'OMe probe and possible metabolites was studied in a VITOTOX® assay from Gentaur [25,26] as shown in Figure 7.3. A serial dilution of the probe was tested ranging from 0.04 µM to 2 µM. The tested concentrations of the probe did not reduce the signal to noise ratio of the treated cytox cultures below 0.8 (C in Figure 7.3). This was also the case after addition of the S9 liver extract in the TA104 pr1 strain, indicating lack of toxicity towards the *S. typhymurium* model and enabling to test for genotoxicity. The signal to noise ratio of the luminescence emitted by the genox strain did not exceeded 1.5 before and after addition of the S9 liver extract (G in Figure 7.3). At the tested concentrations, the activation of the SOS DNA repair mechanism and early signs of genotoxicity elicited by the Cy3_HyP_LNA/2'OMe probe or its possible metabolites could not be observed.

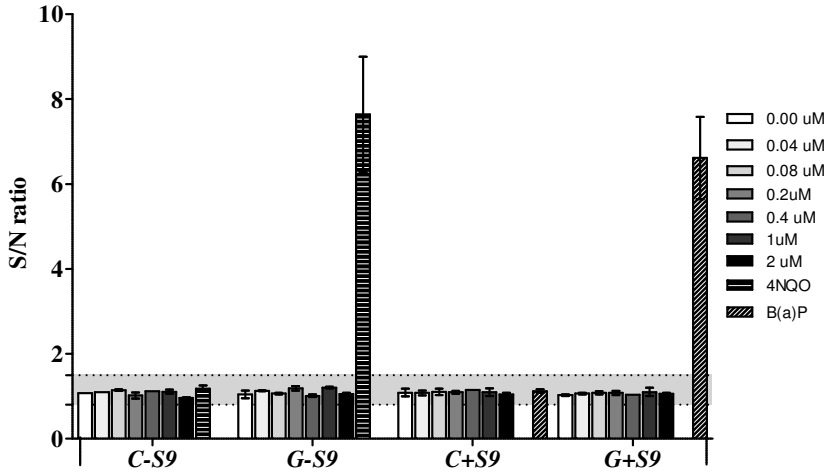

Figure 7.3 - VITOTOX® assay for detection of signs of genotoxicity caused by the Cy3_HyP_LNA/2'OMe probe. Results are expressed as the signal-to-noise (S/N) *ratio* between exposed and unexposed VITOTOX® test bacteria (Genox or Cytox strain) in the absence or presence of S9 mix. Bap:benzo[*a*]pyrene, the positive control, only turns genotoxic after S9 metabolisation.

7.3.3. Fluorescence in situ hybridization (FISH) of Cy3_HP_LNA/2OMe_PS probe on H.pylori SS1 smears

To evaluate whether the Cy3_HP_LNA/2OMe_PS probe is able to detect *H. pylori* SS1 FISH in smears was performed, with different pH values of the hybridization solutions. As it can be observed in Figure 7.4, a high fluorescent signal was detected in *H. pylori* SS1 smears at all conditions tested. This is similar to what it has reported in Chapter VI for smears of other strains of *H. pylori* [22] with, in which high fluorescence obtained using a non-fixative protocol.

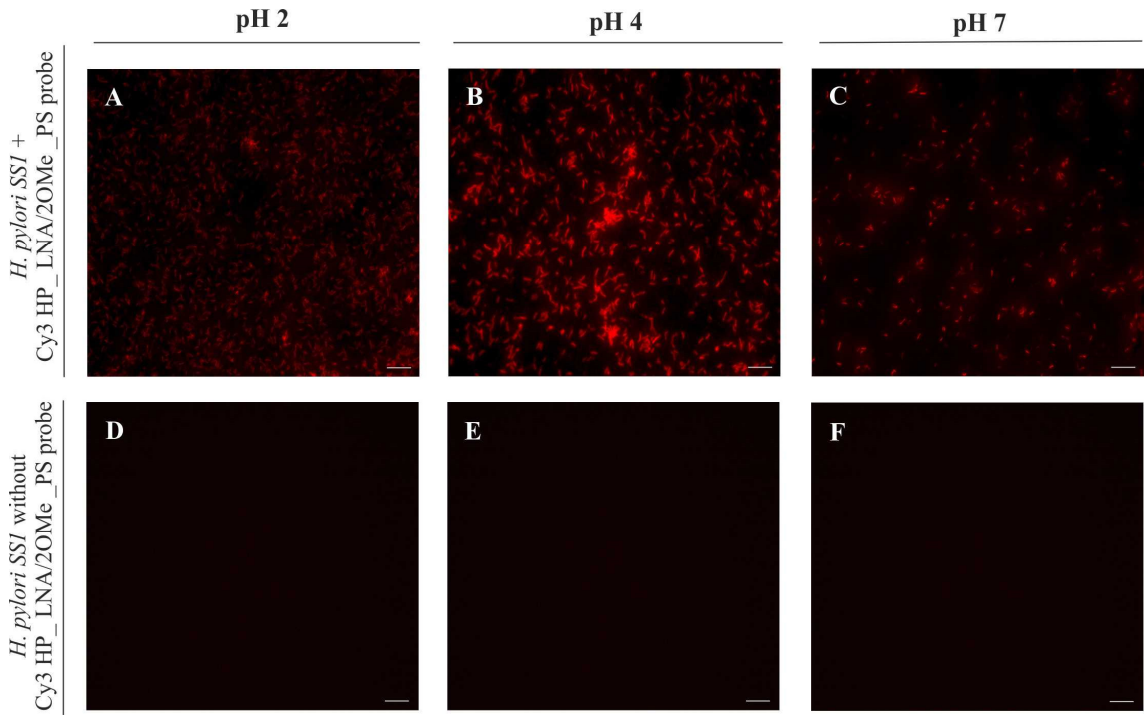

Figure 7.4 - Detection of *H. pylori SS1* in slides, by fluorescence *in situ* hybridization (FISH) using the Cy3_HP_LNA/2OMe_PS probe at different pH values, analyzed by epifluorescence microscopy. A to C - FISH protocol performed on smears of pure cultures of *H. pylori* SS1 incubated with 0.2 µM of probe. D to F - FISH protocol on smears of *H. pylori* SS1 cultures without probe used as negative control. A and D - Experiments performed at pH2. B and E - Experiments performed at pH4. C and F - Experiments performed at pH7. All images were taken at equal exposure times. Scale bar: 10 µm.

7.3.4. Bacteria colonization of the gastric mucosa in C57BL/6 mice

Before the detection of *H. pylori* SS1-infecting C57BL/6 mice by FIVH, the efficiency of colonization in the experimental animal groups was assessed to assure that any difference in FIVH signal was not attributed to differences in the colonization levels of bacteria. For that, the bacterial burden was quantified in the stomach of each infected mice by counting the CFU per gram of stomach tissue (Figure 7.5). At 2 weeks of infection, all mice had an established infection. No differences in bacterial burden were found in the stomachs of infected animals, since CFU levels were equivalent regardless of delivery or not of probe and vehicle. Further, no *H. pylori* were found in the non-infected control animals.

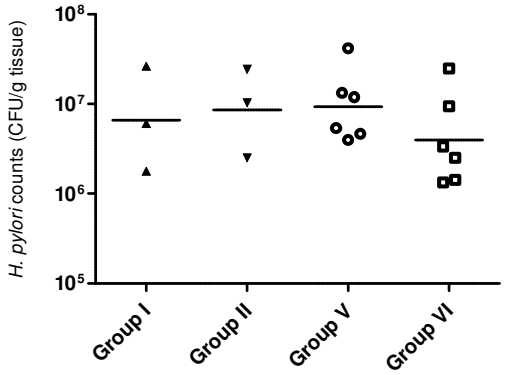

Figure 7.5 – Viable bacterial counts (CFU, colony-forming units) from stomachs of mice infected with *H. pylori* SS1 stain for 2 weeks. Scatter plot of CFU for each animal, with bars representing the medium value.

7.3.5. Assessment of H. pylori in the mice stomach by FIVH

Having demonstrated that *H. pylori* SS1 colonization of C57BL/6 mice was similar in all animal groups tested (Figure 7.5), the efficiency of FIVH experiments was assessed by microscopical observation of both mucus samples (surface mucus layer) and mucosa sections from each mouse. At 2-weeks post-infection, it was possible to observe free-swimming *H. pylori* within the mucus (Figure 7.6), as well as attached to gastric epithelial cells (Figure 7.7 and 7.8), the major locations of *H. pylori* infection in the stomach [28], as identified by the fluorescent signal of the probe. Both concentrations of the Cy3_HP_LNA/2OMe_PS probe studied, 0.5 µM (Figure 7.6A and 7.6B) and 2 µM (Figure 7.6D and 7.6E) were effective in FIVH for mucus samples of test groups V and VI. Mucus samples collected from infected control groups without probe (groups I and II) and from uninfected control groups (groups III and IV) showed no detectable fluorescence emission in the red channel (Figure S12).

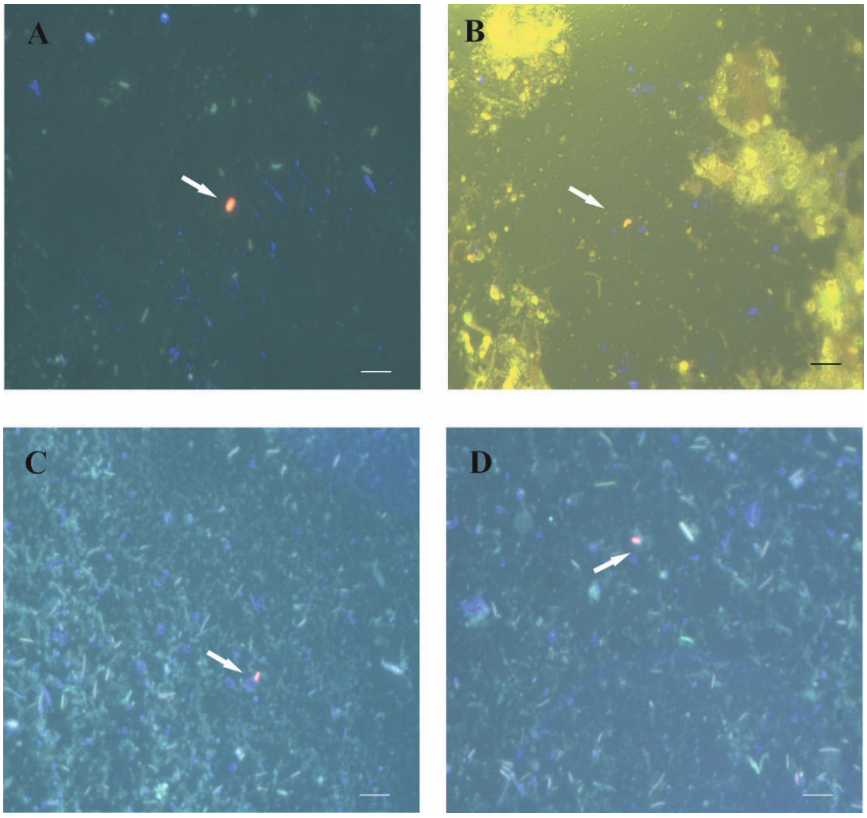

Figure 7.6 – Detection of *H. pylori SS1* in samples of gastric mucus from mice subjected to FIVH with 0.5 µM (A and B; group V) and 2 µM (C and D; group VI) of the Cy3_HP_LNA/2OMe_PS probe. Samples were collected and visualized directly using the epifluorescence microscope. Arrows indicate free-swimming *H. pylori* in gastric mucus. All images were taken at equal exposure times and are representative of the respective test group. Channels red, green and DAPI are overlapped. Scale bars: 10 µm.

Next, for the detection of *H. pylori* SS1 in the gastric mucosa of mice, it was used both cryosections and paraffin-embedded sections of the mice stomach. It has been described that, although physically less stable, cryosections are generally superior for the preservation of the fluorescence signals and therefore for detection by microscopy [29]. As it can be observed in Figures 7.7 and 7.8, the detection of *H. pylori SS1* infection, using FIVH with the Cy3-labeled HP_LNA/2OMe_PS probe, was successful in both frozen and paraffin-embedded stomach sections of the infected test groups V (0.5 µM probe) and VI (2 µM probe).

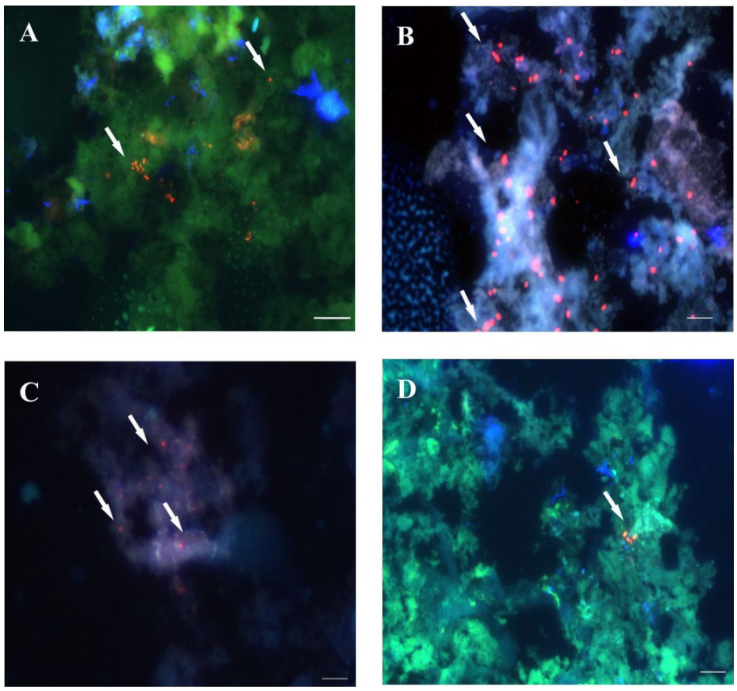

Figure 7.7 - Detection of *H. pylori SS1* in frozen sections of gastric mucosa from mice subjected to FIVH, 30 minutes before euthanasia. A and B: mice from group V (0.5 µM of the Cy3_HP_LNA/2OMe_PS probe), C and D: group VI (2 µM of the Cy3_HP_LNA/2OMe _PS probe). Arrows indicate the presence of *H. pylori* infecting the gastric mucosa. All images were taken at equal exposure times, with overlapping of the red, green and DAPI channels. All the images from each group are representative of *n*= 6 mice. A and C- scale bars: 50 µm. B and D- scale bars: 10 µm.

Although the Cy3_HP_LNA/2OMe _PS probe was effective at detecting bacteria at both concentrations tested, the bacterial morphology was better defined when higher concentration of the probe was used in the case of paraffin-embedded sections (Figure 7.8C and 7.8D). In paraffin-embedded sections it was possible to detect free-swimming bacteria in the mucus layer nearby the surface of epithelial cells, as well as *H. pylori* adhered to the surface mucus cells (Figure 7.8 A-C. Furthermore, it was possible to visualize *H. pylori* colonizing the glands (Figure 7.8B and 7.8D).

A low background in the red channel was observed in infected controls groups (group and II) in cryosections (Figure S13A-D), whereas no detectable red fluorescence emission was found in paraffin-embedded sections (Figure S13A-B). No red fluorescent signal (non-specific signal) was observed in non-infected control groups where the Cy3-labeled probe was administrated without *H. pylori* (Figure S13E-H for cryosections, and Figure S14C-D for paraffin-embedded section; group III and IV).

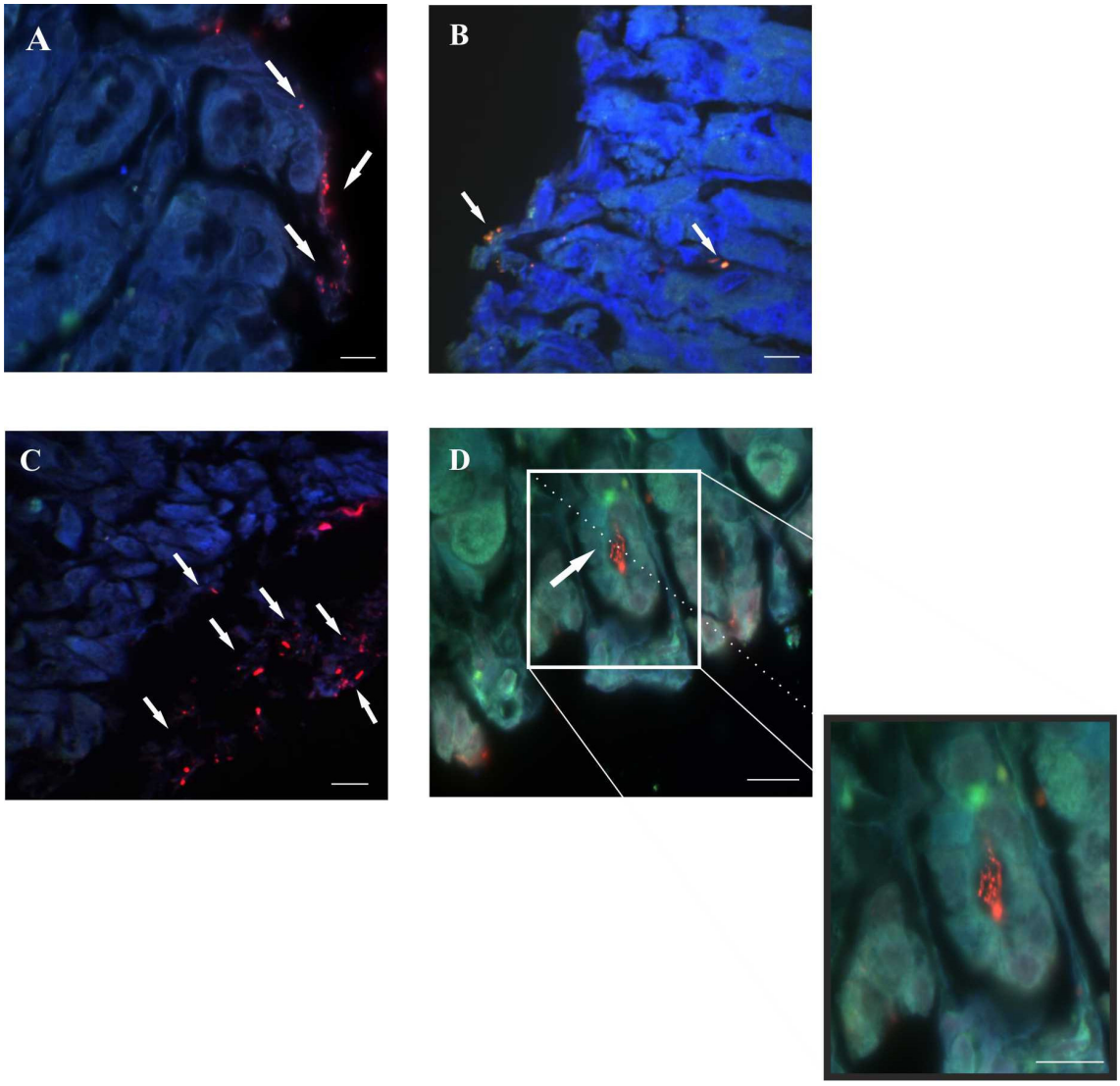

Figure 7.8 – Detection of *H. pylori SS1* in paraffin sections of gastric mucosa from mice test groups subjected to FIVH with the Cy3_HP_LNA/2OMe_PS probe 30 minutes before being sacrificed. A and C. Fluorescence images of the detection in the surface of the gastric mucosa. B and D. Fluorescence images of the detection in the epithelium. A-B images obtained from mouse stomachs from group V. C-D images obtained from mouse stomachs from group VI. Red, green and DAPI channels are overlapped. All the images from each group are representative of *n*= 6 mice. A, B and C scale bars: 10 µm; D scale bars: 50 µm.

To analyze the retention time of the Cy3_HP_LNA/2OMe_PS probe in the gastric mucosa after FIVH, the period post-FIVH was increased from 30 min to 24 hours. The probe was administrated at a concentration of 2 µM to a group of *3* mice at day 5 post-infection. After 24 hours of the FIVH, mice were sacrificed and the infection was confirmed by counting the bacterial CFUs (Figure S15), and the stomach of each mouse was analyzed using fluorescence signal (Figure 7.9). The number of CFUs obtained from the stomach of mice with a 5 days-infection (Figure S4) was lower than that obtained from mice with a 15 days-infection. No signal was observed in the red channel in the mucus samples (Figure 7.9A),

and few bacteria were observed in frozen sections (Figure 7.9B). In contrast, in paraffin-embedded sections it was possible to detect *H. pylori* adhered to gastric epithelial cells (Figure 7.9C), indicating that the probe was retained in the stomach, though the fluorescence intensity was rather lower (Figure 7.9B-C).

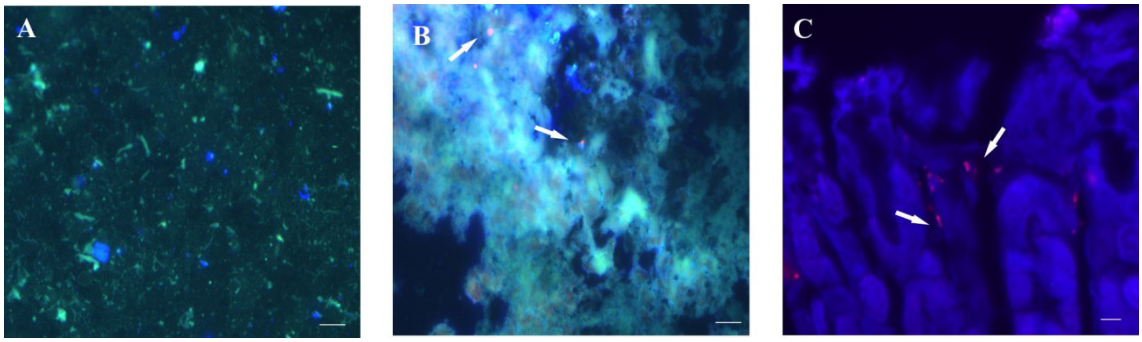

Figure 7.9 –Retention of the Cy3_HP_LNA/2OMe_PS probe in the mouse stomach infected with *H. pylori* SS1 for 5 days, and subjected to a FIVH period of 24 hrs before being sacrificed. A. Sample of gastric mucus. B. Frozen section of mouse gastric mucosa. C. Paraffin section of mouse gastric mucosa. Detection of *H. pylori SS1* by the Cy3-labeled probe is depicted by white arrows. A and B: Red, green and DAPI channels were overlapped. C. Red and DAPI channels are overlapped. All the images from each group are representative of *n*= 3 mice. Scale bars: 10 µm.

7.4. Discussion

In the present study, the efficiency of detection of *H. pylori* was evaluated using *in vivo* labeling with a Cy3_HP_LNA/2OMe_PS probe directed against the 16S rRNA gene, by FIVH on a mouse model. C57BL/6 mice were infected for 15 days with *H. pylori* SS1 strain and FIVH was performed 30 minutes before mice were sacrificed. The results demonstrated that *H. pylori* can be successfully detected in the gastric mucosa of mice. Moreover, the Cy3_HP_LNA/2OMe_PS probe showed high *in vivo* specificity with low background.

The detection and tracking of molecules in living cells constitute an important field of study in biology and medical diagnostics. Therefore, efforts have been done to develop specific methods to target different molecules, such as proteins, mRNA, miRNA, and rRNA, mainly based on fluorescent probes [30-33]. Successful detection of fluorescent probes depend on several characteristics, namely: high fluorescence level and specificity, high *in vivo* stability and high spatial resolution [34]. The FIVH term was introduced by Wiegant *et al.* in 2010, to described a method to microinject a 2'OMe probe into live eukaryotic cells in culture [35]. Later on, other studies have also used fluorescence labeled oligonucleotides to target or regulate molecules *in vivo* [32,36-38]. This *in vivo* labeling methodology can

be applied to address the challenge of a fast diagnosis of microbial infections in humans. The aim is to use FIVH in the future, for real-time detection of *H. pylori* during upper endoscopy using confocal laser endomicroscopy (CLE) [5].

LNA probes have been applied *in vivo* mainly for therapeutic purposes [39,40]. To the best of our knowledge, there are no *in vivo* studies that use LNA probes for diagnostic purposes.

Previously, in Chapter VI, it was reported that the Cy3_HP_LNA/2OMe_PS probe was non-toxic at the concentration of 0.2 µM against the gastric AGS cell line [22]. In the present study, higher concentrations of the probe were needed for *in vivo* experiments. Therefore, viability analysis using a range of concentration between 0.4 µM and 2 µM of the Cy3_ HP_ LNA/2OMe _PS probe was performed in AGS cells. Although selected studies have demonstrated some toxicity associated to LNA probes [41,42], no statistically significant changes in cell viability were observed within the range of probe concentrations tested in this study. Further, the possibility of genotoxic effects induced by the Cy3_HP_LNA/2OMe_PS probe was also investigated. According to the results, the probe was not genotoxic, even at high concentrations. To our knowledge this is the first report that tests the genotoxicity of LNA probes. Since the VITOTOX® test is known to correlate very well with the Ames assay, which is essentially a gene mutation assay [43], we can conclude that the Cy3_HP_LNA/2OMe_PS probe does not induce genotoxicity by an SOS-induction mechanism.

Additionally, the detection of *H. pylori SS1* strain by the Cy3_HP_LNA/2OMe_PS probe was confirmed by FISH on smears of pure cultures of this bacterium, using a range of pH conditions, as well as with a simplified protocol without permeabilization. Although this step is crucial for FISH in bacterial suspensions as we previously reported [22], it is dispensable when using bacteria smears. This simplification of the protocol is relevant for *in vivo* experiments, since it will reduce animal manipulations, time and toxicity of the reagents used.

Regarding the *in vivo* detection of *H. pylori*, the results have shown that the Cy3_HP_ LNA/2OMe_PS probe was effective in detecting *H. pylori*-infected mice at both probe concentrations tested (0.5 µM and 2 µM), and in different locations (within the mucus and attached to gastric epithelial cells). Although we were able to detect *H. pylori* in the surface of the mucus samples collected from infected mice, we did not observe a high concentration of bacteria at this location (Figure 7.6). Contrastingly, a high density of *H. pylori* was found in the mucus layer nearby the stomach surface (e.g. Figure 7.8A and D) or attached to the surface of epithelial cells (e.g. Figure 7.8C and E). This is in agreement with already published reports [28,44-46]. Schreiber *et al.*, described that *H. pylori*

colonizes the mucus layer located 0–25 µm above the tissue surface and that the remaining part of the mucus layer was almost free of bacteria [28]. In fact, one cannot expect a substantial pool of *H. pylori* bacteria to be present in the surface of the mucus, where the pH is low and proximate to the lumen pH, thus an adverse niche for the maintenance and replication of *H. pylori*.

We can also conclude that the Cy3_HP_LNA/2OMe_PS probe had a good retention 24 hrs post-FIVH (Figure 7.9C) in the stomach lining and was able to diffuse into deeper regions of the gastric epithelium (Figure 7.8), since it detected *H. pylori* in the inner mucus layer and at the entrance of gastric pits. It is accepted that the presence of *H. pylori* closer to the epithelial surface probably facilitates exchanges between the adherent and swimming populations of bacteria [28,47].

Importantly, and as mentioned above, the naked Cy3_HP_LNA/2OMe_PS probe is able to diffused well through the mucus and is resistant to the extreme conditions of the stomach without degradation, as it was suggested in Chapter VI [22]. Thus, the stomach environment, known by a limited permeabilization and retention, was not an obstacle for the detection of *H. pylori* using our probe and FIVH conditions.

Improvements in the methodology still have to be addressed in the future in order to include FIVH in the routine clinical practice. The use of CLE is at the moment limited to the equipment available in the market that have an excitation *wavelength* of 488 nm, which is not compatible with the Cy3 fluorochrome (wavelength around 530-560 nm). Thus, it will be necessary to modify the fluorochrome of the probe. In Chapter VI [22], it was shown that fluorescein-labeled probes had low fluorescence when exposed to gastric fluid juice. Therefore, our future work will comprise selection of a different label not only compatible with CLE devices, but also that preserves characteristics such as high brightness, low photobleaching, higher biostability, low toxicity, and a competitive price. Overall, and although there are still some limitations that need to be addressed, the FIVH methodology described herein represents a remarkable advance towards the *in vivo* diagnosis of *H. pylori* infection. Adding to the possibility of detecting pathogens *in vivo*, FIVH will also allow to localize microorganisms directly within the human body. At the moment, a large number of studies have associated gut microbiota with different diseases [49,50], but there are no available technologies to visualize directly the microorganisms and asses their spatial interactions with other microorganisms and with human tissues. The application of FIVH would hence allow to complement the knowledge on the population structure with information about preferred locations of the microorganisms, with a final goal of better understanding the physical-chemical interactions between all the cells of the human complex ecosystem.

7.5. Conclusion

In summary, we have evaluated the *in vivo* diagnostic potential of an LNA based probe for the detection of *H. pylori* by FIVH in an infected C57BL/6 mouse model. Overall, our results showed that the Cy3-labeled HP_LNA/2OMe_PS probe using the developed FIVH protocol allows the detection *H. pylori*, both within gastric mucus and attached to gastric epithelial cells. This holds great promise towards an effective, safe, and immediate method for *in vivo* diagnosis of *H. pylori* infection in human patients, applying a confocal laser endomicroscope. Moreover, this methodology can be applied to the study of the detection patterns of bacteria to different anatomic sites that may be relevant during infection processes and for the identification and localization of different components of the microbiome.

7.6. References

1. Peek RM, Jr., Blaser MJ *Helicobacter pylori* and gastrointestinal tract adenocarcinomas. Nat Rev Cancer (2002); 2: 28-37.
2. Milne AN, Carneiro F, O'Morain C, Offerhaus GJ Nature meets nurture: molecular genetics of gastric cancer. Hum Genet (2009); 126: 615-628.
3. Testerman TL, Morris J Beyond the stomach: an updated view of *Helicobacter pylori* pathogenesis, diagnosis, and treatment. World J Gastroenterol (2014); 20: 12781-12808.
4. Lopes AI, Vale FF, Oleastro M *Helicobacter pylori* infection - recent developments in diagnosis. World J Gastroenterol (2014); 20: 9299-9313.
5. Gheonea DI, Cartana T, Ciurea T, Popescu C, Badarau A, Saftoiu A Confocal laser endomicroscopy and immunoendoscopy for real-time assessment of vascularization in gastrointestinal malignancies. World J Gastroenterol (2011); 17: 21-27.
6. Kiesslich R, Burg J, Vieth M, Gnaendiger J, Enders M, Delaney P, et al. Confocal laser endoscopy for diagnosing intraepithelial neoplasias and colorectal cancer *in vivo*. Gastroenterology (2004); 127: 706-713.
7. Neumann H, Gunther C, Vieth M, Grauer M, Wittkopf N, Mudter J, et al. Confocal laser endomicroscopy for *in vivo* diagnosis of Clostridium difficile associated colitis - a pilot study. PLoS One (2013); 8: e58753.
8. Shahid MW, Crook JE, Meining A, Perchant A, Buchner A, Gomez V, et al. Exploring the optimal fluorescein dose in probe-based confocal laser endomicroscopy for colonic imaging. J Interv Gastroenterol (2011); 1: 166-171.
9. Paramsothy S, Leong RW Endoscopy: Fluorescein contrast in confocal laser endomicroscopy. Nat Rev Gastroenterol Hepatol (2010); 7: 366-368.
10. Ji R, Li Y-Q, Gu X-m, Yu T, Zuo X-L, Zhou C-j Confocal laser endomicroscopy for diagnosis of *Helicobacter pylori* infection: A prospective study. Journal of Gastroenterology and Hepatology (2010); 25: 700-705.
11. McNulty CAM, Lehours P, Mégraud F Diagnosis of *Helicobacter pylori* Infection. Helicobacter (2011); 16: 10-18.
12. Wiegant J, Brouwer AK, Tanke HJ, Dirks RW Visualizing nucleic acids in living cells by fluorescence *in vivo* hybridization. Methods Mol Biol (2010); 659: 239-246.
13. Cerqueira L, Azevedo NF, Almeida C, Jardim T, Keevil CW, Vieira MJ DNA mimics for the rapid identification of microorganisms by fluorescence *in situ* hybridization (FISH). Int J Mol Sci (2008); 9: 1944-1960.
14. Shi H, He X, Cui W, Wang K, Deng K, Li D, et al. Locked nucleic acid/DNA chimeric aptamer probe for tumor diagnosis with improved serum stability and extended imaging window in vivo. Anal Chim Acta (2014); 812: 138-144.
15. Mook O, Vreijling J, Wengel SL, Wengel J, Zhou C, Chattopadhyaya J, et al. *In vivo* efficacy and off-target effects of locked nucleic acid (LNA) and unlocked nucleic acid (UNA)

modified siRNA and small internally segmented interfering RNA (sisiRNA) in mice bearing human tumor xenografts. Artif DNA PNA XNA (2010); 1: 36-44.

16. Zhao X, Wang N, Ren X, Zhang J, Wang J, Han J, et al. Preparation and Evaluation of 99mTc-Epidermal Growth Factor Receptor (EGFR)-Peptide Nucleic Acid for Visualization of EGFR Messenger RNA Expression in Malignant Tumors. J Nucl Med (2014); 55: 1008-1016.
17. Fontenete S, Guimaraes N, Wengel J, Azevedo NF Prediction of melting temperatures in fluorescence *in situ* hybridization (FISH) procedures using thermodynamic models. Crit Rev Biotechnol (2015): 1-12.
18. Fontenete S, Barros J, Madureira P, Figueiredo C, Wengel J, Azevedo NF Erratum to: Mismatch discrimination in fluorescent *in situ* hybridization using different types of nucleic acids. Appl Microbiol Biotechnol (2015).
19. Nedosekin DA, Juratli MA, Sarimollaoglu M, Moore CL, Rusch NJ, Smeltzer MS, et al. Photoacoustic and photothermal detection of circulating tumor cells, bacteria and nanoparticles in cerebrospinal fluid *in vivo* and *ex vivo*. Journal of Biophotonics (2013); 6: 523-533.
20. Lorenz U, Schäfer T, Ohlsen K, Tiurbe GC, Bühler C, Germer CT, et al. *In Vivo* Detection of Staphylococcus aureus in Biofilm on Vascular Prostheses Using Non-invasive Biophotonic Imaging. European Journal of Vascular and Endovascular Surgery (2011); 41: 68-75.
21. Hoerr V, Tuchscherr L, Huve J, Nippe N, Loser K, Glyvuk N, et al. Bacteria tracking by *in vivo* magnetic resonance imaging. BMC Biol (2013); 11: 63.
22. Fontenete S, Leite M, Guimaraes N, Madureira P, Ferreira RM, Figueiredo C, et al. Towards Fluorescence *In Vivo* Hybridization (FIVH) Detection of *H. pylori* in Gastric Mucosa Using Advanced LNA Probes. PLoS One (2015); 10: e0125494.
23. Fontenete S, Guimaraes N, Leite M, Figueiredo C, Wengel J, Filipe Azevedo N Hybridization-based detection of *Helicobacter pylori* at human body temperature using advanced locked nucleic acid (LNA) probes. PLoS One (2013); 8: e81230.
24. Cappoen D, Claes P, Jacobs J, Anthonissen R, Mathys V, Verschaeve L, et al. 1,2,3,4,8,9,10,11-Octahydrobenzo[j]phenanthridine-7,12-diones as New Leads against Mycobacterium tuberculosis. Journal of Medicinal Chemistry (2014); 57: 2895-2907.
25. Verschaeve L, Van Gompel J, Thilemans L, Regniers L, Vanparys P, van der Lelie D VITOTOX® bacterial genotoxicity and toxicity test for the rapid screening of chemicals. Environmental and Molecular Mutagenesis (1999); 33: 240-248.
26. Westerink WMA, Stevenson JCR, Lauwers A, Griffioen G, Horbach GJ, Schoonen WGEJ Evaluation of the Vitotox™ and RadarScreen assays for the rapid assessment of genotoxicity in the early research phase of drug development. Mutation Research/Genetic Toxicology and Environmental Mutagenesis (2009); 676: 113-130.
27. Lee A, O'Rourke J, De Ungria MC, Robertson B, Daskalopoulos G, Dixon MF A standardized mouse model of *Helicobacter pylori* infection: introducing the Sydney strain. Gastroenterology (1997); 112: 1386-1397.

28. Schreiber S, Konradt M, Groll C, Scheid P, Hanauer G, Werling HO, et al. The spatial orientation of *Helicobacter pylori* in the gastric mucus. Proc Natl Acad Sci U S A (2004); 101: 5024-5029.
29. Shi S-R, Liu C, Pootrakul L, Tang L, Young A, Chen R, et al. Evaluation of the Value of Frozen Tissue Section Used as "Gold Standard" for Immunohistochemistry. American Journal of Clinical Pathology (2008); 129: 358-366.
30. Weil TT, Parton RM, Davis I Making the message clear: visualizing mRNA localization. Trends Cell Biol (2010); 20: 380-390.
31. Zelenka J, Alán L, Jabůrek M, Ježek P Import of desired nucleic acid sequences using addressing motif of mitochondrial ribosomal 5S-rRNA for fluorescent *in vivo* hybridization of mitochondrial DNA and RNA. Journal of Bioenergetics and Biomembranes (2014); 46: 147-156.
32. Wang Y, Chen L, Liu X, Cheng D, Liu G, Liu Y, et al. Detection of Aspergillus fumigatus pulmonary fungal infections in mice with 99mTc-labeled MORF oligomers targeting ribosomal RNA. Nuclear Medicine and Biology (2013); 40: 89-96.
33. Yamamichi N, Shimomura R, Inada K, Sakurai K, Haraguchi T, Ozaki Y, et al. Locked nucleic acid *in situ* hybridization analysis of miR-21 expression during colorectal cancer development. Clin Cancer Res (2009); 15: 4009-4016.
34. Hövelmann F, Gaspar I, Loibl S, Ermilov EA, Röder B, Wengel J, et al. Brightness through Local Constraint—LNA-Enhanced FIT Hybridization Probes for In Vivo Ribonucleotide Particle Tracking. Angewandte Chemie International Edition (2014); 53: 11370-11375.
35. Wiegant J, Brouwer A, Tanke H, Dirks RVisualizing Nucleic Acids in Living Cells by Fluorescence In Vivo Hybridization. In: Bridger JM, Volpi EV, editors. Fluorescence in situ Hybridization (FISH). (2010): Humana Press. pp. 239-246.
36. Li L, Tong R, Chu H, Wang W, Langer R, Kohane DS Aptamer photoregulation in vivo. Proceedings of the National Academy of Sciences (2014); 111: 17099-17103.
37. Kam Y, Rubinstein A, Nissan A, Halle D, Yavin E Detection of endogenous K-ras mRNA in living cells at a single base resolution by a PNA molecular beacon. Mol Pharm (2012); 9: 685-693.
38. Shi H, Cui W, He X, Guo Q, Wang K, Ye X, et al. Whole cell-SELEX aptamers for highly specific fluorescence molecular imaging of carcinomas in vivo. PLoS One (2013); 8: e70476.
39. Fluiter K, ten Asbroek AL, de Wissel MB, Jakobs ME, Wissenbach M, Olsson H, et al. In vivo tumor growth inhibition and biodistribution studies of locked nucleic acid (LNA) antisense oligonucleotides. Nucleic Acids Res (2003); 31: 953-962.
40. Gupta N, Fisker N, Asselin MC, Lindholm M, Rosenbohm C, Orum H, et al. A locked nucleic acid antisense oligonucleotide (LNA) silences PCSK9 and enhances LDLR expression in vitro and in vivo. PLoS One (2010); 5: e10682.
41. Stanton R, Sciabola S, Salatto C, Weng Y, Moshinsky D, Little J, et al. Chemical modification study of antisense gapmers. Nucleic Acid Ther (2012); 22: 344-359.

42. Swayze EE, Siwkowski AM, Wancewicz EV, Migawa MT, Wyrzykiewicz TK, Hung G, et al. Antisense oligonucleotides containing locked nucleic acid improve potency but cause significant hepatotoxicity in animals. Nucleic Acids Res (2007); 35: 687-700.
43. Verschaeve LHigh-Throughput Bacterial Mutagenicity Testing: Vitotox™ Assay. High-Throughput Screening Methods in Toxicity Testing. (2013): John Wiley & Sons, Inc. pp. 213-232.
44. Ilver D, Arnqvist A, Ogren J, Frick IM, Kersulyte D, Incecik ET, et al. *Helicobacter pylori* adhesin binding fucosylated histo-blood group antigens revealed by retagging. Science (1998); 279: 373-377.
45. Mahdavi J, Sonden B, Hurtig M, Olfat FO, Forsberg L, Roche N, et al. *Helicobacter pylori* SabA adhesin in persistent infection and chronic inflammation. Science (2002); 297: 573-578.
46. Sigal M, Rothenberg ME, Logan CY, Lee JY, Honaker RW, Cooper RL, et al. Helicobacter pylori Activates and Expands Lgr5 Stem Cells Through Direct Colonization of the Gastric Glands. Gastroenterology (2015).
47. Kirschner DE, Blaser MJ The dynamics of *helicobacter pylori* infection of the human stomach. Journal of Theoretical Biology (1995); 176: 281-290.
48. Lai SK, Wang YY, Hanes J Mucus-penetrating nanoparticles for drug and gene delivery to mucosal tissues. Adv Drug Deliv Rev (2009); 61: 158-171.
49. Karlsson FH, Tremaroli V, Nookaew I, Bergstrom G, Behre CJ, Fagerberg B, et al. Gut metagenome in European women with normal, impaired and diabetic glucose control. Nature (2013); 498: 99-103.
50. Koeth RA, Wang Z, Levison BS, Buffa JA, Org E, Sheehy BT, et al. Intestinal microbiota metabolism of L-carnitine, a nutrient in red meat, promotes atherosclerosis. Nat Med (2013); 19: 576-585.

Chapter VIII

General discussion

8.1. Discussion

H. pylori is the main cause of gastroduodenal ulcers and of gastric cancer [1,2]. An early diagnosis is fundamental to an effective treatment and cure of the infection before the development of gastric diseases. As described in Section 1.2 of Chapter I, several methods can be used to diagnose *H. pylori* infection. However, there is not a single test that can be considered the gold standard [3,4]. Consequently, the improvement of the sensitivity, the elimination of sampling error and the reduction of the time of the diagnosis will be critical in the development of a more efficient clinical diagnosis method.
FISH is a molecular technique that has been used in clinical microbiology to identify and detect bacteria. This technique has been demonstrated to be useful for the detection of pathogens in blood cultures as well as in other clinical specimens [5-8]. The evaluation of standard DNA FISH as a non-culture-based method to detect *H. pylori* has been studied [9,10]. However, as discussed in section 1.5 of Chapter I and confirmed in Chapter IV, DNA oligonucleotides are not sufficiently reliable and versatile to be used in robust FISH methodologies. To overcome these problems, new synthetic monomers comprising novel chemical modifications with stronger target affinities are started to be used.

Earlier, LNA probes were used for the detection of bacteria using FISH [11,12], but this nucleic acid mimic remained as one of the less well-studied mimics for FISH applications. Therefore, Chapter II focused on assessing which parameters impact the design of LNA probes. As such, probe length, the introduction of interspersed 2'OMe monomers and of backbone modifications (PS linkages instead of standard PO) were tested for LNA probe efficiency in *H. pylori* detection. It was concluded that the hybridization is strongly influenced by the design of FISH probes containing LNA. Moreover, it was observed that short LNA probes containing 2'OMe monomers and PS linkages in the backbone can work efficiently at low temperatures.

In order to accurately compare different probes, it is necessary to use systems that are able to quantify fluorescence, such as flow cytometry. Nonetheless, as many of the FISH experiments are performed in attached cells (or smears), quantification should also be applicable to images obtained by microscopy. A few programs and software are already available to quantify fluorescence from microscope images [13,14], but these methods are not user-friendly and are in general very time-consuming when several images have to be studied and compared. Consequently, to allow a quantitative and fast analysis of FISH performed in bacterial smears, in Chapter III bioinformatics tools (FISHji) were developed and integrated in the online platform *ImageJ*® [15]. Of the 5 developed methods, the

automatic FISHji 4 and FISHji 5) methods showed the highest correlations with flow cytometry. Additionally, FISHji 4 and FISHji 5 allowed the analysis of a greater number of images in a short time. Thus, it is expected that these methods can be in the future very useful for all scientific community.

One of the most challenging aspects of FISH is the design of probes with high specificity and sensitivity against the sequence target [16]. Specificity can be limited when another sequence that differs only by a single nucleotide from the target is present [17]. The specificity of a probe is critical in clinical assays to avoid false positive results. Synthetic modifications on the probes used in FISH protocols have shown significant improvement in assay specificity [11,18,19]. Higher binding energies of probe-target duplexes offered by PNA or LNA probes are an advantage yielding high binding affinities. This characteristic is crucial for the shorter probe designs reducing non-specific interactions [20]. Although the advantages of nucleic acid mimics are well-known, a systematic comparison using LNA and PNA probes to discriminate mismatches in FISH has not been performed before.

In Chapter IV, and bearing in mind that specificity is one of the most important factors in FISH, the ability of the different types of nucleic acid mimics to discriminate mismatches was compared. These assays used both naked DNA/RNA and rRNA in whole cells (standard FISH) as targets. A specific sequence present in *H. pylori* and *H. acinonychis* was selected, because in this sequence only a central mismatch exists between these two species. Several probes were designed, including DNA, PNA, LNA/DNA, LNA/2'OMe and LNA/UNA probes. LNA-based probes were designed using the results obtained in Chapter II. The results showed that both PNA and LNA/2'OMe probes had a high discriminatory capacity and could be used to develop more robust FISH methods for the detection of microorganisms. Additionally, it was demonstrated that studies using only naked DNA are not sufficient to evaluate the specificity of the probes in FISH because they fail to consider the complex intracellular environment present in *in vitro* analysis. Furthermore, in this chapter it was demonstrated that LNA/UNA probes should not be used as short probes in FISH. The main reason was probably the reduction of T_m (T_m decrease of 5-10 °C per UNA monomer) [21]. Consequently, a higher number of LNA monomers are needed to overcome this destabilization.

An *in vivo* diagnosis method has to work at human body conditions (e.g. normotemperature, 37 °C). However, FISH protocols are normally performed at temperatures between 55 °C to 65 °C [22-24]. In Chapter V, the use of LNA-based probes

at normotemperature was tested. *In vitro* studies using fluorescence microscopy and cytometry revealed that the smallest LNA/2'OMe probes designed in Chapter II (10 mer HP_ LNA/2OMe _PO and HP_ LNA/2OMe _PS), can efficiently work at 37 °C. Nevertheless, the probe with the PS backbone showed a higher fluorescence signal comparatively to its PO counterpart. The use of different *Helicobacter spp.*, *H. pylori* strains, *non-Helicobacter* and clinical isolates allowed to confirm the high specificity and sensitivity of this probe (HP_ LNA/2OMe _PS). Here, was the first demonstration of the possibility of using nucleic acid mimic probes to hybridize at low temperatures.

To perform hybridization in the gastric mucosa, the probe used in FIVH has not only to work at normotemperature, but also in the presence of gastric juice and low pH, as observed in stomach. In Chapter VI, the HP LNA/2OMe PS probe was used in a large range of pH. Additionally, several studies to mimic human stomach mucosa were performed showing that HP_ LNA/2OMe _PS probe can resist at low pH.
Though, *in vivo* experiments require also non-toxic reagents. Therefore the use a fast and non-toxic FISH protocol must be developed to be used *in vivo*. For that reason, in Chapter VII a simple FISH methodology which combines high signal-to-noise and high specificity was developed.

Low stringency hybridization conditions are currently not used in FISH experiments as the probe can hybridize to sequences which are partially but not entirely complementary to the probe sequence. In this study, it was shown that although we used low temperature and high salt concentrations, the HP_ LNA/2OMe _PS probe maintains high specificity and sensitivity. The sensitivity and resolution of fluorescence imaging *in vivo* is often limited by autofluorescence or background noise [25]. For *in vitro* cell studies, results obtained by confocal microcopy did not revealed unspecific binding and showed the detection of the internalised *H. pylori* in case of infected samples. Then, the background fluorescence of animal cells was not considered relevant. To study the effect of the HP_ LNA/2OMe _PS probe in the viability of gastric cells, toxicity studies were performed and a minimum level death rate was observed. Moreover, additional studies using the Vitotox® test and described in Chapter VII showed that this probe does not demonstrate *in vitro* genotoxicity. These results provided good indications for the potential application of this probe for *in vivo* studies.

Because *in vitro* results do not always reflects the *in vivo* conditions, animal studies are pivotal. *In vivo* studies were performed in C*57*BL/*6* infected with *H. pylori* SS1 strain as described in Chapter VII. In this chapter FIVH was performed using 0.5 and 2 µM of HP_

LNA/2OMe _PS probe in infected C*57*BL/6 mice. A strong fluorescence was observed in the mice stomach collected 30 minutes after oral gavage in both concentrations tested. In contrast, the stomachs of the control group of mice that were not infected did not show fluorescence. Therefore, not only an efficient detection of *H. pylori SS1* was observed but also a specific probe binding. *H. pylori* SS1 was detected more frequently in the mucus layer and only a few bacteria have been found attached to the surface of epithelial cells at the entrance of the gastric pits. This observation is in keeping with the previously described preferential localization for this bacterium [26,27]. The detection of bacteria in the gastric epithelium indicates an effective diffusion of the probe through the mucus layer. Additionally, HP_ LNA/2OMe _PS probe showed a good retention in the gastric tissue after 24 hours.

The selection of the Cy3 fluorochrome was based on the lower background obtained in tissues. Oppositely, high background signals in the green (488 nm) and blue (358 nm) channels were observed. So far, all CLE available on the market are equipped with a 488 nm laser, and consequently_it was not possible to use these apparatuses with this fluorochrome. Although the use of other types of fluorochromes such as fluorescein was a possibility, as observed in chapter VI, the use of this fluorochrome in extreme acidic conditions did not provide good results *in vitro*, and was therefore not tested *in viv*o. Other types of fluorescence molecules such as Alexa Fluor® 488 can be used in future *in vivo* experiments with detection using CLE. Still, cytotoxicity and genotoxicity evaluation should be performed before, because to the best of our knowledge no toxicity-related data exists so far.

CLE with fluorochromes, such as FITC and acriflavine, has shown good results in the esophagus, gastric, intestine and liver epithelium of both humans and animals for detection of neoplasias or inflammatory conditions [28-32]. Additionally, the visualization of bacteria *in vivo* using CLE has been reported before using transformed bacteria or non-specific staining [33,34]. Enteric bacteria transformed with a plasmid carrying the *egfp* gene (expression of enhanced green fluorescent protein) were identified in the small intestine of an anaesthetized mouse [35]. Moreover, Wang *et al.* identified *H. pylori*-infected mucosa in the human stomach using fluorescein as a staining agent [34]. Nevertheless, these authors agree that the specificity of fluorescein is low. Although *in vivo* experiments in mice performed in Chapter VII may differ for human essentially in mucus layer, some studies have used CLE in combination with mucolytic agents (chymotrypsin) to eliminate the slime layer of the stomach and consequently allow better visualization (from the top layer to 250 µm beneath the surface) [34].

Consequently, the use of specific probes such as HP_ LNA/2OMe _PS probe developed in this thesis could contribute to a more efficient diagnosis of *H. pylori* infection in an early stage before the damage of the tissue.

8.2. References

1. Caruso M.L., Fucci L. Histological identification of Helicobacter pylori in early and advanced gastric cancer. J Clin Gastroenterol (1990); 12: 601-602.
2. Graham D.Y. Helicobacter pylori: its epidemiology and its role in duodenal ulcer disease. J Gastroenterol Hepatol (1991); 6: 105-113.
3. Patel S.K., Pratap C.B., Jain A.K., Gulati A.K., Nath G. Diagnosis of Helicobacter pylori: what should be the gold standard? World J Gastroenterol (2014); 20: 12847-12859.
4. Koido S., Odahara S., Mitsunaga M., Aizawa M., Itoh S., Uchiyama K., et al. [Diagnosis of Helicobacter pylori infection: comparison with gold standard]. Rinsho Byori (2008); 56: 1007-1013.
5. Oliveira K., Brecher S.M., Durbin A., Shapiro D.S., Schwartz D.R., De Girolami P.C., et al. Direct Identification of Staphylococcus aureus from Positive Blood Culture Bottles. Journal of Clinical Microbiology (2003); 41: 889-891.
6. Rigby S., Procop G.W., Haase G., Wilson D., Hall G., Kurtzman C., et al. Fluorescence In Situ Hybridization with Peptide Nucleic Acid Probes for Rapid Identification of Candida albicans Directly from Blood Culture Bottles. Journal of Clinical Microbiology (2002); 40: 2182-2186.
7. Hayden R.T., Uhl J.R., Qian X., Hopkins M.K., Aubry M.C., Limper A.H., et al. Direct Detection of Legionella Species from Bronchoalveolar Lavage and Open Lung Biopsy Specimens: Comparison of LightCycler PCR, In Situ Hybridization, Direct Fluorescence Antigen Detection, and Culture. Journal of Clinical Microbiology (2001); 39: 2618-2626.
8. Hogardt M., Trebesius K., Geiger A.M., Hornef M., Rosenecker J., Heesemann J. Specific and Rapid Detection by Fluorescent In Situ Hybridization of Bacteria in Clinical Samples Obtained from Cystic Fibrosis Patients. Journal of Clinical Microbiology (2000); 38: 818-825.
9. Contreras M., Salazar V., García-Amado M.A., Reyes N., Aparcero M., Silva O., et al. High frequency of Helicobacter pylori in the esophageal mucosa of dyspeptic patients and its possible association with histopathological alterations. International Journal of Infectious Diseases (2012); 16: e364-e370.
10. Yilmaz Ö., Demiray E., Tümer S., Altungöz O., Yörükoğlu K., Soytürk M., et al. Detection of Helicobacter pylori and Determination of Clarithromycin Susceptibility Using Formalin-Fixed, Paraffin-Embedded Gastric Biopsy Specimens by Fluorescence In Situ Hybridization. Helicobacter (2007); 12: 136-141.
11. Kubota K., Ohashi A., Imachi H., Harada H. Improved In Situ Hybridization Efficiency with Locked-Nucleic-Acid-Incorporated DNA Probes. Applied and Environmental Microbiology (2006); 72: 5311-5317.
12. Robertson K.L., Vora G.J. Locked Nucleic Acid and Flow Cytometry-Fluorescence In Situ Hybridization for the Detection of Bacterial Small Noncoding RNAs. Applied and Environmental Microbiology (2012); 78: 14-20.

13. Daims H., Lucker S., Wagner M. daime, a novel image analysis program for microbial ecology and biofilm research. Environ Microbiol (2006); 8: 200-213.
14. Konsti J., Lundin J., Jumppanen M., Lundin M., Viitanen A., Isola J. A public-domain image processing tool for automated quantification of fluorescence in situ hybridisation signals. J Clin Pathol (2008); 61: 278-282.
15. Collins T.J. ImageJ for microscopy. Biotechniques (2007); 43: 25-30.
16. Wright E.S., Yilmaz L.S., Corcoran A.M., Ökten H.E., Noguera D.R. Automated Design of Probes for rRNA-Targeted Fluorescence In Situ Hybridization Reveals the Advantages of Using Dual Probes for Accurate Identification. Applied and Environmental Microbiology (2014); 80: 5124-5133.
17. Bonnet G., Tyagi S., Libchaber A., Kramer F.R. Thermodynamic basis of the enhanced specificity of structured DNA probes. Proc Natl Acad Sci U S A (1999); 96: 6171-6176.
18. Rigby S., Procop G.W., Haase G., Wilson D., Hall G., Kurtzman C., et al. Fluorescence in situ hybridization with peptide nucleic acid probes for rapid identification of Candida albicans directly from blood culture bottles. J Clin Microbiol (2002); 40: 2182-2186.
19. Machado A., Castro J., Cereija T., Almeida C., Cerca N. Diagnosis of bacterial vaginosis by a new multiplex peptide nucleic acid fluorescence in situ hybridization method. PeerJ (2015); 3: e780.
20. Spaulding D. Peptide Nucleic Acids: Robust Probe Hybridization Technology. In: Taylor C.R. RL, editor. Immunohistochemical Staining Methods.(2013): Dako, An Agilent Tecnhologies Company
21. Jensen T.B., Langkjaer N., Wengel J. Unlocked nucleic acid (UNA) and UNA derivatives: thermal denaturation studies. Nucleic Acids Symp Ser (Oxf) (2008): 133-134.
22. Almeida C., Cerqueira L., Azevedo N.F., Vieira M.J. Detection of Salmonella enterica serovar Enteritidis using real time PCR, immunocapture assay, PNA FISH and standard culture methods in different types of food samples. Int J Food Microbiol (2013); 161: 16-22.
23. Cerqueira L., Fernandes R.M., Ferreira R.M., Carneiro F., Dinis-Ribeiro M., Figueiredo C., et al. PNA-FISH as a new diagnostic method for the determination of clarithromycin resistance of Helicobacter pylori. BMC Microbiol (2011); 11: 101.
24. Harris D.M., Hata D.J. Rapid identification of bacteria and Candida using PNA-FISH from blood and peritoneal fluid cultures: a retrospective clinical study. Ann Clin Microbiol Antimicrob (2013); 12: 2.
25. Sarkar S.K., Bumb A., Wu X., Sochacki K.A., Kellman P., Brechbiel M.W., et al. Wide-field in vivo background free imaging by selective magnetic modulation of nanodiamond fluorescence. Biomed Opt Express (2014); 5: 1190-1202.
26. Schreiber S., Konradt M., Groll C., Scheid P., Hanauer G., Werling H.O., et al. The spatial orientation of Helicobacter pylori in the gastric mucus. Proc Natl Acad Sci U S A (2004); 101: 5024-5029.

27. Sigal M., Rothenberg M.E., Logan C.Y., Lee J.Y., Honaker R.W., Cooper R.L., et al. Helicobacter pylori Activate and Expand Lgr5 Stem Cells Through Direct Colonization of the Gastric Glands. Gastroenterology (2015).
28. Goetz M., Vieth M., Kanzler S., Galle P.R., Delaney P., Neurath M.F., et al. In vivo confocal laser laparoscopy allows real time subsurface microscopy in animal models of liver disease. J Hepatol (2008); 48: 91-97.
29. Goetz M., Fottner C., Schirrmacher E., Delaney P., Gregor S., Schneider C., et al. In-vivo confocal real-time mini-microscopy in animal models of human inflammatory and neoplastic diseases. Endoscopy (2007); 39: 350-356.
30. Pech O., Rabenstein T., Manner H., Petrone M.C., Pohl J., Vieth M., et al. Confocal laser endomicroscopy for in vivo diagnosis of early squamous cell carcinoma in the esophagus. Clin Gastroenterol Hepatol (2008); 6: 89-94.
31. Zhang J.N., Li Y.Q., Zhao Y.A., Yu T., Zhang J.P., Guo Y.T., et al. Classification of gastric pit patterns by confocal endomicroscopy. Gastrointest Endosc (2008); 67: 843-853.
32. Buchner A.M., Wallace M.B. In-vivo microscopy in the diagnosis of intestinal neoplasia and inflammatory conditions. Histopathology (2015); 66: 137-146.
33. Nanda S. Imaging: Visualizing intraepithelial bacteria in vivo with confocal endomicroscopy. Nat Rev Gastroenterol Hepatol (2011); 8: 64.
34. Wang P., Ji R., Yu T., Zuo X.L., Zhou C.J., Li C.Q., et al. Classification of histological severity of Helicobacter pylori-associated gastritis by confocal laser endomicroscopy. World J Gastroenterol (2010); 16: 5203-5210.
35. Moussata D., Goetz M., Gloeckner A., Kerner M., Campbell B., Hoffman A., et al. Confocal laser endomicroscopy is a new imaging modality for recognition of intramucosal bacteria in inflammatory bowel disease in vivo. Gut (2010).

Chapter IX

Concluding remarks and future perspectives

9.1. General conclusion

The ultimate goal of this thesis was to develop a new FISH methodology able to work *in vivo*. Additionally, this work also aimed to improve the knowledge on FISH-based methods employing other nucleic acid mimics such as LNA, 2'OMe and UNA. The novel FIVH method was directed towards *H. pylori*, a bacterium that infects half of the world's population and is the major cause of gastric carcinogenesis and other gastric diseases.

The first results of this work led to conclude that LNA-based probes are a robust and specific nucleic acid mimic to detect *H. pylori*. The flexibility in the design of these probes allowed the development of a FISH method able to work at normo-temperature and in acidic environments. In order to analyse the capacity of mismatch discrimination, part of this work reported the *in silico* design and development of nucleic acid mimics probes for the detection of *H. pylori* and discrimination of *H. pylori* and *H. acinonychis*. The PNA and LNA/2'OMe probes demonstrated high theoretical specificities *in vitro*. Although obtained only for the specific detection of *H. pylori*, these findings are important for the design and performance of LNA-FISH in other microorganisms, as they provide the first evidence about the potential use of these oligonucleotides as diagnostic tools.

Given these findings, LNA-based probes were tested in specific conditions, namely low temperatures and acid pH. Results highlighted the ability of LNA probes to specifically detect *H. pylori* under low stringency conditions. Since these results showed that the HP_ LNA/2OMe _PS probe performed well *in vitro*, the next step consisted in evaluating the probe *in vivo* using a *H. pylori*-infected mouse model. The HP_ LNA/2OMe _PS probe can detect *H. pylori in vivo*, with high specificity and long retention in the gastric mucosa.

Although additional *in vivo* experiments are necessary to improve the diagnostic efficiency of the HP_ LNA/2OMe _PS probe, this work provides a successful proof-of-concept for future clinical applications in the diagnostic of microorganisms.

9.2. Future perspectives

Based on the results obtained here, there are some perspectives for future work that could provide important outcomes to implement this method in clinical diagnostics. The first one is the time needed to carry out the experiment. As described in Chapters VI and VII, the time necessary for the hybridization of the oligonucleotide (approx. 30 min), should be reduced for *in vivo* diagnosis in humans. The use of nanoparticles might help in the delivery and reduce the time necessary to achieve hybridization [1]. Therefore, in the follow-up of the work described in this thesis it would be of interest to link HP_ LNA/2OMe_PS probe with nanoparticles. Although some nanoparticles demonstrated improvement in the diffusivity properties, they have so far failed in their capacity to

efficiently penetrate the mucus layers [2]. Additionally, and in order to optimize the delivery, this probe could also be coupled with site-specific biomolecules recognizing a target in the *H. pylori* outer membrane. Consequently, in order to penetrate mucus and bind specifically to bacteria, different engineered nanoparticles approaches should be tested.

This method could also be improved by using probes not only for the detection of *H. pylori* but also for the identification of clarithromycin resistance. As described in Chapter I, the resistance to this antibiotic is increasing worldwide, leading to the loss of the efficiency of the clarithromycin-based *H. pylori* eradication treatment [3]. The resistance to this antibiotic in *H. pylori* is the consequence of mutations in *23S* rRNA gene [4]. Essentially, three point mutations are recurrent: two nucleotide positions 2142 (A2142G and A2142C) and 2143 (A2143G) in the peptidyl transferase loop. These mutations lead to a conformational change and therefore decrease the binding of the antibiotic [5].

Finally, it would be of relevance to assess the distribution of the hybridized HP_ LNA/2OMe _PS probe in healthy and in infected mice using *in vivo* molecular imaging systems, such as CLE. The resolution of the probe equipment used in CLE is 1 µm, and consequently it should be possible to detect and identify *H. pylori* in the gastric mucosa *in vivo* with this technology [6].

The analysis of the FIVH results could also be improved using non-invasive monitoring infection models. *In vivo* molecular imaging is a developing area that allows generating pictures of organs and tissues throughout the body at an increased resolution. The analysis of 3D images of the mice stomach would allow the study of the infection distribution and also to monitor host response. Multispectral imaging (MSI) fluorescence-based methodologies (e.g. Maestro *In-Vivo* Imaging System) can also be used in *in vivo* mouse-models [7]. This technology allows imaging of the fluorochromes used in biomedical research *in vivo* at emission wavelengths between 500 and 950 [8,9]. In the way, this type of technology could provide interesting non-invasive data for complementing the pre-clinical results obtained in this thesis. Additionally, this type of optical imaging offers the possibility of real-time acquisition where the use of multiple fluorochromes allow multiplex imaging [10,11]. Therefore, this methodology can be applied in the future for polymicrobial infections or for targeting multiple species simultaneously. Although *in vivo* molecular imaging has turned the corner, there are many drawbacks that still need to be circumvented, such as finding ways of eliminating autofluorescence and amplifying the correct signal. The resolution is considered high (25 microns/pixel), but it is not enough to identify single bacteria. Nonetheless, it has already been used to study infections [12]. The use of new fluorescent agents and labels with wavelengths spanning the near infrared-emitting spectrum, the use of quantum dot

technology, or the use of nanoparticles-based fluorochromes with excellent phostostability proprieties, would allow a better *in vivo* performance [13]. Additionally, improvements in the tomographic approach should be performed to allow the detection of signals at depth, as in the stomach signals may become very diffuse and hard to localize. Even though non-invasive *in vivo* imaging technologies still have problems that need to be overcome, this is a burgeoning field. Specifically, the methodologies focused on fluorescent-based optimal techniques have unique characteristics, such as high spatial resolution, high throughput, relative low cost, avoidance of ionizing radiation, and high levels of multiplexing [7,9,10].

These studies could constitute the basis for the diagnosis of other infectious diseases *in vivo* and monitoring host response.

9.3. References

1. Lai S.K., Wang Y.Y., Hanes J. Mucus-penetrating nanoparticles for drug and gene delivery to mucosal tissues. Adv Drug Deliv Rev (2009); 61: 158-171.
2. Lai S.K., O'Hanlon D.E., Harrold S., Man S.T., Wang Y.Y., Cone R., et al. Rapid transport of large polymeric nanoparticles in fresh undiluted human mucus. Proc Natl Acad Sci U S A (2007); 104: 1482-1487.
3. Megraud F. The challenge of Helicobacter pylori resistance to antibiotics: the comeback of bismuth-based quadruple therapy. Therap Adv Gastroenterol (2012); 5: 103-109.
4. Kim J.M., Kim J.S., Kim N., Kim Y.J., Kim I.Y., Chee Y.J., et al. Gene mutations of 23S rRNA associated with clarithromycin resistance in Helicobacter pylori strains isolated from Korean patients. J Microbiol Biotechnol (2008); 18: 1584-1589.
5. Megraud F., Lehours P. Helicobacter pylori detection and antimicrobial susceptibility testing. Clin Microbiol Rev (2007); 20: 280-322.
6. Chauhan S.S., Abu Dayyeh B.K., Bhat Y.M., Gottlieb K.T., Hwang J.H., Komanduri S., et al. Confocal laser endomicroscopy. Gastrointestinal Endoscopy (2014); 80: 928-938.
7. Levenson R.M., Lynch D.T., Kobayashi H., Backer J.M., Backer M.V. Multiplexing with Multispectral Imaging: From Mice to Microscopy. ILAR Journal (2008); 49: 78-88.
8. Eisenstein M. Helping cells to tell a colorful tale. Nat Meth (2006); 3: 647-655.
9. Franke-Fayard B., Janse C.J., Cunha-Rodrigues M., Ramesar J., Buscher P., Que I., et al. Murine malaria parasite sequestration: CD36 is the major receptor, but cerebral pathology is unlinked to sequestration. Proc Natl Acad Sci U S A (2005); 102: 11468-11473.
10. Mansfield J.R., Gossage K.W., Hoyt C.C., Levenson R.M. Autofluorescence removal, multiplexing, and automated analysis methods for in-vivo fluorescence imaging. Journal of Biomedical Optics (2005); 10: 041207-041207-041209.
11. Levenson R.M., Mansfield J.R. Multispectral imaging in biology and medicine: slices of life. Cytometry A (2006); 69: 748-758.
12. Wang W., Chen S.W., Zhu J., Zuo S., Ma Y.Y., Chen Z.Y., et al. Intestinal alkaline phosphatase inhibits the translocation of bacteria of gut-origin in mice with peritonitis: mechanism of action. PLoS One (2015); 10: e0124835.
13. Tholouli E., Hoyland J.A., Di Vizio D., O'Connell F., MacDermott S.A., Twomey D., et al. Imaging of multiple mRNA targets using quantum dot based in situ hybridization and spectral deconvolution in clinical biopsies. Biochemical and Biophysical Research Communications (2006); 348: 628-636.

Supplemental Material

Chapter II

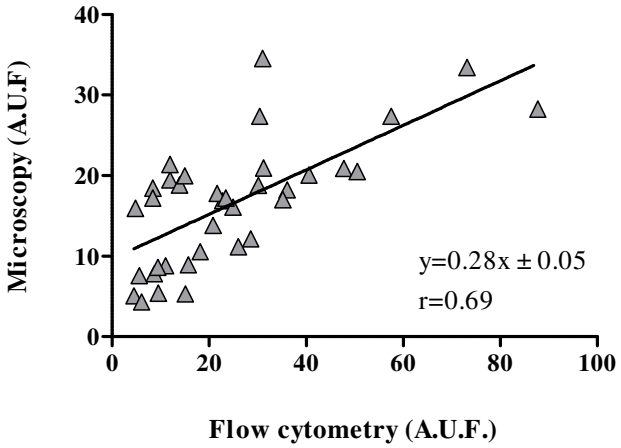

Figure S1 - Analysis of the correlation between fluorescence intensity (A.U.F.) obtained by microscopy versus the fluorescence intensity (A.U.F.) obtained by flow cytometry, for optimal hybridization temperatures. The regression line and the correlation coefficient (r) are displayed for each data comparison. Data are means of two independent experiments.

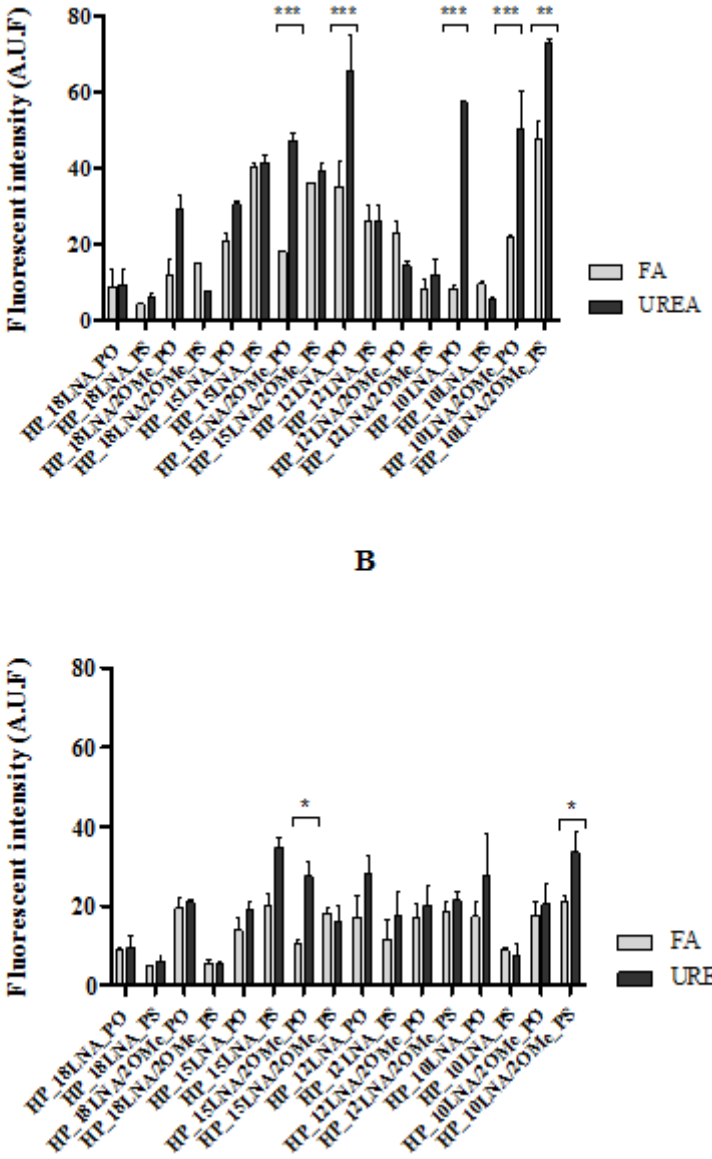

Figure S2 - Quantification of fluorescence hybridization signals from *in situ* detection of 16S rRNA of *H.pylori* with LNA advanced probes. Hybridizations were performed in two different buffers with 50(v/v) FA or 4M urea. Data are means of two independent experiments A. Cytometry; B. Microscopy, * $p \leq 0.05$; . ** $p \leq 0.01$; *** $p \leq 0.001$.

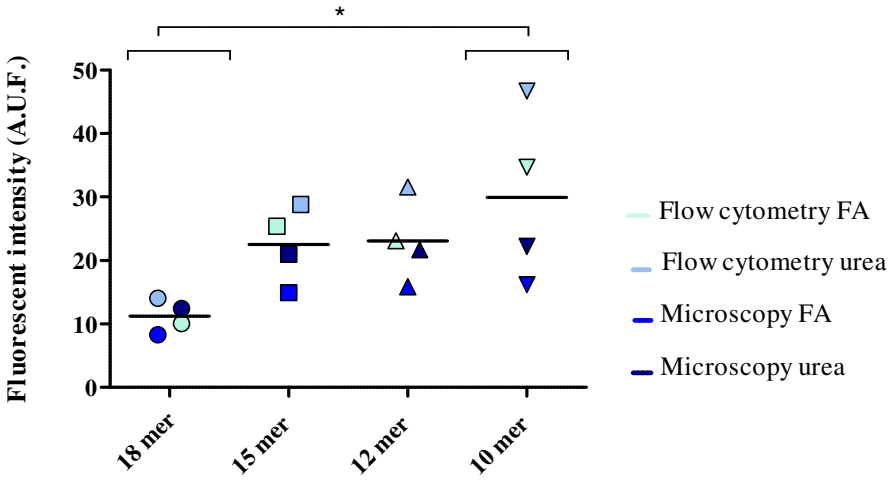

Figure S3 - Analysis of fluorescence intensities obtained by flow cytometry and microscopy for probes of different length. . Data are means of two independent experiments. * $p \leq 0.05$. A.U.F.: Arbitrary Units of Fluorescence. FA: formamide.

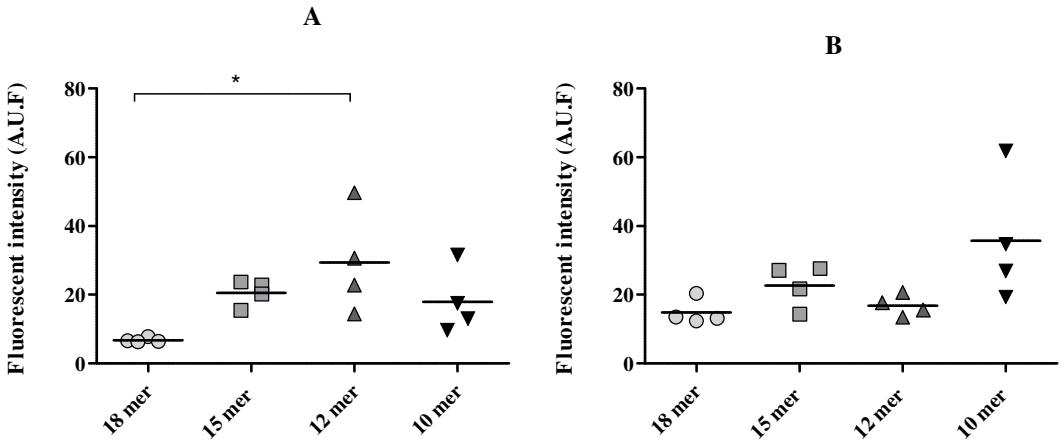

Figure S 4 - Analysis of fluorescence intensities obtained by length of the probe and nucleic acid mimic. A- LNA oligonucleotide. B- LNA/2'OMe oligonucleotide. * $p \leq 0.05$.

Table S1 - Results of thermal denaturation experiments in different types of buffers for different types of probes and hybridization temperature in *H. pylori* 26695 strain. The DNA complementary oligonucleotide has the following sequence: 5'-TTCCTCCCGTTTCTGTGTGGTC-3'. The DNA reference has the following sequence: 5'- CTGGAGAGACTAAGCCCTCCAA-3'. nd- not determined

	Melting temperatures			
	Medium salt buffer	Medium salt buffer with FA	Low salt buffer with FA	High salt buffer with urea
Probes analysed	DNA complement T_m (°C)	DNA complement T_m (°C)	DNA complement T_m (°C)	DNA complement T_m (°C)
REF	62	48	48	67
HP_18LNA_PO	>85 °C	72	68	>85 °C
HP_18LNA_PS	78	66	64	>85 °C
HP_18LNA/2OMe_PO	81	70	68	>85 °C
HP_ 18LNA/2OMe _PS	80	66	42	>85 °C
HP_15LNA_PO	79	64	57	>85 °C
HP_15LNA_PO_2	65	52	49	69
HP_15LNA_PS	71	62	59	80
HP_15LNA_PS_2	58	49	44	61
HP_15LNA/2OMe_PO	79	63	60	>85 °C
HP_ 15LNA/2OMe _PS	68	58	53	74
HP_12LNA_PO	70	57	47	74
HP_12LNA_PS	62	49	50	66
HP_12LNA/2OMe_PO	67	55	51	74
HP_ 12LNA/2OMe _PS	59	49	48	65
HP_10LNA_PO	61	49	46	65
HP_10LNA_PS	56	45	43	61
HP_10LNA/2OMe_PO	59	47	43	61
HP_ 10LNA/2OMe _PS	55	45	43	59

Chapter III

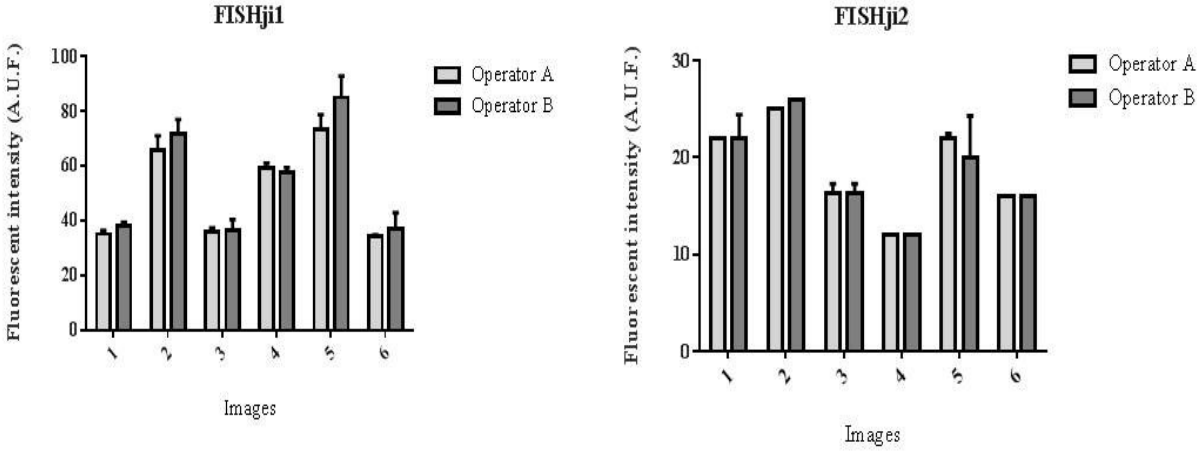

Figure S5 - Variability test between operators in FISHji 1 and FISHji 2. For all the methods we can observe very small differences between the operators in each sample. There are not statistically differences between the operators.

Chapter V

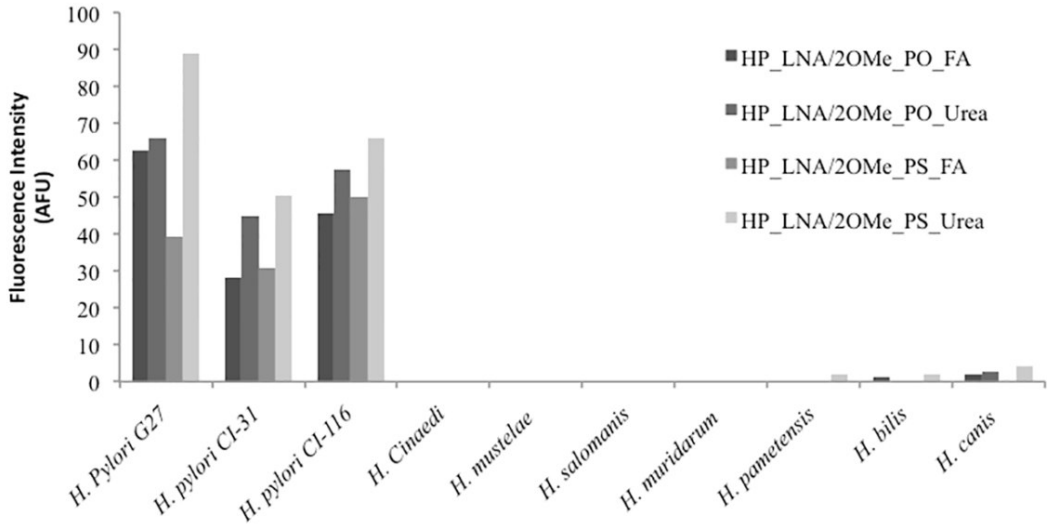

Figure S6- Fluorescence intensity results of Helicobacter strains (non 26695 (ATCC 700392) tested in this study. The results represent the positive signal of each sample after the subtraction of the respective control.

Chapter VI

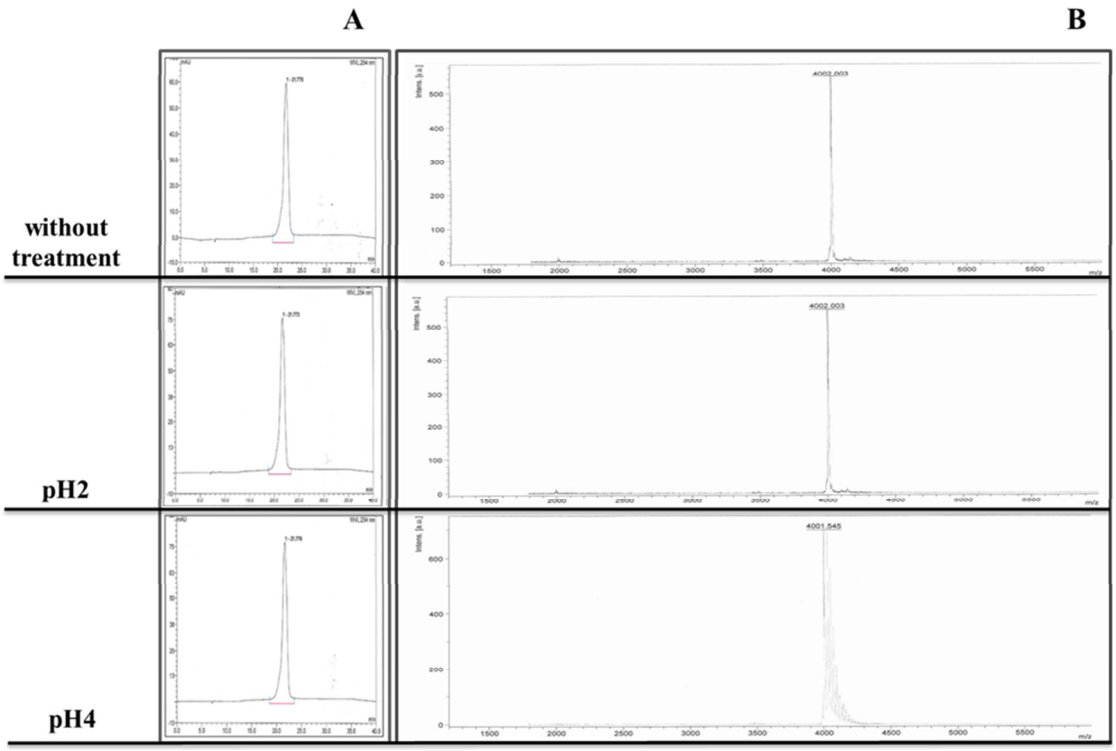

Figure S7- A. IC-HPLC analysis of FAM HP_ LNA/2OMe _PS oligonucleotide probe. The spectrum from FAM HyP-PS without treatment shows similar retention time comparatively to the spectrum from FAM HP_ LNA/2OMe _PS oligonucleotide probe after treatment in a pH2 buffer and pH4 buffer. **B.** Mass spectrum of FAM HP_ LNA/2OMe _PS oligonucleotide obtained by MALDI-TOF. The spectrum from the probe without treatment is similar to the spectrum after treatment in a pH2 buffer and pH4 buffer.

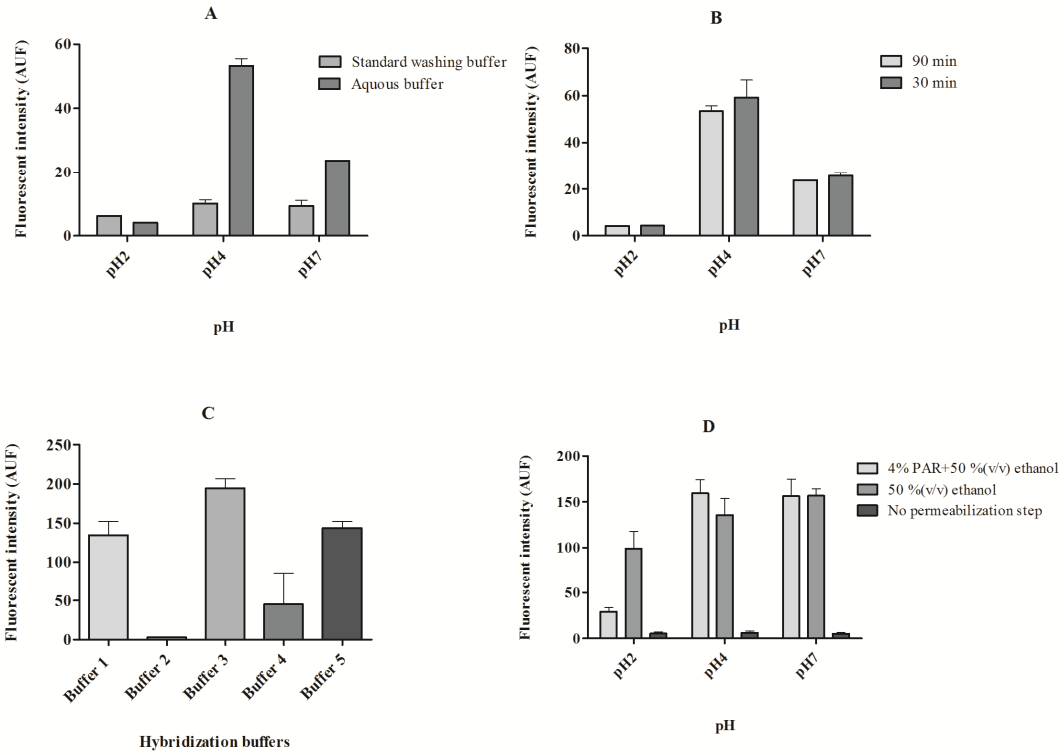

Figure S8 - Optimization of hybridization condition of HP_ LNA/2OMe _PS oligonucleotide probe in pure culture of *H. pylori* strain 26695 (ATCC 700392) at different types of pH **A.** Optimization of washing step using a standard buffer or an aqueous buffer during 15 min **B.** Optimization of hybridization time. Hybridizations steps are performed using a standard hybridization buffer and a washing step during 15 min with aqueous buffer. **C.** Use of different types of hybridization buffer at 30 minutes of hybridization. Buffer 1: 0.1% (v/v) Triton-X, 5 mM of EDTA disodium salt 2-hydrate, 4M urea and 900 mM NaCl. Buffer 2: 0.1% (v/v) Triton-X, 5 mM of EDTA disodium salt 2-hydrate and 900 mM NaCl. Buffer 3: 4M urea and 900 mM NaCl. Buffer 4: 2M urea and 900 mM NaCl. Buffer 5: 0.5M urea and 900 mM NaCl. **D.** Optimization of permeabilization step. Hybridization step was performed using 0.5M urea and 900 mM NaCl during 30 min. The washing step used in these experiments was with aqueous buffer during 15 min.

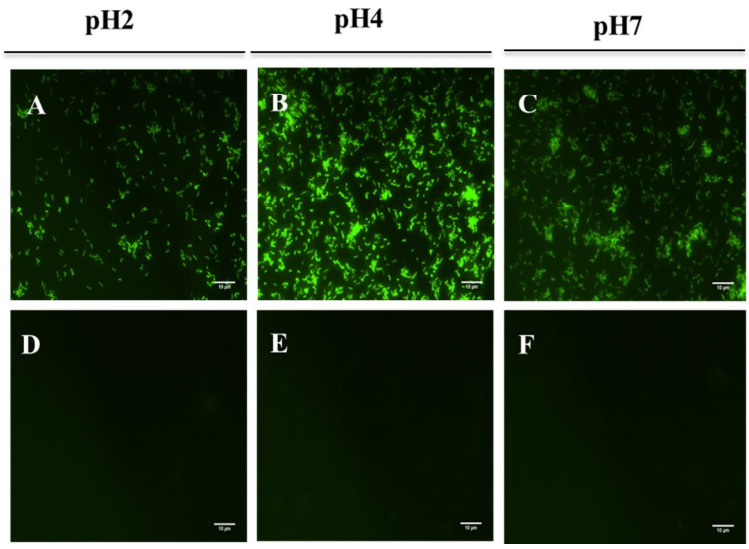

Figure S9- Detection of *H. pylori* using the FAM HP_ LNA/2OMe _PS oligonucleotide probe, without permeabilization. Smear of pure culture of *H. pylori* strain 26695 (ATCC 700392) observed by epifluorescent microscopy. A-C. Experiment using 200 nM of HyP_PS probe. D-F. Smears without probe were used as negative control. All images were taken at equal exposure times. Original magnification: 1000x**.** Scale bar = 10 µm.

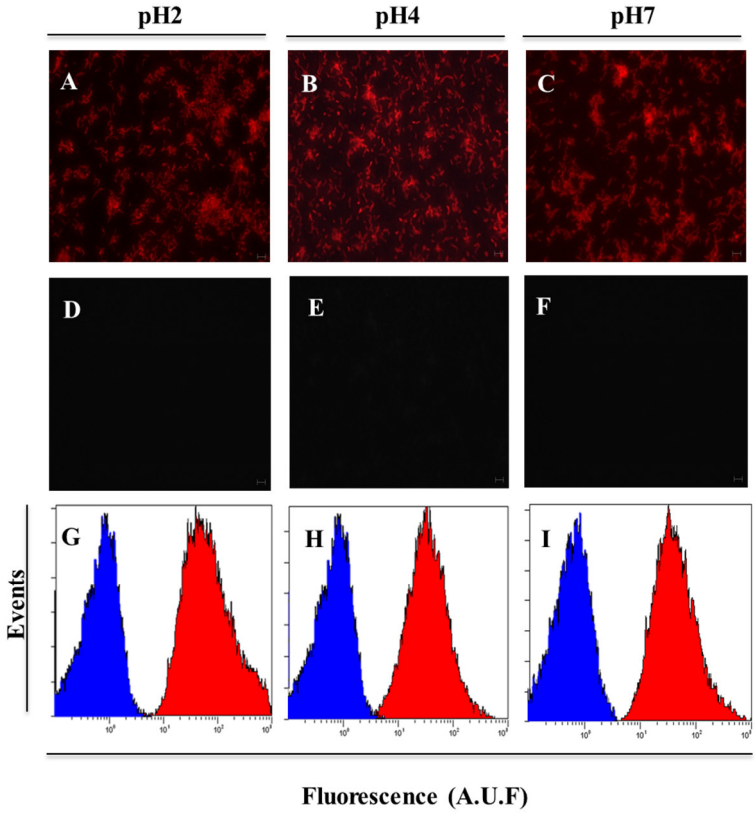

Figure S10- Detection of *H. pylori* using the red fluorescent HP_ LNA/2OMe _PS oligonucleotide probe. A-F Smear of pure culture of *H. pylori* strain 26695 (ATCC 700392) observed by epifluorescent microscopy. A-C. Experiment using 200 nM of HP_ LNA/2OMe _PS oligonucleotide probe. D-F. Smears without probe were used as negative control. All images were taken at equal exposure times. Original magnification: 1000x**.** G-I. Relative fluorescence histograms of LNA-FISH targeting *H. pylori* in different pH for two different assays – Blue: negative control with no probe; Red: positive sample. Scale bar = 5 µm.

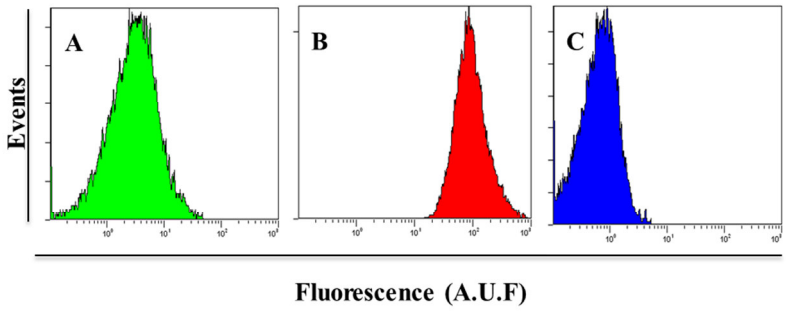

Figure S11- Detection of *H. pylori* at pH1 using gastric simulated juice by FAM HP_ LNA/2OMe _PS and Cy3 HP_ LNA/2OMe _PS oligonucleotide probes. A. FAM HP_ LNA/2OMe _PS oligonucleotide probe. B. Cy3 HP_ LNA/2OMe _PS oligonucleotide probe. C. negative control.

Table S2 - Experimental design matrix and corresponding observed results of arbitrary fluorescence intensity (AUF)

Run	Factor 1: Time	Factor 2: pH	Response: Fluorescence intensity (AFU)
1	52.75	4.50	898.00
2	15.50	2.00	613.00
3	52.75	4.50	1064.00
4	90.00	7.00	329.76
5	15.50	7.00	464.58
6	52.75	4.50	984.30
7	90.00	2.00	815.96
8	52.75	0.96	2347.78
9	52.75	8.04	90.49
10	52.75	4.50	217.60
11	0.07	4.50	80.00
12	105.43	4.50	344.26
13	52.75	4.50	215.77
14	52.75	4.50	227.74

Table S3 - Analysis of variance (ANOVA) for linear model. The adequacy of the model was checked using analysis of variance

Model	Sequential p-value	Lack of fit p-value	R-square
Linear	0.0178	0.0001	0.5543

Chapter VII

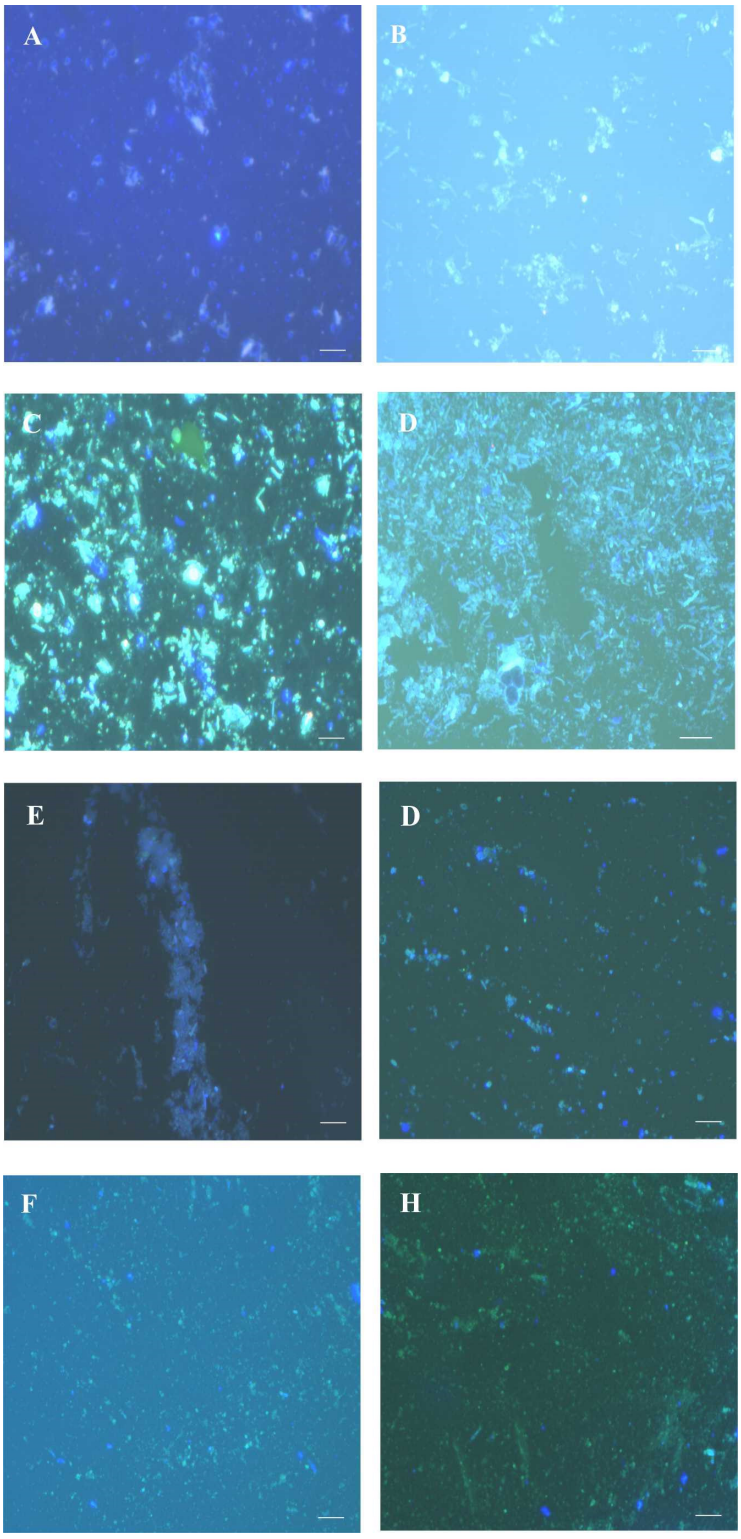

Figure S12- Analysis of the specificity of Cy3 HP_ LNA/2OMe _PS probe and the background *in vivo* in samples of gastric mucus from control groups. Samples were collected and analyzed directly under the epifluorescence microscope. A and B: group I, C and D: group II, E and F: group III, G and H: group IV. All images were taken at equal exposure times. Channel red, green and DAPI were overlapping. Scale bars: 10 µm.

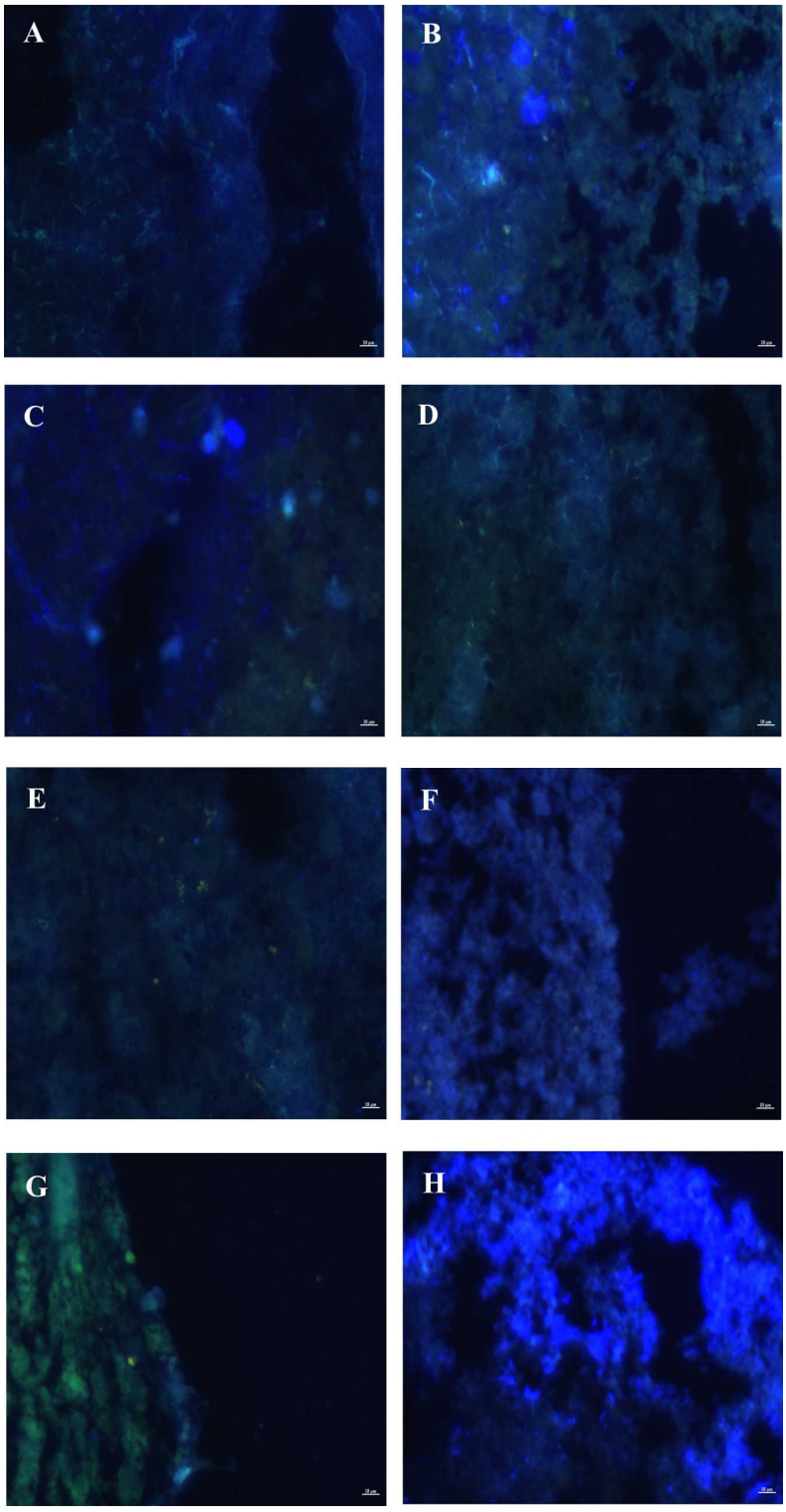

Figure S13- Analysis of the specificity of Cy3 HP_ LNA/2OMe _PS probe and the background *in vivo* in cryosections from gastric mucosa of control groups. A and B: group I, C and D: group II, E and F: group III, G and H: group IV. All the images are representative of n=3 mice. All images were taken at equal exposure times. Channel red, green and DAPI were overlapping. Scale bars: 10 µm.

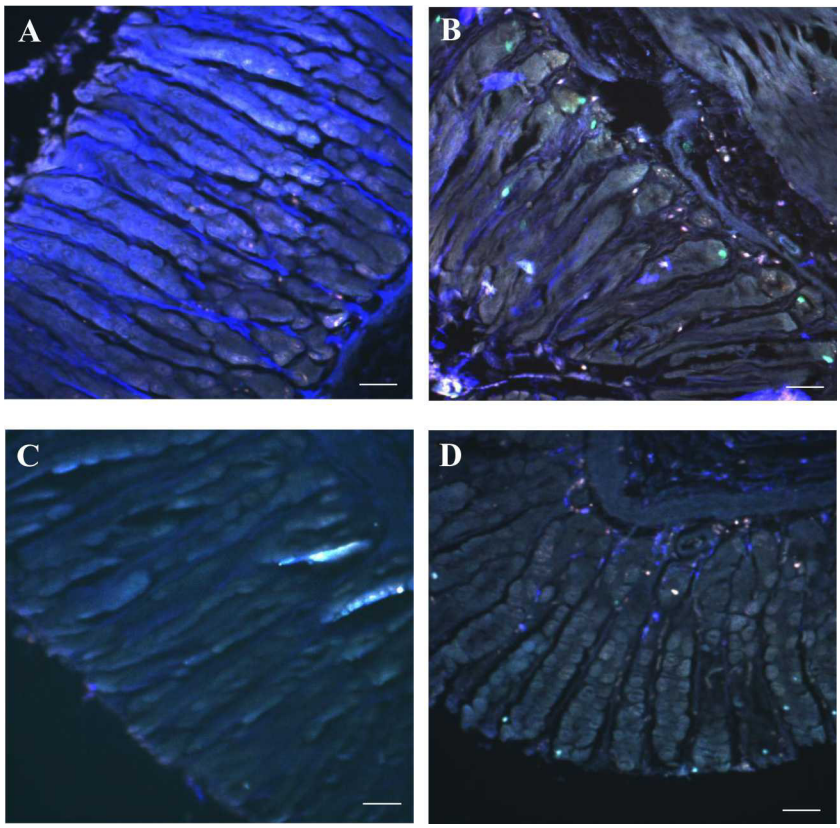

Figure S14- Analysis of specificity of Cy3 HP_ LNA/2OMe and background in paraffin sections of mouse stomach from control groups. A-B: Background obtained using the vehicle and water from group I and II, respectively. C - D. Distribution of Cy3 HP_ LNA/2OMe _PS probe in mouse stomach of group III and IV, respectively. All the images are representative of *n*=3 mice. All images were taken at equal exposure times. Channel red, green and DAPI were overlapping. Scale bars: 50 µm.

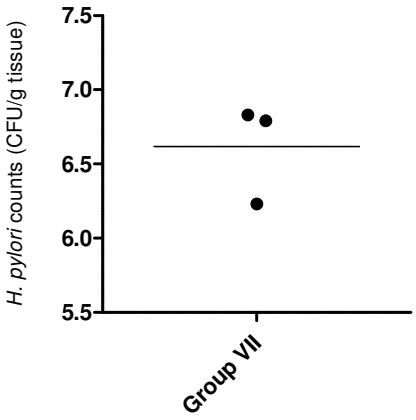

Figure S15- Quantification of bacterial burden in the stomach of *H. pylori*-infected mice with 5 days of post-infection. Bars represent medium values.

Appendix I

Critical Reviews in Biotechnology

http://informahealthcare.com/bty
ISSN: 0738-8551 (print), 1549-7801 (electronic)

Crit Rev Biotechnol, Early Online: 1–12
 DOI: 10.3109/07388551.2014.993589

informa healthcare

REVIEW ARTICLE

Prediction of melting temperatures in fluorescence *in situ* hybridization (FISH) procedures using thermodynamic models

Sílvia Fontenete[1,2,3,4]*, Nuno Guimarães[1,2,3]*, Jesper Wengel[3], and Nuno Filipe Azevedo[1]

[1]*Department of Chemical Engineering, Faculty of Engineering, LEPABE, University of Porto, Porto, Portugal,* [2]*Institute of Molecular Pathology and Immunology of the University of Porto, Porto, Portugal,* [3]*Department of Physics, Chemistry and Pharmacy, Nucleic Acid Center, University of Southern Denmark, Odense M, Denmark, and* [4]*ICBAS, Institute of Biomedical Sciences Abel Salazar, University of Porto, Porto, Portugal*

ABSTRACT

The thermodynamics and kinetics of DNA hybridization, i.e., the process of self-assembly of one, two or more complementary nucleic acid strands, has been studied for many years. The appearance of the nearest-neighbour model led to several theoretical and experimental papers on DNA thermodynamics that provide reasonably accurate thermodynamic information on nucleic acid duplexes and allow estimation of the melting temperature. Because there are no thermodynamic models specifically developed to predict the hybridization temperature of a probe used in a fluorescence in situ hybridization (FISH) procedure, the melting temperature is used as a reference, together with corrections for certain compounds that are used during FISH. However, the quantitative relation between melting and experimental FISH temperatures is poorly described. In this review, various models used to predict the melting temperature for rRNA targets, for DNA oligonucleotides and for nucleic acid mimics (chemically modified oligonucleotides), will be addressed in detail, together with a critical assessment of how this information should be used in FISH.

Keywords: DNA, peptide nucleic acids (PNA), locked nucleic acids (LNA), nucleic acid mimics.

Definition list: Ea: activation energy; FA: formamide; FISH: fluorescence *in situ* hybridization; G: *gibbs free energy;* H: enthalpy; LNA: locked nucleic acid; NN: nearest-neighbour model; PNA: peptide nucleic acid; RMM: retrained mechanistic model; S: entropy; T_H: hybridization temperature; T_m : melting or mid-transition temperature; 2'OMe RNA: 2'-O-methyl nucleotide .

1. General Concepts

Fluorescence in situ hybridization (FISH) is a powerful molecular method with widespread use in environmental and in medical applications for the identification, visualization, and quantification of organisms of interest in microbial communities [1-6]. The FISH procedure is based on the detection of nucleic acids sequences by a fluorescently labelled nucleic acid probe that hybridizes specifically to complementary target sequences within intact microbial and animal cells [7]. It involves five major steps: fixation, permeabilization, hybridization, washing and visualization. Fixation and permeabilization is typically joined in one operation with the objective to render the cell wall permeable to the nucleic acid probe entry, while, at the same time, guaranteeing that cell lysis and extensive nucleic acid degradation will not occur. During hybridization, the probe is placed in contact with the target cells, and if complementary (or near-complementary) sequences are present, hybridization will take place. The specificity of this binding event, i.e. the ability of the method to discriminate the target organisms from the remaining cells, is further ensured by a washing step where all loosely-bound probes are washed away. Specificity can be theoretically predicted using 16S rRNA comparative sequence analysis, as probes are designed to confer a required level of taxonomic specificity (e.g. species, genus, class), and then implemented in the laboratory by optimizing the hybridization and washing conditions [8]. Finally, visualization by either fluorescence microscopy or flow cytometry allows the researcher to observe if successful hybridization has occurred.

A successful hybridization is dependent on several factors such as the conditions at which the hybridization step is carried out and the ribosomal content of cells [9]. The effect of ribosomal proteins, the affinity of the probe and technical factors like the type of fluorophore used, and the microscope's optical quality are also very important [5,9-11]. Due to this large number of factors involved, the development of new FISH procedures remains highly empirical and time-consuming. One of the ways to decrease the effort associated with method development is to be able to predict under what conditions a new probe will work. For instance, if a suitable mathematical model is available that allows the researcher to predict the temperature at which the hybridization step should be carried out, the need for trial-and-error experiments where several temperatures are tested can be avoided or at least minimized.

When FISH first appeared, most studies were performed at the same temperature (46 °C) during the hybridization step [12-14]. This temperature was maintained constant by testing different probe designs and altering the concentration of a denaturing agent, such as formamide, in the hybridization solution. The arrival of multiplex methods (the use of more than one probe in the same experiment to detect multiple microorganisms), together with a better understanding of the hybridization mechanisms, changed this approach. Because in a multiplex experiment probes have to operate at the same temperature and concentrations of denaturing agents, now researchers tend to try and predict the temperature at which the probes will work based on the sequence of the probe and taking into account the compounds of the hybridization solution used in the experiment [15-17]. However, to date, there are no mathematical models that can accurately predict the optimal hybridization temperature (T_H) for a given oligonucleotide probe. As such, the more easily calculated melting or mid-transition temperature (T_m) of an oligonucleotide is calculated instead [18]. T_m can be defined as the temperature at which half of the nucleic-acid strands are forming a duplex and the other half are single stranded, i.e. the temperature at which the dissociation factor is 0.5 [19]. Typically, T_m is used as an indication for the hybridization temperature, but the relationship between these temperatures has not been clearly defined in the literature. It appears sensible to state, however, that for hybridization to occur as efficiently as possible, it would be desirable that all targets sites have bound probes. It hence follows that T_m overestimates T_H by a value that is related to the slope of the melting curve and to the dissociation fraction that is considered acceptable for the FISH procedure (Figure 1). For strands that are not completely complementary, i.e. that contain one or more mismatches to the target sequence, it is usually desirable that the dissociation factor is close to 1 at the hybridization temperature.

Examining Figure 1, it would be reasonable to consider that the hybridization would be successful if it was performed at a temperature equal or lower than the T_H. However, in the initial state of the dissociation fraction curves, the nucleic acids are already in the duplex configuration, and as such do not require energy - so called activation energy (Ea) - to form a duplex. FISH, on the other hand, starts with two single stranded strands that will require Ea to hybridize [20]. This implies that low temperatures will make the hybridization process very slow, and consequently there is a narrow range of T_H at which FISH will provide satisfactory results. This narrow range allows researchers to increase the temperature to minimize non-target hybridization, if specificity is an issue, whereas the opposite may be true if sensitivity is the biggest issue.

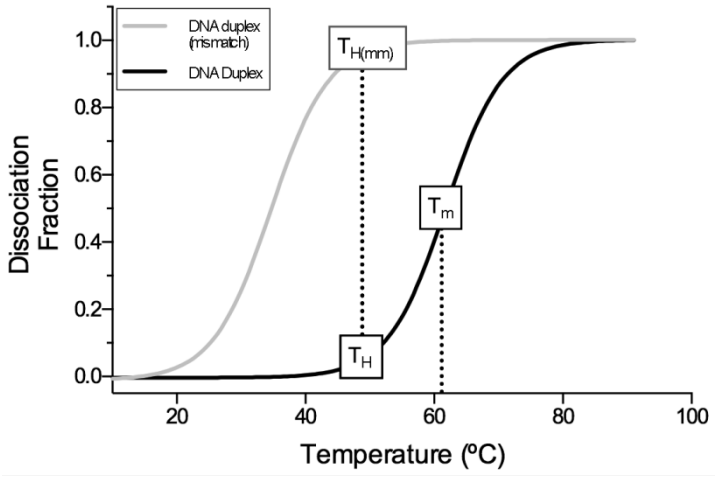

Figure 1 - Melting temperature (T_m) and dissociation fraction curves are showed for completely complementary strands (DNA duplex) and for strands with one mismatch (DNA duplex mismatch). The hybridization temperature (T_H) is presented as the hybridization temperature for DNA duplex and T_H (mm) represents the hybridization temperature for the DNA duplex containing one mismatch (DNA duplex (mismatch)). The values used to design the curves are hypothetical.

T_m is intrinsically related with other thermodynamic properties such as the *Gibbs Free Energy* (G). This energy is a thermodynamic quantity which can be used as an indicator of whether a reaction is thermodynamically favourable or not. When ΔG is negative (ΔG<0) the reaction will be favourable or spontaneous, and the more negative the value the more favourable is the reaction. An estimation of these parameters (and also their correlation) can now be obtained by the nearest-neighbour model (NN), which relies on the assumption that the stability of a base pair depends on the identity and orientation of the adjacent base pair (neighbour base pair) [21,22]. While very useful, the NN model was developed to deal with the thermodynamics of nucleic acid hybridization in general, and does not take into account all parameters and chemical compounds involved in the hybridization step of a FISH procedure.

Here, we will critically review existing models for prediction of the T_m value and describe corrections (e.g. for salt and formamide constituents) that exist to approximate the theoretical model to the chemical micro-environmental conditions of typical FISH procedures. Most of the modelling work and FISH procedures have been developed for DNA probes, and as such we will start by reviewing models for DNA molecules. Nonetheless, DNA probes in FISH are being replaced by better performing nucleic acid mimics, such as peptide nucleic acid (PNA) and locked nucleic acid (LNA). Consequently, the existing models for these novel types of mimics and respective corrections will also be presented. Furthermore, while in the microbiology area the probe target is mostly a RNA molecule, the existing T_m models were originally developed for a DNA target. While some

of these models have been adapted to RNA [23,24], we decided for consistency to present first the models targeting DNA and only afterwards, when available, mention the adaptations for RNA. The last section of the review compares the predicted values of T_m against T_H obtained in the laboratory and provides some explanations for observed discrepancies and suggestions for future work.

2. Melting temperature prediction of oligonucleotide probes

2.1. Melting temperature of DNA duplexes and DNA:RNA hybrids

The prediction of a precise T_m for DNA duplexes was an early concern of many researchers (Figure 2). In 1962, Marmur had already proposed a simple formula to predict this temperature from the GC content of a sequence (T_m = 4GC+2AT) [25]. However, this model is simplistic because it only considers the type and number of nucleic acid bases of a sequence.

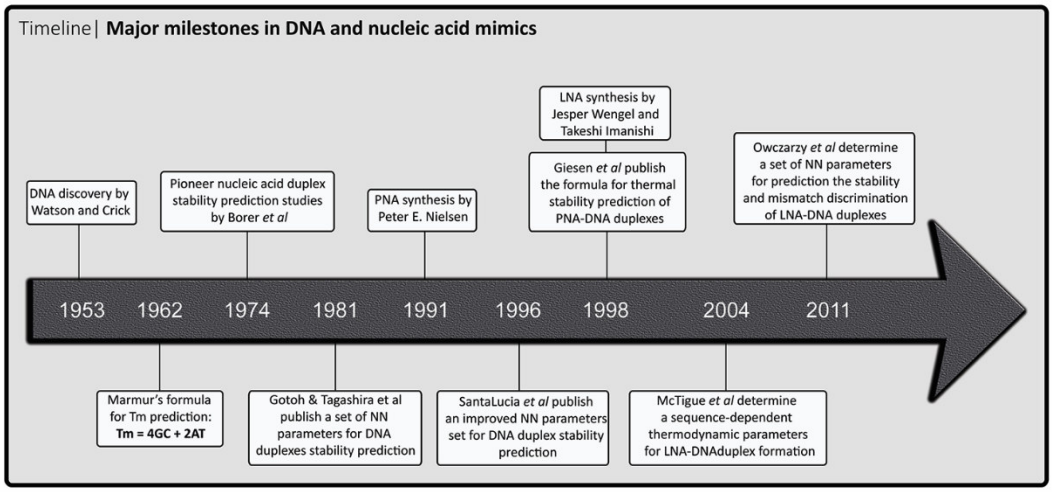

Figure 2 - Major milestones in DNA and nucleic acid mimics.

In order to improve from the previous equation, various studies have reported thermodynamic values for calculating DNA stability from the order of bases within a sequence based on the NN model, and several NN parameter sets for predicting DNA duplex stability are described in the literature [26-28]. From all these parameter sets, the NN parameters published by SantaLucia *et al.* [18] are the most commonly used for the calculation of thermodynamic values.

The NN model starts by assuming that enthalpy (ΔHo) and entropy (ΔSo) are independent. It is then possible to determine the ΔG^o for nucleic acid duplexes of different lengths as a sum of 2 base pair duplexes (ΔG^o_T). The ΔG^o_T value is obtained through

equation 1 using ΔHo and ΔSo values ((T is in Kelvin, ΔHo is in cal.mol^{-1} and ΔSo is in units of cal K^{-1} mol^{-1})[18].

$$\Delta G^{O}_{T} = \Delta H^{o} - T\Delta S^{o} \quad (1)$$

A derivation of equation 1 can be used to determine the T_m on the basis of the thermodynamic parameters. In fact, T_m (°C) may be calculated by equation 2, where R is the gas constant 1.9872 cal/K - mol, C_t is the total strand probe concentration (mM) and x is the symmetry factor (where x is equal to 1 for self-complementary oligonucleotide duplexes and equal to 4 for non-self-complementary oligonucleotide duplexes) [18].

$$T_m = \Delta H^{o} \times 1000/(\Delta S^{o} + R \times \ln(C_t/x)) - 273.15 \quad (2)$$

The deviation of this model has been estimated to be 2.3 °C for DNA duplexes but so far efforts to obtain a better model have been unsuccessful [18,29]. This model can also be used for DNA:RNA duplexes by simply adapting the NN parameters for this type of situation with an average error of 0.6% [23].

2.2. Melting temperature of PNA:DNA duplexes

PNA is an uncharged synthetic DNA analogue which is resistant to nuclease and protease degradation. PNA forms various hybrid complexes such as PNA:PNA, PNA:DNA and PNA:RNA duplexes, and PNA:PNA:PNA and PNA:DNA:PNA triplexes [30]. Due to its thermodynamic characteristics, PNA presents several advantages for FISH experiments. For instance, PNA:target duplexes proved to be more stable under physiological salt conditions and to have more favourable hybridization properties than the corresponding unmodified DNA or RNA duplexes [31-33]. PNA probes can be shorter than nucleic acid probes due to their enhanced binding properties [34], and, because PNA is an uncharged oligonucleotide analogue , it has a higher capacity of penetrating untreated bacterial cell walls than their negatively charged nucleic acid counterparts [35]. Due to its neutral charge, PNA has very high affinity for DNA/RNA due to the lack of charge repulsion of the peptide-like backbone [31,36,37]. The higher specificity and sensitivity have been exploited in order to develop several diagnostic applications [38-40] .

Several authors have described that the higher T_m of PNA-containing duplexes depends on the sequence and length of the duplexes [37,41] and generally can be explained by an enthalpy increase [41]. Theoretical predictions of the thermodynamic behaviour of

PNA:DNA duplexes have employed NN values and empirical thermodynamic parameters [42]. Since these models were initially built for T_m prediction of DNA:DNA duplexes, not surprisingly they proved inaccurate when applied to PNA:DNA duplexes [42]. Accordingly, these models are also not applicable to predict accurate PNA T_H values. It was therefore necessary to determine a new set of thermodynamic parameters to represent the average contribution of each PNA base in order to be able to accurately predict the T_m values for PNA-containing duplexes [41].

In another approach, Giesen *et al. [37]* developed an empirical formula based on the T_m value as calculated for the corresponding DNA:DNA duplex [19]. This formula includes terms for the pyrimidine content (f_{pyr} and length of the PNA (equation 3).

$$T_{m_{pred}} = c_0 + c_1 \times T_{m_{nmDNA}} + c_2 \times f_{pyr} + c_3 \times length \quad (3)$$

The constants were determined to be c_0 = 20.79, c_1 = 0.83, c_2 = -26.13 and c_3 = 0.44. However, the thermodynamic values calculated from the above mentioned models are not nearly as accurate as values calculated from the DNA duplex models [37,42], likely because PNA models have been much less studied than their DNA counterparts. Therefore, the development of a more accurate thermodynamic model for PNA is a priority to be able to predict more accurately not only hybridization reactions of PNA:DNA duplexes but also PNA:RNA duplexes.

2.3. Melting temperature of LNA:DNA duplexes

Locked nucleic acid (LNA) is another nucleic acid mimic that has recently began to be used in FISH [15,17,43,44]. The pentose ring of LNA nucleotides is conformationally locked in a C3'-*endo/N-type* sugar conformation by an O2' to C4' methylene linkage [45,46], and has been used as an antisense molecule both *in vitro* and in *vivo*, exhibiting very high affinity and specificity toward complementary DNA and RNA [43,47,48]. The use of LNA residues in oligonucleotides allows the stabilization of the duplex during the hybridization and permits a more sensitive detection [17]. Additionally, this stability is evident in biological media where only the presence of three LNAs at the 5' and 3' ends is enough to increase the half-life of the oligonucleotide [49]. LNA has important advantages comparatively to PNA, namely the possibility of being synthesized using conventional phosphoramidite chemistry which allows automated synthesis of chimeric oligonucleotides such as DNA+LNA or LNA+RNA. Additionally, PNA probe synthesis is limited in terms of length and sequence, which increases the difficulty of designing PNA probes with enough specificity [50]. For this reason, LNA probes offer high design flexibility comparatively to

the PNA probes. The introduction of LNA into an oligonucleotide raises the T_m of the hybrid, depending on the length and the position in the oligonucleotide. It has been shown that the number of LNA substitutions needs to be optimized to allow a higher hybridization efficiency and specificity [17,51]. It also been proved that single LNA modifications in the inner positions of the duplexes has equal effect on the stability, in spite of the chemical nature of the LNA nucleotides used [47,52]. However, the additive behaviour of multiple LNA substitutions was only observed if the LNA nucleotides were separated at least by one 2'-O-methyl nucleotide (2'OMe RNA) [53]. Similarly, LNA/DNA probes in which LNA and DNA nucleotides alternate have shown strong increase of affinity [17]. However, the thermodynamic origin of LNA's enhanced base pairing stability has not been clearly delineated, although it has been suggested that decreased entropy of duplex formation and improved stacking in the duplex both play a part [54].

Similarly to PNA, LNA parameters differ from the DNA parameters used in the NN models, but several authors, such as McTigue *et al. [55]* and more recently Owczarzy *et al. [54],* have determined a set of unique LNA parameters that could be used for prediction of thermodynamic parameters of the hybridization of LNA oligonucleotides to their all-DNA complements. McTigue *et al* have determined the thermodynamic parameters for the hybridization of DNA oligonucleotides with a single LNA nucleotide to their all-DNA complements [55]. The variation in the enthalpy parameter due to the LNA nucleotide ($\Delta\Delta H$ °) was estimated by the equation below:

$$\Delta\Delta H^\circ \equiv \Delta H^\circ_{\text{LNA+DNA:DNA}} - \Delta H^\circ_{\text{DNA:DNA}} \quad (4)$$

Where LNA+DNA:DNA refers to the duplex with a single LNA nucleotide incorporated in one strand and DNA:DNA refers to the reference DNA duplex. The $\Delta\Delta S^\circ$, $\Delta\Delta G^\circ_{37}$ and $\Delta\Delta T_M$ can be obtained by analogous expressions. After evaluating the accuracy of the experimental parameters in the test set of oligonucleotides, the authors combined the data of all the 100 oligonucleotides used and derived a 32 NN thermodynamic parameter sets for LNA incorporation [55] (Table 1 and 2). The 32 NN parameter set gives a prediction of the T_m of a new single LNA-substituted sequence. To use it, the ΔH° and ΔS° of the corresponding all-DNA duplex is calculated using the already described DNA parameters [56]. Then the ΔΔH° and ΔΔS° values from the 32 NN set for the two LNA NN pairs are added and the T_m calculated using equation 2. According to the authors, the sets of ΔΔH°, ΔΔS° and $\Delta\Delta G^\circ_{37}$ parameters for all the 32 possible NN for LNA+DNA:DNA hybridization provides T_m estimates accurate within 2 ˚C for oligonucleotides containing a single LNA nucleotide.

Table 1 - Models from the literature for T_m prediction of an oligonucleotide

Models for T_m prediction	Units	Characteristics	Authors/Studies
$T_{m=}\,\Delta H^{\circ}/(\Delta S^{\circ} + R\ln(\mathrm{C_A} - \mathrm{C_B}/2))$	K	Use for non-self-complementary oligonucleotides duplexes, if the strands are different concentration	[22]
$T_{m=}\,\Delta H^{\circ}/(A + \Delta S^{O}_{NN} + R\ln(\mathrm{C_t}))\mathrm{N}73.15$	˚ C	Including all the changes between self-complementary and non-self-complementary oligomers	[57]
$T_m = (\Delta H_{duplex} + \Delta H_{nuc})$ $/\left(R\ln\left(\frac{C_T}{\alpha}\right) + \Delta S_{duplex} + \Delta S_{nuc}\right)$ ΔH (cal/mol); mS (cal.mol $^{-1}$.K^{-1});Ct (µM)	K	Duplex sequences as a function of strand concentration	[58]
$T_{m=}\,\Delta H^{\circ} \times 1000/(\Delta S^{\circ} + R\ln(\mathrm{C_t}/\mathrm{x})) - 273.15$ ΔH (kcal/mol); (S (cal.mol $^{-1}$.K^{-1});Ct (mM);R(cal/K-mol)	˚ C	Use for self and no self-complementary oligonucleotides duplexes, where x equal 1 or 4 respectively	[18]

Table 2 - Different models for ΔG prediction existing in the literature for an oligonucleotide

Models for ΔG prediction (cal/mol)	Characteristics	Authors/Studies
$\Delta G^{O}_{T=}\ \Delta H^{o} - T\Delta S^{o}$ ΔH (cal/mol); (S (cal.mol $^{-1}$ .K^{-1});T (K)	Use at a different temperatures (when ΔH and ΔS are temperature independent)	[18]
$\Delta G^{o}{}_{1}=\Delta H^{o}{}_{duplex}$ - $T\Delta S^{o}{}_{duplex}$	For DNA/RNA duplexes	[59]
$\Delta G_{duplex} = \sum_{ij} N_{ij}(\Delta H_{ij} - T\Delta S_{ij})$	Use for duplex stability	[58]
$\Delta G^{o}{}_{1,mismatched} = \Delta G^{o}{}_{1,\ perfect\ complementary} + \Delta\Delta G^{o}{}_{1}$	When a mismatch form is present.	[59]
$\Delta G^{o}{}_{i}[FA] = \Delta G^{o}{}_{i,0\ \%} + m_i[FA]$	For probe dissociation with increasing formamide percentage.	[59]
$\Delta\Delta G^{o}{}_{1} = \Delta G^{o}\langle\frac{5'\alpha\beta\gamma_{3'}}{3'\alpha_c\mu\gamma c_{5'}}\rangle - \left(\Delta G^{o}\langle\frac{5'\alpha\beta_{3'}}{3'\alpha_c\beta_{c5'}}\rangle + \Delta G^{o}\langle\frac{5'\beta\gamma_{3'}}{3'\beta\gamma_{5'}}\rangle\right)$	If a mismatch forms a trinucleotide.	[20]

Although this study presented important progress on LNA thermodynamics, the LNA parameter set is incomplete because most probes have more than just a single LNA incorporation. For instance, a triplet of LNA nucleotides appears to maximize mismatch discrimination and improves single-nucleotide polymorphism assays [60], genomic DNA sequences can be selectively captured by fully LNA-modified probes [61], and LNA incorporations induce higher specificities increasing the mismatch discrimination of FISH probes [17]. In fact, using values determined experimentally and from previous NN parameters [18,55], Owczarzy *et al* establish a new set of NN parameters that represent the effects on thermodynamic parameters of consecutive LNAs nucleotides (table 1 of reference [54]). Since these values represent deviations from native DNA duplexes in order to calculate the total enthalpy of a LNA-modified sequence, one predicts the transition enthalpy for the native DNA duplex ($\Delta H°$) and adds the differential parameters ($\Delta\Delta H°$) to take into account the LNA-mediated effects (equation 5).

$$\Delta H° = \sum_{i=1}^{N_{bp}-1} \Delta H°_{i,i+1} + \Delta H°_{init} + \sum^{LNA} \Delta\Delta H° \qquad (5)$$

To simplify the calculation of thermodynamic values, Owczarzy *et al* (2011) presented a full set of thermodynamic parameters for consecutive and isolated LNA modifications (table 2 of reference [54]. Instead of having to calculate the thermodynamics of the native DNA duplex and then add the differential parameters caused by the LNA modifications, Owczarzy *et al* (2011) combines the parameters of an isolated LNA modification (table 4 of ref [55]) or consecutive LNA modifications (table 1 of reference [54]) with the corresponding DNA NN parameters (table 1 of reference [18]) which gives full NN LNA parameters. The full set of NN parameters allows a faster calculation of thermodynamic values involving an LNA-modified sequence. Similarly for PNA, there are no parameters for LNA:RNA duplexes and as such it is expected that these models present many deviations from the reality.

3. Models currently available to make reaction parameter corrections that affect the variation of Tm

In Section 2 we have described the more commonly used models for the theoretical prediction of the melting temperatures for DNA, PNA and LNA probes. These models provide an approximation of the possible behaviour of the probe in study, however the results are far from being precise, partly due to the fact that these models do not consider the effects of several compounds used in the FISH procedure that have crucial influence in the hybridization. Having this in mind several authors have proposed models to predict the effect that these parameters have on the T_m values. As before, these models are mostly developed for DNA probes and only very limited adaptations for nucleic acid mimics exist.

3.1. Models used for hybridization with DNA probes

The denaturing agent formamide (FA) and sodium ions are two of the most important ingredients used in FISH reactions with DNA probes, and are also two of the most likely to impact hybridization temperature.

3.2. Effect of formamide on the stability of duplex

FA is used to adjust the stringency of the hybridization. It acts by allowing a more exposed surface in the molecule, leading in turn to a thermodynamically more favourable reaction [20]. Earlier studies suggested that this effect of FA was due to its ion-solvating power [62,63] and the ability to increase the solubility of free bases [62]. In fact, by increasing the hydrophobic character of the solvent, the activity coefficients and free energies of the bases were decreased, favouring the denatured state [64-66]. Initially, it was

demonstrated that the T_m of DNA duplexes decrease linearly by approximately 0.65°C per volume fraction (x100) of FA ([67-70]. However, these earlier studies consider the effects of FA independent of base content of the DNA.

Consequently, it is necessary to achieve the optimal denaturing conditions that allow specific hybridization. Some studies determined these conditions based on FA dissociation profiles, which show the variation of brightness of hybridized cells with the change of FA concentration [20]. These FA curves allow the determination of melting points and can be used to compare models prediction with experimental results [71]. Yilmaz (2006) has developed a FA-based probe dissociation model where the ΔG° values for each reaction in the equilibrium model must be obtained for different FA concentrations. The changes in ΔG° values are obtained with equation 6, where the "m-value" is used to formulate the linear relationship between FA concentrations and the ΔG° values.

$$\Delta G^{\circ}{}_{i}[\mathrm{FA}] = \Delta G^{\circ}{}_{i,0\,\%} + m_i[\mathrm{FA}] \quad (6)$$

However, this model is independent of the sequence, although it has been demonstrated previously that the FA effect is dependent of base content of the DNA [72].

This model was improved by Wright *et al*. (2014), through the use of a retrained mechanistic model (RMM). The RMM model was developed based on the improvement of the prediction of FA curves for perfectly matched hybrids, using new thermodynamic calculations and data sets. These data sets were calibrated and validated on 106 probes targeting five different organisms [71]. Therefore, the prediction of hybridization efficiency is defined by the ratio of probe-bound rRNA molecules ([PR]) to total rRNA ($[R]_0$) (equation 7).

$$\frac{[PR]}{[R]_0} = \frac{[P]_0 K_{overall}}{1+[P]_0 K_{overall}} \quad (7)$$

This ratio is related with the overall equilibrium constant ($K_{overall}$) and the molar concentration of probe used ($[P]_0$). The $K_{overall}$ constant (equation 8) is further defined as a function of three ΔG° changes (i=1,2,3) representing the reactions for probe:target duplex formation, probe folding, and target folding, respectively.

$$K_{overall} = \frac{exp(-\frac{\Delta G^0_{1\%} - m_1[FA]}{RT})}{[1+exp\left(-\frac{\Delta G^0_{1\%} - m_2[FA]}{RT}\right)][1+exp\left(-\frac{\Delta G^0_{1\%} - m_3[FA]}{RT}\right)]} \quad (8)$$

In this equation, R is the ideal gas law constant ($1.99X10^{-3}$ kcal/mol K), and T is the hybridization temperature in K.

In order to improve predictions of formamide denaturation in FISH another approach was used from the same authors for microarrays hybridizations [73], the single-reaction computationally model (SRM) [71]. The SRM model converts the ΔG values from DNA/RNA NN rules to a specific ΔG using a linear relationship with only two parameters, instead of 17, and was considered the best model in predicting the melting point, with the error being less than 10%. Nevertheless, because SRM cannot predict probe affinity, the authors use in parallel RMM to predict hybridization efficiency as a function of FA (with predicted ΔG° values and known probe concentration).

The effects of FA in complementary duplexes containing mismatches are still poorly understood. It is known that an optimal range of FA concentrations enhance the mismatch discrimination due to the occurrence of a more rapid discrimination in duplexes with mismatches [59]. Therefore, the mismatch discrimination in FISH can be associated with how much the mismatches change the FA dissociation profile of a probe comparatively to that obtained with a target microorganism [74].

Finally, it is important to mention that several studies proved that different denaturants could replace FA (e.g. urea, SDS) [15,17,75], and have showed that the use of FA is not always beneficial for the best outcome of the FISH procedure [76].

3.3. Effects of mismatches on melting temperature

The appearance of mismatches leads to a less favourable free energy binding when compared to the original and perfectly sequence-matched duplex [77] with a decrease in the efficiency of the reaction. This phenomenon is purely chemical, since the loss of connections and the surrounding area of the mismatch are matched with a more rigid structure forming a not so perfect duplex [77]. Increasing the size of the probe is usually performed in an attempt to create a higher affinity with the target sequence. However, this elongation can increase the nonspecific binding of the probe, leading to small mismatches. Therefore the systematic characterization of mismatches stability is an upmost requirement in FISH. However, this is a complicated process due to several variables associated with this particular parameter and uncertainties in the estimation of it. According to the NN model, the “G” base is the one which will have the tendency to form the highest number of mismatches, while the “C” base has the most propensity to form very few mismatches [18]. Therefore, the stability predictions could help determining false positives, consequently foreseeing the published probe specificity.

The quantification of the effect of internal mismatches is therefore important to understand the cross-hybridization effect, which could have some practical consequences for optimal probe design [78]. The calculation of the $\Delta G^{o}{}_{1}$, in equation 9, is essential to determine the duplex stability.

$$\Delta G^{o}{}_{1,\text{mismatched}} = \Delta G^{o}{}_{1,\text{ perfect complementary}} + \Delta\Delta G^{o}{}_{1} \quad (9)$$

The difference in $\Delta G^{o}{}_{1}$, referred as $\Delta\Delta G^{o}{}_{1}$, represents the effect of stability mismatch on the duplex DNA:RNA. Subsequently, the $\Delta\Delta G^{o}{}_{1}$ needs to be calculated to incorporate single mismatches into the theoretical framework. The NN theory suggests that the stability of a mismatch is dependent of the mismatch type and the base pairs adjacent to the mismatch [79].

The screening of FISH probes for potential non-target bindings against a large rRNA databases of rRNA sequences is crucial to reduce the number of candidate probes before undertake laborious experimental validation process. There are some programs that can be used to help in this process, such as ARB software. ARB, provide a prediction of mismatch stability, where a weighted mismatch score is calculated based on the type of mismatch and the relative perfect match [80]. Yilmaz *et al.,* compare the mismatch scores obtained by this software with the experimental results of the effect of single mismatch on FA dissociation profiles. Although the authors agree with the importance of stability predictors to evaluate the specificity of probes, they reefer that the parameters of ARB should be improve [74]. Additionally, this software does not consider insertions and deletions sites, which can outcome false positive FISH results if the ΔG^{o} of the loop structure is less than 4 kcal/mol [81]. The software tool LoopOut allow the screening of FISH probes for non-target binding containing single nucleotide insertions or deletions. This tool generates all possible insertion/deletion combinations and the theoretical ΔG^{o} and ΔG°_{bulge} values for each variant for a FISH probe. ΔG°_{bulge} values were calculated based on the following equation 10 and 11 for pyrimidine and purine bases, respectively [82].

$$\Delta G^{\circ}_{\text{bulge}} = 3.9 + 0.1\,\Delta G^{\circ}_{\text{nn}}\ \text{kcal/mol} \quad (10)$$

$$\Delta G^{\circ}_{bulge} = 3.3 + 0.3\,\Delta G^{\circ}_{nn}\ kcal/mol \quad (11)$$

ΔG°_{nn} is the calculated free energy of the neighbouring base pair of the bases flanking the bulge [82]. Several correlations to these models can also be applied according with the type of insertions/deletions [81-83].

Even though several approaches have been analysed to characterize mismatch stability in FISH, this is a very complex subject. The use of different microorganisms with mismatches on the target site, lead to a different ΔGo values for the target site, and makes the calculation uncertain [74]. Therefore, experimental and theoretical methodology should be combined to obtain more accuracy results.

The improvement of the specificity of FISH probes has been investigated. One of these approaches is the application of dual probes with distinct fluorophores. These probes should be design to have similar melting points and a mathematical modelling study should be determined to analyse the potential false negative results based on mismatch thermodynamics [71]. The increase of stringency conditions (e.g. higher FA concentration) [20,84] and the use of unlabeled competitor probes (Kirschner et al., 2012,[85] are other strategies used to minimize the cross-hybridization with mismatch non-targets and enhanced the fluorescence signal. However, the use of stable DNA mimics it is a simpler approach to help to overleap the mismatch problem. Although several studies have already found that destabilization occurs in the presence of mismatches in both DNA:DNA, PNA:DNA and LNA:DNA duplexes, the ability of discrimination of nucleic acid mimics is usually higher than when only DNA is used [31,86-88].

3.4. Effects of sodium on prediction of melting temperatures

The relationship between sodium ion concentration and T_m of a DNA duplex has been widely studied with several algorithms [22,56,58], with the algorithm developed by Owczarzy *et al.* (2004) being the most accurate. According to this model, the T_m calculation can be adjusted to the salt concentration trough equation 12, however DNA concentration and the sequence length are not considered [89].

$$\frac{1}{T_{M\,(2)}} = \frac{1}{T_{M(1)}} + (4{,}29f(G.C) - 3.95) \times 10^{-5} \ln \frac{[Na^+]_2}{[Na^+]_1} + 9.40 \times 10^{-6} (\ln^2 [Na^+]_2 - \ln^2 [Na^+]_1) \quad (12)$$

In sum, despite the existence of various models for T_m value prediction and correction parameters, they were not developed for FISH, they are not accurate enough for this specific application. In fact, the model for DNA duplexes proposed by SantaLucia *et al.* [18,19] is still one of the most used.

3.5. Models used for hybridization with PNA probes

The influence of the different parameters in FISH using PNA probes is well known. Some authors reported the change in solubility associated with T_m values in duplexes of PNA [90]. It thus seems that differences in hydration of PNA:DNA duplexes can severely influence the duplexes stability [33].

The influence of sodium ion on PNA hybridization has been controversial. Some authors described that the concentration of sodium ion has an influence on thermodynamic parameters (Griffin and Smith, 1998) while other studies reported no significant effects of the ionic strength on the stabilities of duplexes of PNA [33,91].

In particular, the stability of PNA duplexes is dependent not only on the percentage of GC content but also on the purine proportion present [37]. This occurs because PNA:DNA duplexes containing a pyrimidine-rich PNA strand are enthalpically disfavoured in solvents like water [33].

Although several thermodynamic models have been described these models are mostly incomplete, very complex and principally do not include the most important parameter in FISH experiments, as FA. Therefore more studies including PNA components is needed in order to develop a simple model capable of predicting complete thermodynamic values of PNA-containing duplexes.

4. Software for thermodynamic prediction

There are different online programs which use thermodynamic formulae for T_m calculation. The most usual programs only give the user the T_m value, thus merely allowing the selection of some parameters that influence this temperature. Table 3 describes some of the programs that are available online, together with some of the characteristics associated to each program.

Table 3 - Software for thermodynamic parameter prediction available online

Software	**Adjustments**	**Notes**
Oligonucleotide Properties Calculator software	Salt and length	Only accepts symmetric sequences, fixed pH (*pH* 7.0), and denaturant agents are not included
LNA™ Oligo Tm Prediction	-	Only valid for neutral solutions (7 to 8), defined oligonucleotides concentrations and specific salt concentration.
OligoAnalyzer software	Salt	The presence of denaturant agents is not included
mathFISH	Salt, probe concentration, temperature	Very complete software which performed all available simulations for a probe and a target/nontarget sequence.

ProbeMelt	Target molecule (RNA or microarrays)	Predictions are performed for a defined temperature (46°C) and specific salt concentration (1M sodium concentration).

The *Oligonucleotide Properties Calculator software* (http://www.basic.northwestern.edu/biotools/oligocalc.html) is a DNA and RNA specific software. In essence, this program uses the strategy described in Breslauer *et al*. to calculate thermodynamic properties [28] and the values published by Sugimoto *el al*., [92].

The *LNA™ Oligo Tm Prediction* tool (http://www.exiqon.com/ls/Pages/ExiqonTMPredictionTool.aspx) allow the prediction of the duplex Tm between an oligonucleotide (LNA, DNA or LNA:DNA) and a complementary DNA or RNA strand.

The *OligoAnalyzer* software (http://eu.idtdna.com/analyzer/applications/oligoanalyzer/default.aspx) estimates T_m value from the NN model [19] and it uses the NN parameters already published for DNA:DNA, RNA:DNA, RNA:RNA base pairs from Allawi *et al.,* [93], Sugimoto *et al.,* [23], and Xia *et al.,* [94], respectively. This is one of the most robust softwares for T_m value prediction. There are other similar software packages like PRIDE, PRIMO, AcePrimer and PrimeMaster , however they generally produce deviations greater than, or equal to 6.8 °C [18].

An important tool in the FISH area was developed by Yilmaz *et al.* (2011) and is a web-based program called mathFISH (http://mathfish.cee.wisc.edu/) which incorporates all previous models developed by the authors, specifically the output model for the $\Delta G^{o}_{overall}$ and the linear energy model. This program can simulate the hybridization between a given target/probe sequence and gives the user functional parameters like the thermodynamic parameter set, hybridization efficiency, affinity of a probe, and a predicted FA dissociation profile of the probe. Furthermore, the program also informs if the thermodynamic parameters of the probe are not the most correct [95]. While the program does not predict T_H and provides no information on the properties of PNA and LNA, it is certainly one of the most well adapted for FISH procedures.

The most recent web tool was developed by Wright *et al.,* and it is called DECIPHER's ProbeMelt (http://decipher.cee.wisc.edu/ProbeMelt.html) [71]. With this software it is possible to perform some relevant predictions in DNA probes when FA is used. The mathematic modelling background used was based on the SRM model that has been described above. The user is able to analyse hybridization efficiencies using different levels of stringency and generating denaturant curves. Additionally, ProbeMelt can be used in combination with database searches, allowing the identification of potential targets

and nontargets [71]. Although it is a recent online tool, it is still only possible to analyse DNA or RNA sequences and only the use of FA as a denaturant is considered.

5. Melting temperature vs hybridization temperature

In the previous chapter, we have addressed the thermodynamic models more commonly used for theoretical prediction of melting temperatures of DNA, PNA and LNA probes. Despite the important information that we can obtain from these models, we have shown above several reasons why the T_m obtained from those calculations is still different from the hybridization temperature of the probes. For a better understanding of these differences we have identified studies on FISH that used DNA, PNA and LNA probes and calculated the melting temperature using the respective thermodynamic models described above and compared it with the hybridization temperature that was used by the authors (Figure 3). More specifically, we used the parameters described by Santalucia *et al*. [19] and equation 2 previously described to determine the T_m for DNA probes. To calculate the T_m of PNA probes we used equation 3 described above. The T_m determination of LNA probes was performed based on Owczarzy *et al.* [54] parameters for LNA using equation 2. We did not use the models with corrections for parameters such as salt concentration and formamide. Relatively to the salt concentration, the majority of the published results do not take these conditions in consideration and their impact on the melting or hybridization temperature is comparatively low. Regarding the formamide, the correction models that exist were developed for DNA probes, and since we address in this study not only DNA probes but also other nucleic acid mimics probes the application of the formamides models for these other probes could originate misleading results.

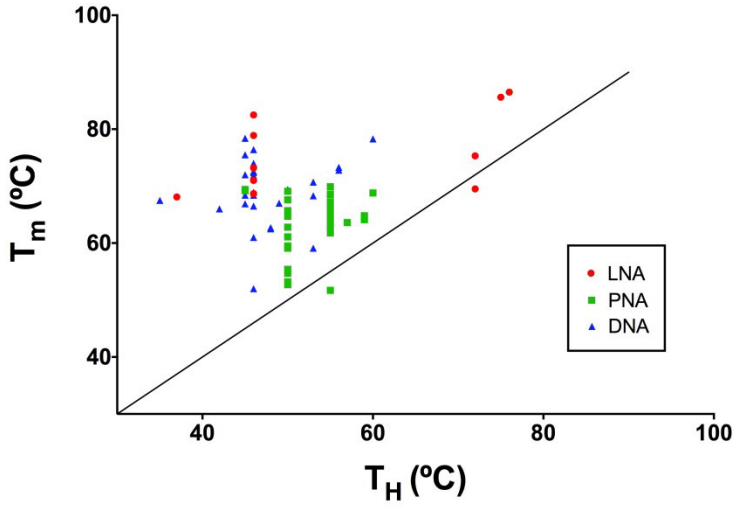

Figure 3 - Predicted melting temperature (T_m) and respective hybridization temperature (T_H) at which the hybridization has been performed.

In Figure 4, the average difference between the T_m predicted for each type of probe, and the hybridization temperature employed by the authors is represented. As expected, the analysis of Figure 3 and 4 shows that in average the T_H is lower than the T_m for all types of probes. Another result that can also be easily explained is the lower standard deviation obtained for DNA and PNA probes, which is likely to be due to the fact that PNA models are adaptations of the DNA models and these DNA models and are much more established than the recent developed models for LNA. LNA probes show a higher variability than DNA and PNA probes, with the T_H being 7 ° C to 37 ° C lower that the predicted melting temperature values. This variability may be due to the fact that, unlike for DNA and PNA probes, many of the LNA probes are constituted by DNA oligonucleotides with LNA insertions. In adding to the number of LNA bases of the probe, the positioning of the LNA bases within the probe also has effects on the thermodynamics of the hybridization [96], implying that Tm predictions are much harder to obtain for LNA probes. In addition, most of the FISH methods performed using LNA are in animal cells. In this case, many of the authors aim at developing the method at 37 °C, and as such might not be interested in identifying the temperature at which the probe will work optimally.

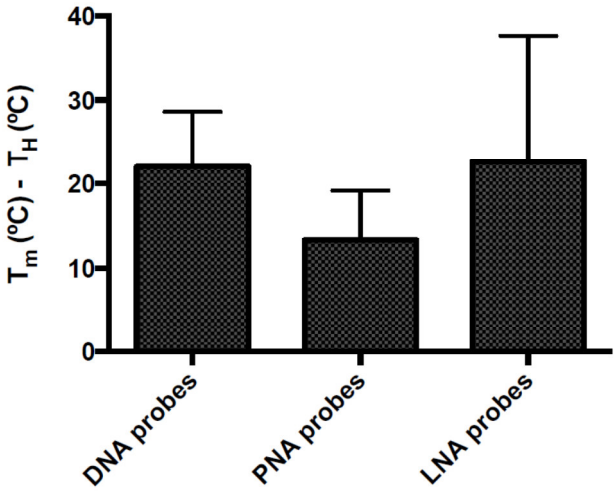

Figure 4 - Difference between predicted melting temperature (T_m) and hybridization temperature (T_H).

The average difference between the T_H and T_m of the PNA probes was lower than the ones for DNA, which could be due to the fact that no correction has been used for parameters such as formamide. In our opinion, it is expected that different types of nucleic acids have different (T_m-T_H) values as the slope of the melting temperature curve showed in Figure 1 might also vary for each nucleic acid. Nonetheless, because of the lack of optimization and large scale verification of at least some of the models, it is too early to

draw any conclusions in relation to the explicit differences between the various probe chemistries.

6. Conclusions

FISH is a powerful molecular method used for the identification and quantification of organisms of interest, both in environmental and in medical samples. This technique has evolved and become more powerful due to the appearance of nucleic acid mimics that have substituted the traditional DNA oligonucleotide probes used.

Despite this development, the optimization of this technique is still a trial and error process, in part due to the lack of precise mathematic models to predict the hybridization temperature of an oligonucleotide probe. The first thermodynamic models were based on thermodynamic parameters calculated for DNA or RNA oligonucleotides, but with the appearance of the new DNA or RNA mimics it has become necessary to adjust these models or to develop novel models. The most used models to calculate thermodynamic parameters for DNA/RNA mimics oligonucleotides have been derived from the ones used for DNA oligonucleotides [37,55,96] and provide important information about the conditions at which the FISH procedure should be performed, helping to decrease the time involved in method optimization. However, the results often lack accuracy because these all models are not specific for FISH since they were designed for other molecular biology techniques, such as *polymerase chain reaction* (PCR). Furthermore, they do not take into account all parameters and chemical compounds involved in the hybridization step of a FISH procedure. If possible, one should always confirm the predicted T_m values through two independent models due to the occurrence of potential deviations (Owczarzy et al., 1997). Furthermore, these methods only allow us to predict the melting temperature which is used as a reference for the hybridization temperature as illustrated above when the Tm values predicted by the models were compared with the T_H's used in the experiments.

FA and sodium ion concentrations are known to have an impact on the hybridization reaction and therefore correction models have been developed. Nevertheless, these models do not give precise results for all kinds of oligonucleotide probes and some of them involve complicated mathematical calculations and are therefore not practical for routine use for most researchers. This obstacle may be alleviated by the use of specialized software to predict the T_H but at present such software must be used carefully because most of them only take a limited number of parameters of the hybridization reaction into account.

In short, the thermodynamic models already developed for DNA, RNA and DNA/RNA mimics only allow researchers to obtain an indication of the range of the hybridization temperature, but a trial and error optimization will still be required until the shortcomings identified in this review are solved.

7. References

1. Guimaraes N., Azevedo N.F., Figueiredo C., Keevil C.W., Vieira M.J. Development and application of a novel peptide nucleic acid probe for the specific detection of Helicobacter pylori in gastric biopsies. J ClinMicrobiol (2007); 45: 3089-3094.
2. Wagner M., Horn M., Daims H. Fluorescence in situ hybridisation for the identification and characterisation of prokaryotes. Current Opinion in Microbiology (2003); 6: 302-309.
3. Amann R., Fuchs B.M. Single-cell identification in microbial communities by improved fluorescence in situ hybridization techniques. Nat Rev Microbiol (2008); 6: 339-348.
4. DeLong E.F., Wickham G.S., Pace N.R. Phylogenetic stains: ribosomal RNA-based probes for the identification of single cells. Science (1989); 243: 1360-1363.
5. Amann R.I., Ludwig W., Schleifer K.H. Phylogenetic identification and in situ detection of individual microbial cells without cultivation. MicrobiolRev (1995); 59: 143-169.
6. Amann R.I., Krumholz L., Stahl D.A. Fluorescent-oligonucleotide probing of whole cells for determinative, phylogenetic, and environmental studies in microbiology. J Bacteriol (1990); 172: 762-770.
7. Moter A., Gobel U.B. Fluorescence in situ hybridization (FISH) for direct visualization of microorganisms. J Microbiol Methods (2000); 41: 85-112.
8. Hugenholtz P., Tyson G.W., Blackall L.L. Design and evaluation of 16S rRNA-targeted oligonucleotide probes for fluorescence in situ hybridization. Methods Mol Biol (2002); 179: 29-42.
9. Behrens S., Fuchs B.M., Mueller F., Amann R. Is the in situ accessibility of the 16S rRNA of Escherichia coli for Cy3-labeled oligonucleotide probes predicted by a three-dimensional structure model of the 30S ribosomal subunit? Appl Environ Microbiol (2003); 69: 4935-4941.
10. Yilmaz L.S., Noguera D.R. Mechanistic approach to the problem of hybridization efficiency in fluorescent in situ hybridization. Appl Environ Microbiol (2004); 70: 7126-7139.
11. Hoshino T., Yilmaz L.S., Noguera D.R., Daims H., Wagner M. Quantification of target molecules needed to detect microorganisms by fluorescence in situ hybridization (FISH) and catalyzed reporter deposition-FISH. Appl Environ Microbiol (2008); 74: 5068-5077.
12. Wagner M., Erhart R., Manz W., Amann R., Lemmer H., Wedi D., et al. Development of an Ribosomal-Rna-Targeted Oligonucleotide Probe Specific for the Genus Acinetobacter and Its Application for in-Situ Monitoring in Activated-Sludge. Appl Environ Microbiol (1994); 60: 792-800.
13. Manz W., Amann R., Szewzyk R., Szewzyk U., Stenstrom T.A., Hutzler P., et al. In-Situ Identification of Legionellaceae Using 16s Ribosomal-Rna-Targeted Oligonucleotide Probes and Confocal Laser-Scanning Microscopy. Microbiology-Sgm (1995); 141: 29-39.
14. Neef A., Amann R., Schleifer K.H. Detection of Microbial-Cells in Aerosols Using Nucleic-Acid Probes. Systematic and Applied Microbiology (1995); 18: 113-122.

15. Fontenete S., Guimarães N., Leite M., Figueiredo C., Wengel J., Filipe Azevedo N. Hybridization-Based Detection of <italic>Helicobacter pylori</italic> at Human Body Temperature Using Advanced Locked Nucleic Acid (LNA) Probes. PLoS ONE (2013); 8: e81230.
16. Cerqueira L., Azevedo N.F., Almeida C., Jardim T., Keevil C.W., Vieira M.J. DNA mimics for the rapid identification of microorganisms by fluorescence in situ hybridization (FISH). Int J Mol Sci (2008); 9: 1944-1960.
17. Kubota K., Ohashi A., Imachi H., Harada H. Improved in situ hybridization efficiency with locked-nucleic-acid-incorporated DNA probes. Appl Environ Microbiol (2006); 72: 5311-5317.
18. SantaLucia J., Jr., Hicks D. The thermodynamics of DNA structural motifs. Annu Rev Biophys Biomol Struct (2004); 33: 415-440.
19. SantaLucia J., Jr., Allawi H.T., Seneviratne P.A. Improved nearest-neighbor parameters for predicting DNA duplex stability. Biochemistry (1996); 35: 3555-3562.
20. Yilmaz L.S., Noguera D.R. Development of thermodynamic models for simulating probe dissociation profiles in fluorescence in situ hybridization. Biotechnol Bioeng (2007); 96: 349-363.
21. Bloomfield V.A. C.D.M., Tinoco I., , editor Nucleic Acids: Structures, Properties, and Functions. 1 edition ed.(2000); Sausalito, CA: University Science Books. 672 pages p.
22. SantaLucia J., Jr. A unified view of polymer, dumbbell, and oligonucleotide DNA nearest-neighbor thermodynamics. Proc Natl Acad Sci U S A (1998); 95: 1460-1465.
23. Sugimoto N., Nakano S., Katoh M., Matsumura A., Nakamuta H., Ohmichi T., et al. Thermodynamic parameters to predict stability of RNA/DNA hybrid duplexes. Biochemistry (1995); 34: 11211-11216.
24. Freier S.M., Kierzek R., Jaeger J.A., Sugimoto N., Caruthers M.H., Neilson T., et al. Improved free-energy parameters for predictions of RNA duplex stability. Proc Natl Acad Sci U S A (1986); 83: 9373-9377.
25. Marmur J., Doty P. Determination of the base composition of deoxyribonucleic acid from its thermal denaturation temperature. J Mol Biol (1962); 5: 109-118.
26. Gotoh O., Tagashira Y. Locations of frequently opening regions on natural DNAs and their relation to functional loci. Biopolymers (1981); 20: 1043-1058.
27. Ornstein R.L., Fresco J.R. Correlation of Tm and sequence of DNA duplexes with delta H computed by an improved empirical potential method. Biopolymers (1983); 22: 1979-2000.
28. Breslauer K.J., Frank R., Blocker H., Marky L.A. Predicting DNA duplex stability from the base sequence. Proc Natl Acad Sci U S A (1986); 83: 3746-3750.
29. Owczarzy R., Vallone P.M., Goldstein R.F., Benight A.S. Studies of DNA dumbbells VII: evaluation of the next-nearest-neighbor sequence-dependent interactions in duplex DNA. Biopolymers (1999); 52: 29-56.
30. Rasmussen H., Kastrup J.S., Nielsen J.N., Nielsen J.M., Nielsen P.E. Crystal structure of a peptide nucleic acid (PNA) duplex at 1.7 A resolution. Nat Struct Biol (1997); 4: 98-101.

31. Egholm M., Buchardt O., Christensen L., Behrens C., Freier S.M., Driver D.A., et al. PNA hybridizes to complementary oligonucleotides obeying the Watson-Crick hydrogen-bonding rules. Nature (1993); 365: 566-568.
32. Seo Y.J., Lim J., Lee E.H., Ok T., Yoon J., Lee J.H., et al. Base pair opening kinetics study of the aegPNA:DNA hydrid duplex containing a site-specific GNA-like chiral PNA monomer. Nucleic Acids Res (2011); 39: 7329-7335.
33. Sen A., Nielsen P.E. Unique properties of purine/pyrimidine asymmetric PNA.DNA duplexes: differential stabilization of PNA.DNA duplexes by purines in the PNA strand. Biophys J (2006); 90: 1329-1337.
34. Demidov V.V., Potaman V.N., Frank-Kamenetskii M.D., Egholm M., Buchard O., Sonnichsen S.H., et al. Stability of peptide nucleic acids in human serum and cellular extracts. Biochem Pharmacol (1994); 48: 1310-1313.
35. Good L., Nielsen P.E. Inhibition of translation and bacterial growth by peptide nucleic acid targeted to ribosomal RNA. Proc Natl Acad Sci U S A (1998); 95: 2073-2076.
36. Jensen K.K., Orum H., Nielsen P.E., Norden B. Kinetics for hybridization of peptide nucleic acids (PNA) with DNA and RNA studied with the BIAcore technique. Biochemistry (1997); 36: 5072-5077.
37. Giesen U., Kleider W., Berding C., Geiger A., Orum H., Nielsen P.E. A formula for thermal stability (Tm) prediction of PNA/DNA duplexes. Nucleic Acids Res (1998); 26: 5004-5006.
38. Cerqueira L., Fernandes R.M., Ferreira R.M., Oleastro M., Carneiro F., Brandao C., et al. Validation of a fluorescence in situ hybridization method using peptide nucleic acid probes for detection of Helicobacter pylori clarithromycin resistance in gastric biopsy specimens. J Clin Microbiol (2013); 51: 1887-1893.
39. Zhang N., Appella D.H. Colorimetric detection of anthrax DNA with a Peptide nucleic acid sandwich-hybridization assay. J Am Chem Soc (2007); 129: 8424-8425.
40. Grossmann T.N., Roglin L., Seitz O. Target-catalyzed transfer reactions for the amplified detection of RNA. Angew Chem Int Ed Engl (2008); 47: 7119-7122.
41. Chakrabarti M.C., Schwarz F.P. Thermal stability of PNA/DNA and DNA/DNA duplexes by differential scanning calorimetry. Nucleic Acids Res (1999); 27: 4801-4806.
42. Griffin T.J., Smith L.M. An approach to predicting the stabilities of peptide nucleic acid:DNA duplexes. Anal Biochem (1998); 260: 56-63.
43. Robertson K.L., Vora G.J. Locked nucleic acid and flow cytometry-fluorescence in situ hybridization for the detection of bacterial small noncoding RNAs. Appl Environ Microbiol (2012); 78: 14-20.
44. Silahtaroglu A., Pfundheller H., Koshkin A., Tommerup N., Kauppinen S. LNA-modified oligonucleotides are highly efficient as FISH probes. Cytogenet Genome Res (2004); 107: 32-37.
45. Kumar R., Singh S.K., Koshkin A.A., Rajwanshi V.K., Meldgaard M., Wengel J. The first analogues of LNA (locked nucleic acids): phosphorothioate-LNA and 2'-thio-LNA. Bioorg Med Chem Lett (1998); 8: 2219-2222.

46. Obika S., Nanbu D., Hari Y., Morio K., In Y., Ishida T., et al. Synthesis of 2'-O,4'-C-methyleneuridine and -cytidine. Novel bicyclic nucleosides having a fixed C-3,-endo sugar puckering. Tetrahedron Letters (1997); 38: 8735-8738.
47. Vester B., Wengel J. LNA (locked nucleic acid): high-affinity targeting of complementary RNA and DNA. Biochemistry (2004); 43: 13233-13241.
48. Zhang Y., Qu Z., Kim S., Shi V., Liao B., Kraft P., et al. Down-modulation of cancer targets using locked nucleic acid (LNA)-based antisense oligonucleotides without transfection. Gene Ther (2011); 18: 326-333.
49. Kurreck J., Wyszko E., Gillen C., Erdmann V.A. Design of antisense oligonucleotides stabilized by locked nucleic acids. Nucleic Acids Res (2002); 30: 1911-1918.
50. Perry-O'Keefe H., Rigby S., Oliveira K., Sorensen D., Stender H., Coull J., et al. Identification of indicator microorganisms using a standardized PNA FISH method. J Microbiol Methods (2001); 47: 281-292.
51. Piao X., Yan Y., Yan J., Guan Y. Enhanced recognition of non-complementary hybridization by single-LNA-modified oligonucleotide probes. Anal Bioanal Chem (2009); 394: 1637-1643.
52. Kaur H., Arora A., Wengel J., Maiti S. Thermodynamic, counterion, and hydration effects for the incorporation of locked nucleic acid nucleotides into DNA duplexes. Biochemistry (2006); 45: 7347-7355.
53. Petersen M., Bondensgaard K., Wengel J., Jacobsen J.P. Locked nucleic acid (LNA) recognition of RNA: NMR solution structures of LNA:RNA hybrids. J Am Chem Soc (2002); 124: 5974-5982.
54. Owczarzy R., You Y., Groth C.L., Tataurov A.V. Stability and mismatch discrimination of locked nucleic acid-DNA duplexes. Biochemistry (2011); 50: 9352-9367.
55. McTigue P.M., Peterson R.J., Kahn J.D. Sequence-dependent thermodynamic parameters for locked nucleic acid (LNA)-DNA duplex formation. Biochemistry (2004); 43: 5388-5405.
56. SantaLucia J., Jr., Allawi H.T., Seneviratne P.A. Improved nearest-neighbor parameters for predicting DNA duplex stability. Biochemistry.(1996); 1996/03/19 ed. pp. 3555-3562.
57. Borer P.N., Dengler B., Tinoco I., Jr., Uhlenbeck O.C. Stability of ribonucleic acid double-stranded helices. J Mol Biol (1974); 86: 843-853.
58. Owczarzy R., Vallone P.M., Gallo F.J., Paner T.M., Lane M.J., Benight A.S. Predicting sequence-dependent melting stability of short duplex DNA oligomers. Biopolymers (1997); 44: 217-239.
59. Yilmaz L.S. Development of Thermidynamic Models for the Optimization of Fluorescence in Situ Hybridization. (2006): University of Wisconsin-Madison. 244 p.
60. You Y., Moreira B.G., Behlke M.A., Owczarzy R. Design of LNA probes that improve mismatch discrimination. Nucleic Acids Res (2006); 34: e60.
61. Jacobsen N., Bentzen J., Meldgaard M., Jakobsen M.H., Fenger M., Kauppinen S., et al. LNA-enhanced detection of single nucleotide polymorphisms in the apolipoprotein E. Nucleic Acids Res (2002); 30: e100.

62. Levine L., Gordon J.A., Jencks W.P. The relationship of structure to the effectiveness of denaturing agents for deoxyribonucleic acid. Biochemistry (1963); 2: 168-175.
63. Helmkamp G.K., Ts'O P.O. Secondary structures of nucleic acids in organic solvents. III. Relationship of optical properties to conformation. Biochim Biophys Acta (1962); 55: 601-608.
64. Herskovits T.T., Singer S.J., Geiduschek E.P. Nonaqueous solutions of DNA. Denaturation in methanol and ethanol. Arch Biochem Biophys (1961); 94: 99-114.
65. Geiduschek E.P., Herskovits T.T. Nonaqueous solutions of DNA. Reversible and irreversible denaturation in methanol. Arch Biochem Biophys (1961); 95: 114-129.
66. Sander H., Alkemeyer M., Haensel R. [On Solanum dulcamara L. 4. Chemical differentiation of the inner half of the species and isolation of soladulcidine tetraoside]. Arch Pharm (1962); 295/67: 6-12.
67. McConaughy B.L., Laird C.D., McCarthy B.J. Nucleic acid reassociation in formamide. Biochemistry (1969); 8: 3289-3295.
68. Record M.T., Jr. Electrostatic effects on polynucleotide transitions. I. Behavior at neutral pH. Biopolymers (1967); 5: 975-992.
69. Casey J., Davidson N. Rates of formation and thermal stabilities of RNA:DNA and DNA:DNA duplexes at high concentrations of formamide. Nucleic Acids Res (1977); 4: 1539-1552.
70. Hutton J.R. Renaturation kinetics and thermal stability of DNA in aqueous solutions of formamide and urea. Nucleic Acids Res (1977); 4: 3537-3555.
71. Wright E.S., Yilmaz L.S., Corcoran A.M., Okten H.E., Noguera D.R. Automated Design of Probes for rRNA-Targeted Fluorescence In Situ Hybridization Reveals the Advantages of Using Dual Probes for Accurate Identification. Appl Environ Microbiol (2014); 80: 5124-5133.
72. Blake R.D., Delcourt S.G. Thermodynamic effects of formamide on DNA stability. Nucleic Acids Res (1996); 24: 2095-2103.
73. Yilmaz L.S., Loy A., Wright E.S., Wagner M., Noguera D.R. Modeling formamide denaturation of probe-target hybrids for improved microarray probe design in microbial diagnostics. PLoS ONE (2012); 7: e43862.
74. Yilmaz L.S., Bergsven L.I., Noguera D.R. Systematic evaluation of single mismatch stability predictors for fluorescence in situ hybridization. Environ Microbiol (2008); 10: 2872-2885.
75. Simard C., Lemieux R., Cote S. Urea substitutes toxic formamide as destabilizing agent in nucleic acid hybridizations with RNA probes. Electrophoresis (2001); 22: 2679-2683.
76. Matthiesen S.H., Hansen C.M. Fast and non-toxic in situ hybridization without blocking of repetitive sequences. PLoS One (2012); 7: e40675.
77. Ratilainen T., Holmen A., Tuite E., Nielsen P.E., Norden B. Thermodynamics of sequence-specific binding of PNA to DNA. Biochemistry (2000); 39: 7781-7791.
78. Hooyberghs J., Van Hummelen P., Carlon E. The effects of mismatches on hybridization in DNA microarrays: determination of nearest neighbor parameters. Nucleic Acids Res (2009); 37: e53.

79. Sugimoto N., Nakano M., Nakano S. Thermodynamics-structure relationship of single mismatches in RNA/DNA duplexes. Biochemistry (2000); 39: 11270-11281.
80. Ludwig W., Strunk O., Westram R., Richter L., Meier H., Yadhukumar, et al. ARB: a software environment for sequence data. Nucleic Acids Res (2004); 32: 1363-1371.
81. McIlroy S.J., Tillett D., Petrovski S., Seviour R.J. Non-target sites with single nucleotide insertions or deletions are frequently found in 16S rRNA sequences and can lead to false positives in fluorescence in situ hybridization (FISH). Environ Microbiol (2011); 13: 33-47.
82. Znosko B.M., Silvestri S.B., Volkman H., Boswell B., Serra M.J. Thermodynamic parameters for an expanded nearest-neighbor model for the formation of RNA duplexes with single nucleotide bulges. Biochemistry (2002); 41: 10406-10417.
83. Pozhitkov A., Noble P.A., Domazet-Loso T., Nolte A.W., Sonnenberg R., Staehler P., et al. Tests of rRNA hybridization to microarrays suggest that hybridization characteristics of oligonucleotide probes for species discrimination cannot be predicted. Nucleic Acids Res (2006); 34: e66.
84. Kirschner A.K., Rameder A., Schrammel B., Indra A., Farnleitner A.H., Sommer R. Development of a new CARD-FISH protocol for quantification of Legionella pneumophila and its application in two hospital cooling towers. J Appl Microbiol (2012); 112: 1244-1256.
85. Fuchs B.M., Glockner F.O., Wulf J., Amann R. Unlabeled helper oligonucleotides increase the in situ accessibility to 16S rRNA of fluorescently labeled oligonucleotide probes. Appl Environ Microbiol (2000); 66: 3603-3607.
86. Johnson M.P., Haupt L.M., Griffiths L.R. Locked nucleic acid (LNA) single nucleotide polymorphism (SNP) genotype analysis and validation using real-time PCR. Nucleic Acids Res (2004); 32: e55.
87. Chou L.S., Meadows C., Wittwer C.T., Lyon E. Unlabeled oligonucleotide probes modified with locked nucleic acids for improved mismatch discrimination in genotyping by melting analysis. Biotechniques (2005); 39: 644, 646, 648 passim.
88. Mouritzen P., Nielsen A.T., Pfundheller H.M., Choleva Y., Kongsbak L., Moller S. Single nucleotide polymorphism genotyping using locked nucleic acid (LNA). Expert Rev Mol Diagn (2003); 3: 27-38.
89. Owczarzy R., You Y., Moreira B.G., Manthey J.A., Huang L., Behlke M.A., et al. Effects of sodium ions on DNA duplex oligomers: improved predictions of melting temperatures. Biochemistry (2004); 43: 3537-3554.
90. Spink C.H., Chaires J.B. Effects of hydration, ion release, and excluded volume on the melting of triplex and duplex DNA. Biochemistry (1999); 38: 496-508.
91. Tomac S., M. Sarkar, T. Ratilainen, P. Wittung, P. E. Nielsen, B. Nordén, and A. Graslund. Ionic Effects on the Stability and Conformation of Peptide Nucleic Acid Complexes. J Am Chem Soc (1996); 24: 5544-5552.
92. Sugimoto N., Nakano S., Yoneyama M., Honda K. Improved thermodynamic parameters and helix initiation factor to predict stability of DNA duplexes. Nucleic Acids Res (1996); 24: 4501-4505.

93. Allawi H.T., SantaLucia J., Jr. Thermodynamics and NMR of internal G.T mismatches in DNA. Biochemistry (1997); 36: 10581-10594.

94. Xia T., SantaLucia J., Jr., Burkard M.E., Kierzek R., Schroeder S.J., Jiao X., et al. Thermodynamic parameters for an expanded nearest-neighbor model for formation of RNA duplexes with Watson-Crick base pairs. Biochemistry (1998); 37: 14719-14735.

95. Yilmaz L.S., Parnerkar S., Noguera D.R. mathFISH, a web tool that uses thermodynamics-based mathematical models for in silico evaluation of oligonucleotide probes for fluorescence in situ hybridization. Appl Environ Microbiol (2011); 77: 1118-1122.

96. Kierzek E., Ciesielska A., Pasternak K., Mathews D.H., Turner D.H., Kierzek R. The influence of locked nucleic acid residues on the thermodynamic properties of 2'-O-methyl RNA/RNA heteroduplexes. Nucleic Acids Res (2005); 33: 5082-5093.